

Vladimir Dvorkin

Stochastic and Private Energy System Optimization

Ph.D. Thesis, December 2020

Kgs. Lyngby, Denmark

DANMARKS TEKNISKE UNIVERSITET
Center for Electric Power and Energy (CEE)
DTU Electrical Engineering

Stochastic and Private Energy System Optimization

Ph.D. Thesis, by Vladimir Dvorkin

Supervisors:

Professor Pierre Pinson, Technical University of Denmark

Associate Professor Jalal Kazempour, Technical University of Denmark

DTU - Technical University of Denmark, Kgs. Lyngby - December 2020

Stochastic and Private Energy System Optimization

This thesis was prepared by:

Vladimir Dvorkin

Supervisors:

Professor Pierre Pinson, Technical University of Denmark

Associate Professor Jalal Kazempour, Technical University of Denmark

Dissertation Examination Committee:

Associate Professor Spyros Chatzivasileiadis

Department of Electrical Engineering, Technical University of Denmark

Professor Alexander Shapiro

H. Milton Stewart School of Industrial and Systems Engineering, Georgia Institute of Technology,
USA

Professor Adam Wierman

Department of Computing and Mathematical Sciences, California Institute of Technology, USA

Center for Electric Power and Energy (CEE)

DTU Electrical Engineering

Elektrovej, Building 325

DK-2800 Kgs. Lyngby

Denmark

Tel: (+45) 4525 3500

Fax: (+45) 4588 6111

E-mail: cee@elektro.dtu.dk

Release date: December 2020

Edition: 1.0

Class: Internal

Field: Electrical Engineering

Remarks: The dissertation is presented to the Department of Electrical Engineering
of the Technical University of Denmark in partial fulfillment of the require-
ments for the degree of Doctor of Philosophy.

Copyrights: Vladimir Dvorkin, 2020

ISBN: 000-00-00000-00-0

Imagination is its own form of courage

— Francis Joseph Underwood

46th President of the United States

To my family

Preface

This thesis is prepared at the Department of Electrical Engineering of the Technical University of Denmark (DTU) in partial fulfillment of the requirements for acquiring the degree of Doctor of Philosophy in Engineering. The Ph.D. project was funded by an internal DTU scholarship.

This dissertation summarizes the work carried out by the author during his Ph.D. project. It started on 1st September 2017 and was completed on 31st December 2020. During this period, he was hired by the Technical University of Denmark as a Ph.D. student at the Center for Electric Power and Energy (CEE) at the Department of Electrical Engineering.

The thesis is composed of four chapters which summarize the six attached scientific papers, four of which have been peer-reviewed and published, one of which has been submitted to a peer-reviewed journal and the remaining one is a preprint to be submitted to a peer-reviewed journal.



Vladimir Dvorkin
December 2020

Acknowledgements

Pursuing this degree has been a journey shared with many people who – directly or not – contributed to my work. Their advice and friendship matured into relationships of great importance to me.

First, I would like to thank my mentors Pierre Pinson and Jalal Kazempour. Thank you Pierre for giving me the chance to pursue this degree. Your permanent advice, inspiration, and genuine support, that spans beyond professional matters, resulted in invaluable returns to me. Thank you Jalal for all the time you have invested in my projects and specifically for lifting my ambitions towards exploring new research directions and to publish in journals and venues which I previously thought were unavailable to me. You both taught me your approach to research and academic values – the legacy which I take to my post-graduate path.

In 2019 I visited the Georgia Institute of Technology, where I worked with Pascal Van Hentenryck and Ferdinando Fioretto. This time takes a special place in my memories thanks to the very style of Pascal's guidance and his leadership by example. I am grateful to Pascal and Nando for helping me succeed in privacy research. I also thank the students, postdocs and faculty members I met at Georgia Tech for the inspiring conversations, let alone for welcoming me in a foreign country that felt more like home by the end of my stay.

My PhD path would be different had I not been a member of *ELMA* team - the very special ecosystem that made my PhD time so joyful - and I thank all current and past *ELMA* members for their friendship. Thank you Lejla for introducing me to the team and for remaining a close friend even after we went our separate ways. Thank you Christos for introducing me to the PhD life; I always appreciated how much we think alike and how we inspire one another. Thank you Stefanos for helping me with my first paper, it made every next paper much easier. Thank you Andrea Marin and Anubhav for making our collaboration a pleasure. Thank you Stefanos, Christos, Tiago and Anubhav for the comments to this thesis and Morten for translating the abstract. Thank you Maxim for your friendship. Although I am about to depart, we will stay in touch. *Vi ses!*

I am grateful to my brother Yury for lending me a hand whenever it was needed and for introducing me to Robert, Jip, Ali and Samrat - you all made my visits to the US memorable.

My parents Evgeniya and Yury have always taught meritocratic values and that education is above all - thank you, now that I followed your advice, I realize how many opportunities come to my hands. I thank my *babushka* Svetlana who taught the importance of hard work and cemented family values in me. I was always inspired by my *dedushka* Vladimir who – despite the age of 84 – remains dedicated to his research work. Thank you for your example. I am grateful to my brothers Dmitry and Yury who have never been reluctant to exercise their elder-brother rights and remind me to be the last among us to earn this degree. You were nothing but extremely supportive during my time abroad and gave me the vision to pursue this path. I also thank your spouses Anna and Olga – who were always behind your personal successes – for their friendship. Last but not least, I thank Claudia – my *sputnik* and the greatest discovery of my PhD time – for understanding my passion and for your unconditional support.

Vladimir

Kgs. Lyngby, Denmark, December 2020

Table of Contents

Preface	i
Acknowledgements	iii
Table of Contents	v
List of Figures	vii
List of Tables	vii
Abstract	ix
Resumé	xi
1 Introduction	1
1.1 Context and motivation	1
1.2 Research directions	2
1.2.1 Advancing stochastic energy system optimization	2
1.2.2 Providing privacy guarantees in power system optimization	4
1.3 Scientific contributions	7
1.4 Thesis outline	8
1.5 List of publications	8
2 Stochastic Optimization of Energy Systems	11
2.1 Stochastic energy system optimization	11
2.1.1 Convex counterpart of non-convex optimization	12
2.1.2 From infinite- to finite-dimensional stochastic programming	12
2.1.3 Stochastic market properties	15
2.2 Policy-based control and pricing for uncertainty energy systems	17
2.2.1 Uncertainty- and variability-aware policy optimization	17
2.2.2 Uncertainty- and variability-aware energy payments	19
2.3 Cost recovery and revenue adequacy beyond expectation	20
2.3.1 Deterministic versus stochastic energy system dispatch	20
2.3.2 Approximating stochastic solutions within deterministic settlements	22
2.4 Stochastic market settlement under information asymmetry	24
3 Privacy-Preserving Optimization in Energy Systems	27
3.1 Optimal power flow problem	27

3.1.1	Power network equations	27
3.1.2	Centralized optimization of the optimal power flow problem	28
3.1.3	Distributed optimization of the optimal power flow problem	28
3.2	Privacy breaches in optimal power flow computations	29
3.2.1	OPF computation problem as a mechanism	30
3.2.2	Reconstruction models of privacy attacks	30
3.2.3	Tracing models of privacy attacks	31
3.3	Differential privacy: main definitions and results	33
3.4	Differentially private distributed OPF optimization	35
3.4.1	Differentially private ADMM-based OPF algorithm	35
3.4.2	Privacy guarantee for a single iteration	36
3.4.3	Convergence and optimality loss trade-offs	37
3.4.4	Controlling privacy loss beyond one iteration	38
3.5	Differentially private centralized OPF optimization	38
3.5.1	Internalizing Laplace and Gaussian mechanisms	39
3.5.2	Feasibility guarantees	42
3.5.3	Controlling optimally loss and solution variance	44
4	Conclusions and Perspectives	47
4.1	Overview of contributions	47
4.2	Future research	48
Bibliography		51
Collection of relevant publications		59
[Paper A] Stochastic control and pricing for natural gas networks	61	
[Paper B] Setting reserve requirements to approximate the efficiency of the stochastic dispatch	73	
[Paper C] Electricity market equilibrium under information asymmetry	87	
[Paper D] Differentially private distributed optimal power flow	95	
[Paper E] Differentially private convex optimization with feasibility guarantees	103	
[Paper F] Differentially private optimal power flow for distribution grids	119	

List of Figures

1.1	Illustration of the differential privacy principle	5
2.1	Results of uncertainty- and variability-aware control policy optimization	19
2.2	Expected operating cost as a function of wind penetration level	23
2.3	Equilibrium prices as a function of agent information	25
3.1	Illustration of the node-wise decomposition of a 3-node power network	29
3.2	Example of a tracing privacy attack on the centralized OPF computation	32
3.3	Example of a tracing privacy attack on the distributed OPF computation	32
3.4	OPF optimization as a mechanism	33
3.5	Results of the privacy attack on the ε -differentially private ADMM OPF algorithm . .	37
3.6	Evolution of the primal residual over ADMM iterations	38
3.7	Composition for privacy loss control beyond one iteration	39
3.8	Stylized projections of randomized optimization solutions onto feasible space	40
3.9	Obfuscation of customer load profile in power flow measurements	42
3.10	Optimality-variance trade-offs	44

List of Tables

3.1	Optimality loss induced by ε -differentially private ADMM algorithms	38
3.2	Identity query summary for 100 optimization dataset samples	43

Abstract

Modern energy systems are undergoing the green transition towards renewable-based operations. This transition promises an emission-neutral and equal-access energy supply that finds tremendous public and governmental support. To succeed, the responsible parties must account for a range of engineering, economic and ethical challenges arising from the uncertain nature of renewables and utilization of vast amounts of data required to facilitate this transition. This thesis addresses those challenges using mathematically rigorous methods of optimization and privacy preservation.

There is a growing consensus that the methods from *stochastic optimization* are critical enablers of this transition. By leveraging the probabilistic information on uncertainty, they produce control and market signals that ensure secure operations and competitive energy trading. In this thesis, we utilize those methods to develop new operational and market policies that enumerate the contributions of various actors to uncertainty and variability control. While guiding energy systems towards secure operations, these policies enable a stochastic market settlement to price energy under uncertainty and variability. To immunize the desired market properties of this settlement against any uncertainty realizations, this thesis develops stochastic approximations to trade cost efficiency for the satisfaction of market properties. To complete stochastic market settlements, we provide market redesign solutions to accommodate private forecasts in energy market clearing and to satisfy individual stochastic preferences of market participants.

This thesis improves conventional data protection practices in energy systems by providing strong privacy guarantees to data owners, thus addressing the ethical challenges in utilizing vast amounts of energy data. These guarantees originate from rendering the standard optimization algorithms as *differentially private* mechanisms – the mechanisms that add a calibrated noise to computations to obfuscate the input optimization datasets when querying optimization results. By calibrating the noise to the privacy preferences of energy system users, these mechanisms encourage information sharing across energy systems without exposing sensitive data attributes, such as energy load patterns. The differentially private optimization mechanisms are designed for distributed and centralized optimization methods and allow for trade-offs between the level of privacy and the utility of noisy optimization outcomes.

Resumé

Moderne energisystemer er midt i en grøn omstilling imod drift baseret på vedvarende energi. I omstillingen findes løftet om en energiforsyning der er emissionsneutral og med lige adgang for alle, hvilket nyder gevaldig opbakning i offentligheden og blandt regeringer. For at lykkes, må de ansvarlige parter tage højde for en række ingeniørfaglige, økonomiske og etiske udfordringer der stammer fra den vedvarende energis usikre natur og udnyttelsen af de vældige datamængder der er krævet for at facilitere omstillingen. Denne afhandling adresserer disse udfordringer ved brug af matematisk stringente metoder til optimering samt beskyttelse af privatlivets fred. Der er en voksende konsensus om at metoderne fra *stokastisk optimering* er afgørende for at muliggøre denne omstilling. Ved at udnytte probabilistisk information om usikkerhed, producerer de kontrol- og markedssignaler der sikrer sikker drift samt konkurrencedygtig handel med energi.

I denne afhandling udnytter vi disse metoder til at udvikle nye operationelle og markeds politikker der opregner forskellige aktørers bidrag til usikkerheds- og variabilitetskонтrol. Imens de styrer energisystemer mod sikker drift, muliggør disse politikker en stokastisk markedsafregning der prissætter energi under hensyntagen til usikkerhed og variabilitet. For at immunisere de ønskede markedsegenskaber af denne afregningsform imod realiseringer af usikkerhed, udvikler denne afhandling stokastiske approksimationer der bytter omkostningseffektivitet for opfyldelse af markedsegenskaber. For at fuldføre stokastisk markedsafregning, foreskriver vi re-design af markedslösninger til at imødekomme private prognoser til energimarkedsafregning og for at tilfredsstille markedsdeltageres individuelle stokastiske præferencer.

Denne afhandling forbedrer konventionelle energisystemsdatabeskyttelsespraktikker ved at sikre dataejerne stærke privatlivsgarantier, og således adressere de etiske udfordringer der ligger i at udnytte store mængder energidata. Disse garantier stammer fra at genge de standard optimeringsalgoritmer som *differentielt private* mekanismer – de mekanismer der tilføjer en kalibreret støj til beregninger for at obfuscere inputoptimeringsdatasæt når der laves forespørgsler på optimeringsresultater. Ved at kalibrere støjen til brugerne af energisystemernes privatlivspræferencer, tilskynder disse mekanismer informationsdeling på tværs af energisystemer uden at eksponere følsomme dataattributter såsom energibelastningsmønstre. De differentielt private optimeringsmekanismer er designede til distribuerede og centraliserede optimeringsmetoder og tillader afvejninger mellem privatlivsniveau og nytteværdi af støjpåvirkede optimeringsresultater.

CHAPTER 1

Introduction

1.1 Context and motivation

Widely popularized environmental policies, such as the European Green Deal and the Green New Deal in the US, facilitate the global transition towards renewable-based and emission-free energy systems. While this transition brings about large shares of stochastic energy producers, deterministic operational and market policies in energy systems are now revisited to ensure energy supply security and fair energy market competition under uncertainty [1]. Since these goals are well formalized in the field of mathematical programming, there is a growing consensus that its sub-field *stochastic optimization* is among the main keys to this green transition.

The advantage of stochastic methods lies in their capacity to securely operate energy systems with an uncertain and variable renewable energy supply. Stochastic methods have the potential to extend conventional market practices to include uncertainty and variability into energy price formation and to design competitive markets for the green transition. However, while stochastic methods are popularized in the academic literature, there is a significant professional mistrust as they fundamentally alter the existing operational and market procedures. To address these professional concerns, there is a considerable effort to make stochastic methods interpretable and facilitate the transition from deterministic to stochastic optimization of energy infrastructures.

To a great extent, the benefits from stochastic energy system optimization are contingent on the availability and quality of optimization datasets. With growing digitization, these datasets become increasingly detailed, and modern hardware contributes to their powerful collection and curation, thus enabling more precise formulations of optimization tasks. For instance, active data exchange contributes to the coordination between transmission and distribution grids [2] or between independent system operators [3]. Energy market competition is facilitated by providing open access to the core operational and market data [4]. Modern distribution grids enable permanent data transfers from consumers to utilities to reduce operating cost and improve grid reliability [5].

As system operators continuously benefit from data availability, the risk of malicious misuse of this data also increases. Combined with side information, such as customer identity and online footprints, demand profiles are used for private and commercial surveillance in distribution grids [6]. Recent advances in statistical inference and inverse optimization provide new tools that expose private information involved in energy market clearing. Together with strategic market participation, the extraction of confidential market bids has shown to damage social welfare in electricity markets substantially [7]. This risk further originates from recent advances in machine learning that recognize repeated dispatch patterns and establish non-parametric dependencies between network loads and dispatch decisions [8]. This way, the load data can be revealed from partial operational information. Online learning algorithms are used to identify the preferences of grid customers, e.g., in demand response programs [9]. As a mathematical construct, these algorithms do not require an explicit declaration of intent, neither customer consent.

When the green energy transition is in urgent need of interpretable stochastic optimization methods to address operational and market challenges, the energy system data required to implement these methods needs an additional privacy-preserving layer to ensure information integrity. Although the methods from stochastic programming and privacy preservation have been historically considered independently in the energy industry, they can be used in combination to meet operational, economic, and privacy goals in energy systems.

1.2 Research directions

The thesis work is organized following two research directions. The first research direction investigates operational and economic aspects of stochastic programming applications to energy system optimization. Starting with control policy design to accommodate uncertainty in energy networks, this direction develops an optimal market design with robust market properties to price energy commodities. The second research direction focuses on preserving information integrity in energy system operations by developing and accommodating robust privacy guarantees in energy system operations using stochastic optimization methods.

1.2.1 Advancing stochastic energy system optimization

As energy system optimization is traditionally a two-stage problem, including planning and real-time stages, it has been addressed using the methods from robust optimization [10], scenario-based and chance-constrained stochastic programming [11]. While stochastic methods promise to guide energy systems under uncertainty efficiently, there is a range of operational and economic obstacles that prevent their real-world implementation. First, energy system operations are governed by non-linear and non-convex physical laws. To produce efficient control policies to guide stochastic system operations, one needs to establish a convex dependency of controllable variables on system uncertainty [12], which requires producing a high-fidelity convex counterpart of the original non-convex problem. Second, as energy markets are closely aligned with system operations, these control policies should provide remunerations and charges for system agents under uncertainty that satisfy fundamental competitive market properties. Last, the ideal competitive control policies are non-discriminatory and satisfy the preferences of all agents in the system. Following this line of arguments, this thesis addresses the following directions to facilitate the transition from deterministic to stochastic energy system optimization.

Developing stochastic control policies and pricing for energy systems. While energy system parameters, such as energy demand and renewable in-feed, are varying and uncertain, energy system operators must account for the system state's stochasticity in operational planning. Ideally, a system operator needs to allocate and optimize control policies to govern active system components in response to uncertainty realizations. For example, under the affine generator response policy proposed in [13], nodal voltages and network flows become representable through uncertain system parameters and generator dispatch decisions. Using a chance-constrained optimization of those policies, a system operator accommodates system uncertainty in a feasible manner and with security guarantees. Recent work in [14] also finds that these policies can be optimized to guarantee minimal variability of the network state. However, to enable performance guarantees, one needs to establish a convex dependency of the system state on uncertain parameters [12], which is not always the case for non-convex physics of energy systems. This can be overcome, for

instance, through convex relaxations of energy network equations. Although relaxations can be very tight, the analysis in [15] shows that even a marginal relaxation gap disables performance guarantees. Alternatively, one may explore the linearization of non-convex equations to obtain linear sensitivities of system variables to uncertain parameters [16].

The optimized stochastic control policies have a strong potential to produce financial remunerations, because they explicitly define the contribution of each system component to uncertainty and variability control. This property of stochastic policies has been recognized in [17], where the prices for stochastic power delivery, uncertainty and variability control are obtained through the dual solution of the chance-constrained policy optimization problem. These prices are shown to internalize the feasibility and variability requirements imposed by a system operator, while exploiting the moments of underlying uncertainty distribution and its ambiguity. Following this line of work, it is relevant to explore an explicit payment scheme to remunerate active system components, such as flexible gas suppliers or compressors in gas systems, and to charge those system elements that induce uncertainty, such as wind power producers in power networks. To ensure the efficiency of this market settlement, the theoretical market properties of cost recovery and revenue adequacy¹ must be investigated. Since the chance-constrained solution is often obtained through convex approximations, the dependency of these market properties on approximation errors must also be established.

Preserving fundamental market properties in stochastic energy system optimization. The fundamental market properties in the stochastic energy system optimization pertain to the underlying optimization criterion. If the stochastic energy dispatch is optimized under the minimum expected cost criterion, the associated cost recovery and revenue adequacy properties hold only in expectation, and their per-scenario satisfaction is not guaranteed [18]. This is because stochastic programs tend to violate the merit-based energy procurement² to satisfy some expected scenario of uncertainty realization. Although a stochastic solution is more efficient than the deterministic one in terms of operational cost, the violation of the fundamental market properties prevents its practical implementation. To preserve the market properties' satisfaction irrespective of uncertainty realizations, energy operations and pricing are still guided by deterministic dispatch solutions.

The problem of providing stochastic dispatch efficiency while satisfying market properties for all uncertainty realizations boils down to approximating stochastic solutions within deterministic procedures. The work in [19] develops a new planning-stage optimization according to which stochastic energy suppliers are dispatched to a value different from the mean forecast, which has shown to reduce the expected system cost significantly. This, however, requires altering the submitted price-quantity pairs of stochastic producers, thus violating existing market codes. Alternatively, the stochastic dispatch efficiency has been attained within deterministic settlements by designing new market products, e.g., flexiramps introduced to develop ramping capabilities of Californian power system [20]. By procuring ramping capacity up to prescribed needs, this procedure resembles the stochastic dispatch, which inherently finds the optimal allocation of flexible resources between energy and ramping services. Similarly, several US system operators

¹The cost recovery property ensures that the payment to each system component is greater than or equal to its operating cost, while the revenue adequacy property ensures that the total charges of energy consumers is greater than or equal to the total payments to energy providers.

²Energy procurement strategy where cheap energy suppliers are dispatched first followed by more expensive suppliers.

have introduced an operating reserve demand curve mechanism, which adjusts electricity prices to reflect the scarcity value of reserves and to incentivize the arbitrage between energy and reserve markets [21]. A system operator approximates the cost-optimal energy and reserve allocations provided by the stochastic dispatch procedure through a proper price calibration. In one way or another, the solutions proposed by [19]-[21] require market interventions or changes in market codes to attain the desired result. Thus, it is relevant to investigate the approximation of the stochastic efficiency within existing dispatch procedures.

Addressing information inconsistency in energy systems under uncertainty. Since the work of Samuelson in [22], it has been established that the optimal solution of a centralized optimization problem is a solution to a competitive equilibrium problem. That is, the primal and dual solutions of a centralized optimization problem constitute a solution to a competitive economy, where agents compete based on their preferences (merits) without any external interventions. Therefore, to analyze the centralized dispatch efficiency, its solution is often benchmarked against an equilibrium solution, see, for example, [23, Chapter 2]. If the two solutions match, the market organization based on a centralized optimization problem is said to be complete. Otherwise, a centralized market organization is incomplete as it does not satisfy the underlying agent preferences. Consequently, incomplete markets risk producing incorrect price signals in energy systems.

When solving stochastic energy dispatch and market-clearing problems, it is often assumed in the technical literature that a centralized organization is complete and the information on the underlying uncertainty is consistent among system agents. While this assumption is convenient from the modeling standpoint, there is often no postulate that it holds, and the problem of information asymmetry has not been fully addressed in the literature. Aside from natural causes of information asymmetry, e.g., forecasts are sourced from different providers, information asymmetry occurs even when agents have full access to data, but they utilize it differently. For example, a risk attitude directly affects the construction of uncertainty and scenario sets in local optimizations of market participants [24],[25]. Disregarding a risk attitude, the scenario construction is affected by irrational preferences, captured by prospect theory [26]: agents acting on the same set of plausible uncertainty scenarios tend to favor some scenarios over others, depending on their subjective beliefs about scenario likelihood. It is thus relevant to analyze the impacts of such information asymmetry and to investigate whether it can be internalized in a centralized market organization.

1.2.2 Providing privacy guarantees in power system optimization

To formally guarantee privacy for energy optimization data, it is imperative to rely on a robust privacy definition. *Differential privacy* is such a definition [27] originated in the analysis of large datasets with sensitive data items, e.g., private health, insurance, and bank records. The goal of differential privacy research is to provide a formal promise that individual records in a dataset remain private, undisclosed when this dataset is used in computations. Differential privacy guarantees are attained through randomization of the computation of interest, e.g., by adding a calibrated random noise to the results of a computation, as shown in Figure 1.1. The virtue of a differentially private computation is to produce statistically similar results on datasets different in one item (hence, *differential*), i.e., irrespective of the presence of any individual record in a dataset, thus establishing individual privacy guarantees.

As power systems enjoy a drastic increase in available data, differential private optimization algorithms would provide power system users with a formal promise that their private data

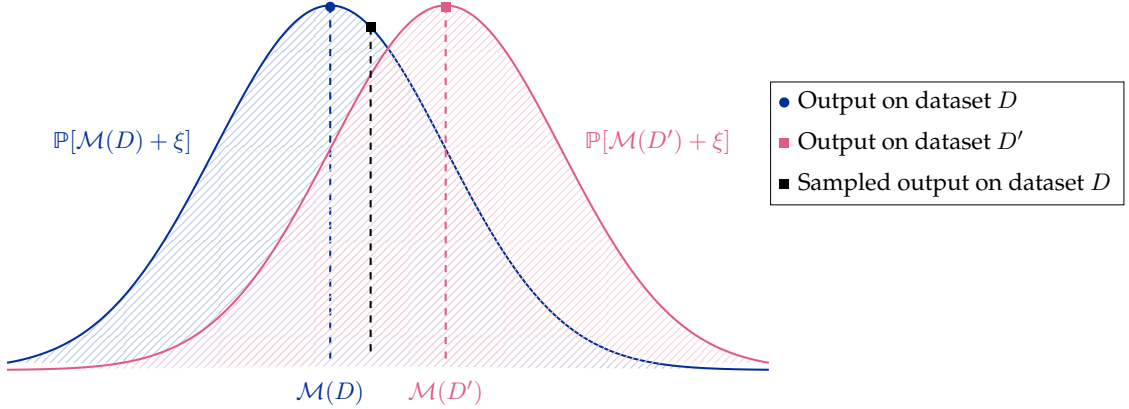


Figure 1.1: Illustration of the differential privacy principle: $\mathcal{M} : \mathbb{R}^n \mapsto \mathbb{R}$ is a mechanism (mapping) of interest, $D, D' \in \mathbb{R}^n$ are two datasets different in one item, and ξ is a zero-mean random noise. By augmenting the output of \mathcal{M} with the random noise ξ , the outputs on two different datasets D and D' are made statistically similar. By observing a sample from the output distribution, an observer cannot identify which dataset (thus, the difference in one item) is used in computations.

will not be exposed, thus facilitating the user engagement. As privacy guarantees arise from the randomization of the underlying optimization task, the application of differential privacy to power systems requires addressing many challenges. In this thesis, these challenges are organized into three categories. The first category focuses on providing formal privacy guarantees for optimization data by internalizing private algorithms within power system computational problems. The second category concerns resolving the risks of producing infeasible private outcomes and develops robust feasibility guarantees for private power system optimization algorithms. The third category is motivated by the utility loss associated with noisy private algorithms and develops the means to control the optimization utility.

Providing privacy guarantees to power system computations. Any power system optimization problem can be formalized as a mechanism that maps datasets to the output(s) of interest, e.g., an optimization solution or some of its statistics. Differentially private guarantees for this mechanism can be attained by means of randomization using the standard input and output *perturbation strategies*. The input perturbation strategy implies the addition of random noise to the input dataset [28], which has been applied in the power system context for a private release of high-fidelity network test cases [29] and a private release of aggregated dispatch statistics [30]. The output perturbation ensures privacy by adding a calibrated noise to optimization results and has been explored in the context of the private distributed electrical vehicle charging problem [31]. As input and output perturbation strategies are agnostic to many operational aspects of power systems, e.g., operational feasibility, their application to operational tasks is limited. This necessitates to develop an alternative mechanism perturbation strategy that does not alter the input datasets nor perturb optimization solution, but internalizes the noise within computations.

The central challenge of differentially private optimization is noise calibration. To a great extent, the noise calibration depends on the chosen noise distribution, e.g., Laplace or Gaussian distribution commonly used in private statistical analysis, key differential privacy parameters such as privacy loss, and the sensitivity of the optimization solution to the input datasets [32]. If the noise distribution and privacy loss are exogenous inputs, the mechanism sensitivity is an inherent

property of an optimization problem of interest. As constrained optimization problems commonly address power system optimization tasks, obtaining the exact sensitivity is only available for simple, symmetric feasible regions [33]. To establish privacy guarantees for non-trivial constrained optimization problems, it is imperative to provide at least an upper bound on mechanism sensitivity.

Some optimization problems in power systems are solved in a distributed manner, when optimization datasets are distributed among sub-problems that perform local computations and only exchange certain coordinating signals [34]. Although distributed algorithms are often regarded as privacy-preserving, they do not establish any formal guarantee that the exchange of coordination signals does not leak local datasets. By calibrating the noise to the sensitivity of algorithms' sub-problems to local datasets, the distributed algorithms can be made formally private by augmenting the noise into local computations. Since not all optimization problems in energy are decomposable and due to institutional reasons, many operational problems are solved centrally by system operators. It is thus not less relevant to offer privacy guarantees for centralized computations. Moreover, the privacy guarantees in centralized computations are known to be stronger than those offered by locally private computations [27].

Ensuring feasibility of differentially private optimization outcomes. As differential privacy guarantees originate from randomization, differentially private constrained optimization cannot be ignorant of infeasibility issues. The input perturbation strategy, for example, does not guarantee that the perturbed input dataset admits a feasible solution. Even if the solution space is non-empty, the differentially private solution can still be infeasible for the original optimization dataset. The output perturbation strategy is also ignorant of optimization constraints, thus involving similar infeasibility risks. Although these infeasibility issues can be addressed with post-processing [35], feasibility restoration for operational problems requires using original private data, thus involving privacy losses. This necessitates a mechanism perturbation strategy that internalizes the feasibility criteria within private computations of optimization tasks.

Utility-aware private optimization. While providing privacy guarantees for optimization datasets, it is important to characterize and control the loss of optimization utility due to random perturbations. In the context of power systems, the optimization utility is often translated into solution optimality. The pursuit of optimality brings the benefits of improved operations [36] and market efficiency [37]. When adding noise to power system computations, however, these benefits diminish with increasing privacy requirements. Moreover, noise additive private algorithms risk producing significant variations of private optimization results, which poses additional operational challenges in the power system domain. It has been recognized in [14] that the random fluctuations in the network, e.g., random wind power in-feed, lead to highly variable network power flows, voltage profiles, etc. It is thus not less relevant to develop privacy-preserving strategies that produce randomized private results with controllable variance.

Although the optimization utility can be improved by relaxing noise parameters, this would involve weaker privacy guarantees: one of the fundamental results in data privacy argues that it is not possible to improve task utility without incurring additional privacy loss [38]. While the average optimization utility cannot be improved for prescribed privacy parameters, it appears relevant to develop private algorithms that enable a trade-off between the average and the worst-case utility *without* altering privacy guarantees. Using stochastic programming methods, this would imply for power system operational tasks that the worst-case realization of the additional operating cost can

be reduced at the expense of an increasing expected value. Similarly, the accumulated variance of private optimization results can be reduced at the expense of increasing operating costs.

1.3 Scientific contributions

The thesis first contributes by advancing stochastic programming applications to energy system optimization through [Paper A]–[Paper C]. Starting with stochastic natural gas system operations under uncertainty of gas extractions, [Paper A] develops stochastic control policies for flexible gas injections, compressors and valves, that ensure real-time feasibility of operations. The non-linear and non-convex gas system operations are approximated through a convex counterpart, which paves the foundation for a chance-constrained optimization of those policies. The optimized policies quantify active system components' contribution to system state uncertainty and variability, thus enabling competitive financial remunerations for system components. Their competitive market properties, i.e., the cost recovery and revenue adequacy, are conditioned to system design and shown to hold in expectation.

As market properties of cost recovery and revenue adequacy in stochastic systems are commonly satisfied only in expectation, [Paper B] develops a mechanism that compromises stochastic solution efficiency in terms of operational cost, but ensures the satisfaction of market properties for any uncertainty realization. Unlike standard stochastic programs, the mechanism does not alter conventional deterministic procedures, but identifies the optimal reserve margins that approximate the stochastic solution efficiency. It was shown in [Paper B] that in the context of sequential reserve-energy power system dispatch, this mechanism attains the maximum expected cost efficiency of conventional dispatch procedures given the need to satisfy market properties.

This work line concludes with analyzing stochastic energy systems under asymmetry of information on the underlying uncertainty source. [Paper C] contributes by analyzing energy prices as a function of agent private forecasts and shows high sensitivities of market outcomes to private information. From the information standpoint, the models developed in [Paper C] identify a significant gap between stochastic solutions in complete and incomplete markets. However, this gap is shown to reduce through information sharing and market redesign solutions that accommodate private forecasts in the existing energy system procedures.

This thesis is among the first to recognize the privacy risks involved in the optimization of power system operational tasks. The next contribution of this thesis is to resolve these privacy risks by developing a systematic approach to provide the routine power system computations with a privacy-preserving layer and rigorous privacy guarantees. The main privacy-related contributions of this thesis are based on publications [Paper D] - [Paper F].

This line of work first identifies privacy breaches in centralized and distributed power system computations by designing adversarial models that infer optimization datasets from optimization results. The models are suitable for the omniscient privacy adversaries with almost full knowledge of the optimization task of interest as in [Paper D] and for weaker adversaries with partial knowledge of the system as in [Paper D] and [Paper F]. These adversarial models play a seminal role in formulating achievable privacy goals and dispelling the common belief about the privacy-preserving power of conventional distributed optimization algorithms in power systems.

This thesis is the first work to provide formal privacy guarantees for operational power system tasks based on differential privacy. These guarantees are provided for distributed computation

with several private distributed algorithms in [Paper D] and for centralized computations in [Paper E] and [Paper F]. Both distributed and centralized private computation algorithms have been successfully applied to the standard set of power system test cases.

To provide both privacy guarantees for optimization datasets and feasibility guarantees for private optimization outcomes, the thesis develops centralized private optimization algorithms at the interface of differential privacy and stochastic optimization methods. To enable privacy guarantees, an optimization outcome of interest is made dependent on a carefully calibrated random perturbation, which in turn allows for a chance-constrained problem formulation with feasibility guarantees. Moreover, to enable a trade-off between the average and worst-case optimization utility, e.g., optimality loss or solution variance, the variance and conditional value-at-risk measures are internalized into the chance-constrained formulation to enable optimization utility control. This theory is mainly established in [Paper E], while the application to distribution grid operations is provided in [Paper F].

1.4 Thesis outline

The thesis provides a brief summary of the attached six papers.

Chapter 2 presents the contributions towards interpretability of stochastic programming applications to energy systems. In the 1st part, the chapter introduces stochastic optimization methods to solve operational problems in energy systems under uncertainty and discusses the properties of the corresponding stochastic market settlement. The remainder guides the reader through the main results of [Paper A]–[Paper C]. The 2nd part presents the chance-constrained stochastic control policies and pricing scheme for energy networks. The 3rd part is devoted to the method of approximating the stochastic cost efficiency within deterministic market settlements. The 4th and last part revisits the properties of the stochastic market settlement under asymmetry of information and provides market redesign solutions to accommodate agents' private uncertainty forecasts.

Chapter 3 presents thesis contributions to privacy-preserving energy system optimization according to [Paper D]–[Paper F]. The 1st part of this chapter introduces the OPF optimization problem and its centralized and distributed computations, while the 2nd part explores the inherent privacy leakages in these computations. The 3rd part reviews the main differential privacy definitions and results that are used in the proposed distributed and centralized privacy-preserving OPF algorithms, presented respectively in the 4th and 5th parts.

Chapter 4 summarizes the main results and outlines perspective directions for future research.

Notation: Operation \circ is the element-wise product. Operator $\text{diag}[x]$ returns an $n \times n$ diagonal matrix with elements of vector $x \in \mathbb{R}^n$. When not clear from the context, for a $n \times n$ matrix A , $[A]_i$ returns an i^{th} row ($1 \times n$) of matrix A , $\langle A \rangle_i$ returns an i^{th} column ($n \times 1$) of matrix A . Operator $\text{Tr}[A]$ returns the trace of matrix A . Symbol $^\top$ stands for transposition, vector 1 ($\mathbb{1}$) is a vector of ones (zeros), and $\|\cdot\|_p$ denotes a p -norm. The notation is coherent with the attached papers, but we recommend to familiarize with the notation of each paper before reading.

1.5 List of publications

The publications at the core of this thesis are listed as follows:

- [**Paper A**] V. Dvorkin, A. Ratha, P. Pinson. and J. Kazempour. "Stochastic control and pricing for natural gas networks." *Submitted to the IEEE Transactions on Control of Network Systems*, 2020.
- [**Paper B**] V. Dvorkin, S. Delikaraoglou and J. M. Morales. "Setting reserve requirements to approximate the efficiency of the stochastic dispatch." in *IEEE Transactions on Power Systems*, vol. 34, no. 2, pp. 1524-1536, 2019.
- [**Paper C**] V. Dvorkin, J. Kazempour and P. Pinson. "Electricity market equilibrium under information asymmetry." in *Operations Research Letters*, vol. 47, no. 6, pp. 521-526, 2019.
- [**Paper D**] V. Dvorkin, P. Van Hentenryck, J. Kazempour and P. Pinson. "Differentially private distributed optimal power flow." in *59th Conference on Decision and Control*, to appear, 2020.
- [**Paper E**] V. Dvorkin, F. Fioretto, P. Van Hentenryck, P. Pinson and J. Kazempour. "Differentially private convex optimization with feasibility guarantees," *Preprint (Marginally rejected at the 2020 Conference on Neural Information Processing Systems: Scores 6/6/5/5.)*, 2020.
- [**Paper F**] V. Dvorkin, F. Fioretto, P. Van Hentenryck, P. Pinson and J. Kazempour. "Differentially private optimal power flow for distribution grids." in *IEEE Transactions on Power Systems*, to appear, 2020, DOI: [10.1109/TPWRS.2020.3031314](https://doi.org/10.1109/TPWRS.2020.3031314).

The following publications have been prepared over the course of Ph.D. studies, but not included in this thesis:

- [**Paper G**] V. Dvorkin, J. Kazempour and P. Pinson. "Chance-constrained equilibrium in electricity markets with asymmetric forecasts." in *16th International Conference on Probabilistic Methods Applied to Power Systems*, pp. 1-6, 2020.
- [**Paper H**] A. M. Radoszynski, V. Dvorkin and P. Pinson. "Accommodating bounded rationality in pricing demand response." in *2019 IEEE Milan PowerTech Conference*, pp. 1-6, 2019.
- [**Paper I**] V. Dvorkin, J. Kazempour, L. Baringo and P. Pinson. "A consensus-ADMM approach for strategic generation investment in electricity markets." in *57th Conference on Decision and Control*, pp. 780-785, 2018.

CHAPTER 2

Stochastic Optimization of Energy Systems

This chapter presents the contributions of this thesis to the interpretability of stochastic programming applications to energy systems. We start by formulating a reference energy optimization problem in Section 2.1 and we discuss how stochastic methods solve it under uncertainty. We further provide general results on the fundamental properties of the resulting stochastic market settlement. The rest of the narrative guides the reader through the main results of [Paper A]–[Paper C] using this reference problem. In Section 2.2, we introduce stochastic control policies for energy system optimization whose objective is two-fold: to quantify the contribution of each system component to the accommodation of uncertainty and variability, and to provide an efficient energy pricing under uncertainty and variability. Although the optimized policies yield the minimum expected cost, we find that they ensure fundamental market properties (e.g., cost recovery) only in expectation, hence limiting their practical applications. To address this issue, in Section 2.3, we explain how to approximate the efficiency of stochastic solutions within deterministic market procedures that ensure the desirable market properties for any realizations of uncertainty. Finally, in Section 2.4, we discuss market completeness from the information standpoint, i.e., the ability of stochastic market settlements to satisfy the objectives of market participants given their private information on uncertainty. To complete the market and guarantee desirable market properties under information asymmetry, we explore market redesign solutions.

2.1 Stochastic energy system optimization

We begin by considering the operations of an energy network guided by the solution of the following deterministic program:

$$\min_{\vartheta, \varphi} \quad c(\vartheta) \tag{2.1a}$$

$$\text{s.t.} \quad A\varphi = \vartheta - \delta, \quad F(\vartheta, \varphi) = 0, \tag{2.1b}$$

$$\underline{\vartheta} \leq \vartheta \leq \bar{\vartheta}, \quad \underline{\varphi} \leq \varphi \leq \bar{\varphi}, \tag{2.1c}$$

in control variables $\vartheta \in \mathbb{R}^n$ and in state variables $\varphi \in \mathbb{R}^m$. The objective function (2.1a) computes the operating costs using a convex function $c : \mathbb{R}^n \mapsto \mathbb{R}$ associated with the deployment of controllable actions. Equality constraints (2.1b) guide the system operations according to the underlying physical laws. The first equation in (2.1b) is the energy conservation law that balances control and state variables with network loads $\delta \in \mathbb{R}^n$, where $A \in \mathbb{R}^{n \times m}$ is a weighted incidence matrix that describes a system topology and encodes specific network parameters. The second entry in (2.1b) is the non-convex equation that relates control and state variables according to underlying physical laws. In the power system context, $F : \mathbb{R}^{n+m} \mapsto \mathbb{R}^m$ relates network flows,

losses and voltages to active and reactive generator set-points according to the AC power flow equations [39]. In natural gas networks, F is the Weymouth equation that conditions network flows on non-linear pressure drops [40]. Inequality constraints in (2.1c) require control and state variables to be within network limits $\underline{\vartheta}, \bar{\vartheta} \in \mathbb{R}^n$ and $\underline{\varphi}, \bar{\varphi} \in \mathbb{R}^m$.

2.1.1 Convex counterpart of non-convex optimization

Although problem (2.1) is non-convex, it has been successfully solved using many techniques, e.g., using convex relaxations in power systems [41] and natural gas networks [42]. However, as parameters become uncertain, the stochastic counterpart of (2.1) becomes computationally intractable, while convex relaxations risk to yield unsatisfactory relaxation gaps [15]. To overcome this difficulty, consider a linearization of the non-convex equation in (2.1b) around a stationary point $(\dot{\vartheta}, \dot{\varphi})$, retrieved by solving problem (2.1) to stationarity, such that $F(\vartheta, \varphi) = 0$ at the stationary point becomes

$$\underbrace{\nabla_{\vartheta} F(\dot{\vartheta}, \dot{\varphi})}_{F_{\vartheta}} \vartheta + \underbrace{\nabla_{\varphi} F(\dot{\vartheta}, \dot{\varphi})}_{F_{\varphi}} \varphi + \underbrace{F_0(\dot{\vartheta}, \dot{\varphi})}_{F_0} = 0, \quad (2.2)$$

where $F_{\vartheta} \in \mathbb{R}^{m \times n}$ and $F_{\varphi} \in \mathbb{R}^{m \times m}$ are the gradients of the non-linear equation with respect to optimization variables and $F_0 \in \mathbb{R}^m$ is a free term. Unless $(\dot{\vartheta}, \dot{\varphi})$ is a bifurcation point, the gradients are well-defined. Consider the following convex counterpart of problem (2.1):

$$\min_{\vartheta, \varphi} c(\vartheta) \quad (2.3a)$$

$$\text{s.t. } A\varphi = \vartheta - \delta, \quad (2.3b)$$

$$F_{\vartheta}\vartheta + F_{\varphi}\varphi + F_0 = 0, \quad (2.3c)$$

$$\underline{\vartheta} \leq \vartheta \leq \bar{\vartheta}, \quad \underline{\varphi} \leq \varphi \leq \bar{\varphi}. \quad (2.3d)$$

The key property of problem (2.3) is that its Karush-Kuhn-Tucker (KKT) optimality conditions are equivalent to the KKT conditions of problem (2.1) at the stationary point, and thus (2.3) solves (2.1) at this point. However, this linearization procedure may produce a rank-deficit system of equations (2.3c), and for the fixed control variables, there may be infinitely many solutions to state variables. This issue can be resolved by fixing one of the state variables to a reference value, as discussed in [Paper A].

2.1.2 From infinite- to finite-dimensional stochastic programming

Operations of energy systems are subject to the uncertainty of system parameters. System design parameters, such as a cost function, network topology and technical limits, remain constant in the short run, while energy demand δ is uncertain. Since control decisions must be made before uncertainty realizes, it makes sense to consider uncertain demand as a random variable $\tilde{\delta}(\xi) = \delta + \xi$, where $\delta \in \mathbb{R}^n$ is the nominal (mean) component and $\xi \in \mathbb{R}^n$ is a vector of random forecast errors. Throughout the chapter, we assume that probability distribution \mathbb{P}_{ξ} and covariance $\Sigma \in \mathbb{R}^{n \times n}$ of the random vector are known, and that \mathbb{P}_{ξ} is centered at 0, which is not restrictive when demand realizations are repetitive, such that the distribution can be estimated from a sufficiently large amount of historical observations. To optimize system operations in this situation, consider the following stochastic program:

$$\min_{\tilde{\vartheta}(\xi), \tilde{\varphi}(\xi)} \mathbb{E}_{\mathbb{P}_{\xi}} [c(\tilde{\vartheta}(\xi))] \quad (2.4a)$$

$$\text{s.t. } A\tilde{\varphi}(\xi) = \tilde{\vartheta}(\xi) - \tilde{\delta}(\xi), \quad (2.4b)$$

$$F_\vartheta\tilde{\vartheta}(\xi) + F_\varphi\tilde{\varphi}(\xi) + F_0 = 0, \quad (2.4c)$$

$$\underline{\vartheta} \leq \tilde{\vartheta}(\xi) \leq \bar{\vartheta}, \quad \underline{\varphi} \leq \tilde{\varphi}(\xi) \leq \bar{\varphi}, \quad \xi \sim \mathbb{P}_\xi, \quad (2.4d)$$

whose objective function is to minimize the expected value of operating costs with respect to probability distribution \mathbb{P}_ξ , and whose optimization variables are random. Unfortunately, problem (2.4) is *infinite-dimensional* since it optimizes over infinite-dimensional variables, and thus it is computationally intractable. To cope with this difficulty, each variable can be seen as a two-stage decision, i.e.,

$$\tilde{\vartheta}(\xi) = \vartheta_1 + \vartheta_2(\xi), \quad \tilde{\varphi}(\xi) = \varphi_1 + \varphi_2(\xi), \quad (2.5)$$

where ϑ_1 and φ_1 are the first-stage decisions independent from uncertainty realizations, and $\vartheta_2(\xi)$ and $\varphi_2(\xi)$ are variable recourse decisions dependent on uncertainty realizations. Computationally tractable counterparts of problem (2.4) are obtained by limiting recourse decisions to finite-dimensional functions using different methods from stochastic programming. In the following, we consider two methods: scenario-based and chance-constrained programming.

Scenario-based stochastic programming. By sampling a finite number of forecast error realizations from \mathbb{P}_ξ , i.e., S scenarios $\hat{\xi}_1, \dots, \hat{\xi}_S$ with probabilities $\pi \in \mathbb{R}_+^S$, such that $\pi_1 + \dots + \pi_S = 1$, the solution to the infinite-dimensional program (2.4) can be approximated through the first-stage decisions ϑ_1, φ_1 and a finite number of recourse decisions, $\vartheta_{21}, \dots, \vartheta_{2S}$ and $\varphi_{21}, \dots, \varphi_{2S}$, optimized using the following finite-dimensional program:

$$\min_{\vartheta_1, \vartheta_2, \varphi_1, \varphi_2} \sum_{s=1}^S \pi_s c(\vartheta_1 + \vartheta_{2s}) \quad (2.6a)$$

$$\text{s.t. } A(\varphi_1 + \varphi_{2s}) = \vartheta_1 + \vartheta_{2s} - \delta - \hat{\xi}_s, \quad (2.6b)$$

$$F_\vartheta(\vartheta_1 + \vartheta_{2s}) + F_\varphi(\varphi_1 + \varphi_{2s}) + F_0 = 0, \quad (2.6c)$$

$$\underline{\vartheta} \leq \vartheta_1 + \vartheta_{2s} \leq \bar{\vartheta}, \quad \underline{\varphi} \leq \varphi_1 + \varphi_{2s} \leq \bar{\varphi}, \quad \forall s = \{1, \dots, S\}, \quad (2.6d)$$

$$\vartheta_1 \in \mathbb{R}^n, \vartheta_2 \in \mathbb{R}^{n \times S}, \varphi_1 \in \mathbb{R}^m, \varphi_2 \in \mathbb{R}^{m \times S}, \quad (2.6e)$$

where (2.6a) is the scenario-based approximation of the expected value and where network equations and limits are enforced through (2.6b)–(2.6d) for each prescribed uncertainty realization. In this formulation, recourse variables are modeled explicitly for each uncertainty realization scenario. With an increasing number of scenarios from \mathbb{P}_ξ , by the Law of Large Numbers, the solution of problem (2.6) will converge to the optimal solution to problem (2.4).

Chance-constrained stochastic programming. Another computationally tractable version of problem (2.4) can be obtained by restricting recourse decisions to affine functions of forecast errors. Consider an explicit parameterization of control variables on a random forecast error of the form

$$\tilde{\vartheta}(\xi) = \vartheta_1 + \vartheta_2(\xi) = \vartheta_1 + \alpha\xi, \quad (2.7)$$

where $\vartheta_1 \in \mathbb{R}^n$ is the first-stage decision as prescribed before, and $\alpha \in \mathbb{R}^{n \times n}$ is a finite-dimensional variable recourse decision. To be consistent with the original proposal [43], we term (2.7) a *control policy*, because it produces control inputs to each network component, such as a generator in power systems or a gas supplier in natural gas networks, with respect to any realization of the random

variable $\xi \in \mathbb{R}^n$. This explicit dependency for the state variables is not enforced because they are not controllable from the system operator's perspective. However, they can be expressed as affine functions of random forecast errors through control recourse decisions, i.e., from (2.4c) we have

$$\begin{aligned}\tilde{\varphi}(\xi) &= -F_\vartheta^{-1}(F_0 + F_\vartheta\tilde{\vartheta}(\xi)) \\ \xrightarrow{\text{from (2.7)}} \tilde{\varphi}(\xi) &= -F_\vartheta^{-1}(F_0 + F_\vartheta(\vartheta_1 + \alpha\xi)) \\ \xrightarrow{\text{from (2.3c)}} \tilde{\varphi}(\xi) &= \varphi_1 - F_\vartheta^{-1}F_\vartheta\alpha\xi,\end{aligned}\tag{2.8}$$

where φ_1 is the first-stage decision as prescribed before, and the last term is the state variable recourse defined through recourse variable α and the random forecast errors ξ .

Since recourse decision α is a finite-dimensional optimization variable, random variables $\tilde{\vartheta}(\xi)$ and $\tilde{\varphi}(\xi)$ become finite-dimensional, thus enabling a computationally efficient reformulation of problem (2.4). Specifically, a control policy (2.7) enables the satisfaction of stochastic network equations (2.4b) and (2.4c) for any realization of random forecast errors when properly constraining the variable recourse. In [Paper A] we show that when requiring recourse decisions to obey $\alpha^\top \mathbf{1} = 1$, the system of stochastic equations (2.4b) and (2.4c) is equivalent to

$$A\varphi_1 = \vartheta_1 - \delta, \quad \alpha^\top \mathbf{1} = 1, \tag{2.9a}$$

$$F_\vartheta\vartheta_1 + F_\vartheta\varphi_1 + F_0 = 0. \tag{2.9b}$$

Furthermore, under control policy (2.7), the expected cost in (2.4a) is reformulated analytically using the covariance $\Sigma \in \mathbb{R}^{n \times n}$ of forecast errors. Assume a quadratic cost function with the first- and second-order coefficients $c_1 \in \mathbb{R}^n$ and $c_2 \in \mathbb{R}^n$, respectively. The expected cost thus admits the following closed-form solution:

$$\begin{aligned}\mathbb{E}_{\mathbb{P}_\xi}[c(\tilde{\vartheta}(\xi))] &= \mathbb{E}_{\mathbb{P}_\xi}[c_1^\top(\vartheta_1 + \alpha\xi) + (\vartheta_1 + \alpha\xi)^\top \text{diag}[c_2](\vartheta_1 + \alpha\xi)] \\ \xrightarrow{\mathbb{E}_{\mathbb{P}_\xi}[\xi]=0} \mathbb{E}_{\mathbb{P}_\xi}[c(\tilde{\vartheta}(\xi))] &= c_1^\top \vartheta_1 + \mathbb{E}_{\mathbb{P}_\xi}[(\vartheta_1 + \alpha\xi)^\top \text{diag}[c_2](\vartheta_1 + \alpha\xi)] \\ \xrightarrow{\mathbb{E}_{\mathbb{P}_\xi}[\xi\xi^\top]=\Sigma} \mathbb{E}_{\mathbb{P}_\xi}[c(\tilde{\vartheta}(\xi))] &= c_1^\top \vartheta_1 + \vartheta_1^\top \text{diag}[c_2]\vartheta_1 + \text{Tr}[\alpha^\top \text{diag}[c_2]\alpha\Sigma],\end{aligned}\tag{2.10}$$

which is convex in optimization variables ϑ_1 and α . For linear costs, the last two terms in (2.10) are disregarded and the expected cost amounts to the cost of the first-stage control decisions only.

With these results at hand, the chance-constrained counterpart of stochastic program (2.4) is

$$\min_{\vartheta_1, \varphi_1, \alpha} \quad c_1^\top \vartheta_1 + \vartheta_1^\top \text{diag}[c_2]\vartheta_1 + \text{Tr}[\alpha^\top \text{diag}[c_2]\alpha\Sigma] \tag{2.11a}$$

$$\text{s.t.} \quad A\varphi_1 = \vartheta_1 - \delta, \quad \alpha^\top \mathbf{1} = 1, \tag{2.11b}$$

$$F_\vartheta\vartheta_1 + F_\vartheta\varphi_1 + F_0 = 0, \tag{2.11c}$$

$$\mathbb{P}_\xi \left[\begin{array}{l} \underline{\vartheta} \leq \vartheta_1 + \alpha\xi \leq \bar{\vartheta}, \\ \underline{\varphi} \leq \varphi_1 - F_\vartheta^{-1}F_\vartheta\alpha\xi \leq \bar{\varphi}, \end{array} \right] \geq 1 - \varepsilon, \tag{2.11d}$$

where the last constraint (2.11d) is the joint chance constraint that requires network limit satisfaction with a prescribed probability $1 - \varepsilon$, and ε is a typically small constraint violation probability. This constraint can be reformulated into a set of linear constraints by enforcing all its entries on a finite number of samples from \mathbb{P}_ξ [44]. This sample-based reformulation provides a joint constraint satisfaction guarantee by extracting sufficiently many samples up to the prescribed parameter

ε . An alternative approach to (2.11d) is to represent it through the union of individual chance constraints [45]. Since entries of (2.11d) are convex with respect to random forecast errors, the individual chance constraints admit analytical second-order cone reformulations [12], allowing for a computationally efficient substitute of (2.11d).

Discussion. Both scenario-based and chance-constrained programming can be used to approximate the solution of stochastic problem (2.4): in **[Paper A]** we use a chance-constrained formulation of the natural gas network control problem under uncertainty, while **[Paper B]** and **[Paper C]** consider scenario-based stochastic electricity market problem formulations. However, the consequences of their applications differ from various modeling perspectives.

First, problem (2.6) ensures solution feasibility for all uncertainty realizations within the prescribed set of scenarios, but it does not provide any out-of-sample feasibility guarantee. The chance-constrained formulation (2.11), instead, provides formal a priori guarantees that policy (2.7) provides feasible real-time control actions in $(1 - \varepsilon)\%$ scenarios of uncertainty realization.

Furthermore, the recourse in chance-constrained formulation (2.11) is an explicit function of the random and control variables. This has significant operational implications because control variables can be optimized anticipating their impact on the system state (e.g., on the system state variability) – a control opportunity which is not explicitly offered by the scenario-based program (2.6). Moreover, the optimization of the affine recourse enables explicit quantification of control variable contributions to maintaining secure system operations under uncertainty and minimizing the variability of network parameters.

Despite these benefits of chance-constrained programs over scenario-based programs, a computationally tractable reformulations of expected costs (2.11a) and chance constraint (2.11d) are enabled due to affine dependency of recourse decisions on random forecast errors. This affine recourse is optimal only in a few real-world applications, i.e., proportional generator response to frequency deviations in power systems. Whenever affine recourse is sub-optimal in an engineering system of interest, the scenario-based problem formulation in (2.6), which does not enforce this affine relation, provides a less conservative solution in terms of expected costs.

2.1.3 Stochastic market properties

Using either scenario-based or chance-constrained approximations of stochastic program (2.4), it is possible to internalize operational uncertainty into energy market clearing and derive meaningful energy prices [18, 37]. Here, we briefly review the fundamental market properties of such pricing, including efficiency, cost recovery, and revenue adequacy [46]. The efficiency property implies that the primal and dual solutions to problem (2.4) result in minimum operational cost and competitive profits for market agents, e.g., power or gas producers. This property is attained with truthful market participation, i.e., the so-called incentive compatibility property [47]. The cost recovery implies that the cost incurred by each control action is compensated for through sufficient demand charges. Finally, the revenue adequacy property holds when the total demand charges suffice to compensate energy suppliers' total revenue. However, in the stochastic market settlement, e.g., using a scenario-based method in [18], it is known that these properties hold only in expectation. Below, we provide these results irrespective of the chosen method to treat uncertainty.

Consider the following stochastic program:

$$\min_{\vartheta_1, \varphi_1} \mathbb{E}_{\mathbb{P}_\xi}[c(\vartheta_1, \vartheta_2(\xi))] \quad (2.12a)$$

$$\text{s.t. } A(\varphi_1 + \varphi_2(\xi)) = \vartheta_1 + \vartheta_2(\xi) - \delta - \xi, \quad : \lambda_1(\xi) \quad (2.12b)$$

$$F_\vartheta(\vartheta_1 + \vartheta_2(\xi)) + F_\varphi(\varphi_1 + \varphi_2(\xi)) + F_0 = 0, \quad : \lambda^f(\xi) \quad (2.12c)$$

$$\underline{\vartheta} \leq \vartheta_1 + \vartheta_2(\xi) \leq \bar{\vartheta}, \quad \underline{\varphi} \leq \varphi_1 + \varphi_2(\xi) \leq \bar{\varphi}, \quad : (\mu_i^\vartheta(\xi), \mu_i^{\bar{\vartheta}}(\xi), \mu_i^\varphi(\xi), \mu_i^{\bar{\varphi}}(\xi)) \quad (2.12d)$$

where each primal variable is modeled as a two-stage decision with the finite-dimensional recourse and where the dual variables are stated after the colon sign. Here, $\lambda_1(\xi)$ is the nodal price of energy supply, while $\lambda^f(\xi)$ is the price associated with maintaining the system operations according to the underlying physical laws. As we show in [Paper A], the primal and dual solutions to problem (2.12) solve a competitive stochastic equilibrium, where each control action $\vartheta_i(\xi)$, $i = 1, \dots, n$ is compensated with the revenue

$$\mathcal{R}_i^\vartheta(\xi) = \lambda_1(\xi)(\vartheta_{1i} + \vartheta_{2i}(\xi)) + \langle F_\vartheta \rangle_i^\top \lambda^f(\xi)(\vartheta_{1i} + \vartheta_{2i}(\xi)), \quad (2.13a)$$

system operator collects the congestion revenue

$$\mathcal{R}^\varphi(\xi) = \lambda_1(\xi)^\top A(\varphi_1 + \varphi_2(\xi)) + \lambda^f(\xi)^\top F_\varphi(\varphi_1 + \varphi_2(\xi)), \quad (2.13b)$$

and demand charges amount to

$$\mathcal{R}^\delta(\xi) = \lambda_1(\xi)^\top (\delta + \xi) + \lambda^f(\xi)^\top F_0. \quad (2.13c)$$

Notice, since the demand is inelastic, the linearization term F_0 is attributed to demand charges, but its allocation among network demands remains an open question. These payments satisfy the following properties.

Lemma 1 (Cost recovery). *Let $\underline{\vartheta}_i = 0, \forall i = 1, \dots, n$. Then, the profit of agent i providing control action $\vartheta_i(\xi)$ is non-negative in expectation, i.e., $\mathbb{E}_{\mathbb{P}_\xi}[\mathcal{R}_i^\vartheta(\xi) - c(\vartheta_{1i}, \vartheta_{2i}(\xi))] \geq 0$.*

Proof. Consider the following expected profit-maximization problem of agent i :

$$\max_{\vartheta_{1i}, \vartheta_{2i}(\xi)} \mathbb{E}_{\mathbb{P}_\xi}[\mathcal{R}_i^\vartheta(\xi) - c(\vartheta_{1i}, \vartheta_{2i}(\xi))] \quad (2.14a)$$

$$\text{s.t. } \underline{\vartheta}_i \leq \vartheta_{1i} + \vartheta_{2i}(\xi) \leq \bar{\vartheta}_i \quad : (\mu_i^\vartheta(\xi), \mu_i^{\bar{\vartheta}}(\xi)). \quad (2.14b)$$

Since this problem is convex, the Slater condition holds, and its objective function equals to the dual objective function in the optimum, such that we have

$$\mathbb{E}_{\mathbb{P}_\xi}[\mathcal{R}_i^\vartheta(\xi) - c(\vartheta_{1i}, \vartheta_{2i}(\xi))] = \mu_i^{\bar{\vartheta}}(\xi)\bar{\vartheta}_i - \mu_i^\vartheta(\xi)\underline{\vartheta}_i. \quad (2.14c)$$

Under the standard assumption that control actions are fully dispatchable, i.e., from zero ($\underline{\vartheta}_i = 0$) to maximum capacity, the right-hand side of (2.14c) is non-negative due to the dual feasibility condition $\mu_i^{\bar{\vartheta}}(\xi) \geq 0$, and thus the profit of agent i is non-negative in expectation. \square

The following result assumes that the lower state variable limit $\underline{\varphi} \leq 0$, e.g., a network flow can be negative up to negative flow capacity, we have the following result.

Lemma 2 (Revenue adequacy). *Let $\underline{\varphi} \leq 0$. Then, stochastic market payments (2.13) are revenue adequate in expectation, i.e., $\mathbb{E}_{\mathbb{P}_\xi}[\sum_{i=1}^n \mathcal{R}_i^\vartheta(\xi) - \mathcal{R}^\delta(\xi)] \geq 0$.*

Proof. By multiplying the stochastic equations of problem (2.12) by their corresponding dual variables, summing up the resulting expressions, and rearranging the terms, we have

$$\begin{aligned} & \lambda_1(\xi)^\top (\vartheta_1 + \vartheta_2(\xi)) + \lambda^f(\xi)^\top F_\vartheta (\vartheta_1 + \vartheta_2(\xi)) - \lambda_1(\xi)^\top (\delta + \xi) - \lambda^f(\xi)^\top F_0 \\ & = \lambda_1(\xi)^\top A(\varphi_1 + \varphi_2(\xi)) + \lambda^f(\xi)^\top F_\varphi (\varphi_1 + \varphi_2(\xi)), \end{aligned} \quad (2.15a)$$

where the mismatch between the total revenue of control agents and demand charges amounts to the congestion rent of the system operator. We thus need to show that $\mathbb{E}_{\mathbb{P}_\xi}[\mathcal{R}^\varphi(\xi)] \geq 0$. The rent-maximization problem formulates as

$$\max_{\varphi_1, \varphi_2(\xi)} \mathbb{E}_{\mathbb{P}_\xi}[\mathcal{R}^\varphi(\xi)] \quad (2.15b)$$

$$\text{s.t. } \underline{\varphi} \leq \varphi_1 + \varphi_2(\xi) \leq \bar{\varphi}, \quad : (\mu^\varphi(\xi), \bar{\mu}^\varphi(\xi)), \quad (2.15c)$$

which is a convex optimization problem. Following the same line of arguments as in Lemma 1, due to $\underline{\varphi} \leq 0$, the expected congestion rent is non-negative, and thus the revenue adequacy holds in expectation. \square

2.2 Policy-based control and pricing for uncertainty energy systems

Control policy (2.7) allows for expressing the optimization variables in (2.4) as explicit functions of random forecast errors and control actions. This section shows how to optimize this policy for secure operations under uncertainty and how to establish the stochastic energy payments. We are interested in uncertainty- and variability-aware policy optimization. By uncertainty-aware, we understand the optimized policy that ensures network limit satisfaction for any realization of energy demand up to a prescribed constraint violation probability. By variability-aware, we understand the policy that results in the minimal variability of state variables across the period of interest. In [Paper A], for example, we optimize control policies for natural gas network components to ensure real-time operational feasibility, while minimizing intraday variability of gas pressures and flows, as well as to obtain competitive payments that compensate network components for their contributions to satisfying constraint violation and variability criteria.

2.2.1 Uncertainty- and variability-aware policy optimization

Uncertainty-aware policy optimization is provided with a tractable reformulation of (2.11d) which splits it into a set of individual chance constraints, i.e.,

$$\mathbb{P}_\xi[\vartheta_{1i} + [\alpha]_i \xi \geq \underline{\vartheta}_i] \geq 1 - \bar{\varepsilon}_i, \quad \forall i = \{1, \dots, n\}, \quad (2.16a)$$

$$\mathbb{P}_\xi[\vartheta_{1i} + [\alpha]_i \xi \leq \bar{\vartheta}_i] \geq 1 - \bar{\varepsilon}_i, \quad \forall i = \{1, \dots, n\}, \quad (2.16b)$$

$$\mathbb{P}_\xi[\varphi_{1i} - [F_\varphi^{-1} F_\vartheta \alpha]_i \xi \geq \underline{\varphi}_i] \geq 1 - \bar{\varepsilon}_i, \quad \forall i = \{1, \dots, m\}, \quad (2.16c)$$

$$\mathbb{P}_\xi[\varphi_{1i} - [F_\varphi^{-1} F_\vartheta \alpha]_i \xi \leq \bar{\varphi}_i] \geq 1 - \bar{\varepsilon}_i, \quad \forall i = \{1, \dots, m\}, \quad (2.16d)$$

where $\bar{\varepsilon} \in \mathbb{R}_+^{2n+2m}$ is a vector of individual constraint violation probabilities; when $\mathbf{1}^\top \bar{\varepsilon} \leq \varepsilon$, individual chance constraints (2.16) provide a guarantee of joint constraint satisfaction with probability $(1 - \varepsilon)$ – the so-called Bonferroni approximation [45]. Since the feasible set of each

chance constraint in (2.16) is convex, they can be reformulated analytically as second-order cone constraints [12], i.e.,

$$\vartheta_{1i} \geq \underline{\vartheta}_i + z_{\bar{\varepsilon}_i} \left\| \Sigma^{\frac{1}{2}} [\alpha]_i^\top \right\|_2, \quad \forall i = \{1, \dots, n\}, \quad (2.17a)$$

$$\vartheta_{1i} \leq \bar{\vartheta}_i - z_{\bar{\varepsilon}_i} \left\| \Sigma^{\frac{1}{2}} [\alpha]_i^\top \right\|_2, \quad \forall i = \{1, \dots, n\}, \quad (2.17b)$$

$$\varphi_{1i} \geq \underline{\varphi}_i + z_{\bar{\varepsilon}_i} \left\| \Sigma^{\frac{1}{2}} [F_\varphi^{-1} F_\vartheta \alpha]_i^\top \right\|_2, \quad \forall i = \{1, \dots, m\}, \quad (2.17c)$$

$$\varphi_{1i} \leq \bar{\varphi}_i - z_{\bar{\varepsilon}_i} \left\| \Sigma^{\frac{1}{2}} [F_\varphi^{-1} F_\vartheta \alpha]_i^\top \right\|_2, \quad \forall i = \{1, \dots, m\}, \quad (2.17d)$$

where $z_{\bar{\varepsilon}_i}$ is a non-negative safety parameter in the sense of [12], which depends on the knowledge of the underlying forecast error distribution, and $\Sigma^{\frac{1}{2}}$ is the factorization of forecast error covariance, i.e., $\Sigma = \Sigma^{\frac{1}{2}} \Sigma^{\frac{1}{2}\top}$. For instance, if ξ obeys a Gaussian distribution, $z_{\bar{\varepsilon}_i}$ amounts to the inverse cumulative distribution function of the standard Gaussian distribution at the $(1 - \bar{\varepsilon}_i)^{\text{th}}$ quantile, for $\bar{\varepsilon}_i < 0.5$. Since the norm terms are also non-negative, the last terms in the right-hand sides of (2.17) are safety margins that ensure constraint satisfaction up to a prescribed constraint violation probability and covariance of forecast errors. By substituting (2.11d) with (2.17), we end up with a tractable chance-constrained optimization of control policies (2.7) that accommodates real-time uncertainty realizations in a feasible manner.

Towards variability-aware control policy optimization, consider the variance of state variables

$$\text{Var}[\tilde{\varphi}_i(\xi)] = \text{Var}[\varphi_{1i} - [F_\varphi^{-1} F_\vartheta \alpha]_i \xi] = [F_\varphi^{-1} F_\vartheta \alpha]_i \Sigma [F_\varphi^{-1} F_\vartheta \alpha]_i^\top, \quad \forall i = \{1, \dots, m\}, \quad (2.18)$$

which is quadratic in recourse decisions. Using a second-order cone formulation, the variability of state variables can be minimized by modeling the following constraint

$$\left\| \Sigma^{\frac{1}{2}} [F_\varphi^{-1} F_\vartheta \alpha]_i^\top \right\|_2 \leq s_i^\varphi, \quad \forall i = \{1, \dots, m\}, \quad (2.19)$$

where $s^\varphi \in \mathbb{R}^m$ is an optimization variable that upper-bounds the standard deviations of state variables. Thus, by penalizing variable s^φ in the objective function of the chance-constrained program, the policies are optimized to provide minimal variability of state variables.

We can thus formulate the following convex reformulation of the chance-constrained optimization problem to produce uncertainty- and variance-aware control policies (2.7):

$$\min_{\vartheta_1, \varphi_1, \alpha, s^\varphi} c_1^\top \vartheta_1 + \vartheta_1^\top \text{diag}[c_2] \vartheta_1 + \text{Tr}[\alpha^\top \text{diag}[c_2] \alpha \Sigma] + \psi^\varphi \top s^\varphi \quad (2.20a)$$

$$\text{s.t. } \lambda_1: A\varphi_1 = \vartheta_1 - \delta, \quad \lambda^r: \alpha^\top \mathbb{1} = 1, \quad (2.20b)$$

$$\lambda^f: F_\vartheta \vartheta_1 + F_\varphi \varphi_1 + F_0 = 0, \quad (2.20c)$$

$$\lambda_i^\varphi: z_{\bar{\varepsilon}_i} \left\| \Sigma^{\frac{1}{2}} [F_\varphi^{-1} F_\vartheta \alpha]_i^\top \right\|_2 \leq \varphi_{1i} - \underline{\varphi}_i, \quad \forall i = \{1, \dots, m\}, \quad (2.20d)$$

$$\lambda_i^{\bar{\varphi}}: z_{\bar{\varepsilon}_i} \left\| \Sigma^{\frac{1}{2}} [F_\varphi^{-1} F_\vartheta \alpha]_i^\top \right\|_2 \leq \bar{\varphi}_i - \varphi_{1i}, \quad \forall i = \{1, \dots, m\}, \quad (2.20e)$$

$$\lambda_i^\vartheta: \left\| \Sigma^{\frac{1}{2}} [F_\varphi^{-1} F_\vartheta \alpha]_i^\top \right\|_2 \leq s_i^\varphi, \quad \forall i = \{1, \dots, m\}, \quad (2.20f)$$

$$z_{\bar{\varepsilon}_i} \left\| \Sigma^{\frac{1}{2}} [\alpha]_i^\top \right\|_2 \leq \vartheta_{1i} - \underline{\vartheta}_i, \quad \forall i = \{1, \dots, n\}, \quad (2.20g)$$

$$z_{\bar{\varepsilon}_i} \left\| \Sigma^{\frac{1}{2}} [\alpha]_i^\top \right\|_2 \leq \bar{\vartheta}_i - \vartheta_{1i}, \quad \forall i = \{1, \dots, n\}, \quad (2.20h)$$

where $s^\varphi \in \mathbb{R}_+^m$ is a penalty factor. The Greek letter λ is reserved to denote the dual variables of coupling constraints, which couple the nominal and recourse variables ϑ_1 and α , respectively, associated with control decisions.

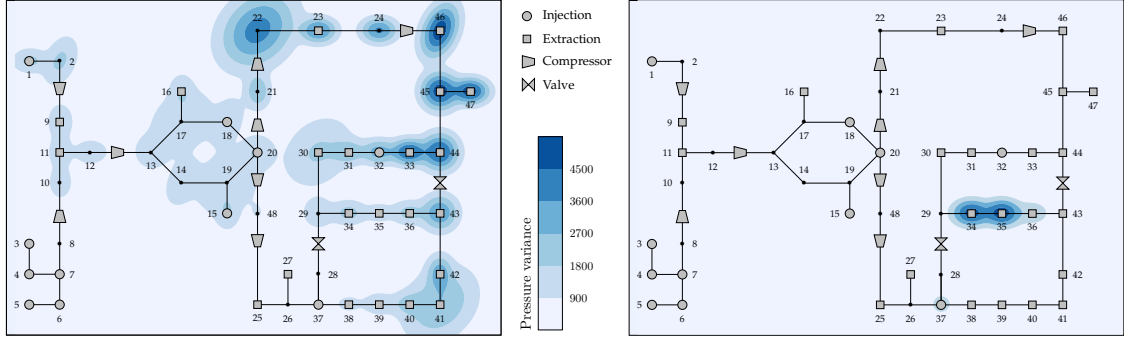


Figure 2.1: Results of uncertainty- and variability-aware control policy optimization in a natural gas network: the variability-agnostic (left) and the variability-aware (right) chance-constrained policy optimization solutions. Refer to the source [Paper A] for the full experiment description.

With Figure 2.1, we illustrate the performance of uncertainty- and variability-aware control policies for flexible injections, compressors, and valves in natural gas networks. Here, the polices are optimized using problem (2.20) to accommodate the uncertainty of gas extractions and to satisfy the criterion of minimal variability of nodal gas pressures. Observe that despite many variable gas extractions, the control policies of network components are jointly optimized to drastically reduce the overall pressure variance, which is localized at a few network nodes. This variability reduction comes at the expense of expected operating costs, thus establishing the cost-variability trade-offs studied in detail in [Paper A].

2.2.2 Uncertainty- and variability-aware energy payments

The optimized control policy (2.7) explicitly defines the contribution of each system component, e.g., flexible gas suppliers in natural gas networks, to uncertainty and variability control. This property of control policies has been recognized as a foundation for uncertainty- and variability-aware prices [17]. In [Paper A] we design an explicit payment scheme that remunerates system components for providing desired network constraint satisfaction and state variability criteria while charging uncertain demands for their adversarial impacts towards the satisfaction of the two criteria. To ensure market efficiency, we further analyze the properties of cost recovery and revenue adequacy of these payments.

To obtain these payments, we invoke the classic linear programming duality theory [48] to decompose the revenue streams associated with linear constraints (2.20b)–(2.20c), and invoke the second-order cone programming duality theory [49] to decompose the revenue streams associated with the reformulated coupling chance constraints (2.20d)–(2.20f). Observe, that unlike linear constraints, the conic constraints are not separable per optimization variables. To overcome this difficulty, in [Paper A], for each conic constraint with a dual variable $\lambda \in \mathbb{R}$ we introduce an auxiliary vector of dual prices $u \in \mathbb{R}^n$, corresponding component-wise to the random vector $\xi \in \mathbb{R}^n$, such that in optimality it always holds that $\|u\|_2 \leq \lambda$. With a set of prices λ, u_1, \dots, u_n , each conic coupling constraint becomes separable, thus enabling the revenue decomposition. Specifically, we show that under a uniform assignment of individual constraint violation probabilities, i.e., $\bar{\varepsilon} = \frac{1}{2n+2m}$, the primal and dual solutions to problem (2.20) solve a competitive equilibrium, where each control action $\vartheta_i(\xi)$, $i = 1, \dots, n$, is compensated with the following revenue

$$\mathcal{R}_i^\vartheta = (\lambda_{1i} + \langle F_\vartheta \rangle_i^\top \lambda^f) \vartheta_{1i} + \left(\lambda^{r\top} + \langle F_\varphi^{-1} F_\vartheta \rangle_i^\top (z_{\bar{\varepsilon}} u^\varphi + z_{\bar{\varepsilon}} u^{\bar{\varphi}} + u^\varphi) \Sigma^{\frac{1}{2}} \right) [\alpha]_i^\top, \quad (2.21)$$

where $u^{\underline{\varphi}}, u^{\overline{\varphi}}, u^{\varphi} \in \mathbb{R}^{m \times n}$ are auxiliary dual prices associated with conic constraints (2.20d)–(2.20f). Here, the first term is a compensation for a nominal control action, and the second term internalizes the contribution of this control action to the satisfaction of stochastic network equations (2.4b) and (2.4c) under uncertainty (through $\lambda^r \in \mathbb{R}^n$), to the satisfaction of state variable limits (2.4d) (through $u^{\underline{\varphi}} \in \mathbb{R}^{n \times n}$ and $u^{\overline{\varphi}} \in \mathbb{R}^{n \times n}$), and to the satisfaction of the variance criteria (through u^{φ}). Observe that this payment is parameterized through the tolerance to constraint satisfaction z_{ε} , covariance factorization of forecast errors $\Sigma^{\frac{1}{2}}$, and variability criteria¹. Similarly, in [Paper A] we show how demand charges and congestion revenues are conditioned to the same set of uncertainty and variability parameters. Furthermore, these payments are shown to satisfy the properties of cost recovery and revenue adequacy in expectation, which is consistent with Lemmas 1 and 2.

2.3 Cost recovery and revenue adequacy beyond expectation

Although stochastic energy system optimization ensures the minimum expected cost, in Section 2.1.3, we established that the stochastic solution guarantees cost recovery and revenue adequacy in expectation only. This may prevent the transition from deterministic to stochastic operational practices, because deterministic market settlements ensure the satisfaction of market properties independently of uncertainty realizations. Through the main contributions of [Paper B], in this section, we explain how the efficiency of the stochastic solution can be approximated within deterministic dispatch procedures to guarantee per-scenario satisfaction of market properties.

2.3.1 Deterministic versus stochastic energy system dispatch

To accommodate fluctuations of the network parameters, system operators arranged energy system optimization in two stages. For instance, power systems are optimized first at the day-ahead stage to meet nominal values of uncertain parameters, followed by the real-time stage where the day-head decisions are adjusted with respect to uncertainty realizations. To ensure sufficient system flexibility in real-time, at the first stage, system operators also impose specific reserve requirements. Building on top of problem (2.3), this first-stage optimization problem writes as

$$\min_{\vartheta_1, \varphi_1, \tilde{\vartheta}} c_1(\vartheta_1, \tilde{\vartheta}) \quad (2.22a)$$

$$\text{s.t. } A\varphi_1 = \vartheta_1 - \delta : \lambda_1, \quad \mathbf{1}^\top \tilde{\vartheta} = R : \lambda^r, \quad (2.22b)$$

$$\underline{\vartheta} + \tilde{\vartheta} \leq \vartheta_1 \leq \bar{\vartheta} - \tilde{\vartheta}, \quad \underline{\varphi} \leq \varphi_1 \leq \bar{\varphi}, \quad \tilde{\vartheta} \geq 0, \quad (2.22c)$$

where $\vartheta_1 \in \mathbb{R}^n$ and $\varphi_1 \in \mathbb{R}^m$ are the nominal values for control and state variables, respectively, and $\tilde{\vartheta} \in \mathbb{R}^n$ is a variable modeling a reserve margin which offsets the minimum and maximum capacity of each control action to ensure enough flexibility in real time. The objective function in (2.22a) is the first-stage convex cost $c_1 : \mathbb{R}^{2n} \mapsto \mathbb{R}$. Equality constraints (2.22b) ensure the balance between the nominal decisions and that reserve margins are procured up to reserve requirement R . Their dual variables $\lambda_1 \in \mathbb{R}^n$ and $\lambda^r \in \mathbb{R}$ respectively constitute the nominal energy and reserve prices. The inequality constraints (2.22c) ensure that nominal control and state variables remain within network limits. Notice, for compactness and without much loss of generality, in formulation (2.22) we drop the linearized equation (2.3c) and assume a symmetric reserve margin for the lower and upper control variable limits.

¹From the dual feasibility conditions of problem (2.20) we have $\|[u^{\varphi}]_i\|_2 \leq \lambda_i^{\varphi}, \forall i = 1, \dots, n$ and from the stationarity conditions of problem (2.20) we know that $\lambda^{\varphi} = \psi^{\varphi}$. Thus prices u^{φ} are implicitly dependent on variability penalty ψ^{φ} . See [Paper A] for details.

At the second stage, the system operator adjusts the nominal decisions to meet a particular realization $\hat{\xi}$ of demand forecast errors using the following optimization:

$$\min_{\vartheta_2, \varphi_2} c_2(\vartheta_2) \quad (2.23a)$$

$$\text{s.t. } A\varphi_2 = \vartheta_2 - \hat{\xi} : \lambda_2, \quad (2.23b)$$

$$-\tilde{\vartheta}^* \leq \vartheta_2 \leq \tilde{\vartheta}^*, \quad (2.23c)$$

$$\underline{\varphi} \leq \varphi_1^* + \varphi_2 \leq \bar{\varphi}, \quad (2.23d)$$

where $\vartheta_2 \in \mathbb{R}^n$ and $\varphi_2 \in \mathbb{R}^m$ are the second-stage adjustment decisions and the optimal solution of the first-stage problem (2.22) is denoted with a subscript $*$. Problem (2.23) minimizes the second-stage cost function $c_2 : \mathbb{R}^n \mapsto \mathbb{R}$ while satisfying the real-time balance constraint (2.23b) and real-time decision limits (2.23c) and (2.23d). The dual variable $\lambda_2 \in \mathbb{R}^n$ of constraint (2.23b) constitutes the price of real-time adjustments.

In problem (2.23), the real-time adjustment of control variables ϑ_2 is made within the procured reserve margins $\tilde{\vartheta}^*$. Therefore, an exogenously set reserve requirement R in problem (2.22) must be sufficient to ensure real-time feasibility. This motivates the following standing assumption.

Assumption 3. *Solutions to problems (2.22) and (2.23) exist.*

Alternatively, a two-stage problem (2.22)–(2.23) can be solved at the minimum of expected cost across a finite set of scenarios using the following scenario-based² stochastic program:

$$\min_{\vartheta_1, \varphi_1, \tilde{\vartheta}, \vartheta_2, \varphi_2} c_1(\vartheta_1, \tilde{\vartheta}) + \sum_{s=1}^S \pi_s c_2(\vartheta_{2s}) \quad (2.24a)$$

$$\text{s.t. } A\varphi_1 = \vartheta_1 - \delta, \quad A\varphi_2 = \vartheta_2 - \hat{\xi}_s, \quad (2.24b)$$

$$\underline{\vartheta} + \tilde{\vartheta} \leq \vartheta_1 \leq \bar{\vartheta} - \tilde{\vartheta}, \quad \tilde{\vartheta} \geq 0, \quad -\tilde{\vartheta} \leq \vartheta_{2s} \leq \tilde{\vartheta}, \quad (2.24c)$$

$$\underline{\varphi} \leq \varphi_1 \leq \bar{\varphi}, \quad \underline{\varphi} \leq \varphi_1 + \varphi_{2s} \leq \bar{\varphi}, \quad \forall s = \{1, \dots, S\}, \quad (2.24d)$$

which does not require the exogenous assignment of reserve requirement R . Instead, it endogenously computes reserve margins $\tilde{\vartheta}$ to minimize the expected system cost over two stages and to ensure solution feasibility within a prescribed set of S uncertainty scenarios.

Despite providing the maximum efficiency in terms of expected cost, the market properties of energy payments based on the dual solution of problem (2.24) hold only in expectation, as per Lemmas 1 and 2. The deterministic market settlement based on problems (2.22) and (2.23), instead, ensures the market properties for any uncertainty realization due to the following results.

Lemma 4 (Cost recovery in the deterministic settlement). *Let $\underline{\vartheta}_i = 0, \forall i = 1, \dots, n$ and let Assumption 3 hold. Then, under deterministic settlement (2.22)–(2.23), the profit associated with control action $\vartheta_i(\xi), i = 1, \dots, n$, is non-negative for any uncertainty realization, i.e., $\lambda_{1i}\vartheta_{1i} + \lambda^r\tilde{\vartheta}_i + \lambda_{2i}\vartheta_{2i} - c_{1i}(\vartheta_{1i}, \tilde{\vartheta}_i) - c_{2i}(\vartheta_{2i}) \geq 0$.*

Proof. The first-stage optimization problem implicitly solves the following profit-maximization problem associated with control variables of each agent i :

$$\max_{\vartheta_{1i}, \tilde{\vartheta}_i} \lambda_{1i}\vartheta_{1i} + \lambda^r\tilde{\vartheta}_i - c_{1i}(\vartheta_{1i}, \tilde{\vartheta}_i) \quad (2.25a)$$

²Here we consider a scenario-based treatment of uncertainty to be consistent with [Paper B]. However, one may consider an affine variable recourse and use a chance-constrained formulation as we explained in Section 2.1.2

$$\text{s.t. } \underline{\vartheta}_i + \tilde{\vartheta}_i \leq \vartheta_{1i} \leq \bar{\vartheta}_i - \tilde{\vartheta}_i, \quad : (\underline{\mu}_{1i}, \bar{\mu}_{1i}) \quad (2.25\text{b})$$

$$\tilde{\vartheta}_i \geq 0. \quad (2.25\text{c})$$

Since this problem is convex, the Slater condition holds, and its objective function equals to the dual objective function in the optimum, such that we have

$$\lambda_{1i}\vartheta_{1i} + \lambda^r\tilde{\vartheta}_i - c_{1i}(\vartheta_{1i}, \tilde{\vartheta}_i) = \bar{\mu}_{1i}\bar{\vartheta}_i - \underline{\mu}_{1i}\underline{\vartheta}_i, \quad (2.25\text{d})$$

where the right-hand side is non-negative because $\bar{\mu}_{1i} \geq 0$ and $\underline{\vartheta}_i = 0$. Thus, the cost recovery holds for the first-stage problem. Next, consider that the second-stage optimization problem implicitly solves the following profit-maximization problem associated with the real-time adjustment of control actions:

$$\max_{\vartheta_{2i}} \lambda_{2i}\vartheta_{2i} - c_{2i}(\vartheta_{2i}) \quad (2.25\text{e})$$

$$\text{s.t. } -\tilde{\vartheta}_i^* \leq \vartheta_{2i} \leq \tilde{\vartheta}_i^*, \quad : (\underline{\mu}_{2i}, \bar{\mu}_{2i}). \quad (2.25\text{f})$$

Since this problem is convex, the Slater condition holds, and its objective function equals to the dual objective function in the optimum, such that we have

$$\lambda_{2i}\vartheta_{2i} - c_{2i}(\vartheta_{2i}) = \bar{\mu}_{2i}\tilde{\vartheta}_i^* + \underline{\mu}_{2i}\tilde{\vartheta}_i^*, \quad (2.25\text{g})$$

where the right-hand side is always non-negative because of dual feasibility conditions $\underline{\mu}_{2i}, \bar{\mu}_{2i} \geq 0$ and that $\tilde{\vartheta}_i^* \geq 0$ due to the primal feasibility condition of the first-stage problem (2.25c). Hence, the cost recovery holds for the second-stage problem, thus completing the proof. \square

Lemma 5 (Revenue adequacy in the deterministic settlement). *Let $\underline{\varphi} \leq 0$ and let Assumption 3 hold. Then, the deterministic settlement (2.22)–(2.23) is revenue adequate for any uncertainty realization, i.e., $\lambda_1^\top \vartheta_1 + \lambda^r \tilde{\vartheta} + \lambda_2^\top \vartheta_2 - \lambda_1^\top \delta - \lambda_2^\top \hat{\xi} \geq 0$.*

Proof. The proof follows the same line of arguments as in the proofs of Lemmas 2 and 4. \square

2.3.2 Approximating stochastic solutions within deterministic settlements

In order to ensure the operational feasibility and the market properties as in Lemmas 4 and 5, a system operator must set a sufficient large reserve requirement R . In practice, this requirement is set using deterministic security criteria, such as the $N - 1$ security rule that requires reserves to cover the largest contingency in the system, or based on a mean forecast load error, as in the PJM [50] and European markets [51]. Motivated by security aspects, these deterministic criteria are agnostic to system operating costs and often lead to overly-conservative solutions. To alleviate the conservatism of the deterministic reserve criteria, in [Paper B], we introduce a cost-optimal computation of reserve requirement R anticipating its impact on the expected operational cost within the deterministic dispatch procedure (2.22)–(2.23).

Towards the goal, we propose the following scenario-based stochastic bilevel problem:

$$\min_{\vartheta_2, \varphi_2, R} c_1(\vartheta_1, \tilde{\vartheta}) + \sum_{s=1}^S \pi_s c_2(\vartheta_{2s}) \quad (2.26\text{a})$$

$$\text{s.t. } A\varphi_{2s} = \vartheta_{2s} - \hat{\xi}_s, \quad (2.26\text{b})$$

$$-\tilde{\vartheta} \leq \vartheta_{2s} \leq \tilde{\vartheta}, \quad (2.26\text{c})$$

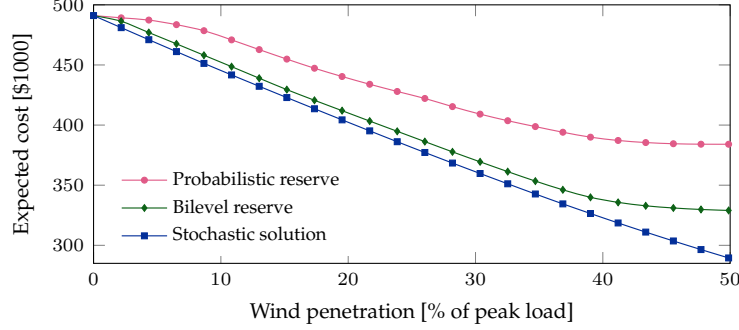


Figure 2.2: Expected operating cost as a function of wind penetration level for different reserve requirements. Refer to the source [Paper B] for detailed model and experiment description.

$$\underline{\varphi} \leq \varphi_1^* + \varphi_{2s} \leq \bar{\varphi}, \quad \forall s = \{1, \dots, S\}, \quad (2.26d)$$

$$\vartheta_1, \varphi_1, \tilde{\vartheta} \in \underset{\vartheta_1, \varphi_1, \tilde{\vartheta}}{\operatorname{argmin}} \quad c_1(\vartheta_1, \tilde{\vartheta}) \quad (2.26e)$$

$$\text{s.t. } A\varphi_1 = \vartheta_1 - \delta, \quad \mathbb{1}^\top \tilde{\vartheta} = R \quad (2.26f)$$

$$\underline{\vartheta} + \tilde{\vartheta} \leq \vartheta_1 \leq \bar{\vartheta} - \tilde{\vartheta}, \quad (2.26g)$$

$$\underline{\varphi} \leq \varphi_1 \leq \bar{\varphi}, \quad \tilde{\vartheta} \geq 0, \quad (2.26h)$$

where the upper-level problem (2.26a)–(2.26d) minimizes the expected cost by optimizing the real-time adjustment decisions and reserve requirement R . Here, the first-stage decisions are considered parameters that are sourced from the lower-level problem (2.26e)–(2.26h). The solution to the lower-level problem is parameterized by reserve requirement R . Hence, by solving the bilevel problem (2.26), a system operator internalizes the criterion of the minimum expected cost into reserve requirement R , thus attaining the maximum cost efficiency of the deterministic dispatch procedure (2.22)–(2.23) on average. Moreover, in line with the stochastic problem (2.24), R is computed to ensure system feasibility within the prescribed set of uncertainty scenarios.

Bilevel optimization problem (2.26), however, is computationally intractable. To resolve this difficulty, in line with [Paper B], convex lower-level problem (2.26e)–(2.26h) is replaced with its KKT optimality conditions to recast the bilevel problem as a single-level mathematical program with equilibrium constraints. The resulting program includes a nonlinear complementary slackness condition, which is replaced with its linear equivalent using special ordered set of type 1 (SOS1) variables, yielding a mixed-integer program.

In Figure 2.2, we illustrate the approximation of stochastic dispatch efficiency in a power system with a varying penetration of wind power generation. The figure compares the cost efficiency of reserve requirements obtained from the bilevel problem with that of (i) ideal stochastic solution and (ii) probabilistic reserve requirements computed according to the state-of-the-art reserve-quantification approach employed by European system operators using probabilistic forecast information³ [51]. Observe that endogenously computed reserve requirements from the bilevel program significantly outperform the dispatch solution obtained with exogenous probabilistic reserves. However, these bilevel requirements only approximate the stochastic efficiency in the interest of preserving the market properties of cost recovery and revenue adequacy.

³Given a cumulative distribution function of wind power generation, these requirements are computed as the distance between the expected wind power generation and specified quantiles in both upward and downward directions. Refer to Section V.B. of [Paper B] for details.

2.4 Stochastic market settlement under information asymmetry

So far, we have discussed the stochastic market settlement and its properties assuming that the information on underlying uncertainty distribution \mathbb{P}_ξ is consistent among all system agents. In this case, the stochastic market settlement is complete as it satisfies all agents' stochastic preferences, i.e., the profits of market participants are maximized in expectation with respect to \mathbb{P}_ξ . This is no longer the case when information on \mathbb{P}_ξ is asymmetric, which leads to incomplete markets from the information standpoint. This section discusses how stochastic settlement can be completed to satisfy stochastic agent preferences under information asymmetry.

Following the assumptions of [Paper C], we simplify the base problem (2.3) by modeling a single producer and a single consumer, optimizing dispatch decisions respecting their stochastic preferences, and disregarding state variables. Specifically, we consider that the renewable power generation is the only source of uncertainty described through a finite set of S scenarios ξ_1, \dots, ξ_S . The producer's decision making is organized in two stages through the first-stage energy supply decision ϑ_1 and a set of second-stage decisions $\vartheta_{21}, \dots, \vartheta_{2S}$ that model the real-time adjustments with respect to uncertainty realizations. Energy supply costs are modeled respectively for the first and second stages by convex functions c_1 and c_2 of one variable. Similarly, consumer's energy demand is modeled as a first-stage variable δ_1 followed by real-time adjustments $\delta_{21}, \dots, \delta_{2S}$ that are governed by the first- and second-stage concave utility functions u_1 and u_2 of one variable. Finally, we assume that producer and consumer decisions belong to compact and convex sets \mathcal{P} and \mathcal{C} , respectively. This setting motivates the following centralized scenario-based stochastic optimization:

$$\min_{\vartheta_1, \delta_1} c_1(\vartheta_1) - u_1(\delta_1) + \sum_{s=1}^S \pi_s^{\text{mo}} (c_2(\vartheta_{2s}) - u_2(\delta_{2s})) \quad (2.27a)$$

$$\text{s.t.} \quad \vartheta_1 + \vartheta_{2s} + \xi_s - \delta_1 - \delta_{2s} = 0, \quad : \lambda_s, \quad \forall s = \{1, \dots, S\} \quad (2.27b)$$

$$(\vartheta_1, \vartheta_{21}, \dots, \vartheta_{2S}) \in \mathcal{P}, \quad (\delta_1, \delta_{21}, \dots, \delta_{2S}) \in \mathcal{C}, \quad (2.27c)$$

which optimizes the expected social cost with respect to a set of probabilities $\pi_1^{\text{mo}}, \dots, \pi_S^{\text{mo}}$, assigned by a central entity, e.g., market operator in this case. The dual variables $\lambda_1, \dots, \lambda_S$ thus reflect the expectation of market operator over stochastic renewable in-feed. These dual variables are also called probability-adjusted electricity prices: in scenario s , the real-time electricity price anticipated by the market operator at the first-stage is retrieved as $\lambda_s / \pi_s^{\text{mo}}$.

This stochastic problem can also be solved through the following equilibrium formulation:

$$\max_{\tilde{\lambda}_s} -\tilde{\lambda}_s [\vartheta_1 + \vartheta_{2s} + \xi_s - \delta_1 - \delta_{2s}], \quad \forall s = \{1, \dots, S\}, \quad (2.28a)$$

$$\max_{\vartheta_1, \vartheta_{21}, \dots, \vartheta_{2S}} \sum_{s=1}^S \pi_s^{\text{p}} \left[\frac{\tilde{\lambda}_s}{\pi_s^{\text{p}}} (\vartheta_1 + \vartheta_{2s}) - c_2(\vartheta_{2s}) \right] - c_1(\vartheta_1), \quad (\vartheta_1, \vartheta_{21}, \dots, \vartheta_{2S}) \in \mathcal{P}, \quad (2.28b)$$

$$\max_{\delta_1, \delta_{21}, \dots, \delta_{2S}} \sum_{s=1}^S \pi_s^{\text{c}} \left[u_2(\delta_{2s}) - \frac{\tilde{\lambda}_s}{\pi_s^{\text{c}}} (\delta_1 + \delta_{2s}) \right] + u_1(\vartheta_1), \quad (\delta_1, \delta_{21}, \dots, \delta_{2S}) \in \mathcal{C}, \quad (2.28c)$$

which is given by a set of optimization problems of three agents. A price-setting agent in (2.28a) seeks equilibrium prices $\tilde{\lambda}_1, \dots, \tilde{\lambda}_S$ in response to system imbalance for each outcome of renewable production. Power producer and consumer, respectively in (2.28b) and (2.28c), optimize the expected profit in response to equilibrium prices by choosing optimal first- and second-stage

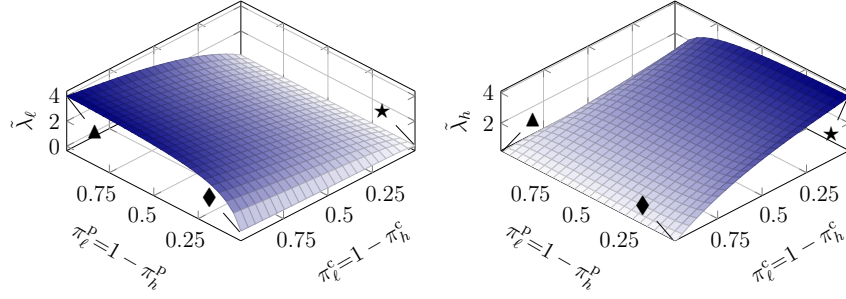


Figure 2.3: Equilibrium prices as a function of agent information. Sourced from [Paper C].

decisions. Problems (2.28b) and (2.28c) optimize the welfare of the two agents with respect to their private probability assignments π_1^P, \dots, π_S^P and π_1^C, \dots, π_S^C . Therefore, equilibrium prices are implicitly functions of the information that agents internalize into their optimization problems.

When information is consistent among market operator in (2.27) and agents in (2.28), i.e., $\pi_s^{mo} = \pi_s^P = \pi_s^C, \forall s = \{1, \dots, S\}$, the solutions to the centralized and equilibrium problems are the same, by equivalence of KKT optimality conditions we have $\lambda = \tilde{\lambda}$. In this case, the centralized stochastic settlement is complete as it satisfies the stochastic preferences of all agents in the equilibrium problem, and thus the result of Lemma 1 holds. This is no longer the case when the information on the underlying distribution is asymmetric among the agents, making the centralized stochastic settlement in (2.27) incomplete.

This necessitates two market redesign solutions proposed in [Paper C]. The first relies on a decentralized computation of equilibrium solution to problem (2.28) that naturally embodies the dynamic price adjustment process (so-called Walrasian auction [52]): the prices are updated followed by producer and consumer updates. The second relies on a centralized computation that requires agents to submit their private probability assignments to the market operator. Through analyzing the technical properties of existence and uniqueness of equilibrium solution, we find in [Paper C] that there exists a centralized optimization problem that solves equilibrium (2.28), i.e.,

$$\min_{\vartheta_1, \delta_1, \dots, \vartheta_{2S}, \delta_{2S}} c_1(\vartheta_1) - u_1(\delta_1) + \sum_{s=1}^S (\pi_s^P c_2(\vartheta_{2s}) - \pi_s^C u_2(\delta_{2s})) \quad (2.29a)$$

$$\text{s.t.} \quad \text{Constraints (2.27b) -- (2.27c),} \quad (2.29b)$$

which makes Lemma 1 hold with respect to the private information of the agents. It is worth noting that this result is possible owing to the linearity of expectation, which is separable in agent optimization variables. This is not always the case if agents are guided by non-separable stochastic measures, such as CVaR risk measure, see for example [25].

We conclude by analyzing electricity prices as functions of private information. In [Paper C] we show that by rearranging the KKT optimality conditions of problem (2.29), the prices admit analytical dependency on probability assignments. For a simple setup with two wind power production scenarios (low ℓ and high h), this dependency is illustrated in Figure 2.3. In case (\blacktriangle), when producer assigns the whole probability mass to outcome ℓ , it leads to a nearly zero price associated with outcome h . A similar situation holds in the opposite case (\star). In a quite critical case (\spadesuit) with a highly asymmetric assignment of probabilities, the equilibrium yields almost zero

prices for both outcomes. This, in turn, has drastic implications on system operations, social welfare, and decentralized computations that are studied in detail in [Paper C].

CHAPTER 3

Privacy-Preserving Optimization in Energy Systems

Solving energy optimization problems requires utilizing large optimization datasets that tend to leak through releases of optimization results. This calls for ethical energy system optimization without involving the risk of disclosing private attributes of these datasets. In this chapter, we introduce privacy-preserving algorithms to solve energy optimization problems while systematically controlling the risks of leaking private optimization datasets, according to the main results of [Paper D]–[Paper F]. We start with Section 3.1, where we introduce the most representative power system optimization task – the optimal power flow (OPF) problem – and discuss its distributed and centralized computations. In Section 3.2, we design adversarial privacy attack models to identify privacy breaches in OPF computations and to substantiate privacy goals. These models are formulated anticipating various types of privacy adversaries, including model-aware and model-agnostic adversaries and those with full or limited access to OPF results. To enable privacy guarantees, we use the notion of differential privacy, whose main definitions and results are presented in Section 3.3. Moving towards private computations, Section 3.4 introduces distributed OPF algorithms that ensure a privacy-preserving information exchange among algorithm sub-problems. Finally, Section 3.5 presents centralized OPF computations with both privacy and feasibility guarantees.

3.1 Optimal power flow problem

The OPF problem is the most representative power system optimization task, which is solved on a daily basis to identify the optimal energy allocations that ensure economically efficient and secure operations [39]. As this problem requires input datasets with many sensitive parameters, e.g., market bids and network parameters, it is of special interest to privacy-preserving computations. Throughout the chapter, we mainly build on top of the DC approximation of this problem, which ignores modeling reactive power, losses, and assumes fixed voltage magnitudes, but often used for market clearing, cross-border coordination and operational planning. This formulation is used in [Paper D] and [Paper E], and we refer to [Paper F] for an AC-OPF formulation.

3.1.1 Power network equations

A power network is modeled as a graph $\Gamma(\mathcal{N}, \Lambda)$, where $\mathcal{N} = \{1, \dots, N\}$ is the set of nodes and $\Lambda = \{1, \dots, L\}$ is the set of edges connecting those nodes. Each edge represents a transmission line with the assigned direction from sending node n to receiving node n' , i.e., if $(n, n') \in \Lambda$, then $(n', n) \notin \Lambda$, yet the energy flows are undirected and can take either positive or negative values. Each line is described through its susceptance $\beta \in \mathbb{R}_+^L$ and maximum transmission capacity $\bar{f} \in \mathbb{R}_+^L$.

Let $\theta \in \mathbb{R}^N$ be a vector of nodal voltage angles. The power flows across the network can be thus computed as

$$f_\ell \triangleq \beta_\ell (\theta_n - \theta_{n'}) , \quad \forall \ell = (n, n') \in \Lambda.$$

Next, consider the network topology through a weighted Laplacian matrix $B \in \mathbb{R}^{N \times N}$, such that

$$B_{nm} = \begin{cases} -\beta_\ell, & \text{if } m = n' \\ \sum_{\ell=(n,:)} \beta_\ell, & \text{if } k = n \\ 0, & \text{otherwise} \end{cases} \quad \forall \ell = (n, n') \in \Lambda.$$

Let vector $d \in \mathbb{R}_+^N$ collect all network loads, and let variable vector $p \in \mathbb{R}^N$ collect real power generation within the minimum and maximum generation capacity of network nodes $\underline{p} \in \mathbb{R}_+^N$ and $\bar{p} \in \mathbb{R}_+^N$, respectively. Then, power flows, generation quantities and loads are balanced for each node through the following power conservation law in a vector form

$$B\theta = p - d,$$

where the left-hand side computes the net power flow injection for all network nodes.

3.1.2 Centralized optimization of the optimal power flow problem

The OPF problem seeks the minimum aggregated generation cost while meeting the technical limits on power flows and generation. Let $c : \mathbb{R}^N \mapsto \mathbb{R}$ be a convex function which computes the aggregated generation cost. Then, the centralized OPF optimization problem formulates as

$$\min_{p, \theta} \quad c(p) \tag{3.1a}$$

$$\text{s.t.} \quad B\theta = p - d, \tag{3.1b}$$

$$-\bar{f}_\ell \leq \beta_\ell (\theta_n - \theta_{n'}) \leq \bar{f}_\ell, \quad \forall \ell = (n, n') \in \Lambda, \tag{3.1c}$$

$$\underline{p} \leq p \leq \bar{p}, \tag{3.1d}$$

where the aggregated cost function (3.1a) is minimized subject to power network equations (3.1b), power flow limits (3.1c), and power generation limits (3.1d).

3.1.3 Distributed optimization of the optimal power flow problem

The OPF problem (3.1) is solved by a central entity, typically by a system operator, who collects optimization data and performs a centralized computation. To enable such a computation, the information about network topology, cost functions, generation limits and loads must be disclosed and made available to a central entity, thus giving rise to privacy risks. Motivated by privacy concerns, it has been proposed to distribute optimization datasets among sub-problems that perform local OPF computations and coordinate over iterations towards the solution of the original OPF problem [53]. Since the optimization dataset is distributed and localized within local OPF computations, this approach is promising to preserve data integrity.

Distributed OPF computations are often performed using a consensus version of an alternating direction method of multipliers (consensus ADMM) algorithm [55] that decomposes a network per individual nodes (or per zones comprising several nodes). Such a nodal network decomposition is illustrated in Figure 3.1. The ADMM algorithm requires duplicating voltage angle variables (3.1),

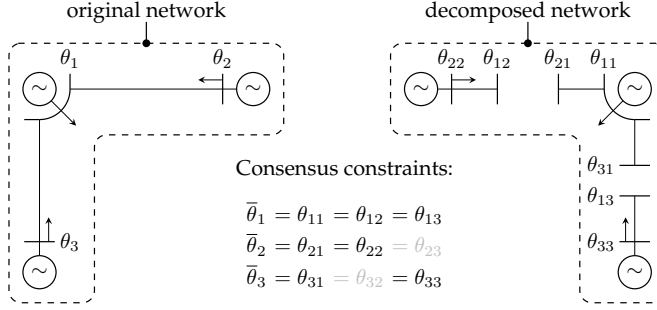


Figure 3.1: Node-wise decomposition of a power network: the original network on the left, and its mirrored decomposed counterpart on the right. The original network is restored by enforcing consensus constraints for every node across its neighborhood. Sourced from [54, arXiv v.1].

such that each n^{th} node stores local copies $\theta_n \in \mathbb{R}^N$ of voltage angles and updates them across iterations to reach the satisfaction of the following consensus constraint:

$$\theta_n - \bar{\theta} = 0 : \mu_n, \quad \forall n \in \mathcal{N}, \quad (3.2)$$

where $\bar{\theta} \in \mathbb{R}^N$ is the vector of consensus variables and $\mu_n \in \mathbb{R}^N$ is the vector of dual variables associated with consensus constraints of each node n . Constraint (3.2) requires that all nodes store identical copies of voltage angles. Let \mathcal{O}_n denote a subset of constraints (3.1b)–(3.1d) specific to node n . By dualizing (3.2), we have the optimization of the following partial Lagrangian function:

$$\max_{\mu} \min_{p, \theta, \bar{\theta}} \mathcal{L}(p, \theta, \bar{\theta}, \mu) := c(p) + \sum_{n=1}^N \mu_n^\top (\bar{\theta} - \theta_n) \quad (3.3a)$$

$$\text{s.t. } p, \theta \in \bigcap_{n=1}^N \mathcal{O}_n, \quad (3.3b)$$

which is separable per each node n . Problem (3.3) can be thus solved in a distributed manner over iterations using Algorithm 1. This algorithm updates the consensus variable $\bar{\theta}$ using the average value over local updates as explained in [55]. The value of dual variables in Step 7 evolves along the decent direction with a suitable step size ρ . The algorithm terminates when the primal and dual residuals are below convergence tolerance \bar{r} or when the iteration counter reaches iteration limit K . The general convergence analysis of this algorithm is provided in [55] and implementation details are available in [Paper D].

3.2 Privacy breaches in optimal power flow computations

Although optimization datasets are not explicitly disclosed in the release of optimization results, the centralized OPF computation in (3.1) and its distributed counterpart in Algorithm 1 tend to leak certain dataset attributes. Here, we overview the privacy attack models that identify the privacy breaches in the centralized and distributed OPF computations. In Section 3.2.1, we first formalize OPF computations through a mathematical mechanism with certain properties, and then introduce two types of attack models: reconstruction models in Section 3.2.2 that are solved by adversaries with almost full knowledge of the underlying computation, and tracing models in Section 3.2.3 that identify the private dataset items through repeated observations of OPF outcomes.

Algorithm 1 Distributed ADMM-based OPF computation

Input: $K, \rho, \bar{\theta}^0, \mu^0$ and \bar{r}
 1: $k \leftarrow 0$
 2: **while** $r^k \leq \bar{r}$ **or** $k \leq K$ **do**
 3: $k \leftarrow k + 1$
 4: Local update $\forall n = 1, \dots, N$:

$$\theta_n^k \leftarrow \underset{p_n, \theta_n}{\operatorname{argmin}} \quad \mathcal{L}_n(p_n, \theta_n, \bar{\theta}^{k-1}, \mu_n^{k-1}) + \frac{\rho}{2} \left\| \theta_n - \bar{\theta}^{k-1} \right\|_2^2, \quad \text{s.t. } p_n, \theta_n \in \mathcal{O}_n$$

- 5: Consensus variable update: $\bar{\theta}_n^k = \sum_{i=1}^N \theta_{in}^k / N, \quad \forall n = 1, \dots, N$
 6: Dual variable update: $\mu_n^k = \mu_n^{k-1} + \rho(\bar{\theta}^k - \theta_n^k), \quad \forall n = 1, \dots, N$
 7: Primal residual update: $r^k = \sum_{n=1}^N \left\| \bar{\theta}^k - \theta_n^k \right\|_2$

8: **end while**

3.2.1 OPF computation problem as a mechanism

From the privacy standpoint, it is convenient to consider an OPF computation as a mechanism $\mathcal{M} : \mathbb{R}^n \mapsto \mathbb{R}^m$, which maps n private dataset items into m computational results released once mechanism \mathcal{M} is executed. For example, centralized OPF optimization problem (3.1) can be seen as a mapping from load, generation, and network topology data into aggregated OPF statistics, such as aggregated generation cost or generation mix. Similarly, consider that the load value d_n of the n^{th} ADMM sub-problem in Algorithm 1 is a private data. The sub-problems are thus seen as mechanisms from their private load values to the local voltage updates released at iteration k . The goal of a privacy adversary is to infer the attributes of any individual item in the private dataset by observing m computational results. Towards the formulation of privacy attack models, we limit our attention to the mechanisms that satisfy the following standing assumption.

Assumption 6. *Mechanism \mathcal{M} is the unique mapping from a dataset to the OPF solution.*

This assumption is introduced to avoid attack models with ambiguous outcomes and allows us to model more powerful privacy adversaries. Assumption 6 is not limiting for OPF problems that admit a unique solution. For instance, the solution of OPF problem (3.1) is unique when cost function $c(p)$ is strictly monotone in variable p and the voltage angle at the reference node $r \in \mathcal{N}$ is set to zero, i.e., $\theta_r = 0$, thus admitting a unique optimal power flow solution [56].

3.2.2 Reconstruction models of privacy attacks

Reconstruction models of privacy attacks are executed by adversaries that are aware of the underlying optimization problem but lack certain input optimization data. Thus, they exploit the knowledge about optimization structure to reconstruct the missing data from the observed optimization results. We consider the following examples of reconstruction models.

Load reconstruction in the centralized OPF computation. Consider a centralized OPF problem as a mapping from private load datasets to generator dispatch decisions. Considering the loads as the only private information, the rest of the parameters are assumed publicly known. Let \hat{p}

denote the optimal dispatch solution released upon solving problem (3.1). Then, the reconstruction privacy attack can be executed by solving the following optimization:

$$\min_{p, \theta, d \geq 0} c(p) + \Upsilon \|p - \hat{p}\|_2^2 \quad (3.4a)$$

$$\text{s.t. } B\theta = p - d, \quad p, \theta \in \text{constraints (3.1c) -- (3.1d)}. \quad (3.4b)$$

In contrast to problem (3.1), here the load vector $d \in \mathbb{R}^N$ is modeled as a decision variable. The objective function (3.4a) is composed of the objective function of the original problem (3.1a) and a regularization term which penalizes the distance between the optimal generator dispatch of problem (3.4) and that of problem (3.1) for some non-negative factor $\Upsilon \in \mathbb{R}_+$. With increasing Υ , the value of objective function (3.4a) converges to that of (3.1a) because of the uniqueness of the global optimal solution to problem (3.1). Therefore, by choosing a sufficiently large factor Υ , problem (3.4) reconstructs the unique dataset d that produces the optimal solution \hat{p} .

Load reconstruction in the distributed OPF computation. Such reconstruction attacks also apply for distributed OPF computations in Algorithm 1, where repeated computations are made on the same input dataset. Indeed, across ADMM iterations, each sub-problem n releases the sequence $\theta_n^1, \dots, \theta_n^k, \dots, \theta_n^K$ of up to K voltage angles computed on the same load value d_n . An adversary can thus solve the following reconstruction problem:

$$\min_{p_n, \hat{\theta}_n, d_n \geq 0} \sum_{k=1}^K \left(\mathcal{L}_n(p_n^k, \hat{\theta}_n^k, \bar{\theta}^{k-1}, \mu_n^{k-1}) + \frac{\rho}{2} \|\hat{\theta}_n^k - \bar{\theta}^k\|_2^2 + \Upsilon \|\hat{\theta}_n^k - \theta_n^k\|_2^2 \right) \quad (3.5a)$$

$$\text{s.t. } B_n^\top \hat{\theta}_n^k = p_n^k - d_n, \quad \forall k = 1, \dots, K, \quad (3.5b)$$

$$p_n^k, \hat{\theta}_n^k \in \text{constraints (3.1c) -- (3.1d)}, \quad \forall k = 1, \dots, K, \quad (3.5c)$$

which identifies the private value d_n by minimizing the distance between the voltage variables and the voltage updates released by sub-problem n across K iterations.

3.2.3 Tracing models of privacy attacks

Unlike reconstruction models that identify missing data items using a single computation, tracing models of privacy attack rely on repeated observations of optimization outcomes to draw conclusions about private data attributes.

Tracing loads in the centralized OPF computation. Consider a centralized OPF computation which is solved repeatedly over time. It can be seen as a mapping $\mathcal{M} : \mathbb{R}^{n \times t} \mapsto \mathbb{R}^{m \times t}$ from n loads across t time periods to m OPF outcomes in the same time periods. A tracing model of privacy attack identifies the changes of loads by observing the changes in the released OPF outcomes. [Paper F] provides an example of this attack in the context of the centralized OPF problem, where a load variation at a single node ($n = 1$) is directly exposed by the changes of the voltage and power flow ($m = 2$) associated with that node across $t = 250$ observations, as shown in Figure 3.2. Here, three periodic load components are exposed by voltage and power flow measurements. A privacy adversary thus identifies the load activity without reconstructing the exact load values.

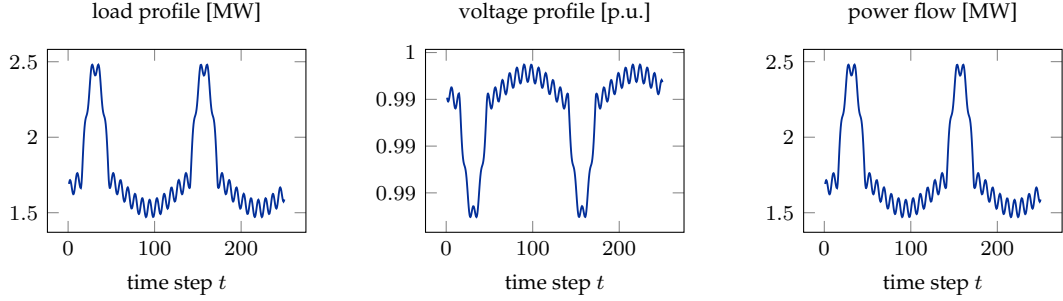


Figure 3.2: Example of a tracing privacy attack on the centralized OPF computation: the voltage at and power flow into the node of interest reveal the load profile used in the computation. Sourced from [Paper F].

Tracing loads in the distributed OPF computation. Tracing privacy attacks also apply to distributed OPF computations in Algorithm 1, where each sub-problem is repeatedly solved across iterations. This enables a privacy adversary to trace the load contained in each sub-problem across iterations. In the preprint version [54, arXiv v.1] of [Paper D], we express the unknown load value as a function of (i) ADMM coordination signals, (ii) algorithmic parameters, and (iii) network data. For quadratic cost functions with the first- and second-order coefficients $c_1 \in \mathbb{R}^N$ and $c_2 \in \mathbb{R}^N$, respectively, the load value of sub-problem n at iteration k can be estimated as:

$$\hat{d}_n^k = \frac{\mu_{nn}^{k-1} + \rho(\bar{\theta}_n^{k-1} - \theta_{nn}^k) - c_{1i}B_{nn}}{2c_{2n}B_{nn}} - \sum_{n'=1}^N B_{nn'}\theta_{nn'}^k + f(\lambda_n), \quad (3.6)$$

where $\lambda_n \in \mathbb{R}^\ell$ is the vector of ℓ dual variables associated with inequality constraints (3.3b) of each sub-problem n , and function $f : \mathbb{R}^\ell \mapsto \mathbb{R}$ is such that $f(\emptyset) = 0$. Using tracing attack model (3.6), a privacy adversary estimates the load value across iterations. Whenever sub-problem's inequalities are non-binding, i.e., $\lambda_n = \emptyset$, a privacy adversary computes the exact load value. An example of such an attack on the second node of the IEEE 14-node Reliability Test System is depicted in Figure 3.3. The figure shows the estimated load observed by an adversary across more than 1,000 ADMM iterations; whenever generator constraints are not binding at the second node, an adversary observes the actual load magnitude at that node. This value also appears to be the most frequent as shown by the empirical density plot in Figure 3.3.

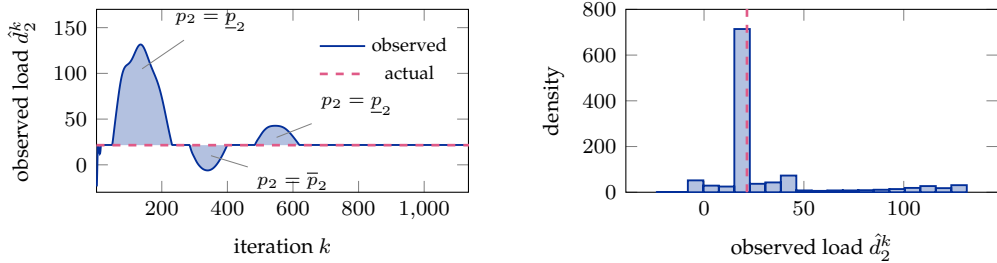


Figure 3.3: Example of a tracing privacy attack on the distributed OPF computation using the IEEE 14-node Reliability Test System: (left) load value in (3.6) across ADMM iterations, (right) empirical density of observed load values. Sourced from [54, arXiv v.1].

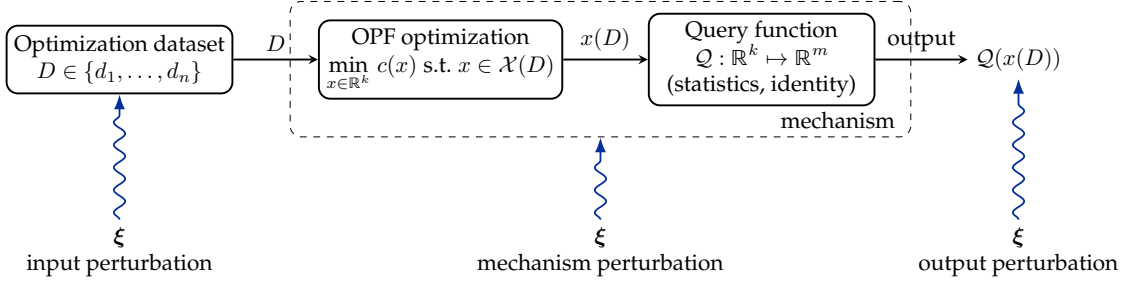


Figure 3.4: OPF optimization as a mechanism that maps datasets into queries over optimization results. Here, the solution space \mathcal{X} of an optimization problem is conditioned to dataset D . This dataset leaks through the queries made over solution x , that may include any linear transformation of x . The blue arrows define three random perturbation strategies that can be used to provide differential privacy for optimization datasets.

3.3 Differential privacy: main definitions and results

The attack models introduced in the previous section identify various privacy breaches in OPF computations. To minimize the risks of OPF dataset exposures, we internalize the notion of differential privacy into OPF computations. This section reviews the main definitions and theoretical results of differential privacy that are at the core of the upcoming private OPF algorithms.

Recall that we consider an OPF computation, either centralized or distributed, as a mechanism $\mathcal{M} : \mathbb{R}^n \mapsto \mathbb{R}^m$ which maps n dataset items into m optimization results, as illustrated in Figure 3.4. For example, Step 5 of Algorithm 1 runs N mechanisms that output identity queries over solutions of ADMM sub-problems. The goal of the differentially private OPF mechanism is to make any two adjacent (different in one item) datasets indistinguishable from the mechanism output. That is, the mechanism output does not disclose the underlying differences between the two datasets. These differences must be measurable and are formalized using the following definition.

Definition 7 (α -adjacency of two datasets [57]). *Two datasets $D = \{e_1, \dots, e_n\}$ and $D' = \{e'_1, \dots, e'_n\}$ are said to be α -adjacent for some parameter $\alpha \in \mathbb{R}_+$, denoted by $D \sim_\alpha D'$, if there exists $k \in \{1, \dots, n\}$ such that $\|e_k - e'_k\|_1 \leq \alpha$ and $e_j = e'_j, \forall j \in \{1, \dots, n\} \setminus k$.*

In the OPF context, a dataset D contains, for example, electrical loads of a given power network. Let electrical loads be normalized such that each load belongs to the interval from 0 to 1. Then, by choosing $\alpha = 1$, one analyzes two datasets D and D' different at position k by exactly one electrical load. This 1-adjacency of two datasets admits the Hamming distance between the two datasets and the mechanism thus obfuscates the presence of a single electrical load. In power systems, however, the presence of loads is often common knowledge. By choosing $\alpha < 1$, the mechanism of interest rather obfuscates the magnitudes of individual dataset items.

The adjacent datasets are obfuscated in the mechanism output by means of randomization using one of the three strategies depicted in Figure 3.4. Regardless of the chosen strategy, consider a randomized counterpart $\tilde{\mathcal{M}}$ of a deterministic OPF mechanism \mathcal{M} . The randomized mechanism is said to be differentially private if it satisfies the following definition.

Definition 8 (Differential Privacy [27]). *A randomized mechanism $\tilde{\mathcal{M}} : \mathcal{D} \mapsto \mathcal{R}$ with domain \mathcal{D} and range \mathcal{R} is (ε, δ) -differential private if, for any output $O \subseteq \mathcal{R}$ and any two adjacent datasets $D \sim_\alpha D' \in \mathcal{D}$*

$$\mathbb{P}[\tilde{\mathcal{M}}(D) \in O] \leq \exp(\varepsilon) \mathbb{P}[\tilde{\mathcal{M}}(D') \in O] + \delta, \quad (3.7)$$

where \mathbb{P} denotes the probability over runs (executions) of $\tilde{\mathcal{M}}$.

In this definition, ε is the privacy loss and $\delta \in (0, 1)$ is the probability of failure; both are differential privacy parameters that respectively bound the multiplicative and additive differences between output distributions obtained on different datasets. Thus, the smaller assignments of ε and δ result in stronger privacy protection. When $\delta \rightarrow 0$, mechanism $\tilde{\mathcal{M}}$ satisfies the pure definition of ε -differential privacy. This privacy property can be relaxed by allowing a typically small probability of failure δ . Finally, observe that Definition 8 requires the mechanism to be differentially private for *any* adjacent pairs D and D' in the mechanism domain. Therefore, differential privacy is provided for any element $k \in \{1, \dots, n\}$ of n -dimensional input dataset, thus addressing individual privacy risks.

To enable formal differential privacy guarantees for optimization datasets, the noise parameters must be calibrated using the sensitivity of a mechanism to optimization datasets. The sensitivity reflects the change of mechanism output with respect to any single change in mechanism input.

Definition 9 (Global sensitivity [32]). *The global sensitivity Δ_n of a mechanism \mathcal{M} is defined by*

$$\Delta_n := \max_{D \sim_\alpha D'} \|\mathcal{M}(D) - \mathcal{M}(D')\|_n, \quad (3.8)$$

where D and D' are α -adjacent datasets in mechanism domain \mathcal{D} .

The sensitivity is global in the sense that it is defined over any α -adjacent load dataset within the mechanism domain. If a dataset D contains private loads, the sensitivity Δ_n shows the maximum change of the OPF solution with respect to any load changes for the given adjacency coefficient α . Unless the adjacency coefficient is marginal, computing Δ_n is difficult and its estimation reduces to finding upper bounds. For instance, if the private data is contained in constraint set, the maximum diameter of the Lowner-John ellipsoid enveloping the constraint set [58, Section 3.7.2.2] admits an upper bound on Δ_n [33]. Alternatively, the upper bound on the global sensitivity can be estimated from the structural properties of the problem of interest, as we establish in [Paper D]–[Paper F].

As the upper bounds on the global sensitivity are known to be conservative, the local mechanism sensitivity is often used to alleviate the conservatism. Unlike the global sensitivity, the local one is computed for any adjacent dataset in the neighbourhood of the original dataset.

Definition 10 (Local sensitivity [27]). *The local sensitivity s_n of a mechanism $\mathcal{M}(D)$ is defined by*

$$s_n := \max_{D'} \|\mathcal{M}(D) - \mathcal{M}(D')\|_n, \quad (3.9)$$

where D' is any α -adjacent to D dataset in mechanism domain \mathcal{D} .

The privacy properties are thus dependent on the choice of local or global mechanism sensitivity. Moreover, various noise distributions allow a data holder to choose between the pure differential privacy and its relaxations. For example, global ℓ_1 -sensitivity Δ_1 underpins the so-called Laplace mechanism, which provides global ε -differential privacy, as per the following result.

Theorem 11 (Laplace mechanism [27]). *Let $\mathcal{M} : \mathbb{R}^n \mapsto \mathbb{R}^m$ be a mechanism that maps n -dimensional datasets to m real numbers, and let Δ_1 be its global ℓ_1 -sensitivity on α -adjacent datasets. The randomized mechanism $\tilde{\mathcal{M}}(D) \triangleq \mathcal{M}(D) + \xi$, where $\xi \in \mathbb{R}^m$ is a zero-mean random vector from the Laplace distribution with scale Δ_1/ε , is ε -differentially private on α -adjacent datasets.*

By choosing ℓ_2 -sensitivity Δ_2 and the Gaussian noise distribution, the global ε -differential privacy is relaxed to allow violations of privacy guarantees with typically small probability δ .

Theorem 12 (Gaussian mechanism [27]). *Let $\mathcal{M} : \mathbb{R}^n \mapsto \mathbb{R}^m$ be a mechanism that maps n -dimensional datasets to m real numbers, and let Δ_2 be its global ℓ_2 -sensitivity on α -adjacent datasets. The randomized mechanism $\tilde{\mathcal{M}}(D) \triangleq \mathcal{M}(D) + \xi$, where $\xi \in \mathbb{R}^m$ is a random vector from a zero-mean Gaussian distribution $\mathcal{N}(0, \text{diag}[\sigma_1, \dots, \sigma_m])$ with $\sigma_i > \sqrt{2\ln(1.25/\delta)}\Delta_2/\varepsilon, \forall i \in \{1, \dots, m\}$, is (ε, δ) -differentially private on α -adjacent datasets.*

Repeated OPF computations on the same dataset accumulate privacy losses. A single run of the randomized mechanism $\tilde{\mathcal{M}}(D)$ induces the privacy loss for dataset D up to quantity ε with probability of failure δ . The same privacy loss is induced with every additional run of the mechanism. Over a course of several runs, the upper bound on the privacy loss induced for the dataset is given by the following result.

Theorem 13 (Sequential composition). *Consider K runs of mechanism $\tilde{\mathcal{M}}$, e.g., $\tilde{\mathcal{M}}^1(D), \dots, \tilde{\mathcal{M}}^K(D)$, such that every run depends on the result of the previous runs, i.e.,*

$$\tilde{\mathcal{M}}^k(D) = \tilde{\mathcal{M}}^k(D, \tilde{\mathcal{M}}^1(D), \tilde{\mathcal{M}}^2(D), \dots, \tilde{\mathcal{M}}^{k-1}(D)).$$

Suppose that $\tilde{\mathcal{M}}^k(D)$ preserves (ε, δ) -differential privacy for all k . Then, the K -tuple mechanism $\tilde{\mathcal{M}}(D) = (\tilde{\mathcal{M}}^1(D), \dots, \tilde{\mathcal{M}}^k(D), \dots, \tilde{\mathcal{M}}^K(D))$ preserves $(\varepsilon K, \delta K)$ -differential privacy.

The rest of the narrative is devoted to applications of these results to distributed and centralized OPF computations.

3.4 Differentially private distributed optimal power flow optimization

Distributed ADMM-based optimization algorithms are often assumed to preserve dataset privacy by avoiding the need of sharing sensitive optimization data. However, as we showed in Section 3.2, adversaries can still infer this information from ADMM coordination signals exchanged across iterations. In this section, we introduce provable privacy guarantees for distributed ADMM-based OPF computations. These guarantees are provided through several algorithms from [Paper D]. Here, we explain those algorithms through the generalized Algorithm 2. We first provide a technical description of the algorithm components. We then explain the privacy guarantees for a single iteration, the trade-offs between algorithm convergence and optimality loss, and how composition of differential privacy is used to extend the guarantee beyond one iteration.

3.4.1 Differentially private ADMM-based OPF algorithm

Relative to the base Algorithm 1, its differentially private counterpart Algorithm 2 includes random perturbations of local updates in Step 7 using function `PRIVATE_LOCAL_UPDATE`, detailed in Appendix A. The function maps datasets and input coordination signals to voltage updates as before, but uses the output perturbation strategy to obfuscate local datasets in voltage releases.

The distribution and calibration of random perturbations depend on privacy preferences expressed through differential privacy parameters (ε, δ) and input parameters `MECH`, `PERT`, `SENS`. The first parameter `MECH` = {LAPLACE, GAUSSIAN} allows to alternate between ε - and (ε, δ) -differential privacy guarantees according to Theorems 11 and 12, respectively. Parameter `PERT` = {STATIC, DYNAMIC}

Algorithm 2 Differentially private ADMM for OPF problem

Input: $K, \rho, \bar{\theta}^0, \mu^0, \bar{r}, \text{MECH, PERT, SENS, } \varepsilon, \delta$

- 1: **if** PERT = STATIC **and** MECH = LAPLACE **then** $\xi_n = \text{LAP}(\varepsilon, \text{SENS}), \forall n = 1, \dots, N$
 - 2: **else if** PERT = STATIC **and** MECH = GAUSSIAN **then** $\xi_n = \text{GAUSS}(\varepsilon, \delta, \text{SENS}), \forall n = 1, \dots, N$
 - 3: **end if**
 - 4: $k \leftarrow 0$
 - 5: **while** $r^k \leq \bar{r}$ **or** $k \leq K$ **do**
 - 6: $k \leftarrow k + 1$
 - 7: Local voltage update $\forall n = 1, \dots, N$:
 - 8: $\tilde{\theta}_n^k \leftarrow \text{PRIVATE_LOCAL_UPDATE}(\text{MECH, PERT, SENS}, \bar{\theta}^{k-1}, \mu_n^{k-1}, \rho, \xi_n)$
 - 9: Consensus variable update: $\bar{\theta}_n^k = \sum_{i=1}^N \tilde{\theta}_{in}^k / N, \quad \forall n = 1, \dots, N$
 - 10: Dual variable update: $\mu_n^k = \mu_n^{k-1} + \rho(\bar{\theta}^k - \tilde{\theta}_n^k), \quad \forall n = 1, \dots, N$
 - 11: Primal residual update: $r^k = \sum_{n=1}^N \|\bar{\theta}^k - \tilde{\theta}_n^k\|_2$
 - 12: **end while**
-

specifies if the perturbations are fixed and drawn prior to iterations in Steps 1-3, or they dynamically updated across iterations in Step 7. Finally, parameter SENS = {GLOBAL, LOCAL} specifies the sensitivity and alternates between global and local privacy guarantees.

The rest of the algorithm steps, including consensus and dual variable updates and the primal residual computation, remain the same as in Algorithm 1 but involve the perturbed local updates.

3.4.2 Privacy guarantee for a single iteration

Without further modifications, Algorithm 2 provides differential privacy guarantees for a single ADMM iteration. These guarantees originate due to the noise augmented to the output voltage angles in Step 7. Regardless of PERT assignment, consider the algorithm settings MECH = LAPLACE and SENS = GLOBAL, which require global ε -differential privacy. To show it analytically, let $\tilde{\mathcal{M}}_n^k : D_n \mapsto \mathbb{R}^N$ denote the randomized mechanism in Step 7 from a private dataset D_n to N voltage angles at iteration k , and let $\tilde{\theta}_n^k$ be some arbitrary result of this computation. Then, the ratio of probabilities that this randomized mechanism returns $\tilde{\theta}_n^k$ on two α -adjacent datasets D_n and D'_n is

$$\begin{aligned}
\frac{\mathbb{P}[\tilde{\mathcal{M}}_n^k(D_n) \in \tilde{\theta}_n^k]}{\mathbb{P}[\tilde{\mathcal{M}}_n^k(D'_n) \in \tilde{\theta}_n^k]} &= \frac{\mathbb{P}[\mathcal{M}_n^k(D_n) + \xi_n \in \tilde{\theta}_n^k]}{\mathbb{P}[\mathcal{M}_n^k(D'_n) + \xi_n \in \tilde{\theta}_n^k]} = \prod_{n'=1}^N \frac{\exp\left(-\frac{\varepsilon \|\xi_{nn'} - \mathcal{M}_{nn'}^k(D_n)\|_1}{\Delta_1^n}\right)}{\exp\left(-\frac{\varepsilon \|\xi_{nn'} - \mathcal{M}_{nn'}^k(D'_n)\|_1}{\Delta_1^n}\right)} \\
&= \prod_{n'=1}^N \exp\left(-\frac{\varepsilon \|\xi_{nn'} - \mathcal{M}_{nn'}^k(D'_n)\|_1 - \varepsilon \|\xi_{nn'} - \mathcal{M}_{nn'}^k(D_n)\|_1}{\Delta_1^n}\right) \\
&\leq \prod_{n'=1}^N \exp\left(\frac{\varepsilon \|\mathcal{M}_{nn'}^k(D_n) - \mathcal{M}_{nn'}^k(D'_n)\|_1}{\Delta_1^n}\right) \\
&= \exp\left(\frac{\varepsilon \|\mathcal{M}_n^k(D_n) - \mathcal{M}_n^k(D'_n)\|_1}{\Delta_1^n}\right),
\end{aligned} \tag{3.10}$$

where the second equality follows from the definition of the probability density function of the zero-mean Laplace distribution with scale Δ_1^n/ε , and the inequality follows from the inequality

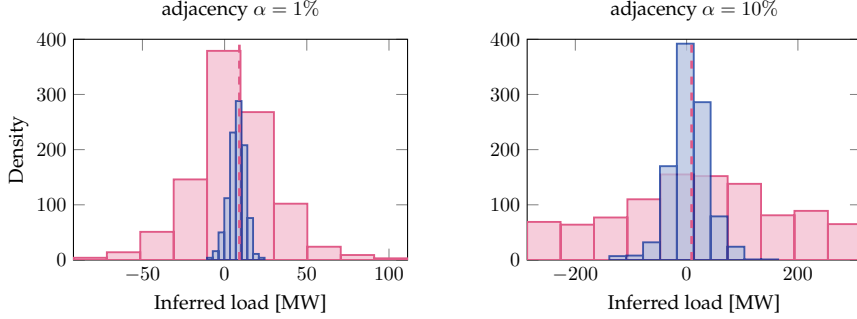


Figure 3.5: Results of the privacy attack on the ε -differentially private ADMM OPF algorithm with static perturbations using load reconstruction model in (3.5). The plots depict the distribution of inferred loads at node 20 of the IEEE 118-node system for 1,000 simulation runs. The left plot is for $\varepsilon = 1$ and $\alpha = 1\%$, while the right plot is for $\varepsilon = 1$ and $\alpha = 10\%$. The red and blue distributions are given for the global and local sensitivities Δ_i and s_i , respectively. The dashed red line depicts the true load value of 9 MW. For more results, refer to the source [Paper D].

of norms. Recall Definition 9 of the ℓ_1 global mechanism sensitivity on α -adjacent datasets. By substituting (3.8) in (3.10), we obtain

$$\mathbb{P}[\tilde{\mathcal{M}}_n^k(D_n) \in \tilde{\theta}_n^k] \leq \exp(\varepsilon) \mathbb{P}[\tilde{\mathcal{M}}_n^k(D'_n) \in \tilde{\theta}_n^k],$$

i.e., ε -differential privacy of mechanism $\tilde{\mathcal{M}}_n^k$. By setting `MECH = GAUSSIAN`, similarly to numerical queries [27, Appendix], it can be shown that Algorithm 2 provides each local dataset with the global (ε, δ) -differential privacy. Regardless of the chosen distribution, the privacy guarantee can be further relaxed by choosing the local mechanism sensitivity instead of the global one.

This privacy property is visualized in Figure 3.5, which shows the distributions of the inferred load across 1,000 runs of Algorithm 2 with settings `MECH = LAPLACE` and `PERT = STATIC`. With no perturbation, the attack model (3.5) successfully reconstructs the load value shown with the red dashed line. With the introduction of the noise, however, at each run of the algorithm a privacy adversary observes only a sample from these distributions. Thus, the privacy properties are stronger when the resulting distribution has a larger variance, which increases in adjacency coefficient α and when using the global mechanism sensitivity.

3.4.3 Convergence and optimality loss trade-offs

The perturbations of local updates affect the convergence and optimality loss of Algorithm 2. In [Paper D] we find that these two algorithmic properties can be traded off by choosing either static noise or dynamically updated perturbations across iterations. Figure 3.6 displays the convergence statistics of Algorithm 2 with static and dynamically updated random perturbations for various assignment of adjacency coefficient α . As dynamic perturbations are updated at every ADMM iteration, the variance of primal residuals increases in adjacency coefficient, thus requiring more iterations towards convergence. In contrast, the static perturbations are fixed across iterations and demonstrate more robust convergence. On the other hand, Table 3.1 collects the optimality loss reported for the two algorithms, showing that the static perturbations result in larger optimality losses. Thus, when providing the same privacy guarantee for a single iteration, Algorithm 2 features inherent trade-offs between the algorithm convergence and OPF optimality loss.

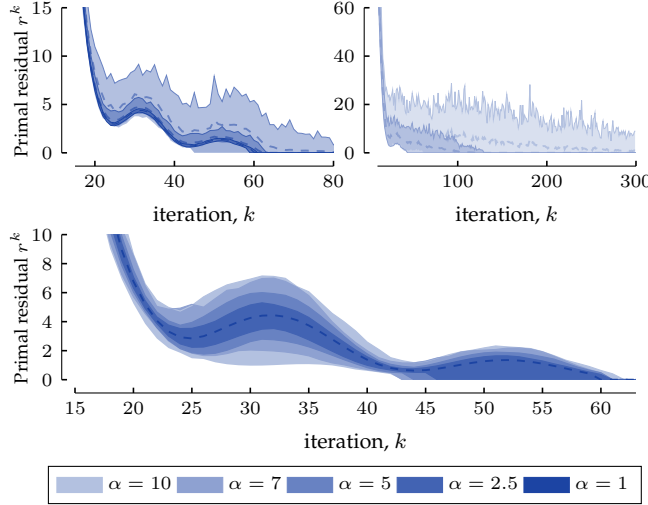


Figure 3.6: Evolution of the primal residual over ADMM iterations with dynamic (top) and static (bottom) random perturbations of local updates. The results are plotted for the 3-zone IEEE 118-node system for different adjacency coefficient α in %. The dashed lines indicate the average residual across 100 runs, whereas the colored areas indicate the spread between the minimum and maximum values of the residual at iteration k . Sourced from [Paper D].

Table 3.1: Optimality loss induced by ε -differentially private ADMM algorithms with static and dynamic perturbations (%). Sourced from [Paper D].

Adjacency coefficient α , %	1	2.5	5	7	10
Dynamic perturbations	0.48	0.92	1.23	1.51	3.83
Static perturbations	0.28	4.33	11.0	11.35	20.41

3.4.4 Controlling privacy loss beyond one iteration

Every new ADMM iteration brings additional privacy losses: Theorem 13 states that the ε -differential privacy guarantee of (any) Algorithm 2 for dataset D diminishes linearly with the number of runs on D . For the OPF problem of interest, this is illustrated with the right plot in Figure 3.7. The figure shows the inference error of the attack model (3.5) when an adversary observes last $K - T, \dots, K$ compromised iterations (attack budget is T iterations) of Algorithm 2 with parameters `MECH = LAPLACE`, `PERT = DYNAMIC` and `SENS = LOCAL`. This error reduces with every additional iteration made available to an adversary, which is consistent with a diminishing privacy guarantee. By scaling the random perturbation with respect to T number of compromised iterations, Algorithm 2 preserves ε -differential privacy guarantee. This is shown with the right plot in Figure 3.7, where the inference error does not reduce with more information revealed.

3.5 Differentially private centralized optimal power flow optimization

In many practical scenarios, the OPF problem is solved centrally by system operators, such that the privacy preservation using Algorithm 2 cannot be achieved. In centralized OPF computations, a system operator acts as a trust-worthy party that collects optimization datasets and performs OPF computations on behalf of all agents in the system. In this section, we introduce privacy-preserving

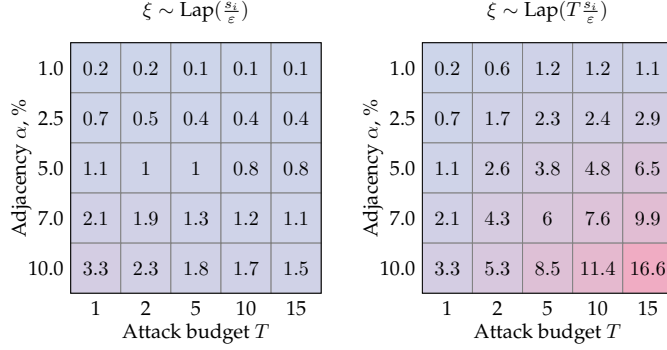


Figure 3.7: Composition for privacy loss control beyond one iteration: mean absolute inference error, i.e., mismatch between the actual and inferred loads in MWh, across last T iterations with (right) and without (left) scaling the noise for 100 simulation runs. Sourced from [Paper D].

centralized OPF computations to ensure that the sensitive information of system agents remains undisclosed when querying OPF solutions.

In the interest of presentation, let us rewrite the centralized OPF problem (3.1) more compactly as

$$\min_{x \in \mathbb{R}^k} c(x) \quad (3.11a)$$

$$\text{s.t. } x \in \mathcal{X}(D), \quad (3.11b)$$

where x is a vector of decision variables, including generator set-points and voltage angles, $c : \mathbb{R}^k \mapsto \mathbb{R}$ is a convex function, and \mathcal{X} represents a convex OPF feasible set, which is parameterized by private dataset D . Hence, the optimal solution x^* is a function of D and the queries on optimization results disclose private attributes of dataset D . These queries include the releases of dispatch decisions and power flows (identity queries), aggregated generation statistics (sum or average queries). To make these queries differentially private, the output perturbation strategy requires adding a calibrated noise to the optimal solution of problem (3.11), as illustrated in Figure 3.8 with a dashed density plot. This approach, however, is agnostic to the feasible set $\mathcal{X}(D)$ and may lead to infeasibility of privacy-preserving optimization results. To ensure solution feasibility, consider solution x , whose perturbation with a random noise yields a feasible solution with a high probability, as shown with a solid density function in Figure 3.8. We therefore seek a systematic way of identifying solution x that enables privacy guarantees for optimization datasets on the one hand, and feasibility guarantees for private optimization results on the other hand. Recognizing that random perturbations affect the utility of the optimization results in terms of optimality loss and solution variance, we aim at finding loss- and variance-aware solution x , whose perturbation results in the minimal impact on operational cost and variability of system operations. To ensure these desirable properties, i.e., privacy, feasibility, controllable optimality loss and OPF variance, we propose internalizing the Laplace and Gaussian mechanisms into constrained optimization problems using chance-constrained programming.

3.5.1 Internalizing Laplace and Gaussian mechanisms

To enable differentially private queries on the solutions of constrained optimization problems, we recast optimization problem (3.11) as the following stochastic program

$$\min_{\tilde{x}(\xi) \in \mathbb{R}^k} \mathbb{E}_\xi[c(\tilde{x}(\xi))] \quad (3.12a)$$

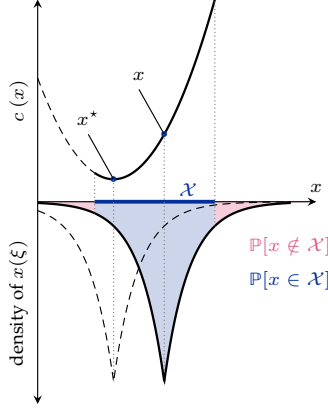


Figure 3.8: Stylized projections of randomized optimization solutions onto feasible space. When perturbing the optimal solution x^* with a random Laplace noise ξ , the probability of violating problem constraints is higher than perturbing solution x . Sourced from [Paper E].

$$\text{s.t. } \mathbb{P}_\xi[\tilde{x}(\xi) \in \mathcal{X}(D)] \geq 1 - \eta, \quad (3.12b)$$

$$\tilde{x}(\xi) \in \mathcal{Q}, \quad (3.12c)$$

which minimizes the expected cost by optimizing variable vector $\tilde{x}(\xi)$ that depends on some random perturbation $\xi \in \mathbb{R}^p, p \leq k$. The problem includes chance constraint (3.12b) that guarantees solution feasibility with the prescribed joint constraint satisfaction probability $1 - \eta$, for some small parameter η . As optimization variables are conditioned on random perturbation, the queries made on $\tilde{x}(\xi)$ are also random. The last constraint (3.12c) is thus enforced to ensure that $\tilde{x}(\xi)$ is distributed according to the query of interest. We focus on *linear* queries that assume any affine transformation of random vector $\tilde{x}(\xi)$, such as identity, sum and average queries. For example, the release of p active power flows in [Paper F] or p power dispatch quantities in [Paper E] are made using identity queries, while p zonal dispatch statistics in [Paper F] are made using the combination of identity and sum queries.

At this stage, chance-constrained problem (3.12) is computationally intractable as it optimizes over infinite-dimensional random variable $\tilde{x}(\xi)$. To overcome computational complexity, we model the random variable as the following affine function

$$\tilde{x}(\xi) \triangleq x + X\xi, \quad (3.13)$$

which consists of a nominal (mean) component x and a recourse component $X\xi$, where $X \in \mathbb{R}^{k \times p}$ is a finite-dimensional optimization variable. As the variable recourse is an affine function with respect to random perturbation ξ , we can obtain a tractable reformulation of chance-constrained problem (3.12) [10]. Observe, however, that the variable recourse X is a function of optimization dataset D , and thus the random components of any query made on $\tilde{x}(\xi)$ carries the information about dataset D as well. To make the random component data independent and thus enable differential privacy guarantees, we define query-specific constraint set $\mathcal{Q}(L)$, where the input matrix $L \in \mathbb{R}^{p \times k}$ is used to specify linear queries on $\tilde{x}(\xi)$, as we show with the following examples.

Example 1 (Identity query). *This query returns elements of vector $\tilde{x}(\xi)$ as $L\tilde{x}(\xi)$. Without loss of generality, consider the release of first p elements of vector $\tilde{x}(\xi)$, then matrix L becomes*

$$L \triangleq \begin{bmatrix} \text{diag}[1_p] & \mathbb{0}_{p \times (k-p)} \end{bmatrix},$$

such that under affine dependency (3.13), the linear query returns

$$L\tilde{x}(\xi) = \begin{bmatrix} x_1 \\ \vdots \\ x_p \end{bmatrix} + \begin{bmatrix} X_{11} & \dots & X_{1p} \\ \vdots & \ddots & \vdots \\ X_{p1} & \dots & X_{pp} \end{bmatrix} \begin{bmatrix} \xi_1 \\ \vdots \\ \xi_p \end{bmatrix},$$

which consists in the nominal (mean) and random components. To make the random component independent from the optimization data, the query-specific constraint set $\mathcal{Q}(L)$ is set as

$$\mathcal{Q}(L) \triangleq \{X | [L \circ X]_{p \times p} = \text{diag}[\mathbb{1}_p],\}$$

such that $L\tilde{x}(\xi) = \begin{bmatrix} x_1 \\ \vdots \\ x_p \end{bmatrix} + \begin{bmatrix} \xi_1 \\ \vdots \\ \xi_p \end{bmatrix}$ in optimality. Notice, when $p = k$, the identity query releases the entire optimization vector.

Example 2 (Release of p sum statistics). This query returns p number of sum statistics on vector $\tilde{x}(\xi)$ as $L\tilde{x}(\xi)$, such that $L_{ij} = 1$ if j element of $\tilde{x}(\xi)$ participates in statistic i , and $L_{ij} = 0$ otherwise. Consider, for example, $p = 2$ and $k = 4$, and the sum query as

$$L\tilde{x}(\xi) = \begin{bmatrix} 1 & 1 & 0 & 0 \\ 0 & 0 & 1 & 1 \end{bmatrix} \begin{bmatrix} \tilde{x}_1(\xi) \\ \vdots \\ \tilde{x}_4(\xi) \end{bmatrix} = \begin{bmatrix} x_1 + x_2 \\ x_3 + x_4 \end{bmatrix} + \begin{bmatrix} X_{11} + X_{21} & X_{12} + X_{22} \\ X_{31} + X_{41} & X_{32} + X_{42} \end{bmatrix} \begin{bmatrix} \xi_1 \\ \xi_2 \end{bmatrix},$$

where the random component can be made independent from the optimization dataset, when the query-specific constraint set $\mathcal{Q}(L)$ is

$$\mathcal{Q}(L) \triangleq \{X | LX = \text{diag}[\mathbb{1}_p]\},$$

such that in optimality we have $L\tilde{x}(\xi) = \begin{bmatrix} x_1 + x_2 \\ x_3 + x_4 \end{bmatrix} + \begin{bmatrix} \xi_1 \\ \xi_2 \end{bmatrix}$.

The main result of [Paper E] is to show that these linear queries on solution $\tilde{x}(\xi)$ can be made differentially private by calibrating the noise parameters and optimizing affine relation (3.13) under query-specific constraints. This result is arranged in two theorems in [Paper E] for identity and sum queries, respectively. As any linear query is representable through matrix L , we provide the following result to encompass the two theorems.

Theorem 14. Let L define the linear query on the solution of problem (3.11), let Δ_1 be the ℓ_1 query sensitivity to α -adjacent optimization datasets, and let $x^*(D)$ and $X^*(D)$ be the optimal solution to the chance-constrained program (3.12) obtained on some dataset D with $\xi \sim \text{Lap}(\Delta_1/\varepsilon)^p$. Then, for some arbitrary query outcome $\hat{O} \in \mathbb{R}^p$ it holds that

$$\mathbb{P}_{\xi}[L(x^*(D) + X^*(D)\xi) \in \hat{O}] \leq \mathbb{P}_{\xi}[L(x^*(D') + X^*(D')\xi) \in \hat{O}] \exp(\varepsilon),$$

for any α -adjacent optimization datasets D and D' .

The proof is identical to the proofs of differentially private identity and sum queries provided in [Paper E]. It first shows data independence of the query's random component, and then repeats the proof of the Laplace mechanism from Theorem 11 outlined in Section 3.4.

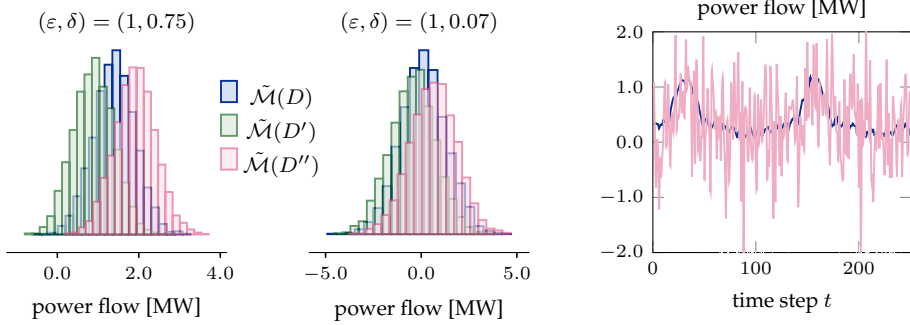


Figure 3.9: Obfuscation of customer load profile from Figure 3.2 in power flow measurements. The two left plots show the overlay of power flow probability densities obtained on the three 0.3MW-adjacent load datasets for different privacy requirements at time step 1 ($D = 2.35$, $D' = 2.05$, $D'' = 2.65$ MW). Observe, with smaller privacy parameters, the similarity of the three distributions improve, thus improving privacy. The right plot shows the mean (blue) and sampled (red) power flow trajectories obtained from the $(1, 0.07)$ -differentially private flow identity queries. The detailed model and experimental description are available in the source [Paper F].

As a consequence of Theorem 14, the privacy-preserving solution to centralized optimization (3.11) is obtained by sampling the result from optimized function (3.13). This way, the Laplace mechanism is internalized into the constrained optimization problem, and we refer to it as the mechanism perturbation in Figure 3.4. While this approach provides identical privacy guarantees as those of input and output perturbation methods, it also ensures solution feasibility. Finally, by choosing the Gaussian distribution of random perturbation ξ and calibrating it to the ℓ_2 -sensitivity Δ_2 , we enable (ε, δ) -differential privacy guarantees for optimization datasets.

Figure 3.9 illustrates how the chance-constrained problem enables differentially private queries of power flows in the face of tracing load privacy attacks discussed in Section 3.2.3. A careful calibration of the noise parameters makes α -adjacent load datasets statistically indistinguishable, such that by observing a sample from the resulting output distribution, an adversary cannot infer the load from the power flow profile, up to the prescribed privacy parameters.

3.5.2 Feasibility guarantees

To guarantee the satisfaction of equality constraints, we separate them into nominal and random components with respect to perturbation ξ . The former requires balancing the nominal optimization variables as dictated by the original deterministic problem, while the random component is constrained to add up to zero for any realization of ξ . Following the discussion in [59, Section 3.2], this provides the equality constraint satisfaction with probability 1.

To enable feasibility guarantees for inequality constraints, we refer to sample-based and analytical convex reformulations of chance constraint (3.12b). The sample-based reformulation due to [44] provides the joint constraint satisfaction guarantee up to the prescribed probability and requires enforcing all inequalities in (3.12b) on a finite number of samples drawn from the distribution of ξ . The number of samples, however, increases in a number of decision variables k , which is shown to affect computational complexity. To alleviate the complexity, the method from [60] enforces the entries of (3.12b) only on the vertices of a rectangular set built upon extracted samples. The number of samples in this case depends on a number of random perturbations p , which results

Table 3.2: The feasibility and optimality summary of private identity queries of OPF dispatch solutions obtained on 100 optimization dataset samples using a series of standard network typologies. The identity query privately releases 30% of nodal power supplies across the network. OP stands for output perturbation method as in Figure 3.4, CCS stands for chance-constrained solution, while appendixes -a and -s indicate analytical and sample-based reformulation of chance constraints, respectively. The detailed experimental description is available in the source [Paper E].

Case ID	$n \times \mathcal{X} $	Empirical constraint violation $\mathbb{P}[x \notin \mathcal{X}] [\%]$						Optimality loss $\Delta C [\%]$			
		OP		CCS-a		CCS-s		CCS-a		CCS-s	
		mean	std	mean	std	mean	std	mean	std	mean	std
3_lmbd	6×17	29.7	23.07	0.64	0.34	0.27	0.31	3.42	3.55	5.72	7.64
5_pjm	10×29	18.32	22.94	0.39	0.41	0.12	0.3	1.22	2.07	2.04	3.03
14_ieee	28×84	52.24	26.85	1.48	0.78	0.27	0.25	1.55	1.33	3.45	2.88
39_epri	78×211	95.56	4.69	4.86	1.32	0.49	0.35	2.17	0.81	4.7	1.68
57_ieee	114×333	98.59	1.91	7.17	1.50	1.28	1.06	2.4	0.78	5.51	5.06
118_ieee	236×728	99.99	0.02	14.35	2.06	1.51	0.47	2.46	0.56	4.89	1.20

in a smaller computational burden as we consider $p \leq k$. This approach is used in [Paper E] to provide joint constraint satisfaction guarantees at scale.

The feasibility guarantees can also be provided with the analytical reformulations of individual chance constraints. The joint chance constraint (3.12b) enforced on N_{\leq} number of inequalities can be recast as the union of individual chance constraints with individual violation probabilities $\bar{\eta} \in \mathbb{R}^{N_{\leq}}$. When the individual probabilities are such that $\mathbf{1}^\top \bar{\eta} \leq \eta$, this approach admits the approximation of the joint chance constraint [45]. Using analytical reformulations of individual chance constraints for the Laplace noise distribution from [61] (result for symmetric and unimodal distributions) and for the Gaussian noise distribution from [11], optimization problem (3.12) transforms into a computationally efficient second-order cone program, as shown in [Paper E] and [Paper F].

Using either sample-based or analytical reformulation of the joint chance constraints, one ensures problem feasibility in $(1 - \eta)\%$ samples from optimized function (3.13). Table 3.2 reports the out-of-sample statistics for the sampled private OPF solutions from the optimized function (3.13). Using the sample-based reformulation, we set the prescribed joint chance-constrained probability as $\eta = 2.5\%$. We set the same prescribed probability for individual chance constraints reformulated in an analytical manner to compare the conservatism of the solution in terms of optimality loss with respect to the non-private, noiseless OPF solution. Observe from the table, that the standard output perturbation mechanism systematically fails to ensure private solution feasibility even for small problem instances, while the chance-constrained solution holds the promise of either joint (sample-based reformulation) or individual (analytical reformulation) constraint satisfaction guarantee. Observe further, that holding the promise of joint constraint satisfaction induces a significantly larger optimality loss than that under individual constraint satisfaction guarantees.

It is important to note that if the sampling of the private optimization result from (3.13) returns an infeasible instance (with probability η), the re-sampling from (3.13) will induce additional privacy loss as per differential privacy composition (Theorem 13). With Theorem 5 in [Paper E] we show that this privacy loss can be avoided with a proper scaling of the noise parameters.

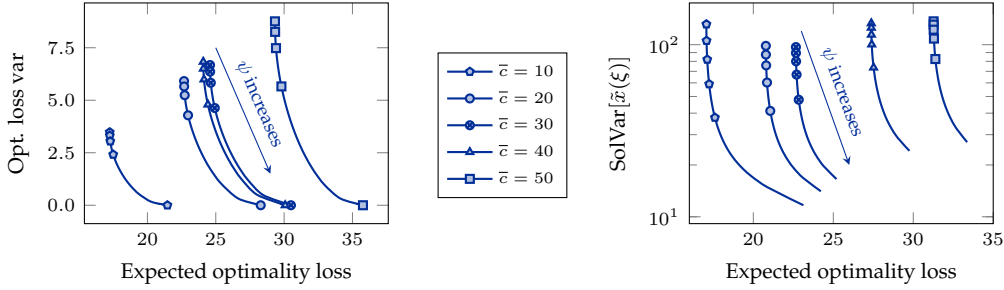


Figure 3.10: Trade-offs obtained for the private sum statistics of OPF dispatch variables for the IEEE 118-node test system for various supply cost sparsity: expected value versus variance of optimality loss (left) and expected optimality loss versus solution variance (right). The results are given for $c \sim U[1, \bar{c}]$ and averaged over 100 runs. The detailed experiment description is available in the source [Paper E].

3.5.3 Controlling optimality loss and solution variance

When producing differentially private queries using the criterion of the minimum expected cost, chance-constrained program (3.12) yields the probability density of candidate private solutions to problem (3.11) irrespective of the worst-case realization of optimality loss. Moreover, under the same criterion, the chance-constrained program optimizes function (3.13) disregarding the variance of the optimization solution, thus leading to a possible large variability of the OPF solutions. These two issues have been addressed in [Paper E] and [Paper F] by internalizing the variance and the conditional value-at-risk (CVaR) measures into chance-constrained program (3.12).

The expected optimality loss ΔC of the privacy-preserving solution with respect to the optimal solution x^* of problem (3.11) expresses as

$$\Delta C = \|c(x^*) - \mathbb{E}_\xi[c(\tilde{x}(\xi))]\|_2. \quad (3.14)$$

Since $c(x^*)$ is a constant value, the optimization of the expected optimality loss boils down to solving chance-constrained program (3.12). Similarly, the variance of the optimality loss is minimized when minimizing the variance of the random cost $\text{CostVar}[c(\tilde{x}(\xi))]$ with respect to random perturbation. Let $\Sigma \in \mathbb{R}^{p \times p}$ be the covariance matrix of p -dimensional random perturbation ξ , and assume the linear cost function $c(x) = c^\top x$. Then, under the affine dependency on random perturbation (3.13), the variance of the cost function (and thus the variance of optimality loss) expresses as

$$\text{CostVar}[c(\tilde{x}(\xi))] = \text{Var}[c^\top(x + X\xi)] = \text{Var}[c^\top x] + \text{Var}[c^\top X\xi] = \text{Tr}[X^\top \text{diag}[c] X \Sigma], \quad (3.15)$$

which is convex with respect to the decision variable x and X and hence can be optimized by modifying problem (3.12) as

$$\min_{x, X} \mathbb{E}_\xi[c^\top(x + X\xi)] + \psi \text{CostVar}[c^\top(x + X\xi)] \quad (3.16a)$$

$$\text{s.t. Equations (3.12b) -- (3.12c),} \quad (3.16b)$$

where ψ is a non-negative parameter to trade off between the expected value and the variance of the random cost. By increasing ψ , the variance of the optimality loss is penalized to reduce its worst-case outcomes. Similarly, the total variance of the random optimization vector $\tilde{x}(\xi)$ under affine dependency on random perturbation expresses as

$$\text{SolVar}[\tilde{x}(\xi)] = \text{Var}[x + X\xi] = \text{Var}[x] + \text{Var}[X\xi] = \text{Tr}[X^\top \text{diag}[1] X \Sigma], \quad (3.17)$$

which can be optimized similarly to problem (3.16). These variance-aware strategies have been adopted in [Paper E] and [Paper F], while the CVaR measure is also internalized into the chance-constrained program in [Paper F].

Figure 3.10 illustrates the trade-offs between (i) the expected optimality loss and its variance and (ii) the expected optimality loss and the overall solution variance. These trade-offs are available without affecting the privacy guarantees of Theorem 14 due to equation (3.12c) on the optimal recourse. As a consequence, the privacy-preserving mechanism perturbation based on the chance-constrained program provides more degrees of freedom to produce differentially private queries over the optimization results, which is not available with the standard variance-agnostic output or input perturbation methods.

CHAPTER 4

Conclusions and Perspectives

This thesis contributes by advancing stochastic optimization applications to and providing privacy guarantees for modern energy system operations. In this chapter, we summarize the main results and outline directions for future research.

4.1 Overview of contributions

This thesis first addressed the interpretability of stochastic method applications to energy system optimization. Starting with [Paper A], we introduced control policies for energy network components to accommodate network parameters' stochasticity. These policies are optimized using chance-constrained programming to guide system operations towards feasible and minimal variance solutions and interpret each system component's contribution to uncertainty and variability control. Furthermore, the dual solution to this chance-constrained optimization established a stochastic market settlement, which yields efficient payments in a stochastic sense: they ensure the fundamental market properties of cost recovery and revenue adequacy in expectation.

The stochastic market settlement properties may prevent the transition from deterministic to stochastic operational practices: negative profits in certain uncertain realizations are noninterpretable to market participants whose cost recovery is always ensured within conventional, deterministic settlements. To facilitate this transition, in [Paper B] we proposed to approximate the stochastic solution within deterministic market settlements through the optimal reserve quantification in power systems. Similar to stochastic methods, the reserves are quantified to provide cost-optimality in expectation and real-time feasibility, while sacrificing the cost efficiency of the stochastic solution to ensure the market properties' satisfaction for all prescribed uncertainty realizations.

We further studied the completeness of stochastic market settlements under asymmetry of agent information on the underlying uncertainty. In [Paper C] we found that the stochastic preferences of market participants are only supported if the underlying market-clearing mechanism is completed and accommodates private uncertainty forecasts. Towards completeness, we proposed market redesign solutions based on centralized and distributed computations of market equilibrium. Although completed, we also find that those markets tend to reduce social welfare if the information is inconsistent among agents. We further found a significant economic, operational, and computational value stemming from information sharing.

Concerning the private optimization of energy systems, [Paper D]–[Paper F] first identified significant privacy risks that originate in optimizing the standard operational tasks. By developing adversarial models of privacy attacks, we showed that sensitive dataset items, such as electrical loads in power systems, are exposed when querying optimization results, thus discouraging privacy-cognizant agents from engaging with energy systems. To minimize privacy violation risks and facilitate ethical data utilization, we developed a systematic approach to augment the routine

optimization tasks with a privacy-preserving layer that provides rigorous privacy guarantees for optimization datasets. These guarantees originate from differential privacy theory, which has been applied to solve operational OPF problems privately in power systems for the first time.

The proposed privacy-preserving algorithms first contribute by dispelling a common belief about the privacy-preserving power of the standard distributed OPF algorithms that distribute and store optimization datasets in algorithm sub-problems but tend to leak those datasets through the exchange of coordination signals. We thus developed in [Paper D] differentially private distributed algorithms that decouple local optimization datasets from coordination signals through their carefully calibrated perturbations. These perturbations offset any adversarial inference of local datasets, provide theoretical privacy guarantees for single and multiple iterations, and tend to converge to near optimality depending on the chosen privacy preferences.

Towards the centralized privacy-preserving power system operations in high-voltage and distribution grids, we developed differentially private stochastic OPF models in [Paper E] and [Paper F], respectively. Unlike the standard input or output perturbation methods that disregard the feasible space of OPF problems, the proposed models provide both privacy and feasibility guarantees a priori, up to prescribed privacy and constraint violation parameters. This way, the OPF datasets can be gradually decoupled from the optimization outcomes without exposing power grids to unsafe operations. Moreover, these differentially private models internalize the variance and CVaR risk measures to control the utility of private optimization results in terms of optimality losses and the variance of OPF state variables.

4.2 Future research

The main results of this thesis motivate several future research directions concerning stochastic and private energy system optimization.

We have discussed the optimization of stochastic control policies from [Paper A] without an explicit account for uncertainty and variability in the coupled energy networks. While natural gas, heat and electricity systems seek efficient stochastic coordination, the proposed policies enable operational and market coordination by offering new cross-system contracts for uncertainty and variability control. For example, natural gas compressors and injections can be rewarded for variability control of voltages in the electricity network. Moreover, the developed control policies manage uncertainty and variability in relation to the *primal* solution feasibility and its variance, disregarding the impacts of random system parameters on *dual* prices used for energy market clearing. Hence, duality-aware policy optimization constitutes a relevant research direction to exploit system flexibility to control the distributional properties of uncertain and variable natural gas, heat and electricity prices.

As we show through [Paper B], the approximation of the stochastic solution within conventional market procedures requires sophisticated decomposition techniques to enable scalability as well as large market datasets that are not always available. A promising research direction is to develop a data-free training of the parameter of interest, e.g. reserve requirements as in [Paper B], to achieve the stochastic approximation. Online machine learning could provide scalable and data-free solution techniques: the parameter of interest can be made a function of uncertainty in the spirit of control policies in [Paper A], which is trained throughout daily-based, repeated dispatch procedures towards cost-optimal and feasible solutions.

Towards completing the market from the information standpoint, in [Paper C] we found that the inconsistency of agent private information on the true distribution leads to significant social welfare losses. This motivates future research towards designing information marketplaces that incentivize information exchange to align private priors and improve private and social welfare.

While developing differentially private ADMM-based OPF algorithms in [Paper D], we found that dynamically updated perturbations of ADMM coordination signals accumulate a large variance of primal residuals, which complicates the algorithm convergence to OPF-feasible operating points. This motivates the research towards feasibility-aware private ADMM designs that accommodate non-zero primal residuals. Since the resulting primal residuals are random at algorithm termination, the algorithm sub-problems can be granted with control policies (as in [Paper E] and [Paper F]), which define post-termination adjustments of the OPF solution with respect to primal residual realizations. To adequately optimize such policies, one needs to study the parameters of the primal residual distribution as a function of privacy preferences.

In line with [Paper A], the differentially private stochastic OPF models in [Paper E] and [Paper F] establish a stochastic market settlement to (i) compensate power producers for accommodating privacy-preserving perturbations and (ii) charge network loads for their privacy preferences encoded in those perturbations. Following marginal pricing schemes, however, the market properties of cost recovery and revenue adequacy are guaranteed only in expectation, as we established with the analysis of stochastic market settlements in Chapter 2. Moreover, network discrimination effects of marginal pricing risk to charge grid customers differently for the same privacy preferences, i.e., privacy cost depends on load position in the network. This motivates research on optimal privacy pricing. As a potential solution, marginal electricity pricing can be complemented with privacy subscriptions that are non-discriminatory towards grid customers but also ensure cost recovery and revenue adequacy of electricity payments beyond expectation.

Bibliography

- [1] E. Ela, F. Billimoria, K. Ragsdale, S. Moorty, J. O’Sullivan, R. Gramlich, M. Rothleder, B. Rew, M. Supponen, and P. Sotkiewicz. Future electricity markets: Designing for massive amounts of zero-variable-cost renewable resources. *IEEE Power and Energy Magazine*, 17(6):58–66, 2019.
- [2] Hélène Le Cadre, Ilyès Mezghani, and Anthony Papavasiliou. A game-theoretic analysis of transmission-distribution system operator coordination. *European Journal of Operational Research*, 274(1):317–339, 2019.
- [3] Lejla Halilbašić, Spyros Chatzivasileiadis, and Pierre Pinson. Coordinating flexibility under uncertainty in multi-area AC and DC grids. In *2017 IEEE Manchester PowerTech*, pages 1–6. IEEE, 2017.
- [4] Frauke Wiese, Ingmar Schlecht, Wolf-Dieter Bunke, Clemens Gerbaulet, Lion Hirth, Martin Jahn, Friedrich Kunz, Casimir Lorenz, Jonathan Mählenpfordt, Juliane Reimann, and Wolf-Peter Schill. Open power system data—frictionless data for electricity system modelling. *Applied Energy*, 236:401–409, 2019.
- [5] Yi Wang, Qixin Chen, Tao Hong, and Chongqing Kang. Review of smart meter data analytics: Applications, methodologies, and challenges. *IEEE Transactions on Smart Grid*, 10(3):3125–3148, 2018.
- [6] Constance Douris. Balancing smart grid data and consumer privacy. Lexington Smart Grid Data Privacy, 2017. https://www.lexingtoninstitute.org/wp-content/uploads/2017/07/Lexington_Smart_Grid_Data_Privacy-2017.pdf. Accessed: December 22, 2020.
- [7] Ruidi Chen, Ioannis Ch Paschalidis, Michael C Caramanis, and Panagiotis Andrianesis. Learning from past bids to participate strategically in day-ahead electricity markets. *IEEE Transactions on Smart Grid*, 10(5):5794–5806, 2019.
- [8] Ferdinando Fioretto, Terrence WK Mak, and Pascal Van Hentenryck. Predicting AC optimal power flows: Combining deep learning and lagrangian dual methods. In *Proceedings of the AAAI Conference on Artificial Intelligence*, volume 34, pages 630–637, 2020.
- [9] Robert Mieth and Yury Dvorkin. Online learning for network constrained demand response pricing in distribution systems. *IEEE Transactions on Smart Grid*, 11(3):2563–2575, 2019.
- [10] Aharon Ben-Tal, Laurent El Ghaoui, and Arkadi Nemirovski. *Robust optimization*, volume 28. Princeton University Press, 2009.
- [11] Alexander Shapiro, Darinka Dentcheva, and Andrzej Ruszczyński. *Lectures on stochastic programming: modeling and theory*. SIAM, 2014.

- [12] Arkadi Nemirovski and Alexander Shapiro. Convex approximations of chance constrained programs. *SIAM Journal on Optimization*, 17(4):969–996, 2007.
- [13] Daniel Bienstock, Michael Chertkov, and Sean Harnett. Chance-constrained optimal power flow: Risk-aware network control under uncertainty. *SIAM Review*, 56(3):461–495, 2014.
- [14] Daniel Bienstock and Apurv Shukla. Variance-aware optimal power flow: Addressing the tradeoff between cost, security, and variability. *IEEE Transactions on Control of Network Systems*, 6(3):1185–1196, 2019.
- [15] Anubhav Ratha, Anna Schewe, Jalal Kazempour, Pierre Pinson, Shahab Shariat Torbaghan, and Ana Virag. Affine policies for flexibility provision by natural gas networks to power systems. *Electric Power Systems Research*, 189, 2020. Article no. 106565.
- [16] Miles Lubin, Yury Dvorkin, and Line Roald. Chance constraints for improving the security of ac optimal power flow. *IEEE Transactions on Power Systems*, 34(3):1908–1917, 2019.
- [17] Robert Mieth, Jip Kim, and Yury Dvorkin. Risk-and variance-aware electricity pricing. *Electric Power Systems Research*, 189, 2020. Article no. 106804.
- [18] Juan M Morales, Antonio J Conejo, Kai Liu, and Jin Zhong. Pricing electricity in pools with wind producers. *IEEE Transactions on Power Systems*, 27(3):1366–1376, 2012.
- [19] Juan M Morales, Marco Zugno, Salvador Pineda, and Pierre Pinson. Electricity market clearing with improved scheduling of stochastic production. *European Journal of Operational Research*, 235(3):765–774, 2014.
- [20] Beibei Wang and B. F. Hobbs. Flexiramp market design for real-time operations: Can it approach the stochastic optimization ideal? In *2013 IEEE Power & Energy Society General Meeting*, pages 1–5, 2013.
- [21] Anthony Papavasiliou and Yves Smeers. Remuneration of flexibility using operating reserve demand curves: A case study of Belgium. *The Energy Journal*, 38(6), 2017.
- [22] Paul A Samuelson. Spatial price equilibrium and linear programming. *The American Economic Review*, 42(3):283–303, 1952.
- [23] Steven A Gabriel, Antonio J Conejo, J David Fuller, Benjamin F Hobbs, and Carlos Ruiz. *Complementarity modeling in energy markets*, volume 180. Springer Science & Business Media, 2012.
- [24] Dimitris Bertsimas and David B Brown. Constructing uncertainty sets for robust linear optimization. *Operations Research*, 57(6):1483–1495, 2009.
- [25] Henri Gérard, Vincent Leclère, and Andy Philpott. On risk averse competitive equilibrium. *Operations Research Letters*, 46(1):19–26, 2018.
- [26] Amos Tversky and Daniel Kahneman. Advances in prospect theory: Cumulative representation of uncertainty. *Journal of Risk and Uncertainty*, 5(4):297–323, 1992.
- [27] Cynthia Dwork and Aaron Roth. The algorithmic foundations of differential privacy. *Foundations and Trends in Theoretical Computer Science*, 9(3-4):211–407, 2014.

- [28] Justin Hsu, Aaron Roth, Tim Roughgarden, and Jonathan Ullman. Privately solving linear programs. In *International Colloquium on Automata, Languages, and Programming*, pages 612–624. Springer, 2014.
- [29] Ferdinando Fioretto, Terrence WK Mak, and Pascal Van Hentenryck. Differential privacy for power grid obfuscation. *IEEE Transactions on Smart Grid*, 11(2):1356–1366, 2020.
- [30] Fengyu Zhou, James Anderson, and Steven H Low. Differential privacy of aggregated DC optimal power flow data. In *2019 American Control Conference (ACC)*, pages 1307–1314, 2019.
- [31] Shuo Han, Ufuk Topcu, and George J Pappas. Differentially private distributed constrained optimization. *IEEE Transactions on Automatic Control*, 62(1):50–64, 2016.
- [32] Cynthia Dwork, Frank McSherry, Kobbi Nissim, and Adam Smith. Calibrating noise to sensitivity in private data analysis. In *Theory of Cryptography Conference*, pages 265–284. Springer, 2006.
- [33] Shuo Han, Ufuk Topcu, and George J Pappas. Differentially private convex optimization with piecewise affine objectives. In *53rd IEEE Conference on Decision and Control*, pages 2160–2166, 2014.
- [34] Daniel K Molzahn, Florian Dörfler, Henrik Sandberg, Steven H Low, Sambuddha Chakrabarti, Ross Baldick, and Javad Lavaei. A survey of distributed optimization and control algorithms for electric power systems. *IEEE Transactions on Smart Grid*, 8(6):2941–2962, 2017.
- [35] Ferdinando Fioretto and Pascal Van Hentenryck. Constrained-based differential privacy: Releasing optimal power flow benchmarks privately. In *International Conference on the Integration of Constraint Programming, Artificial Intelligence, and Operations Research*, pages 215–231. Springer, 2018.
- [36] Andreas Venzke, Lejla Halilbasic, Uros Markovic, Gabriela Hug, and Spyros Chatzivasileiadis. Convex relaxations of chance constrained AC optimal power flow. *IEEE Transactions on Power Systems*, 33(3):2829–2841, 2017.
- [37] Yury Dvorkin. A chance-constrained stochastic electricity market. *IEEE Transactions on Power Systems*, 35(4):2993–3003, 2020.
- [38] Daniel Kifer and Ashwin Machanavajjhala. No free lunch in data privacy. In *Proceedings of the 2011 ACM SIGMOD International Conference on Management of Data*, pages 193–204, 2011.
- [39] Mary B Cain, Richard P O’Neill, and Anya Castillo. History of optimal power flow and formulations. *Federal Energy Regulatory Commission*, 1:1–36, 2012.
- [40] Thorsten Koch, Benjamin Hiller, Marc E Pfetsch, and Lars Schewe. *Evaluating gas network capacities*. SIAM, 2015.
- [41] Steven H Low. Convex relaxation of optimal power flow-Part I: Formulations and equivalence. *IEEE Transactions on Control of Network Systems*, 1(1):15–27, 2014.
- [42] Manish K Singh and Vassilis Kekatos. Natural gas flow solvers using convex relaxation. *IEEE Transactions on Control of Network Systems*, 7(3):1283–1295, 2020.

- [43] Joseph Warrington, Paul Goulart, Sébastien Mariéthoz, and Manfred Morari. Policy-based reserves for power systems. *IEEE Transactions on Power Systems*, 28(4):4427–4437, 2013.
- [44] Marco C Campi and Simone Garatti. The exact feasibility of randomized solutions of uncertain convex programs. *SIAM Journal on Optimization*, 19(3):1211–1230, 2008.
- [45] Weijun Xie, Shabbir Ahmed, and Ruiwei Jiang. Optimized Bonferroni approximations of distributionally robust joint chance constraints. *Mathematical Programming*, pages 1–34, 2019.
- [46] Jalal Kazempour, Pierre Pinson, and Benjamin F Hobbs. A stochastic market design with revenue adequacy and cost recovery by scenario: Benefits and costs. *IEEE Transactions on Power Systems*, 33(4):3531–3545, 2018.
- [47] Lazaros Exizidis. *Electricity markets with high wind power penetration: Information Sharing and Incentive-Compatibility*. PhD thesis, University of Mons, 2017. DOI:[10.5281/zenodo.1195538](https://doi.org/10.5281/zenodo.1195538).
- [48] Leonid V Kantorovich. Mathematical methods of organizing and planning production. *Management Science*, 6(4):366–422, 1960.
- [49] Stephen Boyd, Stephen P Boyd, and Lieven Vandenberghe. *Convex optimization*. Cambridge university press, 2004.
- [50] Yann Rebours and Daniel Kirschen. A survey of definitions and specifications of reserve services. *Report, University of Manchester*, pages 1–38, 2005.
- [51] H. Holttinen, M. Milligan, E. Ela, N. Menemenlis, J. Dobschinski, B. Rawn, R. J. Bessa, D. Flynn, E. Gomez-Lazaro, and N. K. Detlefsen. Methodologies to determine operating reserves due to increased wind power. *IEEE Transactions on Sustainable Energy*, 3(4):713–723, 2012.
- [52] Hirofumi Uzawa. Walras tatonnement in the theory of exchange. *The Review of Economic Studies*, 27(3):182–194, 1960.
- [53] Antonio J Conejo and Jose A Aguado. Multi-area coordinated decentralized DC optimal power flow. *IEEE Transactions on Power Systems*, 13(4):1272–1278, 1998.
- [54] Vladimir Dvorkin, Pascal Van Hentenryck, Jalal Kazempour, and Pierre Pinson. Differentially private distributed optimal power flow. *arXiv preprint arXiv:1910.10136*, 2019.
- [55] Stephen Boyd, Neal Parikh, and Eric Chu. Distributed optimization and statistical learning via the alternating direction method of multipliers. *Foundation and Trends in Machine Learning*, 3(1):1–122, 2010.
- [56] Vanessa Krebs, Lars Schewe, and Martin Schmidt. Uniqueness and multiplicity of market equilibria on DC power flow networks. *European Journal of Operational Research*, 271(1):165–178, 2018.
- [57] Konstantinos Chatzikokolakis, Miguel E Andrés, Nicolás Emilio Bordenabe, and Catuscia Palamidessi. Broadening the scope of differential privacy using metrics. In *International Symposium on Privacy Enhancing Technologies Symposium*, pages 82–102. Springer, 2013.
- [58] Aharon Ben-Tal and Arkadi Nemirovski. *Lectures on modern convex optimization: analysis, algorithms, and engineering applications*. SIAM, 2001.

- [59] Daniel Kuhn, Wolfram Wiesemann, and Angelos Georghiou. Primal and dual linear decision rules in stochastic and robust optimization. *Mathematical Programming*, 130(1):177–209, 2011.
- [60] Kostas Margellos, Paul Goulart, and John Lygeros. On the road between robust optimization and the scenario approach for chance constrained optimization problems. *IEEE Transactions on Automatic Control*, 59(8):2258–2263, 2014.
- [61] Bart PG Van Parys, Paul J Goulart, and Daniel Kuhn. Generalized Gauss inequalities via semidefinite programming. *Mathematical Programming*, 156(1-2):271–302, 2016.

A. Functions used in Algorithm 2

Algorithm 2 makes use of several functions. Function $\text{LAP}(\varepsilon, \text{SENS})$ generates a vector of random variables $\xi \in \mathbb{R}^N$ from the multivariate zero-mean Laplace distribution. The scale of the distribution depends on the differential privacy parameter ε as well as on the global or local sensitivity, depending on the specification of algorithm parameter `SENS`. Simialrly, function $\text{GAUSS}(\varepsilon, \delta, \text{SENS})$ takes differential privacy parameters and `SENS` to produce random samples from the multivariate zero-mean Gaussian distribution. The last function `PRIVATE_LOCAL_UPDATE` computes the local voltage angle updates. If parameter `PERT` set to `STATIC`, the local updates are augmented with a random variables sampled at steps 1-3 of Algorithm 2. Otherwise, with `PERT = DYNAMIC`, the function samples the random variables at every ADMM iteration.

```
1: function LAP( $\varepsilon$ , SENS)
2:   sample random perturbation  $\xi$  using either global  $\Delta_1^n$  (SENS = GLOBAL) or local  $s_1^n$  (SENS = LOCAL) sensitivity and  $\varepsilon$  as in Theorem 11.
3:   return  $\xi$ 
4: end function

5: function GAUS( $\varepsilon, \delta, \text{SENS}$ )
6:   sample random perturbation  $\xi$  using either global  $\Delta_2^n$  (SENS = GLOBAL) or local  $s_2^n$  (SENS = LOCAL) sensitivity,  $\delta$  and  $\varepsilon$  as in Theorem 12.
7:   return  $\xi$ 
8: end function

9: function PRIVATE_LOCAL_UPDATE(MECH, PERT, SENS,  $\bar{\theta}$ ,  $\mu_n$ ,  $\rho$ ,  $\xi$ )
10:  Update  $\theta_n$  as in Step 7 of Algorithm 1
11:  if PERT = DYNAMIC and MECH = LAPLACE then
12:    return  $\theta_n + \text{LAP}(\varepsilon, \text{SENS})$ 
13:  else if PERT = DYNAMIC and MECH = GAUSSIAN then
14:    return  $\theta_n + \text{GAUSS}(\varepsilon, \delta, \text{SENS})$ 
15:  else if PERT = STATIC then
16:    return  $\theta_n + \xi$ 
17:  end if
18: end function
```


Collection of relevant publications

- [Paper A] V. Dvorkin, A. Ratha, P. Pinson. and J. Kazempour. "Stochastic control and market design for natural gas networks." *Submitted to the IEEE Transactions on Control of Network Systems*, 2020.
- [Paper B] V. Dvorkin, S. Delikaraoglou and J. M. Morales. "Setting reserve requirements to approximate the efficiency of the stochastic dispatch." in *IEEE Transactions on Power Systems*, vol. 34, no. 2, pp. 1524-1536, 2019.
- [Paper C] V. Dvorkin, J. Kazempour and P. Pinson. "Electricity market equilibrium under information asymmetry." in *Operations Research Letters*, vol. 47, no. 6, pp. 521-526, 2019.
- [Paper D] V. Dvorkin, P. Van Hentenryck, J. Kazempour and P. Pinson. "Differentially private distributed optimal power flow." in *59th Conference on Decision and Control*, to appear, 2020.
- [Paper E] V. Dvorkin, F. Fioretto, P. Van Hentenryck, P. Pinson and J. Kazempour. "Differentially private convex optimization with feasibility guarantees," *Preprint*, 2020.
- [Paper F] V. Dvorkin, F. Fioretto, P. Van Hentenryck, P. Pinson and J. Kazempour. "Differentially private optimal power flow for distribution grids." in *IEEE Transactions on Power Systems*, to appear, 2020, DOI: [10.1109/TPWRS.2020.3031314](https://doi.org/10.1109/TPWRS.2020.3031314).

[Paper A] Stochastic control and pricing for natural gas networks

Authors:

V. Dvorkin, A. Ratha, P. Pinson. and J. Kazempour.

Submitted to:

IEEE Transactions on Control of Network Systems

Stochastic Control and Pricing for Natural Gas Networks

Vladimir Dvorkin, Anubhav Ratha, Pierre Pinson and Jalal Kazempour

Abstract—We propose stochastic control policies to cope with uncertain and variable gas extractions in natural gas networks. Given historical gas extraction data, these policies are optimized to produce the real-time control inputs for nodal gas injections and for pressure regulation rates by compressors and valves. We describe the random network state as a function of control inputs, which enables a chance-constrained optimization of these policies for arbitrary network topologies. This optimization ensures the real-time gas flow feasibility and a minimal variation in the network state up to specified feasibility and variance criteria. Furthermore, the chance-constrained optimization provides the foundation of a stochastic pricing scheme for natural gas networks, which improves on a deterministic market settlement by offering the compensations to network assets for their contribution to uncertainty and variance control. We analyze the economic properties, including efficiency, revenue adequacy and cost recovery, of the proposed pricing scheme and make them conditioned on the network design.

Index Terms—Chance-constrained programming, conic duality, gas pricing, natural gas network, uncertainty, variance.

I. INTRODUCTION

Deterministic operational and market-clearing practices of the natural gas network operators struggle with the growing uncertainty and variability of natural gas extractions [1]. Ignorance of the uncertain and variable extractions results in technical and economical failures, as demonstrated by the congested network during the 2014 polar vortex event in the United States [2]. The recent study [3] shows that expanding the network to avoid the congestion is financially prohibitive, which encourages us to develop stochastic control policies to gain gas network reliability and efficiency in a short run.

Since the prediction of gas extractions involves errors, a gas network optimization problem has been addressed using the methods from robust optimization [4], scenario-based and chance-constrained stochastic programming [5]. Besides forecasts, they require a network response model to uncertainty, i.e., the mapping from random forecast errors to the network state. The robust solutions [6] optimize the network response to ensure the feasibility within robust uncertainty sets, but result in overly conservative operational costs. To alleviate the conservatism, scenario-based stochastic programs [7] optimize the network response to provide the minimum expected cost and ensure feasibility within a finite number of discrete scenarios. The major drawback of robust and scenario-based programs is their ignorance of the network state within

The authors would like to thank Ana Virág and Hélène Le Cadre for their helpful comments, Jochen Stiasny and Tue Jensen for the advice on visualizations, Robert Mieth and Yury Dvorkin for discussions.

V. Dvorkin, A. Ratha, P. Pinson and J. Kazempour are with the Department of Electrical Engineering, Technical University of Denmark, Lyngby, Denmark. Email: {vladvo, arath, ppin, seykaz}@elektro.dtu.dk

A. Ratha is also with the Flemish Institute of Technological Research (VITO), Boeretang 200, 2400 Mol, Belgium and with EnergyVille, ThorPark 8310, 3600 Genk, Belgium. {anubhav.ratha}@vito.be

the prescribed uncertainty set or outside the chosen scenarios. The chance-constrained programs [8], [9], in turn, yield an optimized network response across the entire forecast error distribution (or a family of those [10]), thus resulting in more advanced prediction and control of uncertain network state.

This work advocates the application of chance-constrained programming to the optimal natural gas network control under uncertainty. By optimal control, we imply the optimization of gas injection and pressure regulation policies that ensure gas flow feasibility and market efficiency for a given forecast error distribution. Towards this goal, we require a network response model with a strong analytic dependency between the network state and random forecast errors. Since natural gas flows are governed by non-convex equations, the design of network response models reduces to finding convex approximations. The work in [8, Chapter 6] enjoys the so-called controllable flow model [11], which balances gas injection and uncertain extractions but disregards pressure variables. It thus does not permit policies for pressure control and corresponding financial remunerations. The work in [9] preserves the integrity of system state variables and relies on the relaxation of non-convex equations. Although the relaxations are known to be tight [12], [13], the results of [9] show that even a marginal relaxation gap yields a poor out-of-sample performance of the chance-constrained solution. Furthermore, the relaxations involve the integrality constraints to model bidirectional gas flows, which prevents extracting the dual solution and thus designing an optimal pricing scheme. One needs to introduce the unidirectional flow assumption to avoid integrality constraints, which is restrictive for gas networks under uncertainty [9].

This work bypasses the simplifying assumptions on network operations through the linearization of the non-convex natural gas equations, and provides a convex network optimization that enables the real-time gas flow feasibility, controls the variability of the network state, and provides an efficient pricing scheme. Specifically, we make the following contributions:

- 1) We propose stochastic control policies for gas injections and pressure regulation rates that provide real-time control inputs for network operators. Through linearization, we describe the uncertain state variables, such as nodal pressures and flow rates as affine functions of control inputs; thus capturing the dependency of the uncertain network response on operator's decisions.
- 2) We introduce a chance-constrained program to optimize the control policies and provide its computationally efficient second-order cone programming (SOCP) reformulation. The policy optimization ensures that the network state remains within network limits with a high probability and utilizes the statistical moments of the state variables to trade-off between the expected cost and the variance of the state variables.
- 3) We propose a conic pricing scheme that remunerates net-

work assets, i.e., gas suppliers, compressors and valves, for their contribution to uncertainty and variance control. Unlike the standard linear programming duality, the conic duality enables the decomposition of revenue streams associated with the coupling chance-constraints. We analyze the economic properties of the conic pricing scheme, e.g. revenue adequacy and cost recovery, and make them conditioned on the network design.

At the operational planning stage, the optimized policies provide the best approximation (up to forecast quality) of the real-time control actions. They can be augmented into preoperational routines of network operators within the deterministic steady-state [13] or transient [14], [15] gas models in the form of gas injection and pressure regulation set-points, while providing the strong foundation for necessary financial remunerations. We corroborate the effectiveness of the proposed policies using a 48-node natural gas network.

Outline: Section II explains the gas network modeling, while Section III describes the stochastic network optimization, control policies and tractable reformulations. Section IV introduces the pricing scheme and its theoretical properties. Section V provides numerical experiments, and Section VI concludes. All proofs are relegated to Appendix.

Notation: Operation \circ is the element-wise product. Operator $\text{diag}[x]$ returns an $n \times n$ diagonal matrix with elements of vector $x \in \mathbb{R}^n$. For a $n \times n$ matrix A , $[A]_i$ returns an i^{th} row ($1 \times n$) of matrix A , $\langle A \rangle_i$ returns an i^{th} column ($n \times 1$) of matrix A , and $\text{Tr}[A]$ returns the trace of matrix A . Symbol \top stands for transposition, vector $\mathbb{1}$ ($\mathbb{0}$) is a vector of ones (zeros), and $\|\cdot\|$ denotes the Euclidean norm.

II. PRELIMINARIES

A. Gas Network Equations

A natural gas network is modeled as a directed graph comprising a set of nodes $\mathcal{N} = \{1, \dots, N\}$ and a set of edges $\mathcal{E} = \{1, \dots, E\}$. Nodes represent the points of gas injection, extraction or network junction, while edges represent pipelines. Each edge is assigned a direction from sending node n to receiving node n' , i.e., if $(n, n') \in \mathcal{E}$, then $(n', n) \notin \mathcal{E}$. The graph may contain cycles, while parallel edges and self-loops should not exist. The graph topology is described by a node-edge incidence matrix $A \in \mathbb{R}^{N \times E}$, such that

$$A_{k\ell} = \begin{cases} +1, & \text{if } k = n \\ -1, & \text{if } k = n' \\ 0, & \text{otherwise} \end{cases} \quad \forall \ell = (n, n') \in \mathcal{E}.$$

Let $\varphi \in \mathbb{R}^E$ be a vector of gas flow rates and let $\delta \in \mathbb{R}_+^N$ be a vector of gas extractions, which must be satisfied by the gas injections $\vartheta \in \mathbb{R}^N$ across the network given their injection limits $\underline{\vartheta}, \bar{\vartheta} \in \mathbb{R}_+^N$. The gas conservation law is thus

$$A\varphi = \vartheta - \delta.$$

The gas flow rates in network edges relate to the nodal pressures through non-linear, partial differential equations [16]. Under steady-state assumptions [13], however, the flows are related to pressures through the Weymouth equation:

$$\varphi_\ell |\varphi_\ell| = w_\ell (\varrho_n^2 - \varrho_{n'}^2), \quad \forall \ell = (n, n') \in \mathcal{E},$$

where $\varrho \in \mathbb{R}^N$ is a vector of pressures contained within technical limits $\underline{\varrho}, \bar{\varrho} \in \mathbb{R}_+^N$, and $w \in \mathbb{R}_+^E$ are constants that encode the friction coefficient and geometry of pipelines. To avoid non-linear pressure drops, let $\pi_n = \varrho_n^2$ be the squared pressure at node n with limits $\underline{\pi}_n = \underline{\varrho}_n^2$ and $\bar{\pi}_n = \bar{\varrho}_n^2$.

To support the desired nodal pressures, the gas network operator regulates the pressure using *active* pipelines $\mathcal{E}_a \subset \mathcal{E}$, which host either compressors $\mathcal{E}_c \subset \mathcal{E}_a$ or valves $\mathcal{E}_v \subset \mathcal{E}_a$, assuming $\mathcal{E}_c \cap \mathcal{E}_v = \emptyset$. These network assets respectively increase and decrease the gas pressure along their corresponding edges. To rewrite the gas conservation law and Weymouth equation accounting for these components, let $\kappa \in \mathbb{R}^E$ be a vector of pressure regulation variables. Pressure regulation is non-negative $\kappa_\ell \geq 0$ for every compressor edge $\ell \in \mathcal{E}_c$ and it is non-positive $\kappa_\ell \leq 0$ for every valve edge $\ell \in \mathcal{E}_v$. This information is encoded in the pressure regulation limits $\underline{\kappa}, \bar{\kappa} \in \mathbb{R}^E$. Pressure regulation involves an additional extraction of the gas mass to fuel active pipelines. Let matrix $B \in \mathbb{R}^{N \times E}$ relate the active pipelines to their sending nodes accounting for conversion factors, i.e.,

$$B_{k\ell} = \begin{cases} b_\ell, & \text{if } k = n, k \in \mathcal{E}_c \\ -b_\ell, & \text{if } k = n, k \in \mathcal{E}_v \\ 0, & \text{otherwise} \end{cases} \quad \forall \ell = (n, n') \in \mathcal{E},$$

where b_ℓ is a conversion factor from the gas mass to the pressure regulation rate. The network equations become

$$A\varphi = \vartheta - B\kappa - \delta, \tag{1a}$$

$$\varphi \circ |\varphi| = \text{diag}[w](A^\top \pi + \kappa), \tag{1b}$$

$$\varphi_\ell \geq 0, \quad \forall \ell \in \mathcal{E}_a. \tag{1c}$$

Here, the gas extraction $B\kappa$ by compressor and valve edges in (1a) is always non-negative. Equation (1b) is the Weymouth equation in a vector form that accounts for both pressure loss and pressure regulation. The absolute value operator in (1b) is understood element-wise. Finally, equality (1c) enforces the unidirectional condition for the gas flow in active pipelines, because they permit the gas flow only in one direction.

B. Deterministic Gas Network Optimization

The gas network optimization seeks the minimum of gas injection costs while satisfying gas flow equations and network limits. Let $c_1 \in \mathbb{R}_+^N$ and $c_2 \in \mathbb{R}_+^N$ be the coefficients of a quadratic gas injection cost function. With a perfect extraction forecast, the deterministic gas network optimization is

$$\min_{\vartheta, \kappa, \varphi, \pi} c_1^\top \vartheta + \vartheta^\top \text{diag}[c_2] \vartheta \tag{2a}$$

$$\text{s.t. } A\varphi = \vartheta - B\kappa - \delta, \tag{2b}$$

$$\varphi \circ |\varphi| = \text{diag}[w](A^\top \pi + \kappa), \tag{2c}$$

$$\underline{\pi} \leq \pi \leq \bar{\pi}, \quad \underline{\vartheta} \leq \vartheta \leq \bar{\vartheta}, \tag{2d}$$

$$\underline{\kappa} \leq \kappa \leq \bar{\kappa}, \quad \varphi_\ell \geq 0, \quad \forall \ell \in \mathcal{E}_a. \tag{2e}$$

Despite the non-convexity of (2), it has been solved successfully using algorithmic solvers [13], [17] or general-purpose solvers [18] when all optimization parameters are known. These solvers no longer apply when the parameters are uncertain, because one needs to establish a convex dependency

of optimization variables on uncertain parameters [19]. This convex dependency is established in this work by means of the linearization of the Weymouth equation (2c).

C. Linearization of the Weymouth Equation

Let $\mathcal{W}(\varphi, \pi, \kappa) = 0$ denote the non-convex constraint (2c), and let $\mathcal{J}(x) \in \mathbb{R}^{E \times n}$ denote the Jacobian of (2c) w.r.t. an arbitrary vector $x \in \mathbb{R}^n$. The relation between the gas flow rates, nodal pressures, and pressure regulation rates can thus be approximated by the first-order Taylor series expansion:

$$\begin{aligned} \mathcal{W}(\varphi, \pi, \kappa) &\approx \mathcal{W}(\dot{\varphi}, \dot{\pi}, \dot{\kappa}) + \mathcal{J}(\dot{\varphi})(\varphi - \dot{\varphi}) \\ &\quad + \mathcal{J}(\dot{\pi})(\pi - \dot{\pi}) + \mathcal{J}(\dot{\kappa})(\kappa - \dot{\kappa}) = 0, \end{aligned} \quad (3)$$

where $(\dot{\varphi}, \dot{\pi}, \dot{\kappa})$ is a stationary point retrieved by solving non-convex problem (2). As $\mathcal{W}(\dot{\varphi}, \dot{\pi}, \dot{\kappa}) = 0$ at a stationary point, equation (3) implies the affine relation:

$$\begin{aligned} \varphi - \dot{\varphi} &= \mathcal{J}(\dot{\varphi})^{-1} \mathcal{J}(\dot{\pi})(\dot{\pi} - \pi) + \mathcal{J}(\dot{\varphi})^{-1} \mathcal{J}(\dot{\kappa})(\dot{\kappa} - \kappa) \\ \Leftrightarrow \varphi &= \underbrace{\mathcal{J}(\dot{\varphi})^{-1} (\mathcal{J}(\dot{\pi})\dot{\pi} + \mathcal{J}(\dot{\kappa})\dot{\kappa})}_{\gamma_1(\dot{\varphi}, \dot{\pi}, \dot{\kappa})} + \dot{\varphi} \\ &\quad - \underbrace{\mathcal{J}(\dot{\varphi})^{-1} \mathcal{J}(\dot{\pi}) \pi}_{\gamma_2(\dot{\varphi}, \dot{\pi})} - \underbrace{\mathcal{J}(\dot{\varphi})^{-1} \mathcal{J}(\dot{\kappa}) \kappa}_{\gamma_3(\dot{\varphi}, \dot{\kappa})} \\ \Leftrightarrow \varphi &= \gamma_1(\dot{\varphi}, \dot{\pi}, \dot{\kappa}) + \gamma_2(\dot{\varphi}, \dot{\pi})\pi + \gamma_3(\dot{\varphi}, \dot{\kappa})\kappa, \end{aligned} \quad (4)$$

where $\gamma_1 \in \mathbb{R}^E$, $\gamma_2 \in \mathbb{R}^{E \times N}$ and $\gamma_3 \in \mathbb{R}^{E \times E}$ are coefficients encoding the sensitivity of gas flow rates to pressures and pressure regulation rates. These coefficients depend on the stationary point. For notational convenience, this dependency is dropped but always implied. In what follows, the Greek letter γ denotes sensitivity coefficients and their transformations.

Remark 1 (Reference node): Since $\text{rank}(\gamma_2) = N - 1$, system (4) is rank-deficient. Since the graph is connected, we have $E > N - 1$, thus resulting in infinitely many solutions to system (4). A unique solution is obtained by choosing a reference node (r) and fixing the reference pressure $\pi_r = \dot{\pi}_r$. The reference node does not host a variable injection or extraction, nor should be a terminal node of active pipelines. In practice, this is a node with a large and constant gas injection.

III. GAS NETWORK OPTIMIZATION UNDER UNCERTAINTY

A. Chance-Constrained Formulation

At the operational planning stage, well ahead of the real-time operations, the unknown gas extractions are modeled as

$$\tilde{\delta}(\xi) = \delta + \xi, \quad (5)$$

where δ is the expectation of the gas withdrawal rates and $\xi \in \mathbb{R}^N$ is a vector of random forecast errors. Having a finite number of historical forecast error samples observed from the true distribution \mathbb{P}_ξ , the network operator approximates its mean and covariance. Without loss of generality, we consider that the sample mean is zero and the description of distribution \mathbb{P}_ξ reduces to its covariance $\Sigma = \mathbb{E}[\xi\xi^\top]$.

The chance-constrained counterpart of the deterministic gas network optimization in (2) writes as

$$\min_{\tilde{\vartheta}, \tilde{\kappa}, \tilde{\varphi}, \tilde{\pi}} \mathbb{E}^{\mathbb{P}_\xi} [c_1^\top \tilde{\vartheta}(\xi) + \tilde{\vartheta}(\xi)^\top \text{diag}[c_2] \tilde{\vartheta}(\xi)] \quad (6a)$$

s.t.

$$\mathbb{P}_\xi \left[\begin{array}{l} A\tilde{\vartheta}(\xi) = \tilde{\vartheta}(\xi) - B\tilde{\kappa}(\xi) - \tilde{\delta}(\xi), \\ \tilde{\varphi}(\xi) = \gamma_1 + \gamma_2\tilde{\pi}(\xi) + \gamma_3\tilde{\kappa}(\xi), \\ \tilde{\pi}_r(\xi) = \dot{\pi}_r \end{array} \right] \stackrel{\text{a.s.}}{=} 1, \quad (6b)$$

$$\mathbb{P}_\xi \left[\begin{array}{l} \underline{\pi} \leq \tilde{\pi}(\xi) \leq \bar{\pi}, \underline{\vartheta} \leq \tilde{\vartheta}(\xi) \leq \bar{\vartheta}, \\ \underline{\kappa} \leq \tilde{\kappa}(\xi) \leq \bar{\kappa}, \varphi_\ell(\xi) \geq 0, \forall \ell \in \mathcal{E}_a \end{array} \right] \geq 1 - \varepsilon, \quad (6c)$$

which optimizes stochastic network variables $\tilde{\vartheta}, \tilde{\kappa}, \tilde{\varphi}$ and $\tilde{\pi}$ to minimize the expected value of the cost function (6a) subject to probabilistic constraints. The almost sure constraint (6b) requires the satisfaction of the gas conservation law and linearized Weymouth equation with probability 1, while the chance constraint (6c) ensures that the real-time pressures together with the injection, pressure regulation and flow rates remain within their technical limits. The prescribed violation probability $\varepsilon \in (0, 1)$ reflects the risk tolerance of the gas network operator towards the violation of network limits.

B. Control Policies and Network Response Model

The chance-constrained problem (6) is computationally intractable as it constitutes an infinite-dimensional optimization problem. To overcome its complexity, it has been proposed to approximate its solution by optimizing stochastic variables as affine, finite-dimensional functions of the random variable [4]. This functional dependency constitutes the model of the gas network response to uncertainty.

The *explicit* dependency on uncertainty is enforced on the controllable variables through the following affine policies

$$\tilde{\vartheta}(\xi) = \vartheta + \alpha\xi, \quad \tilde{\kappa}(\xi) = \kappa + \beta\xi, \quad (7a)$$

where ϑ and κ are the nominal (average) response, while $\alpha \in \mathbb{R}^{N \times N}$ and $\beta \in \mathbb{R}^{E \times N}$ are variable recourse decisions of the gas injections and pressure regulation by active pipelines, respectively. When optimized, policies (7a) provide *control inputs* for the network operator to meet the realization of random forecast errors ξ . As the state variables, such as flow rates and pressures, are coupled with the controllable variables through stochastic equations (6b), they *implicitly* depend on uncertainty through the control inputs.

Lemma 1: Under control policies (7a), the random gas pressures and flow rates are given by affine functions

$$\tilde{\pi}(\xi) = \pi + \check{\gamma}_2(\alpha - \hat{\gamma}_3\beta - \text{diag}[\mathbf{1}])\xi, \quad (7b)$$

$$\tilde{\varphi}(\xi) = \varphi + (\check{\gamma}_2(\alpha - \text{diag}[\mathbf{1}]) - \hat{\gamma}_3\beta)\xi, \quad (7c)$$

both including the nominal and random components, and where $\check{\gamma}_2, \hat{\gamma}_2, \check{\gamma}_3, \hat{\gamma}_3, \gamma_3$ are constants of proper dimensions.

Equations (7) constitute the desired model of the network response to uncertainty. The model is said to be admissible if the stochastic gas conservation law and linearized Weymouth equation in (6b) hold with probability 1, i.e., for any realization of random variable ξ . This is achieved as follows.

Lemma 2: The model of the gas network response (7) is admissible if the nominal and recourse variables obey

$$A\varphi = \vartheta - B\kappa - \delta \quad (8a)$$

$$(\alpha - B\beta)^\top \mathbb{1} = 1, \quad (8b)$$

$$\varphi = \gamma_1 + \gamma_2 \pi + \gamma_3 \kappa, \quad (8c)$$

$$\pi_r = \dot{\pi}_r, [\alpha]_r^\top = 0, [\beta]_r^\top = 0. \quad (8d)$$

Remark 2: The model of the gas network response (7) does not make an assumption on the uncertainty distribution.

C. Expected Cost Reformulation

The expected value of the gas network cost function in (6a) is computationally intractable as it involves an optimization of infinite-dimensional random variable $\tilde{\vartheta}(\xi)$. Under control policy (7a), however, we show that the computation of the expected cost reduces to solving an SOCP problem.

Due to definition of $\tilde{\vartheta}(\xi)$, function (6a) rewrites as

$$\mathbb{E}^{\mathbb{P}_\xi}[c_1^\top (\vartheta + \alpha \xi) + (\vartheta + \alpha \xi)^\top \text{diag}[c_2](\vartheta + \alpha \xi)],$$

where the argument of the expectation operator is separable into nominal and random components. Due to the linearity of the expectation operator, it equivalently rewrites as

$$c_1^\top \vartheta + \vartheta^\top \text{diag}[c_2] \vartheta + \mathbb{E}^{\mathbb{P}_\xi}[c_1^\top \alpha \xi + (\alpha \xi)^\top \text{diag}[c_2] \alpha \xi].$$

A zero-mean assumption made on distribution \mathbb{P}_ξ factors out the first term under the expectation operator. The reformulation of the second term is made recalling that the expectation of the outer product of the zero-mean random variable yields its covariance, i.e., $\mathbb{E}[\xi \xi^\top] = \Sigma$. Thus, the expected value of cost function (6a) reduces to a computation of

$$c_1^\top \vartheta + \vartheta^\top \text{diag}[c_2] \vartheta + \text{Tr}[\alpha^\top \text{diag}[c_2] \alpha \Sigma],$$

which is a convex quadratic function in variables ϑ and α . To bring it to an SOCP form, let vectors $c^\vartheta \in \mathbb{R}^N$ and $c^\alpha \in \mathbb{R}^N$ substitute the quadratic terms of the gas injection and recourse costs. Moreover, let $F \in \mathbb{R}^{N \times N}$ be a factorization of covariance matrix Σ , such that $\Sigma = FF^\top$, and $\hat{c}_2 \in \mathbb{R}^N$ be the factorization of vector c_2 , such that $\text{diag}[c_2] = \hat{c}_2 \hat{c}_2^\top$. Then, for any fixed values of nominal ϑ and recourse α decisions, the expected value of the cost is retrieved by solving the following SOCP problem

$$\min_{c^\vartheta, c^\alpha} c_1^\top \vartheta + \mathbb{1}^\top c^\vartheta + \mathbb{1}^\top c^\alpha \quad (9a)$$

$$\text{s.t. } \|\hat{c}_2 n \vartheta_n\|^2 \leq c_n^\vartheta, \forall n \in \mathcal{N}, \quad (9b)$$

$$\|F[\alpha]_n^\top c_2 n\|^2 \leq c_n^\alpha, \forall n \in \mathcal{N}, \quad (9c)$$

where (9b) and (9c) are rotated second-order cone constraints. Hence, the co-optimization of variables $\vartheta, \alpha, c^\vartheta$ and c^α results in the minimal expected cost. As problem (9) acts on a distribution-free response model (Remark 2), it does not require any assumption on the uncertainty distribution.

D. Variance of State Variables

The optimization of response model (7) using the criterion of the minimum expected cost involves the risks of producing highly variable solutions for the state variables. See, for example, the evidences in the power system domain [20], [21]. However, since the state variables (7b) and (7c) are affine in

control inputs, they can be optimized to provide the minimal-variance solution. To achieve the desired result, however, it is more suitable to optimize the standard deviations of the state variables as they admit conic formulations.

Let $s^\pi \in \mathbb{R}^N$ and $s^\varphi \in \mathbb{R}^E$ be the variables modeling the standard deviations of pressures and flow rates, respectively. For any fixed values of recourse decisions α and β , the standard deviations of pressures and flows rates are retrieved by solving the following SOCP problem

$$\min_{s^\pi, s^\varphi} \mathbb{1}^\top s^\pi + \mathbb{1}^\top s^\varphi \quad (10a)$$

$$\text{s.t. } \|F[\dot{\gamma}_2(\alpha - \dot{\gamma}_3 \beta - \text{diag}[\mathbb{1}])]_n^\top\| \leq s_n^\pi, \quad (10b)$$

$$\|F[\dot{\gamma}_2(\alpha - \text{diag}[\mathbb{1}]) - \dot{\gamma}_3 \beta]_\ell^\top\| \leq s_\ell^\varphi, \quad \forall n \in \mathcal{N}, \forall \ell \in \mathcal{E}, \quad (10c)$$

where (10b) and (10c) are second-order cone constraints, which are tight at optimality. Therefore, the co-optimization of variables α, β, s^π and s^φ yields the optimized system response (7) that ensures the minimal-variance solution for the state variables. We finally note that this co-optimization is also distribution-free.

E. Tractable Chance-Constrained Formulation

It remains to reformulate the joint chance constraint (6c) to attain a tractable reformulation. Given network response model (7), one way to satisfy (6c) is to enforce all its N_{\leq} inequalities on a finite number of samples from \mathbb{P}_ξ [22]. The sample-based reformulation, however, does not explicitly parameterize the problem by the risk tolerance ε of the network operator. We thus proceed by enforcing individual chance constraints with the explicit analytic parameterization of the risk tolerance through individual violation probabilities $\hat{\varepsilon} \in \mathbb{R}_{+}^{N_{\leq}}$. This approach admits the Bonferroni approximation of the joint chance constraint in (6c) when $\mathbb{1}^\top \hat{\varepsilon} \leq \varepsilon$. The joint feasibility guarantee is provided even when the choice of the individual violation probabilities is sub-optimal [23], e.g. $\hat{\varepsilon}_i = \frac{\varepsilon}{N_{\leq}}, \forall i = 1, \dots, N_{\leq}$.

From [19] we know that a scalar chance constraint

$$\mathbb{P}_\xi[\xi^\top x \leq b] \geq 1 - \hat{\varepsilon} \quad (11a)$$

analytically translates into the second-order cone constraint

$$z_{\hat{\varepsilon}} \|Fx\| \leq b - \mathbb{E}_\xi[\xi^\top x], \quad (11b)$$

where $z_{\hat{\varepsilon}} \geq 0$ is a safety parameter in the sense of [19], and the left-hand side of (11b) is the margin that ensures constraint feasibility given the parameters of the forecast errors distribution. Consequently, larger safety parameter $z_{\hat{\varepsilon}}$ improves system security. The choice of $z_{\hat{\varepsilon}}$ depends on the knowledge about distribution \mathbb{P}_ξ [19], yet it always increases as the risk tolerance $\hat{\varepsilon}$ reduces.

Given the network response model (7) and the reformulations in (8)–(11), a computationally tractable version of stochastic problem (6) with the variance awareness formulates as the following SOCP problem:

$$\min_{\varphi} c_1^\top \vartheta + \mathbb{1}^\top c^\vartheta + \mathbb{1}^\top c^\alpha + \psi^\pi \mathbb{1}^\top s^\pi + \psi^\varphi \mathbb{1}^\top s^\varphi \quad (12a)$$

$$\text{s.t. } \lambda^\varphi: A\varphi = \vartheta - B\kappa - \delta, \quad (12b)$$

$$\lambda^r : (\alpha - B\beta)^\top \mathbb{1} = \mathbb{1}, \quad (12c)$$

$$\lambda^w : \varphi = \gamma_1 + \gamma_2 \pi + \gamma_3 \kappa, \quad \pi_r = \dot{\pi}_r, \quad (12d)$$

$$\lambda_n^\pi : \|F[\tilde{\gamma}_2(\alpha - \hat{\gamma}_3\beta - \text{diag}[\mathbb{1}])]_n^\top\| \leq s_n^\pi, \quad (12e)$$

$$\lambda_\ell^\varphi : \|F[\tilde{\gamma}_2(\alpha - \text{diag}[\mathbb{1}]) - \hat{\gamma}_3\beta]_\ell^\top\| \leq s_\ell^\varphi, \quad (12f)$$

$$\lambda_n^\pi : z_{\hat{\varepsilon}} \|F[\tilde{\gamma}_2(\alpha - \hat{\gamma}_3\beta - \text{diag}[\mathbb{1}])]_n^\top\| \leq \bar{\pi}_n - \pi_n, \quad (12g)$$

$$\lambda_n^\pi : z_{\hat{\varepsilon}} \|F[\tilde{\gamma}_2(\alpha - \hat{\gamma}_3\beta - \text{diag}[\mathbb{1}])]_n^\top\| \leq \pi_n - \underline{\pi}_n, \quad (12h)$$

$$\lambda_\ell^\varphi : z_{\hat{\varepsilon}} \|F[\tilde{\gamma}_2(\alpha - \text{diag}[\mathbb{1}]) - \hat{\gamma}_3\beta]_\ell^\top\| \leq \varphi_\ell, * \quad (12i)$$

$$\|\dot{c}_{2n}\vartheta_n\|^2 \leq c_n^\vartheta, \quad (12j)$$

$$\|F\dot{c}_{2n}[\alpha]_n^\top\|^2 \leq c_n^\alpha, \quad (12k)$$

$$z_{\hat{\varepsilon}} \|F[\alpha]_n^\top\| \leq \bar{\vartheta}_n - \vartheta_n, \quad (12l)$$

$$z_{\hat{\varepsilon}} \|F[\alpha]_n^\top\| \leq \vartheta_n - \underline{\vartheta}_n, \quad (12m)$$

$$z_{\hat{\varepsilon}} \|F[\beta]_\ell^\top\| \leq \bar{\kappa}_\ell - \kappa_\ell, \quad (12n)$$

$$z_{\hat{\varepsilon}} \|F[\beta]_\ell^\top\| \leq \kappa_\ell - \underline{\kappa}_\ell, \quad (12o)$$

$$\forall n \in \mathcal{N}, \forall \ell \in \mathcal{E}, * \forall \ell \in \mathcal{E}_a,$$

in variables $\mathcal{P} = \{\vartheta, \kappa, \varphi, \pi, \alpha, \beta, c^\vartheta, c^\alpha, s^\pi, s^\varphi\}$. Problem (12) optimizes the system response model (7) to meet a trade-off between the expected cost and the standard deviation of the state variables up to the given penalties $\psi^\pi \in \mathbb{R}_+^N$ and $\psi^\varphi \in \mathbb{R}_+^E$ for pressures and gas flow rates, respectively. Notice, that the constraints on the optimal recourse with respect to the reference node in (8d) are implicitly accounted for through the conic constraints on the gas injection and pressure regulation (12l)–(12o).

In formulation (12), the Greek letters λ denote the dual variables of the coupling constraints. In the next section, we invoke the SOCP duality theory to establish an efficient pricing scheme for gas networks under uncertainty.

IV. PRICING GAS NETWORKS UNDER UNCERTAINTY

From program (12), we know that network assets participate in the satisfaction of the gas network equations through (12b)–(12d), in state variance reduction (12e)–(12f), and in ensuring the feasibility of the state variables (12g)–(12i). In this section, we establish a pricing scheme that remunerates network assets based on the combination of the classic linear programming duality [24], [25] and the SOCP duality [21], [26]. We refer the interested reader to Appendix C for a brief overview on SOCP duality. For presentation clarity, however, we should stress that for each second-order cone constraint in (12e)–(12i) with a dual variable $\lambda \in \mathbb{R}^1$ there exists a vector of dual prices $u \in \mathbb{R}^N$, corresponding component-wise to random vector $\xi \in \mathbb{R}^N$, such that $\|u\| \leq \lambda$. With a set of prices λ, u_1, \dots, u_N , each conic coupling constraint becomes separable, thus enabling the revenue decomposition associated with constraints (12e)–(12i).

We first show that the primal and dual solutions of program (12) solve a competitive equilibrium. This equilibrium consists of a price-setting problem that seeks the optimal prices associated with the coupling constraints (12e)–(12i), a set of profit-maximizing problems of gas suppliers $n \in \mathcal{N}$, active pipelines $\ell \in \mathcal{E}_a$, and a rent-maximization problem solved by the network operator, as we establish in the proof of the following result; see Appendix D for details.

Theorem 1 (Equilibrium payments): Let \mathcal{P} and \mathcal{D} be the sets of the optimal primal and dual solutions of problem (12), respectively. Then, both sets \mathcal{P} and \mathcal{D} solve a competitive gas network equilibrium with the following payments:

- 1) Each gas supplier $n \in \mathcal{N}$ maximizes the expected profit when receiving the revenue of $\mathcal{R}_n^{\text{sup}}$ as in (13a).
- 2) Each active pipeline $\ell \in \mathcal{E}_a$ maximizes the expected profit when receiving the revenue of $\mathcal{R}_\ell^{\text{act}}$ as in (13b).
- 3) The network operator maximizes the expected network congestion rent when receiving the revenue of $\mathcal{R}^{\text{rent}}$ as in (13c).
- 4) Each consumer $n \in \mathcal{N}$ maximizes the gas extraction utility when it is charged with $\mathcal{R}_n^{\text{con}}$ as in (13d).

Similarly to a deterministic market settlement, the nominal gas injection or extraction is priced by associated locational marginal price λ^c , while the nominal pressure regulation is priced by the dual variable λ^w of the Weymouth equation. The pricing scheme of Theorem 1, however, goes beyond the deterministic payments and provides three additional revenue streams for network assets (13). First, each network asset is paid with the dual variable λ^r to remunerate its contribution to the feasibility of the gas network equations for any realization of uncertainty; see Lemma 2. The dual variables of the reformulated chance constraints (12g)–(12i) are used to compensate network assets for maintaining gas pressures and flow rates within network limits. Observe, this revenue stream is proportional to the safety parameter $z_{\hat{\varepsilon}}$, which increases as risk tolerance $\hat{\varepsilon}$ reduces. The last revenue streams for network assets come from the satisfaction of the variance criteria set by the network operator. From the stationarity conditions (23e) from Appendix D, the variance prices are $\lambda^\pi = \psi^\pi$ and $\lambda^\varphi = \psi^\varphi$, and from the SOCP dual feasibility condition (19) from Appendix D we know that $\|u^\pi\| \leq \lambda_n^\pi$, $\|u^\varphi\| \leq \lambda_\ell^\varphi$, $\forall n \in \mathcal{N}, \ell \in \mathcal{E}$. Thus, these revenue streams are proportional to the variance penalties ψ^π and ψ^φ set by the network operator. The consumer charges, motivated by their individual contributions to uncertainty and state variance, are explained similarly. Finally notice that, in contrast to the deterministic rent, revenue (13c) additionally includes the variance control rent, which is non-zero whenever constraints (12e)–(12f) are binding, i.e., $\psi^\pi, \psi^\varphi > 0$.

The results of Theorem 1, and thus the equivalence between the centralized optimization (12) and its equilibrium counterpart (20)–(22), hold under certain assumptions. First, there exists at least one strictly feasible solution to SOCP problem (12) or to its dual counterpart to ensure that Slater's condition holds [26]. Second, agents must act according to their true preferences, i.e., no exercise of market power. Finally, the information on the uncertainty distribution must be consistent among equilibrium problems [27].

We next analyze the properties of revenue adequacy and cost recovery and make them conditioned on the network design.

Corollary 1 (Revenue adequacy): Let $\gamma_1 = 0$ and $\underline{\pi} = 0$. Then, the payments established by Theorem 1 are revenue adequate, i.e., $\sum_{n=1}^N \mathcal{R}_n^{\text{con}} \geq \sum_{n=1}^N \mathcal{R}_n^{\text{sup}} + \sum_{\ell=1}^E \mathcal{R}_\ell^{\text{act}}$.

As a result, the gas network operator does not incur a financial loss when distributing the payments from consumers to

$$\mathcal{R}_n^{\text{sup}} \triangleq \underbrace{\lambda_n^c \vartheta_n}_{\text{nominal balance}} + \underbrace{[\lambda^r]^\top [\alpha]_n^\top}_{\text{recourse balance}} + \underbrace{z_{\hat{\varepsilon}} (\langle \check{\gamma}_2 \rangle_n^\top (u^{\bar{\pi}} + u^{\pi}) + \langle \dot{\gamma}_2 \rangle_n^\top u^{\varphi}) F[\alpha]_n^\top}_{\text{gas pressure and flow limits}} + \underbrace{(\langle \check{\gamma}_2 \rangle_n^\top u^{\pi} + \langle \dot{\gamma}_2 \rangle_n^\top u^{\varphi}) F[\alpha]_n^\top}_{\text{gas pressure and flow variance}} \quad (13a)$$

$$\mathcal{R}_\ell^{\text{act}} \triangleq \underbrace{((\gamma_3)^\top \lambda^w - \lambda^{c\top} \langle B \rangle_\ell) \kappa_\ell}_{\text{nominal pressure regulation}} - \underbrace{1^\top \langle B \rangle_\ell \lambda^{r\top} [\beta]_\ell^\top}_{\text{recourse balance}} - \underbrace{z_{\hat{\varepsilon}} (\langle \check{\gamma}_2 \dot{\gamma}_3 \rangle_\ell^\top (u^{\bar{\pi}} + u^{\pi}) + \langle \dot{\gamma}_3 \rangle_\ell^\top u^{\varphi}) F[\beta]_\ell^\top}_{\text{gas pressure and flow limits}} - \underbrace{(\langle \check{\gamma}_2 \dot{\gamma}_3 \rangle_\ell^\top u^{\pi} + \langle \dot{\gamma}_3 \rangle_\ell^\top u^{\varphi}) F[\beta]_\ell^\top}_{\text{gas pressure and flow variance}} \quad (13b)$$

$$\mathcal{R}^{\text{rent}} \triangleq \underbrace{(\lambda^{\varphi\top} - \lambda^{w\top} - \lambda^{c\top} A) \varphi}_{\text{flow congestion rent}} + \underbrace{(\lambda^{w\top} \gamma_2 + \lambda^{\pi\top} - \lambda^{\bar{\pi}\top}) \pi + \lambda^{\bar{\pi}\top} \bar{\pi} - \lambda^{\pi\top} \pi}_{\text{pressure congestion rent}} + \underbrace{\lambda^{\varphi\top} s^{\varphi} + \lambda^{\pi\top} s^{\pi}}_{\text{variance rent}} \quad (13c)$$

$$\mathcal{R}_n^{\text{con}} \triangleq \underbrace{\lambda_n^c \delta_n}_{\text{nominal balance}} + \underbrace{\lambda_n^r}_{\text{recourse balance}} + \underbrace{z_{\hat{\varepsilon}} [F]_n (u^{\varphi\top} \langle \check{\gamma}_2 \rangle_n + (u^{\bar{\pi}} + u^{\pi})^\top \langle \dot{\gamma}_2 \rangle_n)}_{\text{gas pressure and flow limits}} + \underbrace{[F]_n (u^{\varphi\top} \langle \check{\gamma}_2 \rangle_n + u^{\pi\top} \langle \dot{\gamma}_2 \rangle_n)}_{\text{gas pressure and flow variance}} \quad (13d)$$

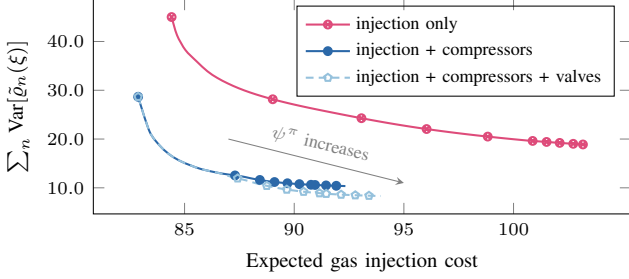


Figure 1. Expected cost versus pressure variance for different assignments of control policies to network assets. Pressure penalty $\psi^\pi \in [10^{-3}, 10^{-1}]$.

network assets. The first condition in Corollary 1 is motivated by the linearization of the Weymouth equation. If $\gamma_1 \neq 0$, there exists an extra revenue term $\lambda^{w\top} \gamma_1$. As consumers are inelastic, this payment can be thus allocated to consumer charges, however its distribution among the customers remains an open question. Finally, the second condition in Corollary 1 allows pressures to be zero at network nodes, which is too restrictive for practical purposes. In the next Section V we show that the revenue adequacy holds in practice even when this condition is not satisfied.

Our last result is to show that the cost recovery for network assets is also conditioned on the network design.

Corollary 2 (Cost recovery): Let $\underline{\vartheta} = 0$, $\kappa_\ell = 0, \forall \ell \in \mathcal{E}_c$, and $\bar{\kappa}_\ell = 0, \forall \ell \in \mathcal{E}_v$. Then, the payments of Theorem 1 ensure cost recovery for suppliers and active pipelines, i.e., $\mathcal{R}_\ell^{\text{act}} \geq 0, \forall \ell \in \mathcal{E}_a$, and $\mathcal{R}_n^{\text{sup}} - c_{1n} \vartheta_n - c_n^\vartheta - c_n^\alpha \geq 0, \forall n \in \mathcal{N}$.

V. NUMERICAL EXPERIMENTS

We run numerical experiments using a 48-node natural gas network depicted in Fig. 2. The network parameters are sourced from [28] with a few modifications: we homogenize the pressure limits across network nodes, add two injections in the demand area at nodes 32 and 37, and install two valves in pipelines connecting nodes (28, 29) and (43, 44). The 22 gas extractions are modeled as $\check{\delta}(\xi) = \delta + \xi$, where δ is the nominal extraction rate reported in [28] and ξ is the zero-mean normally distributed forecast error. The safety parameter $z_{\hat{\varepsilon}}$ is thus the inverse CDF of the standard Gaussian distribution at $(1 - \hat{\varepsilon})$ -quantile [19]. The standard deviation of each gas extraction is set to 10% of the nominal rate. The joint

constraint violation probability ε is set to 1% by default. To retrieve the stationary point in (4), the non-convex problem (2) is solved for the nominal gas extraction rates using the Ipopt solver [18]. The repository [29] contains the input data and code implementation in the JuMP package for Julia [30].

A. Analysis of the Optimized Network Response

We first study the optimized gas network response to uncertainty under deterministic and chance-constrained control policies (7). The deterministic policies are optimized by setting the safety factor $z_{\hat{\varepsilon}}$ in problem (12) to zero. The policies are compared in terms of the expected cost (9a), the aggregated variance of gas pressures and flow rates $\sum_n \text{Var}[\check{\vartheta}_n(\xi)]$ and $\sum_\ell \text{Var}[\check{\varphi}_\ell(\xi)]$, respectively, and the total pressure regulation by compressors $\sum_{\ell \in \mathcal{E}_c} \sqrt{\kappa_\ell}$ and valves $\sum_{\ell \in \mathcal{E}_v} \sqrt{\kappa_\ell}$. Note, we discuss the natural pressure quantities, not their squared counterparts used in optimization.

The policies are also compared in terms of network constraints satisfaction. We first sample control inputs from (7) for $S = 1,000$ realizations of forecast errors and count the violations of network limits (6c). Second, we assess the quality of the control inputs (7a) for the non-convex gas equations, by solving the projection problem

$$\min_{\vartheta_s, \kappa_s, \varphi_s, \pi_s} \|\check{\vartheta}(\xi_s) - \vartheta_s\| + \|\check{\varphi}(\xi_s) - \kappa_s\| \quad (14a)$$

$$\text{s.t. } A\varphi_s = \vartheta_s - B\kappa_s - \delta_s - \xi_s, \quad (14b)$$

$$\text{Constraints (2c) -- (2e),} \quad (14c)$$

for all realizations $\xi_s, \forall s = 1, \dots, S$. A control input is considered feasible if (14a) is zero for a given realization. To characterize this infeasibility numerically, consider the average metrics $\mathcal{P}_{\text{inj}} = \sum_s \|\check{\vartheta}(\xi_s) - \vartheta_s\| / S$ for gas injections and $\mathcal{P}_{\text{act}} = \sum_s \|\check{\varphi}(\xi_s) - \kappa_s\| / S$ for active pipelines.

The results are reported in Table I. Disregarding uncertainty, the deterministic policies optimize the network operation for the nominal gas extraction rates and thus result in the minimum of cost at the operational planning stage. However, the produced control inputs are infeasible for most of the forecast error realizations. The projections \mathcal{P}_{inj} and \mathcal{P}_{act} of deterministic policies require the real-time correction of gas injections by 31.3% and the real-time correction of pressure regulation by active pipelines by 12.7% of the nominal rates on average.

Table I
DETERMINISTIC VERSUS CHANCE-CONSTRAINED OPTIMIZATION OF CONTROL POLICIES

Parameter	Unit	Deterministic control policies	Variance-agnostic	Chance-constrained control policies					
				Pressure variance-aware, ψ^π			Flow variance-aware, ψ^φ		
				10^{-3}	10^{-2}	10^{-1}	1	10^1	10^2
Expected cost	\$1000	80.9	82.5 (100%)	100.5%	105.6%	113.8%	100.1%	102.5%	112.6%
$\sum_n \text{Var}[\tilde{\rho}_n(\xi)]$	MPa ²	217.5	63.4 (100%)	44.2%	18.9%	12.8%	92.8%	46.7%	24.7%
$\sum_\ell \text{Var}[\tilde{\varphi}_\ell(\xi)]$	BMSCFD ²	26.1	58.0 (100%)	83.4%	64.1%	59.2%	93.4%	44.8%	25.9%
$\sum_{\ell \in \mathcal{E}_c} \sqrt{\kappa_\ell}$	kPa	1939	3914	3570	3734	3661	3914	4030	3888
$\sum_{\ell \in \mathcal{E}_v} \sqrt{\kappa_\ell}$	kPa	0	0	0	150	576	0	1	500
Constraint inf.	%	53.7	0.04	0.02	0.02	0.02	0.03	0.02	0.03
Average \mathcal{P}_{inj}	MMSCFD	960.91	0.01	0.03	0.02	0.02	0.04	0.04	0.04
Average \mathcal{P}_{act}	kPa	121.68	0.19	0.08	0.10	0.05	0.28	0.04	0.04

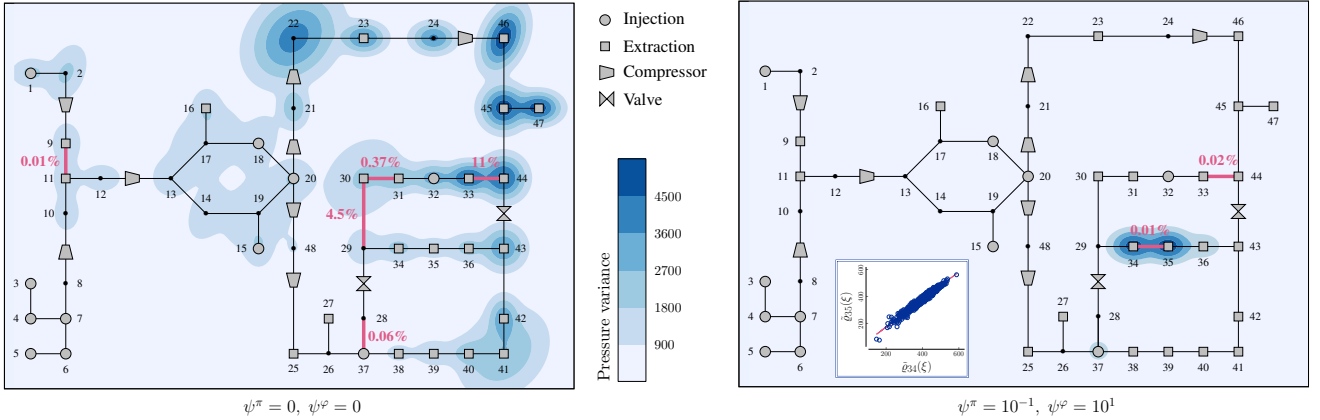


Figure 2. Comparison of the variance-agnostic (left) and the variance-aware (right) chance-constrained control policies in terms of the state variables variance for $\varepsilon = 10\%$. The red values show the probability of flow reversal. The inset plot shows the correlation between the pressures at nodes 34 and 35.

The chance-constrained policies, on the other hand, produce the control inputs that remain feasible with a probability at least $1 - \varepsilon = 99\%$ and require a minimal effort to restore the real-time gas flow feasibility. The variance-agnostic policy requires only a slight increase of the expected cost relative to the deterministic solution by 1.6%, while the variance-aware policies allow to trade-off the expected operational cost for the smaller variations of pressures and flow rates. The variance of gas pressures and flow rates can be reduced by 63.8% and 7.2%, respectively, without any substantial impact on the expected cost. Observe that the subsequent variance reduction is achieved also due to the activation of valves in two active pipelines, that are not operating in the deterministic and variance-agnostic solutions.

Next, we show how the cost-variance trade-offs change with different assignments of control policies (7) to network assets. Figure 1 illustrates the cost-variance trade-offs when the control policies are assigned to gas injections only ($\alpha \in \text{free}, \beta = 0$), to gas injections and compressors ($\alpha, \beta \in \text{free}, [\beta]_\ell^\top = 0, \forall \ell \in \mathcal{E}_v$), and to all network assets including valves ($\alpha, \beta \in \text{free}$). Observe that the variance reduction is achieved more rapidly and at lower costs as more active pipelines are involved into uncertainty and variance control. Hence, the stochastic control becomes more available as the network operator deploys more pressure regulation action by compressors and valves.

With the density plots in Fig. 2, we demonstrate the uncertainty propagation through the network. The variance-agnostic solution results in the large pressure variance in the eastern part of the network with a large concentration of stochastic gas extractions. This solution further allows the probability of the gas flows reversal up to 11% for certain pipelines, thus making the prediction of flow directions difficult. The variance-aware solution with the joint penalization of pressures and flows variance, in turn, drastically reduces the variation of the state variables and localizes the most of the variation only at nodes 34 and 35. Although this variation remains large, the pressures at these nodes are highly correlated. Thus, by Weymouth equation (2c), the flow variance and the probability of flow reversal in edge (34, 35) remain small.

B. Revenue Analysis

Figure 3 depicts the total revenues of active pipelines and gas injections as well as the total charges of gas consumers. It further shows their decomposition into revenue streams defined by the pricing scheme in (13). Relative to the deterministic payments, the chance-constrained policies lead to a substantial increase in payments that further increase due to the variance awareness. Besides the nominal supply revenues, the chance-constrained policies produce the compensations for the uncertainty and variance control that together exceed deterministic payments by 37.3%. Moreover, the payments for

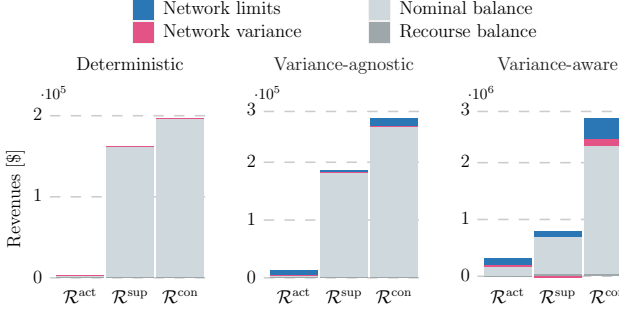


Figure 3. Total payments for active pipelines \mathcal{R}^{act} , suppliers \mathcal{R}^{sup} and consumers \mathcal{R}^{con} under deterministic, chance-constrained variance-agnostic and chance-constrained variance-aware ($\psi^\pi = 0.1, \psi^\varphi = 100$) policies.

the nominal supply under stochastic policies also increase due to several reasons. First, as shown in Table I, the stochastic policies require a larger deployment of gas compressors and valves that extract an additional gas mass for fuel purposes, up to 4.2% of the network demand, thus increasing the marginal cost of gas suppliers. Second, to provide the security margins for chance constraints (12g)–(12i) and (12l)–(12o), the optimized policies require withholding less expensive injections from the purposes of the nominal supply. Last, with increasing assignments of penalty factors ψ^π and ψ^φ , the optimality of the nominal injection cost is altered in the interest of reduced variance of state variables. Finally, the mismatch between the consumer charges and the revenues of gas injections and active pipelines is non-negative, thus satisfying the revenue adequacy in all three instances.

VI. CONCLUSIONS & OUTLOOK

This work has established the stochastic control policies and pricing scheme for the non-convex steady-state gas network operations under gas extraction uncertainty. The work offers an uncertainty- and variance-aware policy optimization that ensures the gas flow feasibility with a high probability and minimal variance of the state variables. Moreover, the work challenged the deterministic market settlement and offered financial remunerations to network assets for their contributions to uncertainty and variance control.

The definition and optimization of gas storage control policies under uncertainty constitute the relevant direction for a future work. In addition, the uncertainty- and variance-aware coordination and financial contracts between the gas and power network operators are valid research directions.

APPENDIX

A. Proof of Lemma 1

The substitution of the linearized Weymouth equation from (6b) and policies (7a) into the gas conservation law in (6b) yields stochastic pressures as

$$\begin{aligned} A\tilde{\varphi}(\xi) &= \tilde{\vartheta}(\xi) - B\tilde{\kappa}(\xi) - \tilde{\delta}(\xi) \\ \Leftrightarrow A(\gamma_1 + \gamma_2\tilde{\pi}(\xi) + \gamma_3(\kappa + \beta\xi)) &= \vartheta + \alpha\xi - B(\kappa + \beta\xi) - \delta - \xi \\ \Leftrightarrow \underbrace{A\gamma_2}_{\hat{\gamma}_2}\tilde{\pi}(\xi) &= \underbrace{\vartheta - (B + A\gamma_3)\kappa - \delta - A\gamma_1}_{\text{from (2b),(4) : } A\gamma_2\pi = \hat{\gamma}_2\pi} \end{aligned}$$

$$+ (\alpha - \underbrace{(B + A\gamma_3)\beta - \text{diag}[1]}_{\hat{\gamma}_3})\xi$$

$$\Leftrightarrow \hat{\gamma}_2\tilde{\pi}(\xi) = \hat{\gamma}_2\pi + (\alpha - \hat{\gamma}_3\beta - \text{diag}[1])\xi$$

$$\Leftrightarrow \tilde{\pi}(\xi) = \pi + \hat{\gamma}_2^{-1}(\alpha - \hat{\gamma}_3\beta - \text{diag}[1])\xi,$$

where $\hat{\gamma}_2 \in \mathbb{R}^{N \times N}$ and $\hat{\gamma}_3 \in \mathbb{R}^{N \times E}$ are auxiliary constants. As $\hat{\gamma}_2 = A\gamma_2$, it is only invertible for the tree network topology. For generality, consider a reference node (r), see Remark 1, and let $\hat{\gamma}_{2 \setminus r}$ be a reduced matrix $\hat{\gamma}_2$ without the rth row and column in $\hat{\gamma}_2$. The invertible counterpart of $\hat{\gamma}_2$ is

$$\check{\gamma}_2 = \begin{bmatrix} \hat{\gamma}_{2 \setminus r}^{-1} & \mathbf{0} \\ \mathbf{0}^\top & 0 \end{bmatrix},$$

and the stochastic pressures become

$$\tilde{\pi}(\xi) = \pi + \check{\gamma}_2(\alpha - \hat{\gamma}_3\beta - \text{diag}[1])\xi, \quad (15a)$$

$$\pi_r = \dot{\pi}_r, [\alpha]_r^\top = \mathbf{0}, [\beta]_r^\top = \mathbf{0}, \quad (15b)$$

for an arbitrary network topology. Here, equation (15b) is enforced to satisfy the reference node definition.

To obtain the stochastic flow rates, substitute (15a) into the linearized Weymouth equation in (6b) and rearrange, i.e.,

$$\begin{aligned} \tilde{\varphi}(\xi) &= \gamma_1 + \gamma_2\tilde{\pi}(\xi) + \gamma_3\tilde{\kappa}(\xi) \\ \Leftrightarrow \tilde{\varphi}(\xi) &= \underbrace{\gamma_1 + \gamma_2\pi + \gamma_3\kappa}_{\text{from (4) : } \varphi} + \underbrace{\gamma_2\check{\gamma}_2}_{\check{\gamma}_2}(\alpha - \text{diag}[1])\xi \\ &\quad - \underbrace{(\gamma_2\check{\gamma}_2\hat{\gamma}_3 - \gamma_3)\beta\xi}_{\hat{\gamma}_3} \\ \Leftrightarrow \tilde{\varphi}(\xi) &= \varphi + (\hat{\gamma}_2(\alpha - \text{diag}[1]) + \hat{\gamma}_3\beta)\xi, \end{aligned}$$

where $\check{\gamma}_2 \in \mathbb{R}^{E \times N}$ and $\hat{\gamma}_3 \in \mathbb{R}^{E \times E}$ are constants.

B. Proof of Lemma 2

Consider the stochastic gas conservation law in (6b):

$$A\tilde{\varphi}(\xi) = \tilde{\vartheta}(\xi) - B\tilde{\kappa}(\xi) - \tilde{\delta}(\xi).$$

From the properties of the edge-node incidence matrix A , we know that $\mathbf{1}^\top A\tilde{\varphi}(\xi) = 0$. By summing up N equations above and by substituting equations (7a), we arrive to equation

$$\mathbf{1}^\top \vartheta - \mathbf{1}^\top B\kappa - \mathbf{1}^\top \delta + \mathbf{1}^\top \alpha\xi - \mathbf{1}^\top B\beta\xi - \mathbf{1}^\top \xi = 0,$$

which is separable into nominal and random components:

$$\mathbf{1}^\top \vartheta - \mathbf{1}^\top B\kappa - \mathbf{1}^\top \delta = 0, \quad (16a)$$

$$\mathbf{1}^\top \alpha\xi - \mathbf{1}^\top B\beta\xi - \mathbf{1}^\top \xi = 0, \quad (16b)$$

where equation (16a) is the deterministic gas conservation law, which is alternatively expressed through (1a), thus providing the first condition in (8a). The second condition in (8b) is provided from (16b), which holds for any realization of ξ if the recourse variables α and β obey $(\alpha - B\beta)^\top \mathbf{1} = \mathbf{1}$.

To obtain condition (8c), substitute (7) into the stochastic linearized Weymouth equation in (6b):

$$\begin{aligned} \varphi &= \gamma_1 + \gamma_2\pi + \gamma_3\kappa - \alpha(\hat{\gamma}_2 - \gamma_2\check{\gamma}_2)\xi \\ &\quad + \beta(\hat{\gamma}_3 - \gamma_2\check{\gamma}_2\hat{\gamma}_3 + \gamma_3)\xi + (\hat{\gamma}_2 - \gamma_2\check{\gamma}_2)\text{diag}[1]\xi \\ &= \gamma_1 + \gamma_2\pi + \gamma_3\kappa, \end{aligned}$$

yielding a deterministic equation due to the definition of constants $\hat{\gamma}_2$ and $\hat{\gamma}_3$. Finally, the stochastic equation for the reference node is satisfied by equations (15b).

C. Dualization of Conic Constraints

The results presented in this section are due to [26, Chapter 5]. Consider the SOCP problem of the form

$$\min_{x \in \mathbb{R}^n} c^\top x, \text{ s.t. } \|A_i x\| \leq b_i^\top x, \quad \forall i = 1, \dots, m, \quad (17a)$$

with $c \in \mathbb{R}^n$, $A_i \in \mathbb{R}^{n_i \times n}$, $b_i \in \mathbb{R}^n$. To dualize the second-order cone constraint, we use the fact that for any pair $\lambda_i \in \mathbb{R}^1$ and $u_i \in \mathbb{R}^{n_i}$ it holds that

$$\begin{aligned} \max_{\substack{u_i, \lambda_i: \\ \|u_i\| \leq \lambda_i}} -u_i^\top A_i x - \lambda_i b_i^\top x &= \max_{\lambda_i \geq 0} -\lambda_i (\|A_i x\| - b_i^\top x) \\ &= \begin{cases} 0, & \text{if } \|A_i x\| \leq b_i^\top x, \\ -\infty, & \text{otherwise.} \end{cases} \end{aligned} \quad (17b)$$

Therefore, the Lagrangian of the SOCP problem writes in variables $x \in \mathbb{R}^n$, $\lambda \in \mathbb{R}^m$ and $u \in \mathbb{R}^{n_i \times n}$ as

$$\max_{\|u_i\| \leq \lambda_i} \min_x \mathcal{L}(x, u, \lambda) = c^\top x - \sum_{i=1}^m (u_i^\top A_i x + \lambda_i b_i^\top x). \quad (17c)$$

Consider another SOCP problem of the form

$$\min_{x \in \mathbb{R}^n} c^\top x, \text{ s.t. } \|A_i x\|^2 \leq b_i^\top x, \quad \forall i = 1, \dots, m, \quad (17d)$$

with the *rotated* second-order cone constraint. To dualize this constraint, we use the fact that for any set of variables $\mu_i \in \mathbb{R}^1$, $\lambda_i \in \mathbb{R}^1$ and $u_i \in \mathbb{R}^{n_i}$ it holds that

$$\begin{aligned} \max_{\substack{u_i, \mu_i, \lambda_i: \\ \|u_i\|^2 \leq \mu_i \lambda_i}} -u_i^\top A_i x - 1/2 \lambda_i - \mu_i b_i^\top x \\ = \max_{\lambda_i \geq 0} -\lambda_i (\|A_i x\|^2 - b_i^\top x) = \begin{cases} 0, & \text{if } \|A_i x\|^2 \leq b_i^\top x, \\ -\infty, & \text{otherwise.} \end{cases} \end{aligned}$$

Therefore, the Lagrangian of the SOCP problem writes in variables $x \in \mathbb{R}^n$, $\mu, \lambda \in \mathbb{R}^m$ and $u \in \mathbb{R}^{n_i \times n}$ as

$$\begin{aligned} \max_{\|u_i\|^2 \leq \mu_i \lambda_i} \min_x \mathcal{L}(x, u, \mu, \lambda) &= c^\top x \\ &- \sum_{i=1}^m (u_i^\top A_i x + 1/2 \lambda_i + \mu_i b_i^\top x). \end{aligned} \quad (17e)$$

D. Proof of Theorem 1

Consider the problem of finding an equilibrium solution among the following set of agents. First, consider a price-setter who seeks the optimal prices to coupling constraints (12b)–(12i) in response to their slacks by solving

$$\begin{aligned} \max_{\lambda^c, \lambda^r, \lambda^w, \lambda^\varphi, \lambda^\pi, \lambda^\varphi, \lambda^\pi, \lambda_\pi} &\lambda^{c^\top} (A\varphi - \vartheta + B\kappa + \delta) \\ &+ \lambda^{r^\top} (\mathbb{1} - (\alpha - B\beta)^\top \mathbb{1}) + \lambda^{w^\top} (\varphi - \gamma_1 - \gamma_2\pi - \gamma_3\kappa) \\ &+ \sum_{\ell=1}^E \lambda_\ell^\varphi (s_\ell^\varphi - \|F[\hat{\gamma}_2(\alpha - \text{diag}[\mathbb{1}]) - \hat{\gamma}_3\beta]_\ell^\top\|) \\ &+ \sum_{n=1}^N \lambda_n^\pi (s_n^\pi - \|F[\hat{\gamma}_2(\alpha - \hat{\gamma}_3\beta - \text{diag}[\mathbb{1}])]_n^\top\|) \\ &+ \sum_{\ell=1}^E \lambda_\ell^\varphi (\varphi_\ell - z_\varepsilon \|F[\hat{\gamma}_2(\alpha - \text{diag}[\mathbb{1}]) - \hat{\gamma}_3\beta]_\ell^\top\|) \\ &+ \sum_{n=1}^N \lambda_\pi^\pi (\bar{\pi}_n - \pi_n - z_\varepsilon \|F[\hat{\gamma}_2(\alpha - \hat{\gamma}_3\beta - \text{diag}[\mathbb{1}])]_n^\top\|) \end{aligned}$$

$$+ \sum_{n=1}^N \lambda_\pi^\pi (\pi_n - \underline{\pi}_n - z_\varepsilon \|F[\hat{\gamma}_2(\alpha - \hat{\gamma}_3\beta - \text{diag}[\mathbb{1}])]_n^\top\|). \quad (18)$$

Problem (18) adjusts the prices respecting the slack of each constraint, e.g., $\lambda^c \downarrow$ if $A\varphi - \vartheta + B\kappa > \delta$, and $\lambda^c \uparrow$ otherwise. From SOCP property (17b), we know that the last five terms associated with the conic constraints rewrite equivalently as

$$\begin{aligned} &- \lambda^{c^\top} s^\varphi - \lambda^{c^\top} s^\pi - \lambda_\ell^\varphi \varphi - \lambda^\pi \pi - \lambda^\varphi \vartheta \\ &- \sum_{\ell=1}^E [u^\varphi + z_\varepsilon u^\varphi]_\ell F[\hat{\gamma}_2(\alpha - \text{diag}[\mathbb{1}]) - \hat{\gamma}_3\beta]_\ell^\top \\ &- \sum_{n=1}^N [u^\pi + z_\varepsilon u^\pi + z_\varepsilon u^\pi]_n F[\hat{\gamma}_2(\alpha - \hat{\gamma}_3\beta - \text{diag}[\mathbb{1}])]_n^\top, \end{aligned}$$

which is linear and separable, and where the dual variables $u^\varphi, u^\varphi \in \mathbb{R}^{E \times N}$ and $u^\pi, u^\pi, u^\pi \in \mathbb{R}^{N \times N}$ are subject to the following dual feasibility conditions

$$\|[u^\pi]_n\| \leq \lambda_n^\pi, \|[u^\pi]_n\| \leq \lambda_n^\pi, \|[u^\pi]_n\| \leq \lambda_n^\pi, \quad (19a)$$

$$\|[u^\varphi]_\ell\| \leq \lambda_\ell^\varphi, \|[u^\varphi]_\ell\| \leq \lambda_\ell^\varphi, \forall n \in \mathcal{N}, \forall \ell \in \mathcal{E}. \quad (19b)$$

By separating the terms with respect to the variables of network assets, network operator, and free terms associated with each consumer, we obtain the revenue functions in (13). Consider next that each gas supplier $n \in \mathcal{N}$ solves

$$\max_{\vartheta_n, [\alpha]_n, c_n^\vartheta, c_\alpha^\vartheta} \mathcal{R}_n^{\text{sup}}(\vartheta_n, [\alpha]_n) - c_{1n}\vartheta_n - c_n^\vartheta - c_\alpha^\vartheta \quad (20a)$$

$$\text{s.t. } \lambda_n^\vartheta : \|\dot{c}_{2n}\vartheta_n\|^2 \leq c_n^\vartheta, \quad (20b)$$

$$\lambda_n^\alpha : \|F\dot{c}_{2n}[\alpha]_n^\top\|^2 \leq c_n^\alpha, \quad (20c)$$

$$\lambda_n^\vartheta : z_\varepsilon \|F[\alpha]_n^\top\| \leq \bar{\vartheta}_n - \vartheta_n, \quad (20d)$$

$$\lambda_n^\vartheta : z_\varepsilon \|F[\alpha]_n^\top\| \leq \vartheta_n - \underline{\vartheta}_n, \quad (20e)$$

to maximize the profit in response to equilibrium prices. Next, consider that each active pipeline $\ell \in \mathcal{E}$ solves

$$\max_{\kappa_\ell, [\beta]_\ell} \mathcal{R}_\ell^{\text{act}}(\kappa_\ell, [\beta]_\ell) \quad (21a)$$

$$\text{s.t. } \lambda_\ell^\vartheta : z_\varepsilon \|F[\beta]_\ell^\top\| \leq \bar{\kappa}_\ell - \kappa_\ell, \quad (21b)$$

$$\lambda_\ell^\kappa : z_\varepsilon \|F[\beta]_\ell^\top\| \leq \kappa_\ell - \underline{\kappa}_\ell, \quad (21c)$$

to maximize the revenue in response to equilibrium prices. Finally, consider a gas network operator which solves

$$\min_{\pi, \varphi, s^\pi, s^\varphi} \mathcal{R}^{\text{rent}}(\pi, \varphi, s^\pi, s^\varphi) \quad (22a)$$

$$\text{s.t. } \lambda_r^\pi : \pi_r = \dot{\pi}_r \quad (22b)$$

to maximize the network rent in response to equilibrium prices. By taking the path outlined in Appendix C, the first-order optimality conditions of equilibrium problems (20)–(22) are given by the following equalities

$$\vartheta : c_1 - u^\vartheta \circ \dot{c}_2 - \lambda^c + \lambda^\vartheta - \lambda^\vartheta = \mathbb{0}, \quad (23a)$$

$$\kappa : [\lambda^{c^\top} B]^\top - [\lambda^{w^\top} \gamma_3]^\top + \lambda^\pi - \lambda^\kappa = \mathbb{0}, \quad (23b)$$

$$\pi : \lambda^\pi - \lambda^\pi - [\lambda^{w^\top} \gamma_2]^\top - \mathbb{I}_r \circ \lambda^\pi = \mathbb{0}, \quad (23c)$$

$$\varphi : [\lambda^{c^\top} A]^\top + \lambda^w - \lambda^\varphi = \mathbb{0}, \quad (23d)$$

$$s^\pi : \lambda^\pi = \psi^\pi, s^\varphi : \lambda^\varphi = \psi^\varphi, \quad (23e)$$

$$c^\vartheta : \mu^\vartheta = \mathbb{1}, c^\alpha : \mu^\alpha = \mathbb{1}, \quad (23f)$$

$$\begin{aligned} [\alpha]_n : F(u^\varphi \langle \gamma_2 \rangle_n + u^\pi \langle \gamma_2 \rangle_n + z_\varepsilon [u^\vartheta + u^\vartheta]_n^\top) \\ + F[u^\alpha]_n^\top \dot{c}_2 + \lambda^r = \mathbb{0}, \end{aligned} \quad (23g)$$

$$[\beta]_\ell: F(u^{\varphi^\top} \langle \hat{\gamma}_3 \rangle_\ell + u^{\pi^\top} \langle \check{\gamma}_2 \hat{\gamma}_3 \rangle_\ell - z_\varepsilon [u^{\bar{\kappa}} + u^{\underline{\kappa}}]_\ell^\top) + \mathbb{1}^\top \langle B \rangle_\ell \lambda^r = 0, \quad (23h)$$

where vector $\mathbb{1}_r \in \mathbb{R}^N$ takes 1 at position corresponding to the reference node, and 0 otherwise. Conditions (23) are identical to those of centralized problem (12), while the set of first-order optimality conditions of problem (18) yields primal constraints (12b)–(12i). Together with the primal constraints of equilibrium problems (20)–(22), they are identical to the feasibility conditions of the centralized problem. Hence, problem (12) solves the competitive equilibrium.

E. Proof of Corollary 1

From the feasibility conditions (12b)–(12d) and complementarity slackness conditions associated with constraints (12e)–(12i), we know that the objective function of the price-setting problem in (18) is zero at optimum. By rearranging the terms of (18), we have

$$\sum_{n=1}^N \mathcal{R}_n^{\text{con}} - \sum_{n=1}^N \mathcal{R}_n^{\text{sup}} - \sum_{\ell=1}^E \mathcal{R}_\ell^{\text{act}} = \mathcal{R}^{\text{rent}} + \lambda^{w^\top} \gamma_1.$$

If let $\gamma_1 = 0$, it remains to show that the congestion rent accumulated by the network is non-negative, i.e.,

$$\underbrace{(\lambda^{\varphi^\top} - \lambda^{w^\top} - \lambda^{c^\top} A) \varphi}_{\text{Term A}} + \underbrace{(\lambda^{w^\top} \gamma_2 + \lambda^{\pi^\top} - \lambda^{\bar{\pi}^\top}) \pi}_{\text{Term B}} + \underbrace{\lambda^{\bar{\pi}^\top} \bar{\pi} - \lambda^{\underline{\pi}^\top} \underline{\pi}}_{\text{Term C}} + \underbrace{\lambda^{\varphi^\top} s^\varphi + \lambda^{\pi^\top} s^\pi}_{\text{Term D}} \geq 0.$$

From optimality condition (23d), we know that term A is zero. Due to (23c), the term B is zero for all nodes but the reference one, and for the reference node it is $\lambda^{\bar{\pi}^\top} \bar{\pi} \geq 0$ from the dual objective function of problem (22). Term D is non-negative, because from (23e) we have that the dual prices λ^φ and λ^π are non-negative, and variables s^φ and s^π are lower-bounded by zero as per (12e) and (12f). In term C, $\lambda^{\bar{\pi}^\top} \bar{\pi}$ and $\lambda^{\underline{\pi}^\top} \underline{\pi}$ are non-negative due conditions (19a). Thus, the rent is always non-negative if and only if the network design allows $\underline{\pi} = 0$.

F. Proof of Corollary 2

We need to show that the functions (20a) and (21a) are non-negative. Both (20a) and (21a) are lower bounded by their corresponding dual functions, i.e.,

$$(20a) \geq 1/2(\lambda_n^\vartheta + \lambda_n^\alpha) + \lambda_n^{\bar{\vartheta}} \bar{\vartheta}_n - \lambda_n^{\underline{\vartheta}} \underline{\vartheta}_n, \quad \forall n \in \mathcal{N},$$

$$(21a) \geq \lambda_\ell^{\bar{\kappa}} \bar{\kappa}_\ell - \lambda_\ell^{\underline{\kappa}} \underline{\kappa}_\ell, \quad \forall \ell \in \mathcal{E}_a.$$

From the complementarity slackness of constraints in (20) and (21), we know that $\lambda^\vartheta, \lambda^\alpha, \lambda^{\bar{\vartheta}}, \lambda^{\underline{\vartheta}} \geq 0$ and $\lambda^{\bar{\kappa}}, \lambda^{\underline{\kappa}} \geq 0$. As injection limits are all non-negative, function (20a) is non-negative if and only if the network design allows $\underline{\vartheta} = 0$. As pressure regulation limits for compressors and valves are respectively non-negative and non-positive, function (21a) is non-negative if and only if the network design allows $\underline{\kappa}_\ell = 0, \forall \ell \in \mathcal{E}_c$ and $\bar{\kappa}_\ell = 0, \forall \ell \in \mathcal{E}_v$.

REFERENCES

- [1] BP Energy Outlook, “2019 edition,” *London, United Kingdom*, 2019.
- [2] PJM Interconnection, “Analysis of operational events and market impacts during the January 2014 cold weather events,” 2014.
- [3] R. Bent *et al.*, “Joint electricity and natural gas transmission planning with endogenous market feedbacks,” *IEEE Trans. Power Syst.*, vol. 33, no. 6, pp. 6397–6409, 2018.
- [4] A. Ben-Tal, L. El Ghaoui, and A. Nemirovski, *Robust optimization*, vol. 28. Princeton University Press, 2009.
- [5] A. Shapiro, D. Dentcheva, and A. Ruszczyński, *Lectures on stochastic programming: modeling and theory*. SIAM, 2014.
- [6] L. A. Roald *et al.*, “An uncertainty management framework for integrated gas-electric energy systems,” *Proc. IEEE*, 2020.
- [7] V. M. Zavala, “Stochastic optimal control model for natural gas networks,” *Comput. Chem. Eng.*, vol. 64, pp. 103 – 113, 2014.
- [8] C. Ordoudis, “Market-based approaches for the coordinated operation of electricity and natural gas systems,” *Ph.D. Thesis*, 2018. Technical University of Denmark.
- [9] A. Ratha *et al.*, “Affine policies for flexibility provision by natural gas networks to power systems,” *Electr. Power Syst. Res.*, vol. 189, 2020. Article no. 106565.
- [10] C. Ordoudis *et al.*, “Energy and reserve dispatch with distributionally robust joint chance constraints,” *Technical Report*, 2018. http://www.optimization-online.org/DB_FILE/2018/12/6962.pdf.
- [11] C. Wang *et al.*, “Strategic offering and equilibrium in coupled gas and electricity markets,” *IEEE Trans. Power Syst.*, vol. 33, no. 1, pp. 290–306, 2017.
- [12] C. Borraz-Sánchez *et al.*, “Convex relaxations for gas expansion planning,” *INFORMS J. Comput.*, vol. 28, no. 4, pp. 645–656, 2016.
- [13] M. K. Singh and V. Kekatos, “Natural gas flow solvers using convex relaxation,” *IEEE Trans. Control. Netw. Syst.*, 2020. to be published.
- [14] A. Zlotnik *et al.*, “Optimal control for scheduling and pricing intraday natural gas transport on pipeline networks,” in *2019 IEEE CDC*, pp. 4887–4894, 2019.
- [15] A. Zlotnik *et al.*, “Pipeline transient optimization for a gas-electric coordination decision support system,” in *PSIG Annual Meeting*, Pipeline Simulation Interest Group, Jun 2019.
- [16] A. Thorley and C. Tiley, “Unsteady and transient flow of compressible fluids in pipelines—a review of theoretical and some experimental studies,” *Int J Heat Fluid Flow*, vol. 8, no. 1, pp. 3–15, 1987.
- [17] M. K. Singh and V. Kekatos, “Natural gas flow equations: Uniqueness and an MI-SOCP solver,” in *2019 IEEE ACC*, pp. 2114–2120, 2019.
- [18] A. Wächter and L. T. Biegler, “On the implementation of an interior-point filter line-search algorithm for large-scale nonlinear programming,” *Math. Program.*, vol. 106, no. 1, pp. 25–57, 2006.
- [19] A. Nemirovski and A. Shapiro, “Convex approximations of chance constrained programs,” *SIAM J. Optim.*, vol. 17, no. 4, pp. 969–996, 2007.
- [20] D. Bienstock and A. Shukla, “Variance-aware optimal power flow: Addressing the tradeoff between cost, security, and variability,” *IEEE Trans. Control. Netw. Syst.*, vol. 6, no. 3, pp. 1185–1196, 2019.
- [21] R. Mieth, J. Kim, and Y. Dvorkin, “Risk-and variance-aware electricity pricing,” *Electr. Power Syst. Res.*, vol. 189, 2020. Article no. 106804.
- [22] M. C. Campi and S. Garatti, “The exact feasibility of randomized solutions of uncertain convex programs,” *SIAM J. Optim.*, vol. 19, no. 3, pp. 1211–1230, 2008.
- [23] W. Xie, S. Ahmed, and R. Jiang, “Optimized bonferroni approximations of distributionally robust joint chance constraints,” *Math. Program.*, pp. 1–34, 2019.
- [24] L. V. Kantorovich, “Mathematical methods of organizing and planning production,” *Manage. Sci.*, vol. 6, no. 4, pp. 366–422, 1960.
- [25] P. A. Samuelson, “Spatial price equilibrium and linear programming,” *The American Economic Review*, vol. 42, no. 3, pp. 283–303, 1952.
- [26] S. Boyd, S. P. Boyd, and L. Vandenberghe, *Convex optimization*. Cambridge university press, 2004.
- [27] V. Dvorkin Jr, J. Kazempour, and P. Pinson, “Electricity market equilibrium under information asymmetry,” *Oper. Res. Lett.*, vol. 47, no. 6, pp. 521–526, 2019.
- [28] S. Wu *et al.*, “Model relaxations for the fuel cost minimization of steady-state gas pipeline networks,” *Math. Comput. Modelling*, vol. 31, no. 2, pp. 197 – 220, 2000.
- [29] *Online repository: Stochastic Control and Pricing for Natural Gas Networks*, 2020 (accessed October 5, 2020). https://github.com/anubhavratha/ng_stochastic_control_and_pricing.
- [30] I. Dunning, J. Huchette, and M. Lubin, “Jump: A modeling language for mathematical optimization,” *SIAM Review*, vol. 59, no. 2, pp. 295–320, 2017.

[Paper B] Setting reserve requirements to approximate the efficiency of the stochastic dispatch

Authors:

V. Dvorkin, S. Delikaraoglou and J. M. Morales.

Published in:

IEEE Transactions on Power Systems

Setting Reserve Requirements to Approximate the Efficiency of the Stochastic Dispatch

Vladimir Dvorkin Jr., *Student member, IEEE*, Stefanos Delikaraoglou, *Member, IEEE*,
and Juan M. Morales, *Senior member, IEEE*

Abstract—This paper deals with the problem of clearing sequential electricity markets under uncertainty. We consider the European approach, where reserves are traded separately from energy to meet exogenous reserve requirements. Recently proposed stochastic dispatch models that co-optimize these services provide the most efficient solution in terms of expected operating costs by computing reserve needs endogenously. However, these models are incompatible with existing market designs. This paper proposes a new method to compute reserve requirements that bring the outcome of sequential markets closer to the stochastic energy and reserves co-optimization in terms of cost efficiency. Our method is based on a stochastic bilevel program that implicitly improves the inter-temporal coordination of energy and reserve markets, but remains compatible with the European market design. We use two standard IEEE reliability test cases to illustrate the benefit of intelligently setting operating reserves in single and multiple reserve control zones.

Index Terms—Bilevel optimization, electricity markets, market clearing, reserve requirements, stochastic programming.

NOMENCLATURE

The main notation used in this paper is stated below. Additional symbols are defined in the paper where needed. All symbols are augmented by index t when referring to different time periods.

A. Sets and Indices

Λ	Set of transmission lines.
$\omega \in \Omega$	Set of wind power production scenarios.
$i \in I$	Set of conventional generation units.
$j \in J$	Set of loads.
$k \in K$	Set of wind power units.
$n \in N$	Set of nodes.
$z \in Z$	Set of reserve control zones.
$\{\}_n$	Mapping of $\{\}$ into the set of nodes.
$\{\}_z$	Mapping of $\{\}$ into the set of reserve control zones.

V. Dvorkin Jr. is with the Technical University of Denmark, Kgs. Lyngby, Denmark (e-mail: vladvo@elektro.dtu.dk).

S. Delikaraoglou is with the ETH Zurich, Zurich, Switzerland (e-mail: delikaraoglou@eeh.ee.ethz.ch).

J.M. Morales is with the University of Malaga, Malaga, Spain (e-mail: juan.morales@uma.es).

The work by Vladimir Dvorkin Jr. was supported in part by the Russian Foundation for Basic Research (RFBR) according to the research project No. 16-36-00389. The work by Juan M. Morales was supported in part by the Spanish Ministry of Economy, Industry and Competitiveness through project ENE2017-83775-P; and in part by the European Research Council (ERC) under the EU Horizon 2020 research and innovation programme (grant agreement No. 755705) and the Research Program for Young Talented Researchers of the University of Malaga through project PPIT-UMA-B1-2017/18.

B. Decision variables

δ_n^{DA}	Day-ahead voltage angle at node n [rad].
$\delta_{n\omega}^{\text{RT}}$	Real-time voltage angle at node n in scenario ω [rad].
$D_z^{\text{U/D}}$	Up-/Downward reserve requirement in zone z [MW].
$L_{j\omega}^{\text{sh}}$	Shedding of load j in scenario ω [MW].
P_i^C	Day-ahead dispatch of conventional unit i [MW].
P_k^W	Day-ahead dispatch of wind power unit k [MW].
$P_{k\omega}^{\text{W,sp}}$	Wind spillage of unit k in scenario ω [MW].
$P_{k\omega}^{\text{W}}$	Wind power realization of unit k in scenario ω [MW].
$R_i^{\text{U/D}}$	Up-/Downward reserve provision from unit i [MW].
$r_{i\omega}^{\text{U/D}}$	Up-/Downward reserve deployment of unit i in scenario ω [MW].

C. Parameters

π_ω	Probability of occurrence of wind power production scenario ω .
C_i	Day-ahead price offer of unit i [\$/MWh].
$C_i^{\text{U/D}}$	Up-/Downward reserve price offer of unit i [\$/MWh].
C^{VoLL}	Value of lost load [\$/MWh].
\bar{F}_{nm}	Capacity of transmission line (n, m) [MW].
L_j	Demand of load j [MWh].
$\bar{P}_i^{\text{U/D}}$	Day-ahead quantity offer of unit i [MW].
$\bar{R}_i^{\text{U/D}}$	Up-/Downward reserve capacity offer of unit i [MW].
\hat{W}_k	Expected generation of wind power unit k [MW].
$W_{k\omega}$	Wind power realization of unit k in scenario ω [MW].
X_{nm}	Reactance of transmission line (n, m) [p.u.].

I. INTRODUCTION

ELECTRICITY markets are commonly organized in a sequence of trading floors in which different services are traded in various time-frames. According to the European market architecture, this sequence consists of reserve and day-ahead markets that are cleared 12-36 hours before actual power system operation and pertain to trading reserve capacity and energy services, respectively. Getting close to actual delivery of electricity, a real-time market is organized to balance deviations from the initial schedule. This market design has been established following a conventional view of power system operation, where uncertainty was induced by equipment contingencies or minor forecast errors of electricity demand. However, considering the increasing shares of renewable generation, this design has limited ability to cope with variable and uncertain energy sources, while maintaining a sufficient level of reliability at a reasonable cost [1].

To account for the uncertain nature of renewable generation, recent literature proposes economic dispatch models [2], [3]

and unit commitment formulations [4]–[6] based on stochastic optimization. Unlike the conventional market design, which downplays the cost of uncertainty, the stochastic model makes use of a probabilistic description of uncertainty and dispatches the system accounting for plausible forecast errors. In this case, reserve requirements are computed endogenously, instead of relying on rule-of-thumb methods such as the N-1 security criterion. Although the resulting *stochastic ideal* schedule provides the most efficient solution in terms of expected operating system costs, this design is not adopted in practice due to still unresolved issues like the violation of the least-cost merit-order principle [7].

There are several research contributions devoted to *approximating* the stochastic ideal solution, i.e., approaching the expected operating cost provided by the stochastic dispatch model while sidestepping its theoretical drawbacks, namely, the violation of *cost recovery* and *revenue adequacy* for certain realizations of the random variables. The cost recovery property guarantees that the profit of each conventional producer is greater than or equal to its operating costs. The revenue adequacy property requires that the payments that the system operator must make to and receive from the participants do not cause it to incur a financial deficit. Authors in [8] propose a new market-clearing procedure according to which wind power is dispatched to a value different than its forecast mean, such that the expected system cost is minimized. This procedure respects the merit order of the day-ahead market and thus ensures cost recovery of the flexible units. An enhanced stochastic dispatch that guarantees both cost recovery and revenue adequacy for every uncertainty realization is introduced in [9]. The main obstacle preventing the implementation of these two models is that they require changing the state of affairs of conventional market structures. Finally, authors in [10] propose a stochastic dispatch model that aims at generating proper price signals that incentivize generators to provide reliability services akin to reserves. This model also guarantees cost recovery and revenue adequacy for every uncertainty realization, but in the meantime it does also require significant changes in market design as well as in the offering strategies of the renewable power producers.

More in line with the current practices of the European market design, [11] proposes a systematic method to adjust available transfer capacities in order to bring operational efficiency of interconnected power systems closer to the stochastic solution. In the US electricity markets, several Independent System Operators (ISOs), e.g., the California ISO (CAISO) and Midcontinent ISO (MISO) are implementing new ramping capacity products to increase the ramping ability of the system during the real-time re-dispatch in order to cope with steep ramps of net load [12]. Essentially, these flexibility products aim to resemble the stochastic dispatch, which inherently finds the optimal allocation of flexible resources between energy and ramping services. In the same vein, several US ISOs, as for instance the New York ISO, the ISO New England, the MISO, and the Pennsylvania-New Jersey-Maryland (PJM) market, have introduced an operating reserve demand curve (ORDC) in their real-time market [13]. Motivated by the two-stage stochastic dispatch model, the ORDC mechanism

adjusts electricity prices to reflect the scarcity value of reserves for the system operator and incentivize market players to dispatch their units according to a socially optimal schedule. The price adjustment through ORDC leads theoretically to perfect arbitrage between energy and reserves in case these two products are co-optimized [14]. However, in the European market that separates energy and reserve capacity trading this arbitrage is inefficient per se, since market players have to value reserves prior to the energy-only market clearing.

This paper proposes an alternative approach to approximate the stochastic ideal dispatch solution through an intelligent setting of zonal reserve requirements in sequentially cleared electricity markets akin to the European architecture. Here, we solely focus on operating reserves, i.e., generation that is dispatched to respond to net load variations based on economic bids, rather than on regulating services that are activated by automatic generation control. Traditionally, requirements for operating reserves are defined based on deterministic security criteria, such as N-1 security constraint violations, where reserves are dimensioned to cover the largest contingency in the system [15], or based on a mean forecast load error and forced outage rate of system components over a certain horizon, as in the PJM market [16]. The main drawback of those approaches is that they ignore the probabilistic nature of renewable generation and neglect the economic impact of reserve needs on subsequent operations. In order to account for the operational uncertainty, recent literature proposes reserve dimensioning methods based on probabilistic criteria, according to which reserve requirements are drawn from the probabilistic description of uncertainties [17]–[26]. For example, [17] suggests to define the reserve needs such that they cover 97.7% (3σ) of the total variation of a Gaussian distribution modeling the joint wind-load uncertainty, disregarding the fact that wind power forecast errors are described by non-Gaussian distributions [24]. As a remedy to this drawback, [25] proposed a method for setting the reserve requirements using non-parametric probabilistic wind power forecasts. Flying brick and probability box methods in [20] and [21], respectively, compute robust envelopes that enclose the net load with a specified probability level. The recent extension of these methods called flexibility envelopes was suggested in [22]. These envelopes are based on the same principles but evolve in time to respect the temporal evolution of reserve requirements. As demonstrated in [20], [21] and [23], the probabilistic reserve concepts might be integrated into the actual energy management system and derive requirements for capacity, ramping capability and ramping duration of flexible units. In contrast to the deterministic practices, the benefit of these methods is that reserve requirements, drawn from accurately predicted distributions, minimize extreme balancing actions provoked by under- or over-procurement of reserves. However, probabilistic requirements are still an exogenous input to the power dispatch, which disregards their potential impact on expected cost.

To this end, we propose a model to determine reserves based on a stochastic bilevel programming problem, which provides the cost-optimal reserve quantities for a European-type market structure. In line with the stochastic dispatch mechanism, our

model computes the reserve requirements that minimize the expected system cost, anticipating their projected impact on the subsequent operations. Additionally, these requirements are defined accounting for the actual decision-making process, i.e., the sequence of market-clearing procedures, zonal representation of the power network and the least-cost merit-order principle in all trading floors. As a result, the implementation of these requirements in a conventional market setting, results in a compromise solution between traditional reserve dimensioning practices and the stochastic dispatch model in terms of expected operating cost. Naturally, our approach has limitations: we consider a simplified market setup with a strictly convex representation. Nevertheless, our results do indicate that the intelligent setting of reserve requirements can enhance the short-run cost efficiency of the conventional market with large shares of renewable generation.

The proposed model can be used as an analytic tool to provide technical and economic insights about the efficacy of different reserve capacity quantification methods, while it can be also used as a decision-support tool by system operators during the reserve setting process. In the latter case, this model can be presumably executed before the day-ahead reserve capacity auction in order to define the reserve requirements that will be used as input in the actual market-clearing process. Nevertheless, the incorporation of this method in the operational strategy of the system operator does not entail any changes in the existing market setup, since the model output is solely under the discretion of the system operator and decoupled from market operations.

The remainder of this paper is organized as follows. Section II describes the conventional market design and its counterfactual stochastic representation. Section III introduces the proposed stochastic bilevel programming problem to compute the optimal reserve requirements that approximate the ideal stochastic solution maintaining the sequential market structure. Section IV explains the solution strategy based on the multi-cut Bender's algorithm for large-scale applications. Section V provides applications of the proposed model to the IEEE-24 and IEEE-96 reliability test systems. Section VI concludes the paper.

II. ELECTRICITY MARKET CLEARING MODELS

In this section, we first describe the conventional market structure and the stochastic dispatch model. We then introduce the necessary modeling assumptions and provide the mathematical formulations of both models.

A. Conventional market and stochastic dispatch framework

In Europe, power markets are cleared in sequential and independent auctions which can be represented by the simplified decision-making process illustrated in Fig. 1(a), which is referred to as the *conventional* market-clearing model. First, the system operator defines zonal reserve requirements \mathcal{D} based on certain security standards. Then, the reserve capacity market is cleared based on the offer prices and quantities submitted by the flexible producers to find the optimal upward and downward reserve allocation Φ^R^* that minimizes reserve

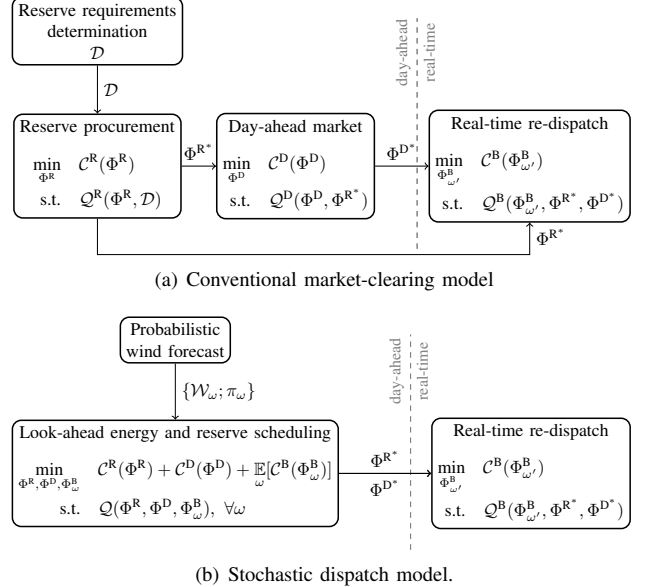


Fig. 1. Decision sequences in conventional (a) and stochastic (b) dispatch models.

procurement costs C^R . This allocation accounts for upward and downward reserve requirement constraints included in the set Q^R . At the next stage, power producers submit their price-quantity offers to the day-ahead market that provides the optimal energy schedule Φ^D^* that minimizes the day-ahead energy cost C^D . The set of day-ahead market constraints Q^D takes into account the reserve capacity Φ^R^* procured at the previous stage. Closer to delivery time, when realization of uncertainty ω' is known, the system operator runs the real-time market to define a set of optimal re-dispatch actions $\Phi_{\omega'}^B$, that minimizes the balancing cost C^B , considering the previously procured reserve Φ^R^* . In this conventional market design, the choice of reserve requirements D has a direct impact on the total expected system cost. In fact, the choice of D influences reserve procurement decisions Φ^R , which in turn affect day-ahead Φ^D and real-time Φ^B energy dispatch decisions.

An alternative model for reserves and energy scheduling is the *stochastic* dispatch model outlined in Fig. 1(b). This is a two-stage stochastic programming model in which first-stage decisions pertain to reserve procurement and day-ahead energy schedule, whereas the second stage models the recourse actions that restore power balance during real-time operation. The stochastic dispatch model takes as input a probabilistic wind power forecast in the form of a scenario set Ω and endogenously computes reserve needs. This way, it naturally coordinates all trading floors by co-optimizing reserve (Φ^R) and energy (Φ^D) schedules, anticipating their impact on the subsequent expected balancing cost $\mathbb{E}_{\omega}[C^B(\Phi_{\omega}^B)]$ estimated over the scenario set Ω . It should be noted that the co-optimization of reserve procurement and energy schedules is a requirement for the implementation of this ideal coordination between the different trading floors.

In the stochastic dispatch, reserve requirements are a byproduct of the energy and reserve co-optimization problem, resulting in the most efficient solution in terms of total expected operating cost. Moreover, unlike the conventional

market model that schedules reserve and day-ahead energy quantities according to the least-cost merit-order principle, the stochastic model schedules generation capacity accounting for potential network congestion during real-time operations, which may lead to expensive balancing actions [2]. This way generators may be scheduled out-of-merit, i.e., more expensive units are dispatched over less expensive ones, in order to minimize the expected costs.

Despite its superiority in terms of cost efficiency, the stochastic model suffers from several drawbacks preventing its practical implementation. As already mentioned, the violation of the merit-order principle results in cost recovery and revenue adequacy only in expectation, while for some uncertainty realizations these two essential economic properties may not hold [2]. This issue disputes the well-functioning of electricity markets in long term, since flexible producers may end up in loss-making positions in one or more scenarios, despite the fact that their expected profit is non-negative. Therefore, these market participants may opt out of the short-run electricity markets or even be discouraged to perform new investments if they are exposed to significant financial risks. In the meantime, the fact that revenue adequacy is only guaranteed in expectation exposes the market operator to the risk of financial deficit. Therefore, a realistic implementation of this market model would require the establishment of out-of-the-market mechanisms, akin to the uplift payments used in the US markets, to provide an ex-post compensation of potential economic deficits. In view of this practical caveats, we do not foresee an actual market clearing implementation of the stochastic dispatch model. Moreover, the co-optimization of day-ahead energy and capacity reserve markets is not compatible with the European market structure, which dictates that the trading of reserves and energy products is organized in independent sequential auctions. However, in this work, we show that the stochastic dispatch solution can be approximated in the conventional market-clearing model by intelligently setting the reserve requirements \mathcal{D} , sidestepping the drawbacks of the stochastic model and improving the efficiency of the existing market setup.

B. Modeling assumptions

We use the following set of assumptions to derive computationally tractable yet sensible formulations of the different dispatch models. Following the European practice, we consider a zonal representation of the network for reserve procurement. In an attempt to build a more generic model, the network topology is included in the day-ahead and real-time dispatch models considering a DC approximation of power flows. Reserve and energy supply functions are linear, and all generators are considered to behave as price takers. System loads are inelastic with a large value of lost load. This way, the maximization of the social welfare is equivalent to cost minimization. Flexible units deploy operating reserves with marginal costs of production. The incentive to provide flexibility services is accounted for in reserve offering prices. Following the prevailing portfolio bidding adopted in the European markets [27], we consider that all unit commitment and inter-temporal constraints are

integrated into the bidding strategies of the generating units. For instance, the commitment of thermal units in practice might be controlled by market participants when offering at either zero price or market price cap. Similarly, offering a part of capacity at zero and even negative price ensures the compliance with the technical minimum constraint of thermal units. This approach is compatible with the European market structure and preserves the convexity of the reserve capacity and day-ahead market-clearing algorithms. In principle, the proposed model can be also applied to market designs that involve non-convex constraints, as for instance the majority of electricity markets in the US, using tight convex relaxations of the unit commitment binary variables. However, this approach lies out of scope of this paper, but we refer the interested reader to [28], [29] for further discussion. Finally, uncertainty is described by a finite set of scenarios and solely induced by stochastic wind power production.

C. Mathematical formulation

1) *Conventional market-clearing model:* The sequential procedure, sketched in Fig. 1(a), for each hour of the next day is modeled by the following three linear optimization problems.

The reserve procurement problem writes as:

$$\min_{\Xi^{\text{OR}}} \sum_{i \in I} (C_i^{\text{U}} R_i^{\text{U}} + C_i^{\text{D}} R_i^{\text{D}}) \quad (1a)$$

$$\text{s.t. } \sum_{i \in I_z} R_i^{\text{U}} = D_z^{\text{U}}, \quad \sum_{i \in I_z} R_i^{\text{D}} = D_z^{\text{D}}, \quad \forall z \in Z, \quad (1b)$$

$$R_i^{\text{U}} + R_i^{\text{D}} \leq \bar{P}_i, \quad \forall i \in I, \quad (1c)$$

$$0 \leq R_i^{\text{U}} \leq \bar{R}_i^{\text{U}}, \quad 0 \leq R_i^{\text{D}} \leq \bar{R}_i^{\text{D}}, \quad \forall i \in I, \quad (1d)$$

where $\Xi^{\text{OR}} = \{R_i^{\text{U}}, R_i^{\text{D}}, \forall i\}$ is the set of optimization variables comprising the upward and downward reserve schedule per each flexible generator. Optimal $\Xi^{\text{OR}*}$ minimizes the reserve procurement cost given by (1a). Equality constraints (1b) ensure that zonal reserve upward and downward requirements, denoted as D_z^{U} and D_z^{D} , respectively, are fulfilled, whereas inequality constraints (1c) - (1d) account for the quantity offers of each flexible generator.

Once reserve allocation $\{R_i^{\text{U}*}, R_i^{\text{D}*}, \forall i\}$ is determined, the least-cost day-ahead energy schedule is computed solving the following optimization problem:

$$\min_{\Xi^{\text{DA}}} \sum_{i \in I} C_i P_i^{\text{C}} \quad (2a)$$

$$\text{s.t. } \sum_{i \in I_n} P_i^{\text{C}} + \sum_{k \in K_n} P_k^{\text{W}} - \sum_{j \in J_n} L_j - \sum_{m:(n,m) \in \Lambda} \frac{\delta_n^{\text{DA}} - \delta_m^{\text{DA}}}{x_{nm}} = 0, \quad \forall n \in N, \quad (2b)$$

$$R_i^{\text{D}*} \leq P_i^{\text{C}} \leq \bar{P}_i - R_i^{\text{U}*}, \quad \forall i \in I, \quad (2c)$$

$$0 \leq P_k^{\text{W}} \leq \widehat{W}_k, \quad \forall k \in K, \quad (2d)$$

$$\frac{\delta_n^{\text{DA}} - \delta_m^{\text{DA}}}{x_{nm}} \leq \bar{F}_{nm}, \quad \forall (n, m) \in \Lambda, \quad (2e)$$

where $\Xi^{\text{DA}} = \{P_i^{\text{C}}, \forall i; P_k^{\text{W}}, \forall k; \delta_n^{\text{DA}}, \forall n\}$ is the set of variables including day-ahead energy quantities for each conventional

and stochastic generator as well as voltage angles at each node. The objective function (2a) to be minimized is the day-ahead energy cost, subject to nodal power balance constraints (2b), offering limits of conventional and stochastic generators (2c)-(2d) and transmission capacity limits (2e). Note that the reserve procurement decisions from the previous stage limit the dispatch of flexible generators at the day-ahead stage. In this design, stochastic production is bounded by the conditional expectation \widehat{W}_k .

Getting closer to real-time operation, any deviation from the optimal day-ahead dispatch $\{P_i^{C*}, \forall i; P_k^{W*}, \forall k; \delta_n^{DA*}, \forall n\}$ has to be covered by proper balancing actions. For a specific realization of stochastic production $W_{k\omega'}$, the optimal re-dispatch is found solving the following linear programming problem:

$$\min_{\Xi^{\text{RT}}} \sum_{i \in I} C_i (r_{i\omega'}^U - r_{i\omega'}^D) + \sum_{j \in J} C^{\text{VoLL}} L_{j\omega'}^{\text{sh}} \quad (3a)$$

$$\begin{aligned} \text{s.t. } & \sum_{i \in I_n} (r_{i\omega'}^U - r_{i\omega'}^D) + \sum_{k \in K_n} (W_{k\omega'} - P_k^{W*} - P_{k\omega'}^{\text{W,sp}}) \\ & + \sum_{j \in J_n} L_{j\omega'}^{\text{sh}} - \sum_{m:(n,m) \in \Lambda} \frac{\delta_{n\omega'}^{\text{RT}} - \delta_n^{\text{DA}*} - \delta_{m\omega'}^{\text{RT}} + \delta_m^{\text{DA}*}}{x_{nm}} \\ & = 0, \quad \forall n \in N, \end{aligned} \quad (3b)$$

$$0 \leq r_{i\omega'}^U \leq R_i^{U*}, \quad 0 \leq r_{i\omega'}^D \leq R_i^{D*}, \quad \forall i \in I, \quad (3c)$$

$$\frac{\delta_{n\omega'}^{\text{RT}} - \delta_{m\omega'}^{\text{RT}}}{x_{nm}} \leq \bar{F}_{nm}, \quad \forall (n, m) \in \Lambda, \quad (3d)$$

$$0 \leq P_{k\omega'}^{\text{W,sp}} \leq W_{k\omega'}, \quad \forall k \in K, \quad (3e)$$

$$0 \leq L_{j\omega'}^{\text{sh}} \leq L_j, \quad \forall j \in J, \quad (3f)$$

where $\Xi^{\text{RT}} = \{r_{i\omega'}^U, r_{i\omega'}^D, \forall i; L_{j\omega'}^{\text{sh}}, \forall j; P_{k\omega'}^{\text{W,sp}}, \forall k; \delta_{n\omega'}^{\text{RT}}, \forall n\}$ is the set of re-dispatch decisions, comprising activation of operating reserves, load shedding, wind spillage and real-time voltage angles. The objective function (3a) to be minimized is the balancing cost. Equality constraints (3b) ensure the real-time nodal power balance. Inequalities (3c) limit activation of upward and downward reserves considering the procured reserve quantities. Constraints (3d) account for the power capacity of transmission lines. Finally, inequalities (3e) and (3f) limit wind spillage and load shedding actions to the actual realization of production and system demand, respectively.

2) *Stochastic dispatch model*: Assuming that wind power uncertainty is described by a finite set of outcomes $W_{k\omega}$ with corresponding probabilities π_ω , the stochastic dispatch procedure outlined in Fig. 1(b) writes as follows:

$$\begin{aligned} \min_{\Xi^{\text{SD}}} & \sum_{i \in I} (C_i^U R_i^U + C_i^D R_i^D + C_i P_i^C) + \\ & \sum_{\omega} \pi_\omega \left(\sum_{i \in I} C_i (r_{i\omega}^U - r_{i\omega}^D) + \sum_{j \in J} C^{\text{VoLL}} L_{j\omega}^{\text{sh}} \right) \end{aligned} \quad (4a)$$

$$\text{s.t. } \text{constraints (1b) - (1d)} \quad (4b)$$

$$\text{constraints (2b) - (2e)} \quad (4c)$$

$$\text{constraints (3b) - (3f)}, \quad \forall \omega \in \Omega \quad (4d)$$

where $\Xi^{\text{SD}} = \{\Xi^{\text{OR}} \cup \Xi^{\text{DA}} \cup \Xi^{\text{RT}}, \forall \omega \cup (D^U, D^D)\}$ is the set of stochastic dispatch variables. The objective function (4a) to be minimized is the reserve and day-ahead energy

cost as well as the expectation of the real-time cost, i.e., the expected cost over the entire decision sequence. Note, that upward and downward reserve requirements D_z^U and D_z^D in (1b) are decision variables and only used to reveal optimal reserve requirements in a stochastic programming sense.

After the optimal reserve procurement and day-ahead energy schedule are obtained, the system operator solves the real-time re-dispatch problem for a specific realization of the stochastic production ω' using formulation (3).

III. APPROXIMATING THE STOCHASTIC IDEAL

On the one hand, the conventional procedure has limited capability to accommodate large shares of stochastic production in a cost efficient manner compared to the stochastic dispatch. On the other hand, the adoption of the stochastic procedure appears to be unrealistic because it does not guarantee revenue adequacy and cost recovery for every uncertainty realization; these are important properties that, in contrast, hold in the sequential market structure [2], [8]. For this reason, our motivation is to enhance the cost-efficiency of the conventional market-clearing procedure without changing the market structure. In this line, we introduce a model that approximates the ideal stochastic solution within the conventional dispatch model by the appropriate setting of zonal reserve requirements. In essence, we aim at finding the reserve requirements that plugged into the conventional market-clearing model (1)-(3) will yield the minimum total expected system cost. To compute them, we use the bilevel programming problem illustrated in Fig. 2.

This model comprises two levels. The objective function of the upper level is the same as (4a) in the stochastic model (4) and aims at minimizing the total expected system cost. The upper-level constraints enforce real-time re-dispatch limits. The lower level consists of two optimization problems, namely, the reserve procurement and day-ahead market clearing problems, which are identical to the corresponding optimization problems (1) and (2) of the conventional model. However, in this bilevel structure, reserve requirements \mathcal{D} are decision variables of the upper-level problem, entering as parameters in the lower-level reserve procurement problem. Hence, reserve requirements \mathcal{D} are not an exogenous input to this model but are internally optimized, accounting for their impact in all three trading floors. As shown in Fig. 2, the upper-level decision on \mathcal{D} affects the reserve procurement schedule in the first lower-level problem, which in turn impacts the day-ahead clearing obtained from the second lower-level problem. In addition, the reserve and energy schedules Φ^R and Φ^D enter the upper level, constraining the real-time re-dispatch decisions.

The structure of this stochastic bilevel model guarantees that the temporal sequence of the different markets follows the existing European paradigm. Having the reserve capacity and day-ahead market clearings as two independent lower-level problems, ensures that reserves and day-ahead schedules are optimized separately, i.e., there is no co-optimization of energy and reserves, while none of these markets have information about the future re-dispatch actions. This property suffices to reproduce the real-time re-dispatch for each scenario indepen-

dently by including the corresponding constraints only in the upper-level problem.

Compared to the stochastic model, the main advantage of this bilevel scheme is that it respects the merit-order principle in the reserve capacity and day-ahead energy markets. In fact, given the same reserve requirements, the solutions of both lower-level problems are identical to the solutions of problems (1) and (2). Nonetheless, the upper-level problem can still anticipate the impact of reserve requirements on all trading floors and consequently on the total expected cost.

Since this model is solved prior to any market-clearing procedure, we assume that the system operator can gather information on the price-quantity offers of market participants. Even in the case of having to use an estimation of price-quantity offers similar to the ORDC mechanism, our approach accounts systematically for the impact of reserve procurement and the structure of forecast errors in all three trading floors. In a more realistic setup, this information can be obtained using inverse optimization techniques as proposed in [30] and [31].

Mathematically, the proposed reserve determination model writes as the following stochastic bilevel programming problem:

$$\min_{\Xi^{\text{RT}}, D_z^{\text{U}}, D_z^{\text{D}}} \quad (4a)$$

$$\text{s.t. constraints (3b) - (3f), } \forall \omega \in \Omega, \quad (5b)$$

$$D_z^{\text{U}}, D_z^{\text{D}} \geq 0, \quad \forall z \in Z, \quad (5c)$$

$$(R_i^{\text{U}}, R_i^{\text{D}}) \in \arg \left\{ \begin{array}{l} \min_{\Xi^{\text{OR}}} \quad (1a) \\ \text{s.t. constraints (1b) - (1d)} \end{array} \right\}, \quad (5d)$$

$$\left(P_i^{\text{C}}, P_k^{\text{W}}, \delta_n^{\text{DA}} \right) \in \arg \left\{ \begin{array}{l} \min_{\Xi^{\text{DA}}} \quad (2a) \\ \text{s.t. constraints (2b) - (2e)} \end{array} \right\}. \quad (5e)$$

According to the mathematical structure of model (5), the lower-level problems (5d) and (5e) guarantee that the reserve capacity and day-ahead energy markets are serially and independently optimized. This property is in accordance with the time-line of these trading floors in the European market framework. This temporal sequence is accomplished considering that upward $R_i^{\text{U}*}$ and downward $R_i^{\text{D}*}$ reserve schedules are variables of the reserve capacity market (5d) but enter as parameters in the day-ahead energy market (5e). Moreover, neither problem (5d) nor (5e) can foresee the outcome of the balancing market, which is included in the upper level of model (5). As a result, both markets have no information about the effect of their decisions on the real-time market. In turn, constraints (5b)-(5c) and the third term of the objective function (4a) clear the real-time market of the conventional model (1)-(3), independently for each scenario $\omega \in \Omega$, considering that the real-time re-dispatch cannot impact the previous trading floors which are ‘fixed’ to the conventional market solution through the lower-level problems (5d) and (5e).

This formulation is computationally intractable, since it consists of an upper-level optimization problem constrained by two lower-level optimization problems. However, since both lower-level problems are convex with linear objective functions and constraints, they can be replaced by their Karush-

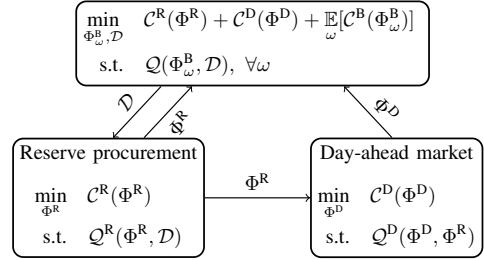


Fig. 2. Bilevel structure of the proposed reserve determination model.

Kuhn-Tucker optimally conditions, such that the problem can be recast as a single-level mathematical program with equilibrium constraints (MPEC). The resulting model includes a set of nonlinear complementary slackness constraints, which can be linearized using disjunctive constraints or SOS1 variables, transforming the MPEC problem into a mixed-integer linear program (MILP) [32].

IV. SOLUTION STRATEGY

The set of integer variables used to linearize the complementarity constraints of the lower-level problems (5d) and (5e) limits the application of the proposed reserve quantification model to power systems of moderate scale. For the large-scale applications, we propose an iterative solution strategy based on the multi-cut Bender’s algorithm [33]. For a fixed reserve and day-ahead dispatch, the set of real-time constraints (3b) - (3f) is independent per scenario. This allows for Bender’s decomposition where each subproblem solves a scenario-specific real-time re-dispatch problem. The subproblems at iteration ν write as follows:

$$\left\{ \begin{array}{l} \min_{\Xi_s^{\text{RTB}}} C_{\omega}^{\text{RT}(\nu)} := \sum_{i \in I} C_i (r_{i\omega}^{\text{U}} - r_{i\omega}^{\text{D}}) + \sum_{j \in J} C^{\text{VoLL}} L_{j\omega}^{\text{sh}} \end{array} \right. \quad (6a)$$

$$\text{s.t. } R_i^{\text{U}} = \tilde{R}_i^{\text{U}(\nu)} : \theta_{i\omega}^{R_i^{\text{U}(\nu)}}, \quad \forall i \in I, \quad (6b)$$

$$R_i^{\text{D}} = \tilde{R}_i^{\text{D}(\nu)} : \theta_{i\omega}^{R_i^{\text{D}(\nu)}}, \quad \forall i \in I, \quad (6c)$$

$$P_k^{\text{W}} = \tilde{P}_k^{\text{W}(\nu)} : \theta_{k\omega}^{P_k^{\text{W}(\nu)}}, \quad \forall k \in K, \quad (6d)$$

$$\delta_n^{\text{DA}} = \tilde{\delta}_n^{\text{DA}(\nu)} : \theta_{n\omega}^{\delta_n^{\text{DA}(\nu)}}, \quad \forall n \in N, \quad (6e)$$

$$\left. \text{constraints (3b) - (3f)} \right\} \quad \forall \omega \in \Omega,$$

where $\Xi_s^{\text{RTB}} = \Xi^{\text{RT}} \cup \{R_i^{\text{U}}, R_i^{\text{D}}, \forall i; P_k^{\text{W}}, \forall k; \delta_n^{\text{DA}}, \forall n\}$ is the set of decision variables of each subproblem of the Bender’s algorithm. Constraints (6b) - (6e) fix the first-stage decisions to their optimal values obtained at the previous iteration, and the corresponding dual variables yield sensitivities of the reserve and day-ahead decisions used in Bender’s cuts.

The master problem of the Bender’s algorithm at iteration ν writes as follows:

$$\min_{\Xi^{\text{M,B}}} \sum_{i \in I} (C_i^{\text{U}} R_i^{\text{U}} + C_i^{\text{D}} R_i^{\text{D}} + C_i P_i^{\text{C}}) + \sum_{\omega \in \Omega} \pi_{\omega} \alpha_{\omega}^{(\nu)} \quad (7a)$$

$$\text{s.t. } \alpha_{\omega}^{(\nu)} \geq C_{\omega}^{\text{RT}(\rho)} + \sum_{i \in I} \theta_{i\omega}^{R_i^{\text{U}(\rho)}} (R_i^{\text{U}} - R_i^{\text{U}(\rho)})$$

$$\begin{aligned}
& + \sum_{i \in I} \theta_{i\omega}^{R_i^D(\rho)} (R_i^D - R_i^{D(\rho)}) \\
& + \sum_{k \in K} \theta_{k\omega}^{P_k^W(\rho)} (P_k^W - P_k^{W(\rho)}) \\
& + \sum_{n \in N} \theta_{n\omega}^{\delta_n^{\text{DA}}(\rho)} (\delta_n^{\text{DA}} - \delta_n^{\text{DA}(\rho)}), \\
& \quad \rho = 1 \dots \nu - 1, \forall \omega \in \Omega, \tag{7b} \\
\alpha_\omega^{(\nu)} & \geq \underline{\alpha}, \quad \forall \omega \in \Omega, \tag{7c} \\
D_z^U, D_z^D & \geq 0, \quad \forall z \in Z, \tag{7d} \\
\text{Linearized KKT conditions of (5d),} & \tag{7e} \\
\text{Linearized KKT conditions of (5e),} & \tag{7f}
\end{aligned}$$

where $\Xi^{\text{M,B}} = \Xi^{\text{OR}} \cup \Xi^{\text{DA}} \cup \alpha_\omega$ is the set of decisions variables of the master problem, and index ρ is used to integrate the fixed values of the corresponding variables at previous iterations. The Bender's cuts are updated at each iteration by (7b) using sensitivities from all previous iterations, while (7c) imposes a lower bound $\underline{\alpha}$ on the auxiliary variable α . Since the subproblems allow for load shedding, they are always feasible, requiring no feasibility cuts in the master problem. The algorithm converges at iteration ν if $\left| \sum_{\omega \in \Omega} \pi_\omega (\alpha_\omega^{(\nu)} - C_\omega^{\text{RT}(\nu)}) \right| \leq \epsilon$, where ϵ is a predefined tolerance.

V. CASE STUDY

In this section, we first describe the test system in Section V-A. In Section V-B and Section V-C we study the impact of reserve requirements on expected operating costs and we assess the remaining efficiency gap of our model with respect to the stochastic solution for a single reserve control zone. In Section V-D we extend our analysis to the case of multiple reserve control zones. In Section V-E we assess the model's performance in the presence of non-convex technical constraints. Finally, in Section V-F we demonstrate the scalability of the model using the proposed Bender's decomposition algorithm.

A. Description of the test system

To assess the performance of the different reserve determination models, a modified version of the IEEE 24-Bus RTS [34] is employed. The system consists of 34 transmission lines, 17 loads and 12 conventional generation units. The total generation capacity amounts to 3,375 MW, from which 1,100 MW is flexible generation that can provide upward and downward reserves. We set upward reserve capacity price offers to be 30% of the marginal costs. Price offers for downward reserve capacity price offers are selected such that they compensate for the potential financial deficit induced by a loss-making position in the day-ahead market. We should note that this is only a heuristic approach to address the possibility that some flexible producers incur financial losses due to their combined positions in the reserve capacity and day-ahead energy markets. This situation may emerge if the downward reserve capacity R_i^{D*} awarded to a generator, and in turn imposed as a lower bound in the day-ahead market constraint

(2c), forces this unit to produce even if the day-ahead energy price is lower than its marginal production cost. This pitfall results from the separation of reserve capacity and energy markets in the European framework. In turn, the physical coupling of these two products is accounted for internally in the trading strategies of the market participants when they submit their price-quantity offers in the corresponding markets according to their risk appetite. A detailed study of this issue constitutes a separate research topic and lies out of the scope of this work, but the interested reader is referred to [35] and [36] for further information on this topic. Apart from conventional generators, there are six wind farms bidding at zero marginal cost and sited as explained in [34]. We consider a 24-hour load profile with a peak value of 2,650 MW obtained from [34]. The loads are assumed to be inelastic with the value of lost load equal to \$500/MW for all operating hours. The relevant GAMS codes and simulation data are provided in the electronic companion of the paper [37].

All simulations are carried out using a standard PC with Intel Core i5 CPU with a clock rate of 2.7 GHz requiring no more than 8GB of RAM. The CPU time required to solve the conventional model (1)-(3), stochastic model (4) and bilevel model (5) in Sections V-B–V-D is kept below 30s when solving per operating hour. The sequential market with unit commitment and inter-temporal constraints is solved in less than a minute in Section V-E. The CPU time corresponding to the last case study is reported separately in Section V-F.

B. Impact of reserve requirements on expected system cost

In this section we assess the expected cost of operating the power system under the conventional market setup (1)-(3), when this is fed with the reserve requirements determined by different approaches for reserve dimensioning, including our proposal. To this end, we consider the time period corresponding to the peak-load hour. Besides, the capacity of each wind power farm is set to 100 MW. Next we discuss the results linked to each reserve dimensioning approach:

- 1) The *probabilistic approach* defines the reserve requirements from the predictive cumulative distribution function (CDF) F of the total wind power portfolio, as the distance between the expected wind power production \widehat{W} and a specified quantile $q^{(\alpha)} = F^{-1}(\alpha)$ with nominal proportion $\alpha \in [0, 1]$. This approach resembles the state-of-the-art reserve-dimensioning processes employed by European system operators using probabilistic forecast information [26]. For a reliability level $\xi = \bar{\alpha} - \underline{\alpha}$, the upward and downward reserve needs are dimensioned as follows:

$$D^U = \widehat{W} - F^{-1}(\bar{\alpha}), \tag{8a}$$

$$D^D = F^{-1}(\underline{\alpha}) - \widehat{W}. \tag{8b}$$

We initially consider $\underline{\alpha} = 5\%$ and $\bar{\alpha} = 1 - \underline{\alpha} = 95\%$ corresponding to a reliability level $\xi = 90\%$. The resulting requirements amount to 127.9 MW and 89.1 MW for upward and downward reserves, respectively.

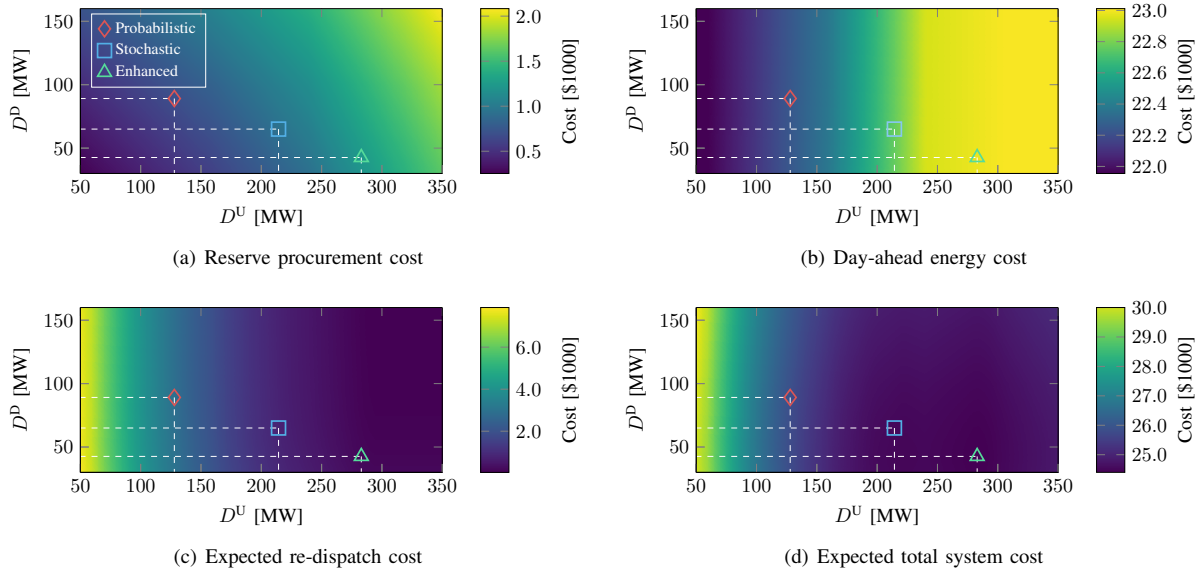


Fig. 3. Impact of downward D^D and upward D^U operating reserve requirements on the reserve (a), day-ahead (b), expected re-dispatch (c) and expected total (d) costs in the conventional procedure (1)-(3). The color density indicates the cost at the considered trading floor.

- 2) *The stochastic approach* derives the reserve requirements from the stochastic dispatch model (4). These requirements are equal to 214.3 MW for upward and 65.0 MW for downward reserves, respectively.
- 3) *The enhanced approach* computes the reserve requirements using the proposed reserve determination model (5). Resulting reserve needs amount to 282.9 MW and 42.6 MW for upward and downward reserves, respectively.

The expected total system costs resulting from the implementation of the probabilistic, stochastic and enhanced operating reserve approaches are \$25,890, \$24,531 and \$24,408, respectively. The total cost break-down is shown in Fig. 3, which demonstrates the impact of the reserve requirements on the cost of the different trading floors in the conventional dispatch procedure. Figure 3(a) shows that the reserve needs computed using the proposed model result in the highest reserve procurement cost among the different approaches, mainly due to a larger volume of upward reserve provision. In turn, efficient flexible generation that could be scheduled in the day-ahead market is now set aside to provide upward reserves. Considering that the price offers for upward reserve are proportional to the day-ahead price offers, the withdrawal of these resources increases the day-ahead energy cost, as shown in Fig. 3(b). Nonetheless, the benefits of the enhanced approach realize in real-time operation as the re-dispatch cost is lower compared to that yielded by the probabilistic and stochastic approaches as illustrated in Fig. 3(c). As a result, the minimum of the expected total costs is achieved with the enhanced approach as demonstrated by Fig. 3(d).

Increasing the reliability level ξ in the probabilistic approach may have a positive impact on the performance of the conventional model. However, Table I shows that this approach never yields the expected cost provided by the proposed model, since the probabilistic approach sets the requirements disregarding their impact on the subsequent op-

TABLE I
COST BREAK-DOWN RESULTING FROM THE IMPLEMENTATION OF A RANGE OF PROBABILISTIC REQUIREMENTS AND ENHANCED REQUIREMENTS.

Approach	Probabilistic approach					Enhanced approach
	Quantiles $q^{(\underline{\alpha}, \bar{\alpha})}$ of wind CDF	$q^{(05/95)}$	$q^{(04/96)}$	$q^{(03/97)}$	$q^{(02/98)}$	
Requirements $D^{U/D}$ [MW]	128/89	168/91	205/93	210/94	283/169	283/43
Exp. total cost [\$1000]	25.89	24.99	24.62	24.61	24.78	24.40
- Reserve	0.69	0.84	0.99	1.01	1.70	1.24
- Day-ahead	22.24	22.43	22.70	22.74	22.99	22.99
- Real-time	2.96	1.72	0.93	0.86	0.88	0.18

erations, including potential wind spillage and load shedding. On the contrary, the proposed model finds the optimal trade-off between reserve procurement and real-time re-dispatch decisions that minimizes the total expected system cost. In this particular case, our model allows more wind curtailment to reduce downward reserve procurement cost.

Regarding the stochastic model, it should be noted that even though reserve requirements are set anticipating the real-time cost, reserve procurement and day-ahead energy schedules are obtained by a co-optimization of these products that is incompatible with the European market structure. As a result, the requirements provided by the stochastic approach lead to larger amounts of load shedding, highlighting that they are practically sub-optimal in a sequential dispatch procedure.

C. Approximating the stochastic dispatch solution

We now investigate to what extent the reserve requirements computed with the proposed model are capable of approximating the ideal stochastic solution within the sequential dispatch procedure. To this end, we compare expected daily system cost of three optimization models for different wind power penetration levels, defined as the ratio between the installed capacity of the entire wind power portfolio and the peak load. The first model represents the sequential market clearing (1)-

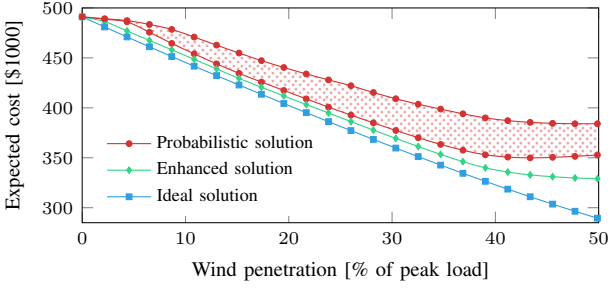


Fig. 4. Expected daily operating cost as a function of wind penetration.

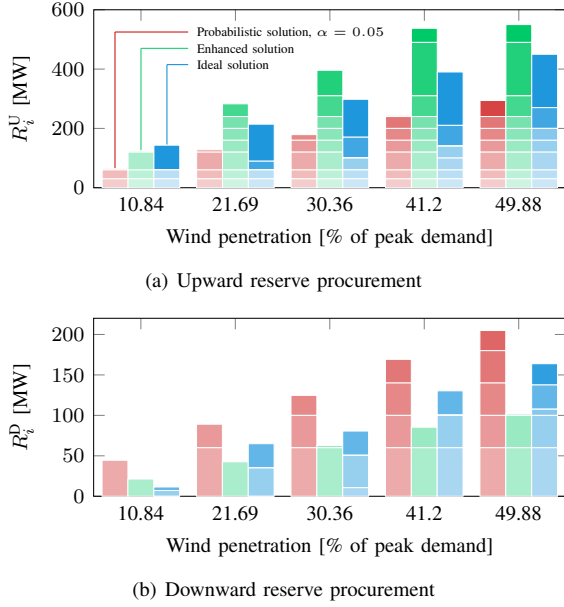


Fig. 5. Reserve procurement from nine flexible generating units for the peak-load hour and different wind penetration levels. Color density ranks generation units according to the reserve capacity price offers.

(3) with reserve requirements computed with the probabilistic approach for a range of reliability levels $\xi \in [0.9, 1]$. The second model also follows the sequential market procedure with reserve requirements computed with the proposed model (5). The third one is the stochastic ideal dispatch model (4) that theoretically attains maximum cost-efficiency, and therefore it is used as a lower bound of the expected system cost. It is worth noting the different role that the stochastic dispatch model plays in this part of the case study, compared to the previous Section V-B. Here, we assume that the solution of the stochastic dispatch model will be implemented as the actual system schedule, presuming that the conventional market setup is replaced with its ideal stochastic counterpart. This is different from the application of the stochastic dispatch model (4) as a reserve-dimensioning approach in Section V-B, where we considered that all trading floors are settled according to the prevailing European market model.

Figure 4 depicts the daily operating cost as a function of the wind power penetration level for the three models. The setting of the reserve requirements provided by the proposed model always results in a lower expected cost than the implementation of the requirements under the probabilistic approach.

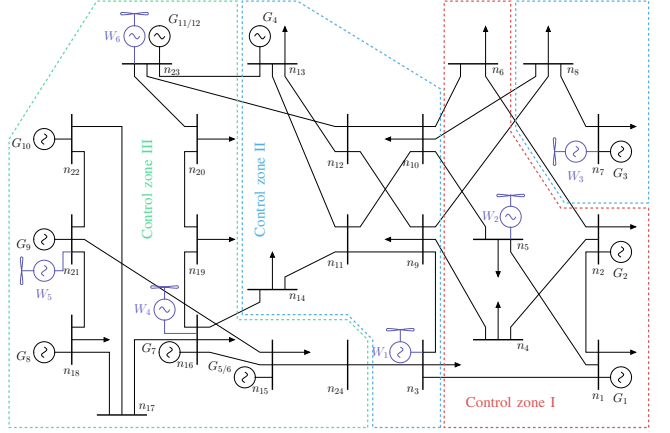


Fig. 6. IEEE 24-Bus reliability test system layout with three reserve control zones.

This figure further indicates that these reserve requirements efficiently approximate the stochastic ideal solution even for a high penetration of wind power.

Figure 5 provides further insights on the difference between the solutions of the three models. Particularly, it shows the procurement of upward and downward reserves from specific flexible units ranked according to their reserve capacity price offers, i.e., from cheap to more expensive units distinguished by increasing color densities. The proposed model controls the trade-off between reserve and real-time costs, ensuring adequate upward reserves to minimize the amount of load shedding and enough downward reserves to prevent wind spillage. In contrast, the probabilistic approach underestimates upward reserve needs, while it overestimates downward reserve requirements.

The enhanced solution for the reserve requirements deviates significantly from the ideal solution given that the stochastic model has more degrees of freedom, i.e., it controls not only the sufficiency of the reserve requirements but also their allocation among the flexible generators. This results in reserve procurement being ‘generator-specific’ which prevents network congestion within the reserve control area. In attempt to minimize expensive balancing actions, the stochastic model may allocate reserves to more expensive units over cheaper providers, violating the least-cost merit-order principle that is inherent in the conventional market design. As a consequence, the requirement imposed in our enhanced approach to respect the merit-order principle in the reserve capacity and day-ahead markets restricts the degree of approximation of the stochastic solution.

D. Optimal zonal reserve requirements allocation

We now consider the optimal reserve dimensioning in a multi-zone setting. For this purpose, the IEEE 24-Bus system is split into three reserve control zones as depicted in Fig. 6. This zonal layout corresponds to the one proposed in [11]. In each control zone there are at least one wind power unit with capacity of 100 MW and at least two flexible generation units. Unlike in the previous instance, the requirements computed with the probabilistic approach are now set for each reserve control zone independently considering the distribution of

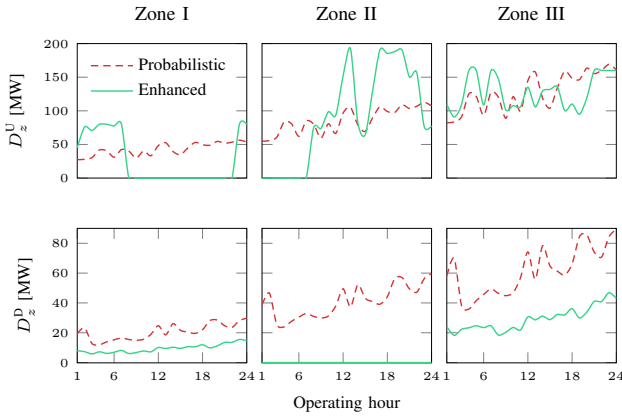


Fig. 7. 24-hour profiles of probabilistic and enhanced reserve requirements in three control zones.

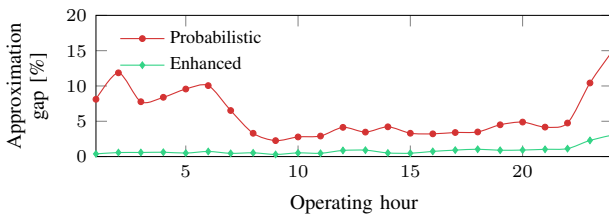
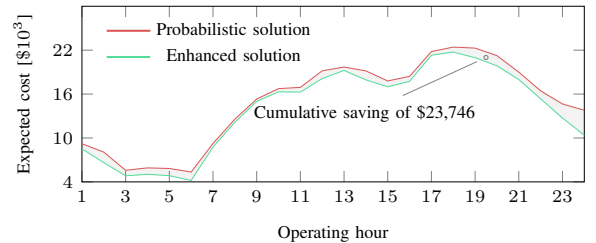


Fig. 8. Approximation gap of the sequential market with probabilistic and enhanced reserve requirements compared to stochastic dispatch.

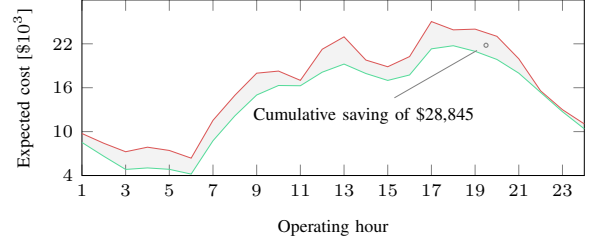
wind power production of each zone. The reliability level ξ is set to 0.98.

The resulting allocation for upward and downward reserve requirements among control zones is summarized in Fig. 7, indicating that the probabilistic approach sets the reserve needs proportionally to the amount of stochastic in-feed in the respective control zone. On the other hand, the proposed model defines the requirements considering not only the zonal wind power in-feed, but also the cost implications of procuring reserve in a specific zone. As a result, the model finds it more efficient to constantly procure upward reserve from the third zone and obtain the remaining upward reserve that is needed either from the first or the second zone depending on the operating hour. In addition, this reserve allocation indicates that it is never optimal to procure downward reserve from the second zone in terms of expected system cost.

This optimal reserve allocation among control zones is supported by the approximation gap depicted in Fig. 8, showing the relative cost difference of the sequential market with respect to the ideal solution. The requirements provided by the proposed model efficiently approximate the ideal solution with nearly zero gap over the first operating hours, and this gap remains relatively small for the subsequent hours as opposed to the large gap when probabilistic requirements are used. The definition of multiple control zones allows to set enhanced reserve requirements that are closer to the ‘generator-specific’ reserve allocation of the stochastic model. Indeed, compared to the single-zone setup in section V-B, the operating cost reduces by 2.5%, from \$24,408 to \$24,034, after the definition of three control zones.



(a) Reliability level $\xi = 98\%$



(b) Reliability level $\xi = 90\%$

Fig. 9. Expected operating cost yielded by the implementation of the probabilistic and enhanced reserve requirements in the conventional market-clearing problem (1)-(3) including the unit commitment constraints (9a)-(9g).

E. Assessing enhanced reserve requirements in the presence of non-convexities

To assess the performance for the proposed reserve quantification model as a proxy model for the power markets with a more comprehensive and non-convex representation of technical constraints, we use the enhanced reserve requirements provided by the proposed model (5) as inputs to the sequential market-clearing problem (1)-(3) with unit commitment and ramping constraints integrated in the day-ahead auction as explained in Appendix A.

Figure 9 shows the hourly profile of expected operating system cost resulting from the implementation of the enhanced requirements in the system with full representation of the technical constraints. This profile is compared against those obtained by setting probabilistic reserve requirements with reliability levels of 98% and 90%. The reserve requirements provided by the proposed model always attain better cost efficiency than the probabilistic requirements, even though the proposed model does not account for the whole set of technical limits of power plants. In the first case in Fig. 9 (a), the model allows savings of \$23,746 that nearly equal to the cost of peak-hour operation, and it allows even larger savings of \$28,845 in the second case in Fig. 9 (b).

F. Application to the IEEE-96 RTS

We now consider the modernized version of the IEEE-96 RTS Test System proposed in [38] to assess the scalability of the proposed model. The test system includes three control zones interconnected by six tie-lines. The system demand follows a 24-hour profile with a peak load of 7.5 GW. The conventional generation is represented by 6 nuclear power plants serving the base load, 3 coal power plants that offer 40% of their capacities for the reserve needs, and 87 gas-fired power plants offering 100% of their capacities to the reserve procurement auction. The reserve offering prices of

TABLE II
CPU PERFORMANCE OF THE BENDER'S ALGORITHM.

Wind penetration [%]	13.8	23.0	36.8
CPU time [min]	32.1	33.5	58.6

TABLE III
DAILY OPERATING COST WITH PROBABILISTIC AND ENHANCED ZONAL RESERVE REQUIREMENTS IN COMPARISON WITH THE STOCHASTIC IDEAL SOLUTION [\$1000].

Wind penetration [%]	Probabilistic solution		Enhanced solution	Ideal solution
	$\xi = 90\%$	$\xi = 98\%$		
13.8	1,912.4	1,888.8	1,877.3	1,850.0
23.0	1,760.8	1,719.3	1,700.8	1,660.5
36.8	1,550.7	1,482.3	1,446.0	1,402.8

flexible units are set to 25% of marginal production cost for both upward and downward reserve needs. There are 19 wind farms distributed among the control zones with the overall capacity of 2.76 GW. Their stochastic output is described by 100 equiprobable scenarios obtained from [39]. The input data and the corresponding GAMS codes are provided in the electronic companion of the paper [37].

The test case is solved for wind penetration levels of 13.8%, 23.0%, and 36.8% of the peak-hour load by implementing the multicut Bender's algorithm explained in Section IV. The tolerance of the algorithm is set to 0.02% requiring three to eight iterations depending on the operating hour. The resulting CPU time is reported in Table II. The CPU time in all three cases is kept below one hour allowing timely day-ahead planning with the proposed model. It is worth mentioning that the CPU time can be reduced at the expense of a marginal deviation from the global optimum with higher tolerance.

The daily operating cost resulting from the implementation of the enhanced zonal reserve requirements computed by the proposed model is always lower than those provided by the probabilistic approach with reliability levels of 90% and 98%, as demonstrated in Table III. The difference in operating cost is explained by the anticipated cost of procuring upward and downward reserves from a specific control zone, while the probabilistic requirements are solely obtained proportionally to the amount of stochastic in-feed in control zones. As a result, the relative cost savings provided by the model increases with the wind penetration level and ranges between 0.6% and 7.2%. Further cost savings towards the ideal solution provided by the stochastic model is limited due to the enforced merit order in both reserve and day-ahead markets. Finally, Table IV illustrates the economic benefit that the proposed model yields as a proxy for the system with the full network representation and technical constraints of power plants described in Appendix A. The results show that in spite of the incomplete description of technical constraints in the lower level of the proposed bilevel model, it still provides a feasible input with a sensible cost reduction for the markets with non-convexities. The economic benefit provided by the model ranges from 0.5% to 1.6%. Moreover, the proposed approach further outperforms the probabilistic one for the largest wind penetration level, where the overestimated requirements provided by the probabilistic approach lead to a reserve schedule that results in an infeasible

TABLE IV
DAILY OPERATING COST WITH PROBABILISTIC AND ENHANCED ZONAL RESERVE REQUIREMENTS WITH FULL REPRESENTATION OF TECHNICAL CONSTRAINTS [\$1000].

Wind penetration [%]	Probabilistic solution		Enhanced solution
	$\xi = 90\%$	$\xi = 98\%$	
13.8	2,072.2	2,073.4	2,061.5
23.0	1,947.9	1,949.1	1,928.6
36.8	1,764.4	infeas.	1,735.9

day-ahead operation.

VI. CONCLUSION

This paper considers the optimal setting of reserve requirements in a European market framework. We propose a new method to quantify reserve needs that brings the sequence of the reserve, day-ahead and real-time markets closer to the ideal stochastic energy and reserves co-optimization model in terms of total expected cost. The proposed model is formulated as a stochastic bilevel problem, which is eventually recast as a MILP problem. To reduce the computational burden of this model, we apply an iterative solution approach based on the multi-cut Bender's decomposition algorithm.

Our numerical studies demonstrate the benefit of properly setting reserve requirements. Our reserve quantification model outperforms both the probabilistic and the stochastic reserve setting approaches due to its preemptive ability to anticipate the impact of day-ahead decisions on the real-time operation, while taking into account the actual market structure. Considering the increasing penetration of stochastic power producers, we show that the reserve requirements provided by the proposed model take the expected system operating cost closer to that given by the ideal energy and reserve co-optimization model, but the degree of this approximation is limited due to the sequential scheduling of reserve and energy in European electricity markets. However, our analysis further indicates that the definition of multiple reserve control zones allows for a more efficient spatial allocation of reserves, which reduces the approximation gap with respect to the ideal stochastic model. Finally, the efficiency of the proposed reserve dimensioning model was tested against market designs whose clearing process explicitly account for inter-temporal and non-convex constraints, i.e. ramping limits and unit commitment constraints. Even though the proposed model does not account for the whole set of technical constraints of such markets, the enhanced reserve requirements still bring the cost of sequential market operation closer to the stochastic ideal, highlighting the importance of the intertemporal coordination between the three trading floors through the intelligent setting of reserve needs.

Future research may focus on the consideration of the tight relaxations of the unit commitment constraints to achieve better approximations for the case of non-convex market designs, and the corresponding tuning of the Bender's decomposition algorithm to better cope with the intertemporal constraints.

APPENDIX

A. Incorporation of unit commitment and ramping constraints

In contrast to the prevailing approach of the European market design, other electricity markets, e.g., the majority of US markets, explicitly model unit commitment constraints and thermal limits of power plants in the market-clearing problem. To assess the performance of the proposed reserve quantification model in markets with unit commitment constraints, the following set of constraints are integrated in the day-ahead market-clearing problem:

$$u_{it}\underline{P}_i \leq P_{it}^C \leq u_{it}\bar{P}_i, \forall i \in I, \forall t \in T, \quad (9a)$$

$$SU_{it} \geq C_i^{\text{SU}}(u_{it} - u_{i(t-1)}), \forall i \in I, \forall t > 1, \quad (9b)$$

$$SU_{it} \geq C_i^{\text{SU}}(u_{it} - u_i^0), \forall i \in I, t = 1, \quad (9c)$$

$$P_{it}^C - P_{i(t-1)}^C \leq R_i^+, \forall i \in I, \forall t > 1, \quad (9d)$$

$$P_{it}^C - P_i^{C,0} \leq R_i^+, \forall i \in I, t = 1, \quad (9e)$$

$$P_{i(t-1)}^C - P_{it}^C \leq R_i^-, \forall i \in I, \forall t > 1, \quad (9f)$$

$$P_i^{C,0} - P_{it}^C \leq R_i^-, \forall i \in I, t = 1, \quad (9g)$$

where $t \in T$ is the set of operating hours, C_i^{SU} is a start-up cost of unit i , R_i^+ and R_i^- are the ramp-up and ramp-down limits, \underline{P}_i is a minimum power output limit, and $P_i^{C,0}$ and u_i^0 are the initial power output and commitment status of unit i . The set of decision variables of the original problem is supplemented with variable $u_{it} \in \{0, 1\}$ that denotes the commitment status of generating units, and variable SU_{it} that computes the cost induced by the start-up of generating units. Now, the generating limits of each unit are additionally enforced by commitment decisions of the system operator by (9a). Binary logic is controlled by (9b) and (9c) and activated by augmenting SU_{it} into the original objective function of problem (2). The ramp limits of generators are accounted for through (9d)-(9g).

REFERENCES

- [1] T. Aigner, S. Jaehnert, G. L. Doorman, and T. Gjengedal, "The effect of large-scale wind power on system balancing in Northern Europe," *IEEE Trans. Sustain. Energy*, vol. 3, no. 4, pp. 751–759, 2012.
- [2] J. M. Morales, A. J. Conejo, K. Liu, and J. Zhong, "Pricing electricity in pools with wind producers," *IEEE Trans. Power Syst.*, vol. 27, no. 3, pp. 1366–1376, 2012.
- [3] F. Bouffard, F. D. Galiana, and A. J. Conejo, "Market-clearing with stochastic security-part I: formulation," *IEEE Trans. Power Syst.*, vol. 20, no. 4, pp. 1818–1826, 2005.
- [4] A. Papavasiliou, S. S. Oren, and B. Rountree, "Applying high performance computing to transmission-constrained stochastic unit commitment for renewable energy integration," *IEEE Trans. Power Syst.*, vol. 30, no. 3, pp. 1109–1120, 2015.
- [5] A. Tuohy, P. Meibom, E. Denny, and M. O'Malley, "Unit commitment for systems with significant wind penetration," *IEEE Trans. Power Syst.*, vol. 24, no. 2, pp. 592–601, 2009.
- [6] J. Wang, M. Shahidehpour, and Z. Li, "Security-constrained unit commitment with volatile wind power generation," *IEEE Trans. Power Syst.*, vol. 23, no. 3, pp. 1319–1327, 2008.
- [7] V. M. Zavala, K. Kim, M. Anitescu, and J. Birge, "A stochastic electricity market clearing formulation with consistent pricing properties," *Eur. Oper. Res.*, vol. 65, no. 3, pp. 557–576, 2017.
- [8] J. M. Morales, M. Zugno, S. Pineda, and P. Pinson, "Electricity market clearing with improved scheduling of stochastic production," *Eur. J. Oper. Res.*, vol. 235, no. 3, pp. 765–774, 2014.
- [9] J. Kazempour, P. Pinson, and B. F. Hobbs, "A stochastic market design with revenue adequacy and cost recovery by scenario: Benefits and costs," *IEEE Trans. Power Syst.*, vol. 33, no. 4, pp. 3531–3545, 2018.
- [10] M. Sarfati, M. R. Hesamzadeh, D. R. Biggar, and R. Baldick, "Probabilistic pricing of ramp service in power systems with wind and solar generation," *Renewable and Sustainable Energy Reviews*, vol. 90, pp. 851 – 862, 2018.
- [11] T. V. Jensen, J. Kazempour, and P. Pinson, "Cost-optimal ATCs in zonal electricity markets," *IEEE Trans. Power Syst.*, vol. 33, no. 4, pp. 3624–3633, 2018.
- [12] B. Wang and B. F. Hobbs, "Flexiramp market design for real-time operations: Can it approach the stochastic optimization ideal?" in *2013 IEEE PESGM*, 2013, pp. 1–5.
- [13] W. W. Hogan, "Electricity scarcity pricing through operating reserves," *EEP*, vol. 2, no. 2, pp. 65–86, 2013.
- [14] A. Papavasiliou and Y. Smeers, "Remuneration of flexibility using operating reserve demand curves: A case study of Belgium," *Energy Journal*, vol. 38, no. 6, 2017.
- [15] Y. Rebours and D. Kirschen, "A survey of definitions and specifications of reserve services," Tech. Rep., 2005.
- [16] "Emergency Operations," *PJM Manual*, Tech. Rep., 2011. [Online]. Available: <http://www.pjm.com/~media/documents/manuals/archive/m13/m13v46-emergency-operations-11-16-2011.ashx>
- [17] G. Strbac, A. Shakoor, M. Black, D. Pudjianto, and T. Bopp, "Impact of wind generation on the operation and development of the UK electricity systems," *Electr. Pow. Syst. Res.*, vol. 77, no. 9, pp. 1214–1227, 2007.
- [18] D. Lee and R. Baldick, "Analyzing the variability of wind power output through the power spectral density," in *2012 IEEE PESGM*, 2012, pp. 1–8.
- [19] R. Doherty and M. O'Malley, "A new approach to quantify reserve demand in systems with significant installed wind capacity," *IEEE Trans. Power Syst.*, vol. 20, no. 2, pp. 587–595, 2005.
- [20] Y. V. Makarov, P. V. Etingov, J. Ma, Z. Huang, and K. Subbarao, "Incorporating uncertainty of wind power generation forecast into power system operation, dispatch, and unit commitment procedures," *IEEE Trans. Sustain. Energy*, vol. 2, no. 4, pp. 433–442, 2011.
- [21] Y. Dvorkin, D. S. Kirschen, and M. A. Ortega-Vazquez, "Assessing flexibility requirements in power systems," *IET GENER. TRANSM. DIS.*, vol. 8, no. 11, pp. 1820–1830, 2014.
- [22] H. Nosair and F. Bouffard, "Flexibility envelopes for power system operational planning," *IEEE Trans. Sustain. Energy*, vol. 6, no. 3, pp. 800–809, 2015.
- [23] ——, "Economic dispatch under uncertainty: The probabilistic envelopes approach," *IEEE Trans. Power Syst.*, vol. 32, no. 3, pp. 1701–1710, 2017.
- [24] M. Lange, "On the uncertainty of wind power predictions analysis of the forecast accuracy and statistical distribution of errors," *J. Sol. Energy Eng.*, vol. 127, no. 2, pp. 177–184, 2005.
- [25] M. A. Matos and R. J. Bessa, "Setting the operating reserve using probabilistic wind power forecasts," *IEEE Trans. Power Syst.*, vol. 26, no. 2, pp. 594–603, 2011.
- [26] H. Holttilinen, M. Milligan, E. Ela, N. Menemenlis, J. Dobshinsky, B. Rawn, R. J. Bessa, D. Flynn, E. Gomez-Lazaro, and N. K. Detlefson, "Methodologies to determine operating reserves due to increased wind power," *IEEE Trans. Sustain. Energy*, vol. 3, no. 4, pp. 713–723, 2012.
- [27] P. N. Biskas, D. I. Chatzigiannis, and A. G. Bakirtzis, "European electricity market integration with mixed market designs—part I: Formulation," *IEEE Trans. Power Syst.*, vol. 29, no. 1, pp. 458–465, 2014.
- [28] S. Kasina, "Essays on unit commitment and interregional cooperation in transmission planning," 2017, Ph.D. thesis.
- [29] J. Kazempour and B. F. Hobbs, "Value of flexible resources, virtual bidding, and self-scheduling in two-settlement electricity markets with wind generation-part I: Principles and competitive model," *IEEE Trans. Power Syst.*, vol. 33, no. 1, pp. 749–759, 2018.
- [30] C. Ruiz, A. J. Conejo, and D. J. Bertsimas, "Revealing rival marginal offer prices via inverse optimization," *IEEE Trans. Power Syst.*, vol. 28, no. 3, pp. 3056–3064, 2013.
- [31] L. Mitridiati and P. Pinson, "A bayesian inference approach to unveil supply curves in electricity markets," *IEEE Trans. Power Syst.*, vol. 33, no. 3, 2017.
- [32] D. Pozo, E. Sauma, and J. Contreras, "Basic theoretical foundations and insights on bilevel models and their applications to power systems," *Ann. Oper. Res.*, pp. 1–32, 2017.
- [33] A. J. Conejo, E. Castillo, R. Minguez, and R. Garcia-Bertrand, *Decomposition techniques in mathematical programming: engineering and science applications*. Springer Science & Business Media, 2006.
- [34] C. Ordoudis, P. Pinson, J. M. Morales, and M. Zugno, "An updated version of the IEEE RTS 24-Bus system for electricity market and power system operation studies," *Technical University of Denmark*, 2016.

- [35] D. J. Swider and C. Weber, "Bidding under price uncertainty in multi-unit pay-as-bid procurement auctions for power systems reserve," *Eur. J. Oper. Res.*, vol. 181, no. 3, pp. 1297 – 1308, 2007.
- [36] M. A. Plazas, A. J. Conejo, and F. J. Prieto, "Multimarket optimal bidding for a power producer," *IEEE Trans. Power Syst.*, vol. 20, no. 4, pp. 2041–2050, 2005.
- [37] V. Dvorkin, S. Delikaraoglou, and J. M. Morales, (2018) Online appendix of the paper "Setting reserve requirements to approximate the efficiency of the stochastic dispatch". [Online]. Available: <https://doi.org/10.5281/zenodo.1408881>
- [38] H. Pandzic, Y. Dvorkin, T. Qiu, Y. Wang, and D. Kirschen, "Unit commitment under uncertainty - GAMS models," Library of the Renewable Energy Analysis Lab (REAL), University of Washington, Seattle, USA. [Online]. Available: http://www.ee.washington.edu/research/real/gams_code.html
- [39] P. Pinson, "Wind energy: Forecasting challenges for its operational management," *Stat. Sci.*, pp. 564–585, 2013.



Vladimir Dvorkin Jr. (S'18) received the B.S. degree in electrical engineering from the Moscow Power Engineering Institute, Russia, in 2012, the M.Sc. degree in Economics from the Higher School of Economics, Russia, in 2014, and the M.Sc. degree in Sustainable Energy from the Technical University of Denmark in 2017. Currently he is pursuing the Ph.D. degree with the Department of Electrical Engineering, Center for Electric Power and Energy, Technical University of Denmark.

His research interests include economics, game theory, optimization, and their applications to power systems and electricity markets.



Stefanos Delikaraoglou (S'14 - M18) received the Dipl.-Eng. degree from the School of Mechanical Engineering, National Technical University of Athens, Greece, in 2010 and the M.Sc. degree in Sustainable Energy from the Technical University of Denmark in 2012. He holds a Ph.D. degree awarded in 2016 by the Department Electrical Engineering at the Technical University of Denmark. He is currently a Postdoctoral Fellow with the EEE-Power Systems Laboratory at the Swiss Federal Institute of Technology (ETH), Zurich, Switzerland.

His research interests include energy markets and multi-energy systems modeling, decision-making under uncertainty, equilibrium models and hierarchical optimization.



Juan M. Morales (S'07-M'11-SM'16) received the Ingeniero Industrial degree from the University of Málaga, Málaga, Spain, in 2006, and a Ph.D. degree in Electrical Engineering from the University of Castilla-La Mancha, Ciudad Real, Spain, in 2010. He is currently an associate professor in the Department of Applied Mathematics at the University of Málaga in Spain.

His research interests are in the fields of power systems economics, operations and planning; energy analytics and optimization; smart grids; decision-making under uncertainty, and electricity markets.

[Paper C] Electricity market equilibrium under information asymmetry

Authors:

V. Dvorkin, J. Kazempour and P. Pinson.

Published in:

Operations Research Letters

Electricity Market Equilibrium under Information Asymmetry

Vladimir Dvorkin Jr., Jalal Kazempour, Pierre Pinson

Technical University of Denmark, Elektrovej 325, 2800 Kongens Lyngby, Denmark

Abstract

We study a competitive electricity market equilibrium with two trading stages, day-ahead and real-time. The welfare of each market agent is exposed to uncertainty (here from renewable energy production), while agent information on the probability distribution of this uncertainty is not identical at the day-ahead stage. We show a high sensitivity of the equilibrium solution to the level of information asymmetry and demonstrate economic, operational, and computational value for the system stemming from potential information sharing.

Keywords: Asymmetry of Information, Distributed Optimization, Electricity Market, Equilibrium, Existence and Uniqueness, Uncertainty

1. Introduction

With increasing shares of renewable energy resources, electricity markets are exposed to uncertainty associated with intermittent power supply. To accommodate this uncertainty, electricity trading in short term has been arranged in several subsequent trading floors, such as day-ahead and real-time markets. At the first stage (day-ahead), market agents, e.g., producers and consumers, compete to contract energy considering the forecast of renewable production, while at the second stage (real-time) they settle power imbalances caused by forecast errors.

Such competition can be modeled as a stochastic *equilibrium* problem in the sense of [1], where each market agent is a self-optimizer and maximizes its welfare, e.g. expected profit for producers or expected utility for consumers. Each agent computes a day-ahead decision while anticipating the real-time outcomes using its *private* information (e.g., probabilistic forecast) about uncertainty. To find the equilibrium among such agents, distributed algorithms as in [2] have been proposed to let agents integrate their private forecasts. After a finite number of iterations, the agents find a set of equilibrium prices that reflect their private information and support the equilibrium. This distributed solution is promising for the operation of local markets [3] or parts of larger systems [4].

In contrast, large electricity markets, such as NordPool or CAISO, use a *centralized* optimization to compute the equilibrium, where the central entity called market operator collects bids from agents and clears the market on its own. To efficiently operate markets with renewables, it has been proposed to cast the centralized optimization as a two-stage stochastic model [5, 6]. This model considers that the operator generates a set of plausible renewable outcomes based on its *own* information about the probability distribution of renewable energy production, and

clears the day-ahead market while accounting for the anticipated real-time imbalances.

The important property of the two problems is that they are equivalent in the case where all market agents in the equilibrium model optimize against the same probability distribution as that of market operator in the centralized model. Under this scenario, the two problems yield the same market-clearing results and the centralized market is complete as it satisfies the preferences of all agents in the equilibrium problem. However, this equivalence no longer holds when agents in the equilibrium problem optimize against different distributions. In this situation, the centralized market settlement is inefficient as it does not support the true preferences of agents. We refer to this situation as *information asymmetry* that typically holds for many reasons. Naturally, agents use different data and forecast tools to build uncertainty distributions. Furthermore, agents may explicitly assign different probabilities across plausible outcomes depending on their rationality, e.g., in the sense of prospect theory [7].

In this line, this letter analyzes electricity market competition among agents that have asymmetric information about a common source of uncertainty. We propose an equilibrium model in which agents may assign different probabilities over a common set of renewable power production outcomes. We show that the centralized model in [5, 6] satisfies the preferences of all market agents only if they all agree on the probability distribution of renewable power production. We discuss the existence and uniqueness of the solution to the equilibrium problem, and refer the stability theory to discuss the challenges associated with its computation. With our analytic results, we point out a high sensitivity of equilibrium prices to the level of information asymmetry. We then propose a distributed algorithm to numerically assess the equilibrium outcomes.

We eventually demonstrate the overall benefits from information sharing, as we show that for any asymmetry in agents information, there exist the loss of social welfare, increase in real-time imbalances, and decrease of the convergence rate of the distributed algorithm.

The letter is outlined as follows. In Section 2 we describe the setup and introduce the stochastic equilibrium model. We proceed with analytical solution to equilibrium prices as a function of agent private forecasts in Section 3. In Section 4 we describe the algorithm to compute equilibrium and provide extensive numerical experiments. All proofs are gathered in an Appendix.

2. Problem statement

2.1. Main notation and assumptions

We consider a finite set of uncertainty outcomes Ω indexed by $\omega = \{1, \dots, \Omega\}$. ξ_ω is the renewable power output that corresponds to outcome ω . The renewable producers are not modeled as market agents, but represented as an aggregated stochastic in-feed. The controllable generation (consumption) is represented by a single producer (consumer). The dispatch of power producer at the day-ahead stage is denoted by $p \in \mathcal{O}$, and it can be adjusted by $r_\omega \in \mathcal{O}$ in real-time if outcome ω realizes. The set \mathcal{O} denotes the feasible operating region of the producer based on its technical constraints. The cost function of the producer is quadratic given by $c(x) = \frac{1}{2}\alpha x^2$, where α is a positive constant. The consumer procures energy at the day-ahead stage in amount of $d \in \mathcal{K}$ that is subject to adjustment $l_\omega \in \mathcal{K}$ in real-time if outcome ω realizes. The set \mathcal{K} exhibits the feasible region of the decision-making problem of the consumer. The utility of the consumer is described by concave function $u(x) = \gamma x - \frac{1}{2}\beta x^2$, where γ and β are positive constants. We assume that both \mathcal{O} and \mathcal{K} are convex and compact sets. The dual price in scenario ω is denoted by λ_ω in the optimization problem. Its counterpart in the equilibrium problem is denoted by $\tilde{\lambda}_\omega$. In this work, we do not consider network, subsidies and unit commitment constraints, that often cause negative electricity prices [8], and exclusively focus on perfect competition. Therefore, both λ_ω and $\tilde{\lambda}_\omega$ belong to a compact set of non-negative reals Λ_+ .

2.2. Centralized model for market-clearing problem

Consider a centralized market organization, where the market operator collects bids of agents and finds socially optimal contracts $\{p, d\}$ at the day-ahead stage, followed by real-time recourse decisions $\{r_\omega, l_\omega\}_{\forall \omega}$. The market operator integrates its own information about underlying uncertainty that is described by a finite set of probabilities $\{\pi_\omega^{\text{mo}}\}_{\forall \omega}$ assigned to uncertain outcomes. This yields

$$\max_{p, r_\omega, d, l_\omega} [u(d) - c(p)] + \sum_{\omega \in \Omega} \pi_\omega^{\text{mo}} [u(l_\omega) - c(r_\omega)], \quad (1a)$$

$$\text{s.t. } p + r_\omega + \xi_\omega - d - l_\omega = 0 : \lambda_\omega, \quad \forall \omega \in \Omega, \quad (1b)$$

$$(p, r_\omega) \in \mathcal{O}, \quad (d, l_\omega) \in \mathcal{K}, \quad \forall \omega \in \Omega, \quad (1c)$$

where objective function (1a) represents the *expected* social welfare seen by the market operator, and constraint (1b) enforces the power balance for each outcome of renewable energy production. A set of dual prices $\{\lambda_\omega\}_{\forall \omega}$ shows the sensitivity of the expected social welfare to the stochastic in-feed and, therefore, is an implicit function of the information of market operator. Hence, the outcomes for market participants are subject to the information available to the market operator.

Remark 1. As dual prices are non-negative, stating (1b) as either equality or inequality constraint is the same.

Remark 2. The real-time electricity price in outcome ω anticipated by the market operator at the day-ahead stage is the probability-removed price $\frac{\lambda_\omega}{\pi_\omega^{\text{mo}}}$ [5].

Remark 3. Unlike settings in [5, 6], we do not explicitly model the day-ahead power balance constraint. Instead, we use the notion of price convergence between day-ahead and real-time stages [9] to obtain the day-ahead electricity price as $\lambda^{\text{DA}} = \sum_\omega \pi_\omega^{\text{mo}} \frac{\lambda_\omega}{\pi_\omega^{\text{mo}}} = \sum_\omega \lambda_\omega$.

2.3. Equilibrium model for market-clearing problem

We now introduce an equilibrium model given by a set of individual optimization of three agents, i.e.,

$$\max_{\tilde{\lambda}_\omega \in \Lambda_+} J_\omega^{\text{Ps}} := -\tilde{\lambda}_\omega [p + r_\omega + \xi_\omega - d - l_\omega], \quad \forall \omega \in \Omega, \quad (2a)$$

$$\max_{(p, r_\omega) \in \mathcal{O}} J^\text{P} := \sum_{\omega \in \Omega} \pi_\omega^\text{P} \left[\frac{\tilde{\lambda}_\omega}{\pi_\omega^\text{P}} (p + r_\omega) - c(r_\omega) \right] - c(p), \quad (2b)$$

$$\max_{(d, l_\omega) \in \mathcal{K}} J^\text{C} := \sum_{\omega \in \Omega} \pi_\omega^\text{C} \left[u(l_\omega) - \frac{\tilde{\lambda}_\omega}{\pi_\omega^\text{C}} (d + l_\omega) \right] + u(d), \quad (2c)$$

The price-setting agent solves (2a) and optimizes a set of equilibrium prices $\{\tilde{\lambda}_\omega\}_{\forall \omega}$ in response to the value of the system imbalance for each outcome of renewable production. For any surplus of generation, problem (2a) yields zero price, while it yields a strictly positive price in case of generation shortage. The power producer optimizes its first- and second-stage decisions p and $\{r_\omega\}_{\forall \omega}$ in (2b) to maximize the expected profit for a given set of prices $\{\tilde{\lambda}_\omega\}_{\forall \omega}$. In its optimization, the producer integrates its own information about the uncertain in-feed characterized by a finite set of probabilities $\{\pi_\omega^\text{P}\}_{\forall \omega}$. Finally, the consumer computes optimal first-stage and recourse decisions d and $\{l_\omega\}_{\forall \omega}$ in (2c) to maximize its expected utility using its own information set $\{\pi_\omega^\text{C}\}_{\forall \omega}$. Observe, that agents in (2b) and (2c) use the probability-removed prices obtained by dividing the equilibrium prices by the associated probabilities [5]. The probability-removed prices define the actual electricity price that each agent expects to receive once uncertainty is resolved.

The three problems are interconnected in the sense that the problem of the price-setter is parametrized by the decisions of the producer and consumer, while their problems are conditioned by the price provided by the price-setting

agent. Similarly to the centralized problem (1a), equilibrium prices provide the sensitivity of the expected social welfare with respect to the marginal change in random in-feed. Therefore, a set of equilibrium prices $\{\tilde{\lambda}_\omega\}_{\forall \omega}$ is implicitly a function of the information that agents integrate into their optimization problems.

Proposition 1. *The solution to the equilibrium problem (2) exists and is unique for any agent information sets.*

Remark 4. *The proof of Proposition 1 relies on the strict monotonicity of agent preferences. In the case of linear preferences, other approaches would be required (see [10, Chapter 2]).*

2.4. Relation between centralized and equilibrium models

The equivalence between centralized and equilibrium market-clearing models is established as follows.

Proposition 2. *Let $\pi_\omega^{mo} = \pi_\omega^p = \pi_\omega^c, \forall \omega \in \Omega$. Then, there exists a set of prices $\{\tilde{\lambda}_\omega^*\}_{\forall \omega}$ that yields the optimal solution $p^*, d^*, \{r_\omega^*, l_\omega^*\}_{\forall \omega}$ in the equilibrium model (2) that solves the centralized model (1). Moreover, $\tilde{\lambda}_\omega^* = \lambda_\omega^*, \forall \omega$.*

However, this equivalence no longer holds when the information of market agents about the renewable in-feed in the equilibrium model is different from that of the market operator in the centralized model. In this scenario, the prices in (1) and (2) are not necessarily identical as they depend on different information sets, making the market based on (1) incomplete in terms of information. In what follows, we study model (2) that reveals the true equilibrium state among agents with private information on uncertainty. Eventually, we show that the system overall benefits when agents agree on a common information set that completes the market.

3. Analytic solution for equilibrium prices

Let us define the demand excess function for renewable power outcome ω as $z_\omega = d + l_\omega - p - r_\omega - \xi_\omega$. We derive the optimality conditions associated with (2b) and (2c) to define variables d, l_ω, p , and r_ω as a function of equilibrium prices $\tilde{\lambda}$. Assuming the agent constraints are not binding, the demand excess function writes as:

$$z_\omega(\tilde{\lambda}) = \frac{\gamma - \Sigma_\omega \tilde{\lambda}_\omega}{\beta} + \frac{\pi_\omega^c \gamma - \tilde{\lambda}_\omega}{\pi_\omega^c \beta} - \frac{\Sigma_\omega \tilde{\lambda}_\omega}{\alpha} - \frac{\tilde{\lambda}_\omega}{\pi_\omega^p \alpha} - \xi_\omega.$$

By solving $z_\omega(\tilde{\lambda}) = 0, \forall \omega \in \Omega$, we obtain a closed-form characterization of equilibrium prices as a function of probabilities that agents assign to uncertain outcomes. In the interest of illustration, let us consider a set $\Omega \in \{\ell, h\}$ with only two outcomes with $\xi_\ell = 1$ and $\xi_h = 3$. For any agent it holds that $\pi_\ell + \pi_h = 1$. Let $\alpha = 1.5$, $\beta = 0.3$, and $\gamma = 5$. Figure 1 depicts the two equilibrium prices $\tilde{\lambda}_\ell$ and $\tilde{\lambda}_h$ as a function of π_ℓ and π_h . We find a clear relationship between the equilibrium prices and agent information. In case (\blacktriangle), where producer assigns the whole probability

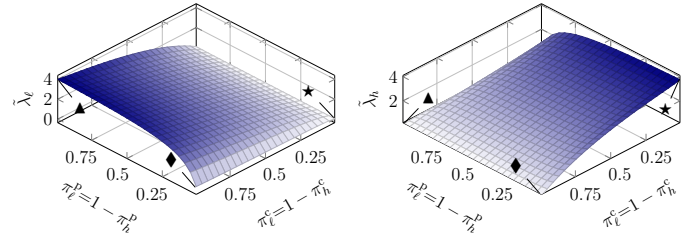


Figure 1: Equilibrium prices $\tilde{\lambda}_\ell$ and $\tilde{\lambda}_h$ as a function of probabilities that agents assign to the two uncertainty outcomes. The black markers indicate the three boundary equilibrium cases.

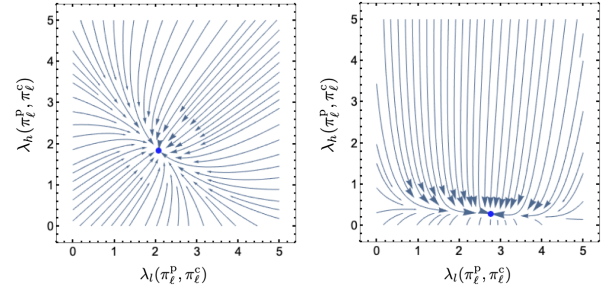


Figure 2: Equilibrium point and vector field around equilibrium point in case of (a) symmetric and (b) asymmetric information.

mass to outcome ℓ , the price associated with outcome h is nearly zero. A similar situation holds in the opposite case (\star). In a quite critical case (\blacklozenge) with highly asymmetric assignment of probabilities, the equilibrium yields almost zero prices for both outcomes. Moreover, we find that the day-ahead price, i.e., $\tilde{\lambda}^{DA} = \tilde{\lambda}_\ell + \tilde{\lambda}_h$, attains maximum with symmetric information, i.e., $\pi_\ell^p = \pi_\ell^c$.

As shown in [2], the unstable equilibrium may not be computable by standard distributed algorithms. To verify the stability of equilibrium under different assignments of probabilities, we consider a dynamic price adjustment process as the following first order differential equation [11]:

$$\frac{d\tilde{\lambda}(t)}{dt} = \tau z(\tilde{\lambda}(t)), \quad \tilde{\lambda}(0) = \tilde{\lambda}_0, \quad (3)$$

where τ is some positive constant, and $\tilde{\lambda}_0$ is a vector of initial prices. We discuss the stability of the equilibrium solution using the following proposition.

Proposition 3 (Adapted from [12]). *If $\tilde{\lambda}$ is a solution of (3) and all the eigenvalues of the Jacobian matrix of z have strictly negative real parts, then $\tilde{\lambda}$ is locally stable. If at least one eigenvalue has strictly positive real part, then $\tilde{\lambda}$ is unstable.*

By verifying the eigenvalues of the Jacobian of z , we find that for any assignment of probabilities, the equilibrium solution is locally stable and, thus, supposedly computable. However, we observe that for asymmetric cases the ratio of the two eigenvalues significantly increases. This ratio heavily affects the convergence rate for gradient search algorithms [13], as illustrated by vector fields in Figure 2 for some choice of $\tilde{\lambda}_0$. In particular, in Figure 2(a), a gradient search is almost uniform in both directions $\tilde{\lambda}_\ell$ and

$\tilde{\lambda}_h$, while in Figure 2(b) the gradient in direction $\tilde{\lambda}_\ell$ is notably smaller than that in direction $\tilde{\lambda}_h$. Next, we demonstrate how large eigenvalue ratios affect the convergence properties of the distributed market-clearing algorithms.

4. Equilibrium computation

In this section, we first introduce a distributed algorithm to compute the solution to the equilibrium problem. We then describe the setup and provide numerical results.

4.1. Algorithm

To compute the equilibrium solution, we use a distributed algorithm that naturally embodies the Walrasian tatonnement [14]. The price-setter in (2a) updates the prices based on the optimal response of the producer and consumer in (2b) and (2c), respectively.

We first show that the price-setter optimization (2a) reduces to a single analytic expression.

Proposition 4. Consider the response of producer $p^\nu, \{r_\omega^\nu\}_{\forall\omega}$ and the response of consumer $d^\nu, \{l_\omega^\nu\}_{\forall\omega}$ to a set of prices $\{\tilde{\lambda}_\omega^{\nu-1}\}_{\forall\omega}$ at some iteration ν . Then, the solution of (2a) converges to optimum over iterations using

$$\tilde{\lambda}_\omega^\nu = \max \left\{ 0, \tilde{\lambda}_\omega^{\nu-1} - \rho [p^\nu + r_\omega^\nu + \xi_\omega - d^\nu - l_\omega^\nu] \right\}, \quad \forall \omega \in \Omega,$$

for some positive constant ρ .

Using the analytic expression for the price-update, we compute the solution of the equilibrium problem (2) using Algorithm 1. As objective function of each agent is strictly monotone in decision variables and its feasibility set is convex and compact, the algorithm provably converges to the global optimum for $\nu \rightarrow \infty$ with rate $\mathcal{O}(\frac{1}{\nu})$, given that the solution exists [15]. The algorithm is implemented in JuMP environment [16] in Julia, and the source code is available in the e-companion [17].

4.2. Setup

We choose $\alpha = 1.5$, $\gamma = 5$, $\beta = 0.3$, $\{\tilde{\lambda}_\omega^0\}_{\forall\omega} = 0$, $\rho = \epsilon = 10^{-5}$. The magnitude of these parameters is kept at the same order as those in [2] and [18]. The outcomes of uncertain renewable production are described by 100 samples drawn from a normal distribution $\mathcal{N}(\mu, \sigma^2)$ with $\mu = 1.5$ and $\sigma^2 = 0.25$. The rationale behind these parameters lies in the fact that the producer and consumer are willing to trade energy for any realization of wind power production, whereas the wind fluctuations bring about observable impacts on the market-clearing outcomes. The practical choice of these parameters is subject to the specifics of a given power system, e.g. cost/utility structure and wind penetration level.

We consider the reference distribution \circledR that assigns equally likely probabilities over 100 samples. We then generate a series of distributions that tweak either mean or variance of the reference distribution \circledR using the probability weighting function of the following form [19, Eq.(3)]:

$$\Phi(\xi) = \frac{\delta[\Phi^{\circledR}(\xi)]^\gamma}{\delta[\Phi^{\circledR}(\xi)]^\gamma + [1 - \Phi^{\circledR}(\xi)]^\gamma}, \quad (4)$$

```

Data:  $\nu_{MAX}, \rho, \tilde{\lambda}_\omega^0 \forall \omega, \epsilon$ 
for  $\nu$  from 1 to  $\nu_{MAX}$  do
    ① For  $\{\tilde{\lambda}_\omega^{\nu-1}\}_{\forall\omega}$ , update producer response
         $p^\nu, \{r_\omega^\nu\}_{\forall\omega} \leftarrow \operatorname{argmax}_{(p, r_\omega) \in \mathcal{O}} J^P(p, r_\omega)$ 
    ② For  $\{\tilde{\lambda}_\omega^{\nu-1}\}_{\forall\omega}$ , update consumer response
         $d^\nu, \{l_\omega^\nu\}_{\forall\omega} \leftarrow \operatorname{argmax}_{(d, l_\omega) \in \mathcal{K}} J^C(d, l_\omega)$ 
    ③ For  $p^\nu, \{r_\omega^\nu\}_{\forall\omega}$  and  $d^\nu, \{l_\omega^\nu\}_{\forall\omega}$ , update prices:
         $\tilde{\lambda}_\omega^\nu = \max \left\{ 0, \tilde{\lambda}_\omega^{\nu-1} - \rho [p^\nu + r_\omega^\nu + \xi_\omega - d^\nu - l_\omega^\nu] \right\}$ 
    ④ Return  $\epsilon$ -equilibrium prices and dispatch if:
         $\|p^\nu + r_\omega^\nu + \xi_\omega - d^\nu - l_\omega^\nu\|^2 \leq \epsilon, \forall \omega \in \Omega,$ 
        otherwise go to ①.
end

```

Algorithm 1: Solution algorithm

Table 1: Descriptive statistics of distributions: \circledR -labeled distributions primarily tweak the mean of the reference distribution \circledR , while \circledS -labeled distributions primarily tweak the variance of \circledR .

Label	\circledP_3^\uparrow	\circledP_2^\uparrow	\circledP_1^\uparrow	\circledR	\circledP_1^\downarrow	\circledP_2^\downarrow	\circledP_3^\downarrow
μ	2.02	1.79	1.65	1.56	1.34	1.22	1.07
σ^2	0.35	0.35	0.34	0.33	0.31	0.30	0.27
Label	\circledS_3^\uparrow	\circledS_2^\uparrow	\circledS_1^\uparrow	\circledR	\circledS_1^\downarrow	\circledS_2^\downarrow	\circledS_3^\downarrow
μ	1.63	1.60	1.57	1.56	1.55	1.55	1.56
σ^2	1.62	0.92	0.54	0.33	0.10	0.04	0.02

where Φ represents the cumulative distribution function of stochastic renewable production, $\delta \in \mathbb{R}_+$ primarily affects the mean of the reference distribution \circledR , and $\gamma \in \mathbb{R}_+$ primarily impacts the variance. By applying (4) to the reference distribution for different δ and γ , we obtain a collection of probability assignments to the same set of outcomes. Table 1 summarizes the distributions that we use in the following analysis.

In our setup, consumer always optimizes against the reference distribution \circledR , while producer optimizes against one of the distributions in Table 1. When producer uses \circledR in its local optimization, the equilibrium solution corresponds to the symmetric case, and any deviation from \circledR corresponds to the asymmetric equilibrium.

4.3. Numerical results

We first consider the impact of information asymmetry on the electricity price at the day-ahead stage depicted in Figure 3. We see that it is maximized when the two agents use the same uncertainty distribution \circledR . Any deviation from \circledR in producer optimization decreases the day-ahead price. The resulting price-supported day-ahead contracts illustrated in Figure 4 show that such deviations in terms

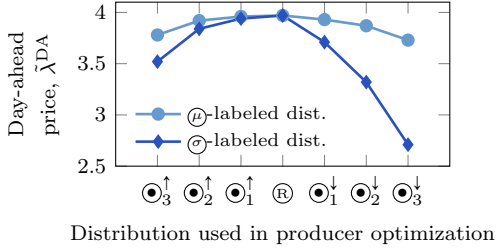


Figure 3: Impacts of information asymmetry on the day-ahead price.

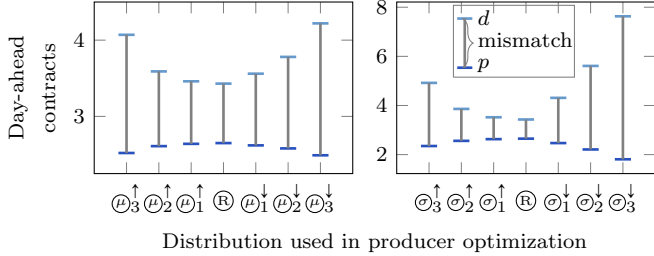


Figure 4: Impacts of information asymmetry on the contracted quantities of consumer (d) and producer (p) at the day-ahead stage.

of either mean or variance lead to increasing power mismatch between controllable generation and consumption.

Next, we compute the realization of the social welfare for each uncertainty outcome as $SW_\omega = [u(d^*) - c(p^*)] + [u(l_\omega) - c(r_\omega)]$, where d^* and p^* are the fixed day-ahead decisions of consumer and producer. They are computed considering symmetric and some asymmetric information cases. The social welfare per outcome SW_ω should not be confused with the expected social welfare $\mathbb{E}_\omega[SW_\omega]$ provided in (1a). The results are summarized in Figure 5. We observe that the social welfare improves in larger realizations of renewable output, and records the maximum when producer employs \mathbb{R} . For any deviation of the producer from the reference distribution, we find a social loss, that is smaller for deviations in terms of the mean rather than variance for given distributions. Moreover, we see the welfare reduces more significantly if the producer assigns smaller variance relatively to that of the consumer.

Finally, we show how the computational performance of the algorithm is affected by the asymmetry of information. Table 2 collects the number of iterations required by the algorithm to converge along with the ratio between the largest and the smallest eigenvalues of Jacobian of the demand excess function. We see that apart from the case of μ_1^\uparrow distribution, the asymmetry of agent information yields larger ratio of eigenvalues, and thus requires more iterations to converge. Moreover, for a highly asymmetric case of a low-variance distribution σ_3^\downarrow , this ratio boosts so that the algorithm does not converge for any iteration limit. The computational time of each iteration, though, is not affected by information asymmetry and kept below a few milliseconds for all distributions.

References

- [1] K. J. Arrow, G. Debreu, Existence of an equilibrium for a competitive economy, *Econometrica: Journal of the Econometric Society* (1954) 265–290.

Table 2: Number of iterations and ratio between the largest and smallest eigenvalues for various distributions used by producer.

Label	μ_3^\uparrow	μ_2^\uparrow	μ_1^\uparrow	\mathbb{R}	μ_1^\downarrow	μ_2^\downarrow	μ_3^\downarrow
# iters	369	347	312	321	362	372	381
ratio	2.4	2.2	2.0	2.0	2.2	2.3	2.5
Label	σ_3^\uparrow	σ_2^\uparrow	σ_1^\uparrow	\mathbb{R}	σ_1^\downarrow	σ_2^\downarrow	σ_3^\downarrow
# iters	379	372	353	321	359	499	∞
ratio	2.7	2.4	2.2	2.0	18.8	1.8e3	1.8e7

- [2] H. Gérard, V. Leclère, A. Philpott, On risk averse competitive equilibrium, *Operations Research Letters* 46 (1) (2018) 19–26.
- [3] F. Moret, P. Pinson, Energy collectives: a community and fairness based approach to future electricity markets, *IEEE Transactions on Power Systems*, in print.
- [4] D. K. Molzahn, F. Dörfler, H. Sandberg, S. H. Low, S. Chakrabarti, R. Baldick, J. Lavaei, A survey of distributed optimization and control algorithms for electric power systems, *IEEE Transactions on Smart Grid* 8 (6) (2017) 2941–2962.
- [5] J. M. Morales, A. J. Conejo, K. Liu, J. Zhong, Pricing electricity in pools with wind producers, *IEEE Transactions on Power Systems* 27 (3) (2012) 1366–1376.
- [6] G. Pritchard, G. Zakeri, A. Philpott, A single-settlement, energy-only electric power market for unpredictable and intermittent participants, *Operations research* 58 (4-part-2) (2010) 1210–1219.
- [7] A. Tversky, D. Kahneman, Advances in prospect theory: Cumulative representation of uncertainty, *Journal of Risk and uncertainty* 5 (4) (1992) 297–323.
- [8] L. Deng, B. F. Hobbs, P. Renson, What is the cost of negative bidding by wind? a unit commitment analysis of cost and emissions, *IEEE Transactions on Power Systems* 30 (4) (2015) 1805–1814.
- [9] W. W. Hogan, Virtual bidding and electricity market design, *The Electricity Journal* 29 (5) (2016) 33–47.
- [10] F. Facchinei, J.-S. Pang, Finite-dimensional variational inequalities and complementarity problems, Springer Science & Business Media, 2007.
- [11] K. J. Arrow, L. Hurwicz, On the stability of the competitive equilibrium, *Econometrica: Journal of the Econometric Society* (1958) 522–552.
- [12] R. Bellman, Stability theory of differential equations, Courier Corporation, 2008.
- [13] G. Goh, Why momentum really works (2017). URL <http://distill.pub/2017/momentum>
- [14] H. Uzawa, Walras' tatonnement in the theory of exchange, *The Review of Economic Studies* 27 (3) (1960) 182–194.
- [15] A. Falsone, K. Margellos, S. Garatti, M. Prandini, Dual decomposition for multi-agent distributed optimization with coupling constraints, *Automatica* 84 (2017) 149–158.
- [16] I. Dunning, J. Huchette, M. Lubin, JuMP: A modeling language for mathematical optimization, *SIAM Review* 59 (2) (2017) 295–320.
- [17] V. Dvorkin, J. Kazempur, P. Pinson, Electronic companion - Electricity market equilibrium under information asymmetry. URL <https://github.com/wdvorkin/EMEuIA>
- [18] Power flow data for IEEE 14 bus test case (2014). URL www.pserc.cornell.edu/matpower/docs/ref/matpower5.0/case14.html
- [19] R. Gonzalez, G. Wu, On the shape of the probability weighting function, *Cognitive psychology* 38 (1) (1999) 129–166.

Appendix A. Proof of Proposition 1

Appendix A.1. Preliminaries

We connect the solution of the equilibrium problem to the solution of variational inequalities.

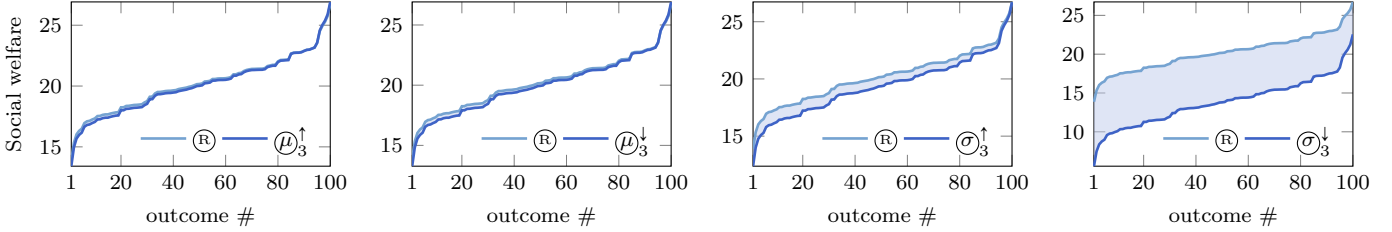


Figure 5: Social welfare for each outcome of renewable production. The 100 outcomes are ordered from the smallest to largest. The colored area between the curves shows the welfare loss caused by asymmetry of information.

Definition 1. Consider a mapping $F : \mathbb{R}^n \rightarrow \mathbb{R}^n$ and a set $K \subseteq \mathbb{R}$. A solution set $\text{SOL}(K, F)$ to the variational inequality problem $\text{VI}(K, F)$ is a vector $x^* \in K$ such that $\langle F(x^*), x - x^* \rangle \geq 0, \forall x \in K$.

We use the results from [10] to establish the existence and uniqueness of the equilibrium solution.

Theorem 1 (Corollary 2.2.5 [10]). Suppose that K is a compact and convex set, and that the mapping F is continuous. Then, the set $\text{SOL}(K, F)$ is nonempty and compact.

Theorem 2 (Theorem 1.3.1 [10]). Let $F : U \rightarrow \mathbb{R}$ be continuously differentiable on the open convex set $U \subseteq \mathbb{R}$. The following three statements are equivalent: (a) there exists a real-valued function θ such that $F(x) = \nabla \theta(x) \forall x \in U$; (b) the Jacobian matrix of $F(x)$ is symmetric $\forall x \in U$; (c) F is integrable on U .

In terms of equilibrium problem (2), $K = \mathcal{O} \times \mathcal{K} \times \Lambda_+$, vector $x = [p, \mathbf{r}, d, \mathbf{l}, \tilde{\lambda}]^\top$, and

$F^\top = [\nabla_p J^P(p, \mathbf{r}) \quad \nabla_{\mathbf{r}} J^P(p, \mathbf{r}) \quad \nabla_d J^C(d, \mathbf{l}) \quad \nabla_{\mathbf{l}} J^C(d, \mathbf{l}) \quad \nabla_{\tilde{\lambda}} J^{Ps}(\tilde{\lambda})]$, where symbols in bold are properly dimensioned vectors. In what follows, by $\text{diag}([x_1, \dots, x_n])$ we denote diagonal $n \times n$ matrix, and by \circ we denote Schur product.

Appendix A.2. Proof

① Existence. Recall that by definition \mathcal{O} , \mathcal{K} and Λ_+ are convex and compact. The map F is continuous as agents' objective functions are differentiable. Thus, the solution to equilibrium exists by Theorem 1.

② Uniqueness. We rely on the symmetry principle that states that if Jacobian of F is symmetric, there exists an equivalent optimization problem that solves $\text{VI}(K, F)$. The Jacobian writes as:

$$\nabla_x F(x) = \begin{pmatrix} \alpha & \mathbf{0}^\top & 0 & \mathbf{0}^\top & -\mathbf{1}^\top \\ \mathbf{0} & \text{diag}(\alpha \boldsymbol{\pi}^P) & \mathbf{0} & \text{diag}(\mathbf{0}) & \text{diag}(-\mathbf{1}) \\ 0 & \mathbf{0}^\top & \beta & \mathbf{0}^\top & \mathbf{1}^\top \\ \mathbf{0} & \text{diag}(\mathbf{0}) & \mathbf{0} & \text{diag}(\beta \boldsymbol{\pi}^C) & \text{diag}(\mathbf{1}) \\ \mathbf{1} & \text{diag}(\mathbf{1}) & -\mathbf{1} & \text{diag}(-\mathbf{1}) & \text{diag}(\mathbf{0}) \end{pmatrix},$$

which includes a symmetric part with entries corresponding to the elements of variable set $x' = \{p, \mathbf{r}, d, \mathbf{l}\}$. We further observe that $F(x')$ is continuous in x' , thus the conditions (b,c) of Theorem 2 hold for the symmetric part, such that there exists a function $\theta(x')$ given by

$$\theta(x') = \int_0^1 F(x'_0 + t(x' - x'_0))^\top (x' - x'_0) dt$$

$$\begin{aligned} x'_0 &\stackrel{\omega}{=} \int_0^1 \begin{pmatrix} t\alpha p \\ t\alpha \boldsymbol{\pi}^P \circ \mathbf{r} \\ -\gamma + t\beta d \\ -\gamma \boldsymbol{\pi}^C + t\beta \boldsymbol{\pi}^C \circ \mathbf{l} \end{pmatrix}^\top \begin{pmatrix} p \\ \mathbf{r} \\ d \\ \mathbf{l} \end{pmatrix} dt \\ &= [\alpha p^2 + \Sigma_\omega \boldsymbol{\pi}_\omega^P \alpha r_\omega^2 + \beta d^2 + \Sigma_\omega \boldsymbol{\pi}_\omega^C \beta l_\omega^2] \int_0^1 t dt \\ &\quad - [\gamma d + \Sigma_\omega \boldsymbol{\pi}_\omega^C l_\omega] \\ &= \frac{1}{2} \alpha p^2 - [\gamma d - \frac{1}{2} \beta d^2] + \Sigma_\omega \boldsymbol{\pi}_\omega^P \frac{1}{2} \alpha r_\omega^2 - \Sigma_\omega \boldsymbol{\pi}_\omega^C [\gamma l_\omega - \frac{1}{2} \beta l_\omega^2]. \end{aligned}$$

If we optimize $\theta(x')$ subject to the stationarity conditions of the price-setting agent, we obtain

$$\max_{p, r_\omega, d, l_\omega} [u(d) - c(p)] + \sum_{\omega \in \Omega} [\boldsymbol{\pi}_\omega^C u(l_\omega) - \boldsymbol{\pi}_\omega^P c(r_\omega)], \quad (\text{A.1a})$$

$$\text{s.t. } p + r_\omega + \xi_\omega - d - l_\omega \geq 0 : \tilde{\lambda}_\omega, \quad \forall \omega \in \Omega, \quad (\text{A.1b})$$

$$(p, r_\omega) \in \mathcal{O}, (d, l_\omega) \in \mathcal{K}, \quad \forall \omega \in \Omega, \quad (\text{A.1c})$$

whose stationarity conditions correspond to those of equilibrium problem (2). We know that optimization (A.1) yields a unique solution due to strict concavity of objective function and convex and compact constraint set. Since the solution of (A.1) constitutes set $\text{SOL}(K, F)$, the solution of original equilibrium problem (2) is also unique.

Appendix B. Proof of Proposition 2.

Since producer and consumer optimize over independent variables, we can optimize problems (2b) and (2c) jointly. If we constrain the joint problem by the optimality conditions of price-setter problem (2a), we obtain

$$\max_{p, r_\omega, d, l_\omega} J^P(p, r_\omega) + J^C(d, l_\omega), \quad (\text{B.1a})$$

$$\text{s.t. } (p, r_\omega) \in \mathcal{O}, (d, l_\omega) \in \mathcal{K}, \quad \forall \omega \in \Omega, \quad (\text{B.1b})$$

$$0 \leq p + r_\omega + \xi_\omega - d - l_\omega \perp \tilde{\lambda}_\omega \geq 0, \quad \forall \omega. \quad (\text{B.1c})$$

This is equivalent to the optimality condition of the centralized problem (1) given that expectations over uncertain renewable production are the same.

Appendix C. Proof of Proposition 4

The descent direction of the price-setter problem writes as

$$-\nabla_{\tilde{\lambda}_\omega} J_\omega^{Ps}(\tilde{\lambda}_\omega) = p^\nu + r_\omega^\nu + \xi_\omega - d^\nu - l_\omega^\nu.$$

Then, the solution of the price-setter problem evolves along the decent direction with a suitable step size ρ as follows:

$$\tilde{\lambda}_\omega^\nu = \tilde{\lambda}_\omega^{\nu-1} - \rho \nabla_{\tilde{\lambda}_\omega} J_\omega^{Ps}(\tilde{\lambda}_\omega),$$

that is bounded from below by zero due to $\tilde{\lambda}_\omega \in \Lambda_+$.

[Paper D] Differentially private distributed optimal power flow

Authors:

V. Dvorkin, P. Van Hentenryck, J. Kazempour and P. Pinson.

Published in:

59th Conference on Decision and Control

Differentially Private Distributed Optimal Power Flow

Vladimir Dvorkin¹, Pascal Van Hentenryck², Jalal Kazempour¹, Pierre Pinson¹

Abstract—Distributed algorithms enable private Optimal Power Flow (OPF) computations by avoiding the need in sharing sensitive information localized in algorithms sub-problems. However, adversaries can still infer this information from the coordination signals exchanged across iterations. This paper seeks formal privacy guarantees for distributed OPF computations and provides differentially private algorithms for OPF computations based on the consensus Alternating Direction Method of Multipliers (ADMM). The proposed algorithms attain differential privacy by introducing static and dynamic random perturbations of OPF sub-problem solutions at each iteration. These perturbations are Laplacian and designed to prevent the inference of sensitive information, as well as to provide theoretical privacy guarantees for ADMM sub-problems. Using a standard IEEE 118-node test case, the paper explores the fundamental trade-offs among privacy, algorithmic convergence, and optimality losses.

I. INTRODUCTION

Centralized OPF computations operate over large datasets of system parameters, such as electrical loads, and their unintended release poses privacy risks for data owners. Recognizing these risks, the literature suggests replacing the centralized computations with distributed algorithms [1], e.g., using the well-known Alternating Direction Method of Multipliers (ADMM). These algorithms distribute OPF computations among sub-problems that coordinate through primal and dual coordination signals without sharing the parameters used in their local computations and thus, preserving privacy. However, in the presence of side information, adversaries can reverse-engineer local parameters from observed coordination signals [2]. To overcome this limitation, this paper augments these ADMM-based OPF algorithms with *differential privacy*.

Differential privacy, first formalized by Dwork *et al.* [3], [4], is a theoretical framework *quantifying* the privacy risk associated with computing functions (queries) on datasets with sensitive information. It ensures that the same query applied to two adjacent datasets, i.e., differing by one item, return essentially similar results (i.e., up to specified parameters), thus preventing adversaries from learning any substantial information over individual items. Chatzikokolakis *et al.* [5] generalized this concept to a metric-based differential privacy for cases where publicly known participants have sensitive data to protect. For instance, in power systems, instead of hiding the presence of industrial customers, their electrical loads may need to be obfuscated (up to a certain threshold)

¹V. Dvorkin, J. Kazempour, and P. Pinson are with the Department of Electrical Engineering, Technical University of Denmark, Lyngby, Denmark. Email: {vladvo, seykaz, ppin}@elektro.dtu.dk

²Pascal Van Hentenryck is with the School of Industrial and Systems Engineering, Georgia Institute of Technology, Atlanta, USA. Email: pascal.vanhentenryck@isye.gatech.edu

to avoid revealing their commercial activities. Traditionally, differential privacy is achieved by adding Laplacian noise to query outputs and the noise can be calibrated using a small set of parameters (e.g., the privacy loss ϵ) to control the differences between the outputs on two adjacent datasets and obtain the guarantee known as ϵ -differential privacy [3].

Contributions: This paper applies differential privacy to distributed OPF computations using a consensus ADMM, where the OPF sub-problems coordinate voltage variables iteratively without disclosing their local load parameters. The paper introduces an adversarial model and shows that, in the presence of additional information, adversaries can infer local load parameters from the sub-problem responses to the coordination signals. To remedy this privacy leak, the paper introduces two privacy-preserving ADMM algorithms for OPF computations using static (SP-ADMM) and dynamic (DP-ADMM) random perturbations of subproblem solutions across iterations. The paper proves that the two algorithms ensure ϵ -differential privacy but differ in the amount of noise they introduce. The DP-ADMM algorithm ensures privacy at each iteration, but needs to scale the noise magnitude in order to minimize the privacy loss across multiple iterations. On the other hand, the SP-ADMM preserves differential privacy across all iterations uniformly but the worst-case sensitivity of its sub-problem solutions to load datasets must be defined ahead of the algorithm iterations. Numerical experiments highlight that, with a fine calibration of privacy parameters, the inference of loads from primal-dual coordination signals is equivalent to random guessing, *even if an adversary acquires all but one unknown sub-problem parameters*. The experiments also explore the convergence properties of the two algorithms and evaluate their fidelity with respect to the non-private ADMM. In particular, despite similar privacy properties, DP-ADMM results in smaller optimality losses, while SP-ADMM exhibits faster convergence rates.

Related work: Differentially private distributed computation was first introduced by Zhang *et al.* [6] for the unconstrained empirical risk minimization (ERM) problem. The authors distribute the ERM problem using ADMM and obtain differential privacy for local training datasets by adding noise to either primal or dual variables. The privacy guarantees, however, are provided for a single ADMM iteration. Moreover, the results hold for the unconstrained ERM problem, and are not appropriate for heavily constrained OPF computations. Han *et al.* [7] build a private distributed projected gradient descent algorithm with gradient perturbations for electrical vehicle charging, preventing the inference of charging power from coordination signals. In the OPF context, Mak *et al.* [8] extend the centralized private release

of OPF test cases [9], [10] to a distributed ADMM-based algorithm. However, the work is meant for the private release of input datasets and does not provide the OPF solution itself.

II. TOWARDS DISTRIBUTED OPF COMPUTATIONS

Consider a power system as an undirected graph $\Gamma(\mathcal{B}, \Lambda)$, where \mathcal{B} is the set of nodes and Λ is the set of transmission lines. Each transmission line has a susceptance $\beta \in \mathbb{R}_+^{|\Lambda|}$ and a capacity $\bar{f} \in \mathbb{R}_+^{|\Lambda|}$. The mapping functions $s : \Lambda \mapsto \mathcal{B}$ and $r : \Lambda \mapsto \mathcal{B}$ are used to return the sending and receiving ends of lines, respectively. The network topology is described by a weighted Laplacian matrix $B \in \mathbb{R}^{|\mathcal{B}| \times |\mathcal{B}|}$, where the weights on the lines are given by their susceptances. The network loads are given by vector $d \in \mathbb{R}_+^{|\mathcal{B}|}$. Each node generates an amount $p \in \mathbb{R}^{|\mathcal{B}|}$ of real power in the interval $[\underline{p}, \bar{p}]$ for a cost given by a quadratic function whose second- and first-order coefficients are $c_2 \in \mathbb{R}_+^{|\mathcal{B}|}$ and $c_1 \in \mathbb{R}_+^{|\mathcal{B}|}$, respectively. The OPF solution amounts to generator set-points $p \in \mathbb{R}^{|\mathcal{B}|}$ and voltage angles $\theta \in \mathbb{R}^{|\mathcal{B}|}$, obtained from the optimization

$$\min_{p, \theta} c(p) = \sum_{i \in \mathcal{B}} c_{2i} p_i^2 + c_{1i} p_i \quad (1a)$$

$$\text{s.t. } \underline{p}_i \leq p_i \leq \bar{p}_i, \forall i \in \mathcal{B}, \quad (1b)$$

$$-\bar{f}_l \leq \beta_{\ell} (\theta_{s(\ell)} - \theta_{r(\ell)}) \leq \bar{f}_l, \forall \ell \in \Lambda, \quad (1c)$$

$$\sum_{j \in \mathcal{B}} B_{ij} \theta_j = p_i - d_i, \forall i \in \mathcal{B}, \quad (1d)$$

which minimizes the total generation cost (1a). Inequality constraints (1b) and (1c) respectively ensure that generation and power flows are within their corresponding limits. Equations (1d) ensure the balance among the load, generation and power flow injection at every network node.

The centralized computation in (1) requires that all network parameters are submitted to a central entity. To avoid the need for sharing network parameters, one may consider instead, a distributed OPF computation, where the network is arbitrarily split into zones $z \in \mathcal{Z}$ [11]. The domestic nodes of each zone z are collected in a set \mathcal{R}_z , such that $\mathcal{R}_z \cap \mathcal{R}_{z'} = \emptyset, \forall z \neq z'$. The extended set \mathcal{V}_z contains the domestic nodes of, and adjacent nodes to, zone z . The set of end nodes from the transmission lines adjacent to zone z is then defined as $\mathcal{M}_z = \mathcal{V}_z \cap \mathcal{V}_{z'}. \forall z \neq z'$. To enable the distributed computation, the voltage angles are duplicated per zone, i.e., they are redefined as $\theta \in \mathbb{R}^{|\mathcal{B}| \times |\mathcal{Z}|}$. Towards the purpose, the following consensus constraint is enforced:

$$\theta_{iz} = \bar{\theta}_i : \mu_{iz}, \forall z \in \mathcal{Z}, \forall i \in \mathcal{M}_z, \quad (2)$$

where θ_{iz} is a local copy of the voltage angle at node i , $\bar{\theta} \in \mathbb{R}^{|\mathcal{B}|}$ is the consensus variable, and $\mu \in \mathbb{R}^{|\mathcal{B}| \times |\mathcal{Z}|}$ is the dual variable of the consensus constraint. This decomposition separates the feasibility region (1b)-(1d) per zone, so we denote the constraint set of each zone by \mathcal{F}_z . Now, the computation boils down to the optimization of the following partial Lagrangian function:

$$\max_{\mu} \min_{p, \theta, \bar{\theta}} \mathcal{L}(\mu, p, \theta, \bar{\theta}) = c(p) + \mu_z^\top (\bar{\theta} - \theta_z)$$

$$\text{s.t. } p, \theta \in \cap_{z \in \mathcal{Z}} \mathcal{F}_z,$$

where the objective function includes the dualized consensus constraint (2) with μ_z and θ_z being z^{th} columns of μ and

θ_z , respectively. The distributed OPF computation is thus enabled by the following ADMM algorithm:

$$\theta_z^{k+1} \leftarrow \operatorname{argmin}_{(p, \theta_z) \in \mathcal{F}_z} \mathcal{L}(\mu^k, p, \theta_z, \bar{\theta}^k) + \frac{\rho}{2} \|\theta^k - \theta_z\|_2^2, \forall z \in \mathcal{Z},$$

$$\bar{\theta}^{k+1} \leftarrow \operatorname{argmin}_{\bar{\theta}} \mathcal{L}(\mu^k, \theta^{k+1}, \bar{\theta}) + \frac{\rho}{2} \sum_{z \in \mathcal{Z}} \|\bar{\theta} - \theta_z^{k+1}\|_2^2,$$

$$\mu_z^{k+1} \leftarrow \mu_z^k + \rho (\bar{\theta}^{k+1} - \theta_z^{k+1}), \forall z \in \mathcal{Z},$$

where k is an iteration index and the squared norms denote the ADMM regularization terms augmented with a non-negative penalty factor ρ . The algorithm is indeed distributed, as it solely requires the exchange and update of primal and dual coordination signals between the neighboring zones.

The rest of the paper makes the following assumption.

Assumption 1: The function $c(p)$ is convex and strictly monotone in p , the set \mathcal{F}_z is compact and convex for all $z \in \mathcal{Z}$, and $\cap_{z \in \mathcal{Z}} \mathcal{F}_z$ has a non-empty interior. As a result, the distributed OPF algorithm converges to a unique optimal solution in a finite number of iterations [12].

III. DIFFERENTIAL PRIVACY FOR OPF

The privacy goal in this paper is to ensure that individual loads cannot be inferred from the outputs of the ADMM subproblems. Each sub-problem is thus considered as a *query* \mathcal{Q}_z^k that maps the dataset of loads $\mathcal{D}_z = \{d_i\}_{i \in \mathcal{R}_z}$ to a vector of all voltage angles $\{\theta_{iz}^{k+1}\}_{i \in \mathcal{M}_z}$ to be released at iteration k . Under Assumption 1, each sub-problem has a unique response for a given load dataset, i.e., it computes a one-to-one mapping of the load dataset to the voltage solution. Hence, the release of the voltage solution leads to the leakage of the load dataset.

The dependencies between sub-problem solutions and their load datasets can be weakened by making queries \mathcal{Q}_z^k differentially private, i.e., by adding a carefully calibrated noise to their outputs. More precisely, the added noise aims at making the outputs for two *adjacent* load datasets \mathcal{D}_z and \mathcal{D}'_z indistinguishable from each other.

Definition 1 (Adjacency [5]): $\mathcal{D}_z = \{d_i\}_{i \in \mathcal{R}_z}$ and $\mathcal{D}'_z = \{d'_i\}_{i \in \mathcal{R}_z}$ are α -adjacent datasets, denoted by $\mathcal{D}_z \sim_{\alpha} \mathcal{D}'_z$, if they differ in one element by α , i.e.,

$$\exists i \text{ s.t. } \|d_i - d'_i\|_1 \leq \alpha \wedge d_j = d'_j, \forall j \neq i.$$

Differential privacy relies on the concept of global sensitivity to calibrate the noise.

Definition 2 (Global Query Sensitivity): The global sensitivity Δ_z of query \mathcal{Q}_z^k is defined by

$$\Delta_z^k := \max_{\mathcal{D}_z \sim_{\alpha} \mathcal{D}'_z} \|\mathcal{Q}_z^k(\mathcal{D}_z) - \mathcal{Q}_z^k(\mathcal{D}'_z)\|_1.$$

where \mathcal{D}_z and \mathcal{D}'_z belong to the universe \mathcal{D}_z of all datasets of interest for zone z . Note that the datasets in \mathcal{D}_z are projections of the globally feasible solutions of interest.

In practice, especially in off-peak hours, the global sensitivity is overly pessimistic. The notion of local query sensitivity can be used to obtain more precise upper bounds.

Definition 3 (Local Query Sensitivity): The local query sensitivity of query \mathcal{Q}_z^k with respect to \mathcal{D}_z , denoted by

Algorithm 1 The SP-ADMM Algorithm

- 1: **Input:** Datasets \mathcal{D}_z , privacy parameters ε, α , algorithmic parameters $\gamma, \rho, K, \bar{\theta}^1, \mu^1$
 - 2: Draw random samples $\xi_z \sim \text{Lap}(\frac{\Delta_z}{\varepsilon})$, $\forall z \in \mathcal{Z}$
 - 3: **while** $k \neq K$ or $\sum_{z \in \mathcal{Z}} \|\tilde{\theta}_z^k - \bar{\theta}^{k+1}\|_2 \leq \gamma$ **do**
 - 4: Update voltage angles θ_z^{k+1} , $\forall z \in \mathcal{Z}$, by solving
$$\min_{(p, \theta_z) \in \mathcal{F}_z} \mathcal{L}_z(\mu^k, p, \theta_z, \bar{\theta}^k) + \frac{\rho}{2} \|\bar{\theta}^k - \theta_z\|_2^2$$
 - 5: Perturb sub-problem solutions $\tilde{\theta}_z^{k+1} = \theta_z^{k+1} + \xi_z$, $\forall z \in \mathcal{Z}$,
 - 6: Update consensus variables $\bar{\theta}_i^{k+1}$, $\forall i \in \mathcal{M}_z, z \in \mathcal{Z}$, as
$$\min_{\bar{\theta}} \mathcal{L}(\mu^k, \tilde{\theta}^{k+1}, \bar{\theta}) + \frac{\rho}{2} \sum_{z \in \mathcal{Z}} \|\bar{\theta} - \tilde{\theta}_z^{k+1}\|_2^2$$
 - 7: Update dual variables μ_z^{k+1} , $\forall z \in \mathcal{Z}$, by solving
$$\mu_z^{k+1} \leftarrow \mu_z^k + \rho (\tilde{\theta}_z^{k+1} - \bar{\theta}_z^{k+1})$$
 - 8: Iteration update $k \leftarrow k + 1$
 - 9: **Output:** Private OPF solution.
-

$\delta_z(\mathcal{D}_z)$, is defined as

$$\delta_z(\mathcal{D}_z) = \max_{\mathcal{D}' \sim_\alpha \mathcal{D}_z} \|\mathcal{Q}_z^k(\mathcal{D}_z) - \mathcal{Q}_z^k(\mathcal{D}')\|_1. \quad (3)$$

For simplicity, when \mathcal{D}_z is clear from the context, δ_z is used to denote $\delta_z(\mathcal{D}_z)$.

Remark 1: The maximal local sensitivity of \mathcal{Q}_z^k depends not only on the magnitude of loads $\{d_i\}_{i \in \mathcal{R}_z}$, but also on their relative position with respect to the nodes in \mathcal{M}_z .

This work introduces noise drawn from a zero-mean Laplace distribution with scale b , denoted by $\text{Lap}(b)$ for short, with a probability density function $\text{Lap}(\xi|b) = \frac{1}{2b} \exp(-\frac{\|\xi\|_1}{b})$. It can be used to attain differential privacy for numerical queries as per the following result [3].

Theorem 1 (Laplace mechanism): Let $\mathcal{Q} : \mathcal{D} \mapsto \mathbb{R}$ be a query that maps dataset \mathcal{D} to real numbers, and let Δ be a query sensitivity. The Laplace mechanism that outputs $\mathcal{Q}(\mathcal{D}) + \xi$ with $\xi \sim \text{Lap}(\Delta/\varepsilon)$ is ε -differential privacy, i.e.,

$$\mathbb{P}[\mathcal{Q}(\mathcal{D}) + \xi] \leq \mathbb{P}[\mathcal{Q}(\mathcal{D}') + \xi] \exp(\varepsilon),$$

where $\mathcal{D} \sim_\alpha \mathcal{D}'$ are any α -adjacent datasets.

The parameter ε , called the *privacy loss*, bounds the multiplicative difference between distributions of query outputs on any two α -adjacent datasets. Stronger privacy requirements can be obtained by choosing smaller values for ε and larger values for α . The last building block is the *sequential composition* theorem [3], which characterizes the guarantees for sequential applications of differential privacy.

Theorem 2 (Sequential composition): Consider T runs of query function $\{\mathcal{Q}_z^t(\mathcal{D}_z)\}_{t=1}^T$ such that every run depends on the result of the previous runs, i.e.,

$$\mathcal{Q}_z^t(\mathcal{D}_z) = \mathcal{Q}_z^t(\mathcal{D}_z, \mathcal{Q}_z^1(\mathcal{D}_z), \mathcal{Q}_z^2(\mathcal{D}_z), \dots, \mathcal{Q}_z^{t-1}(\mathcal{D}_z)).$$

Suppose that \mathcal{Q}_z^t preserve ε_t -differential privacy for $\mathcal{Q}_z^{t'}$ for all $t' < t$. Then, the T -tuple mechanism $\mathcal{Q}_z = (\mathcal{Q}_z^1, \mathcal{Q}_z^2, \dots, \mathcal{Q}_z^t)$ preserves $\sum_{t=1}^T \varepsilon_t$ -differential privacy.

IV. PRIVATE DISTRIBUTED OPF ALGORITHMS

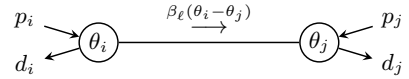
This section presents two differentially private ADMM algorithms for distributed OPF computations.

A. The SP-ADMM Algorithm

The SP-ADMM algorithm relies on a key insight: *the upper bound on the global query sensitivity is independent from the input coordination signals*.

Proposition 1: The global sensitivity of the ADMM subproblem \mathcal{Q}_z^k is upper-bounded by $\max_{\mathcal{D}_z \in \mathcal{D}_z} \max_i \{d_i\}_{i \in \mathcal{R}_z}$.

Proof: The result follows from the nodal balance constraint (1d). Consider that the voltage angle sensitivity to load changes reduces with the size of the network graph. Therefore, the worst-case sensitivity is observed in a minimal size two-node network, i.e.,



where node i is chosen as a reference node, i.e., $\theta_i = 0$. Then, the power balance at node j is $-\beta_l \theta_j = p_j - d_j$. The worst-case sensitivity is provided given that $p_j = 0$, so the change of load directly translates into $\beta_l \theta_j$. As $\beta_l \gg 1$ in power system networks, the change of θ_j is upper-bounded by the magnitude of d_j . In turn, d_j has to be chosen as the largest feasible load in a dataset universe $\mathcal{D}_z, \forall z \in \mathcal{Z}$. ■

As a result, the SP-ADMM algorithm, shown in Algorithm 1, generates the Laplacian noise $\xi_z \in \mathbb{R}^{|\mathcal{M}_z|}, \forall z \in \mathcal{Z}$, once, at the beginning of the algorithm, using an upper bound Δ_z on the global sensitivity. It takes the dataset, privacy and algorithm parameters as inputs, and runs ADMM iterations until reaching iteration limit K or the primal residual is below the tolerance γ . Unlike the conventional ADMM, once a sub-problem produces the optimal response to the dual and consensus variables, the algorithm perturbs the response with the initially generated noise. The perturbed solution $\tilde{\theta}_z^{k+1}$ then participates in the consensus and dual variable updates.

B. The DP-ADMM Algorithm

The DP-ADMM algorithm is fundamentally different: it uses the concept of local query sensitivity to perturb the phase angles differently at each iteration. Its key insight is the recognition that *the local sensitivity of the queries/subproblems can be obtained by solving an optimization problem*. As a result, for each iteration, the DP-ADMM perturbs the phase angles using the local sensitivity. The DP-ADMM is outlined in Algorithm 2. The noise $\xi_z^k \in \mathbb{R}^{|\mathcal{M}_z|}, \forall z \in \mathcal{Z}$, is dynamically updated respecting the change of local sensitivity δ_z^k on α -adjacent datasets. The sensitivity is obtained by identifying the individual load, whose α -change brings the maximal change of the sub-problem solution. The rest of the algorithm is similar to SP-ADMM.

C. Properties

This section reviews the properties of the two algorithms.

Theorem 3: Let $\tilde{\mathcal{Q}}_z^k(\mathcal{D}_z)$ be a randomized sub-problem of zone z acting on optimization dataset \mathcal{D}_z i.e.,

$$\tilde{\mathcal{Q}}_z^k(\mathcal{D}_z) = \theta_z^{k+1} + \xi_z^k.$$

Let δ_z^k be a sensitivity of $\mathcal{Q}_z^k(\mathcal{D}_z)$ for all α -adjacent dataset \mathcal{D}'_z . Then, if the random perturbation ξ_z^k is sampled from the

Algorithm 2 The DP-ADMM Algorithm

- 1: **Input:** Datasets \mathcal{D}_z , privacy parameters ε, α , algorithmic parameters $\gamma, \rho, K, \bar{\theta}^1, \mu^1$
 - 2: **while** $k \neq K$ or $\sum_{z \in \mathcal{Z}} \|\hat{\theta}_z^k - \bar{\theta}^{k+1}\|_2 \leq \gamma$ **do**
 - 3: Update voltage angles $\theta_z^{k+1}, \forall z \in \mathcal{Z}$, by solving
$$\min_{(p, \theta_z) \in \mathcal{F}_z} \mathcal{L}_z(\mu^k, p, \theta, \bar{\theta}^k) + \frac{\rho}{2} \|\bar{\theta}^k - \theta_z\|_2^2$$
 - 4: For μ_z^k and $\bar{\theta}^k$, compute sensitivity $\delta_z^k, \forall z \in \mathcal{Z}$, by solving
$$\delta_z^k = \max_{\mathcal{D}' \in \mathcal{D}} \|\mathcal{Q}_z^k(\mathcal{D}_z) - \mathcal{Q}_z^k(\mathcal{D}'_z)\|_1,$$
s.t. $\|\mathcal{D}_z - \mathcal{D}'_z\|_1 \leq \alpha$
 - 5: Perturb sub-problem solutions by $\xi_z^k \sim \text{Lap}(\frac{\delta_z^k}{\varepsilon}), \forall z \in \mathcal{Z}$,
$$\tilde{\theta}_z^{k+1} = \theta_z^{k+1} + \xi_z^k$$
 - 6: Update consensus variables $\bar{\theta}_i^{k+1}, \forall i \in \mathcal{M}_z, z \in \mathcal{Z}$, as
$$\min_{\bar{\theta}} \mathcal{L}(\mu^k, \bar{\theta}^{k+1}, \bar{\theta}) + \frac{\rho}{2} \sum_{z \in \mathcal{Z}} \|\bar{\theta}_z - \bar{\theta}_z^{k+1}\|_2^2$$
 - 7: Update dual variables $\mu_z^{k+1}, \forall z \in \mathcal{Z}$, by solving
$$\mu_z^{k+1} \leftarrow \mu_z^k + \rho (\bar{\theta}_z^{k+1} - \tilde{\theta}_z^{k+1})$$
 - 8: Iteration update $k \leftarrow k + 1$
 - 9: **Output:** Private OPF solution.
-

probability distribution with density function $\text{Lap}(\frac{\delta_z^k}{\varepsilon})$, then $\tilde{\mathcal{Q}}_z^k(\mathcal{D})$ provides ε -differential privacy at iteration k , i.e.,
$$\mathbb{P}[\tilde{\mathcal{Q}}_z^k(\mathcal{D}_z)] \leq \mathbb{P}[\tilde{\mathcal{Q}}_z^k(\mathcal{D}'_z)] \exp(\varepsilon), \forall \mathcal{D}'_z \in \mathcal{D}_z.$$

Proof: The proof follows a similar line of arguments as for numerical queries. We consider the ratio of probabilities that the query $\tilde{\mathcal{Q}}_z^k$ returns the same solution $\hat{\theta}_z^{k+1}$ on two α -adjacent datasets $\mathcal{D}_z \sim_{\alpha} \mathcal{D}'_z$ at ADMM iteration k :

$$\begin{aligned} \frac{\mathbb{P}[\tilde{\mathcal{Q}}_z^k(\mathcal{D}_z) \in \hat{\theta}_z^{k+1}]}{\mathbb{P}[\tilde{\mathcal{Q}}_z^k(\mathcal{D}'_z) \in \hat{\theta}_z^{k+1}]} &= \frac{\mathbb{P}[\mathcal{Q}_z^k(\mathcal{D}_z) + \text{Lap}(\xi_z | \frac{\delta_z^k}{\varepsilon}) \in \hat{\theta}_z^{k+1}]}{\mathbb{P}[\mathcal{Q}_z^k(\mathcal{D}'_z) + \text{Lap}(\xi_z | \frac{\delta_z^k}{\varepsilon}) \in \hat{\theta}_z^{k+1}]} \\ &= \prod_{i \in \mathcal{M}_z} \frac{\frac{\varepsilon}{2\delta_z^k} \exp\left(-\frac{\|\xi_{iz} - \mathcal{Q}_{iz}^k(\mathcal{D}_z)\|_1}{\delta_z^k}\right)}{\frac{\varepsilon}{2\delta_z^k} \exp\left(-\frac{\|\xi_{iz} - \mathcal{Q}_{iz}^k(\mathcal{D}'_z)\|_1}{\delta_z^k}\right)} \\ &= \prod_{i \in \mathcal{M}_z} \exp\left(\frac{\varepsilon (\|\xi_{iz} - \mathcal{Q}_{iz}^k(\mathcal{D}'_z)\|_1 - \|\xi_{iz} - \mathcal{Q}_{iz}^k(\mathcal{D}_z)\|_1)}{\delta_z^k}\right) \\ &\leq \prod_{i \in \mathcal{M}_z} \exp\left(\frac{\varepsilon \|\mathcal{Q}_{iz}^k(\mathcal{D}_z) - \mathcal{Q}_{iz}^k(\mathcal{D}'_z)\|_1}{\delta_z^k}\right) \\ &= \exp\left(\frac{\varepsilon \|\mathcal{Q}_z^k(\mathcal{D}_z) - \mathcal{Q}_z^k(\mathcal{D}'_z)\|_1}{\delta_z^k}\right), \end{aligned} \quad (4)$$

where the second equality follows from the definition of the probability density function of the Laplace distribution, and the inequality follows from the inequality of norms. Recall Definition 3 of the local sensitivity. Hence, by substituting (3) in (4), we obtain the desired result. ■

Remark 2: Theorem 3 holds not only for the DP-ADMM, but also for the SP-ADMM algorithm when used with an upper bound on the global sensitivity.

Remark 3: Theorem 3 makes use of the local sensitivity δ_z^k , thus attaining local ε -differential privacy. By substituting δ_z^k with the global query sensitivity Δ_z , the algorithms provide global ε -differential privacy. The robustness of the two approaches to privacy attacks is analyzed in Section VI.

Observe that every new iteration of the DP-ADMM algorithm reveals more information to an adversary, thus diminishing the privacy guarantee. Assume that the algorithm implementation can limit the adversary to observing T iterations, e.g., by using secure switching of communication channels. Then, the following result applies.

Theorem 4: Let $\tilde{\mathcal{Q}}_z^k(\mathcal{D}_z) = \theta_z^{k+1} + \xi_z^k$ be a randomized query as specified in Theorem 3 with the difference that the noise ξ_z^k is drawn from $\text{Lap}(T \frac{\delta_z^k}{\varepsilon})$. Then, DP-ADMM preserves ε -differential privacy across T iterations.

Proof: It follows from combining Theorems 2 and 3.

Finally, observe that the feasibility of the OPF solution is not affected by either dynamic or static perturbations, as the two algorithms add noise only to the unconstrained consensus and dual variable updates.

V. ADVERSARIAL PROBLEM

The strength of differentially private algorithms is their robustness to *side* information. The framework guarantees that, even if an adversary obtains information on *all but one* items in a dataset, the privacy of the remaining one item is ensured. This section presents an adversarial problem for this worst-case scenario of privacy attack on OPF sub-problems.

Consider a set $\mathcal{T} = \{k - T, \dots, k\}$ of ADMM iterations observed by an adversary. Let $\hat{\theta}_z^{t+1}$ be a response of each subproblem $z \in \mathcal{Z}$ to dual and consensus variables μ_z^t and $\bar{\theta}_z^t$ at iteration $t \in \mathcal{T}$. For sub-problem z , the adversarial inference problem can be formulated as the following empirical risk minimization problem across T iterations:

$$\begin{aligned} \min_{\hat{p}^t, \hat{\theta}_z^t, \hat{d}_i} \quad & \sum_{t \in \mathcal{T}} c_z(\hat{p}^t) - [\mu_z^t]^\top \hat{\theta}_z^t \\ & + \sum_{t \in \mathcal{T}} \frac{\rho}{2} \|\bar{\theta}_z^t - \hat{\theta}_z^t\|_2^2 \\ & + \Upsilon \sum_{t \in \mathcal{T}} \|\hat{\theta}_z^t - \hat{\theta}_z^{t+1}\|_2 \end{aligned} \quad (5a)$$

$$\text{s.t. Equations (1b) -- (1c), } \forall t \in \mathcal{T}, \quad (5b)$$

$$\sum_{m \in \mathcal{V}_z} B_{nm} \hat{\theta}_{mz}^t = \hat{p}_n^t - d_n, \forall n \in \mathcal{R}_z \setminus i, t \in \mathcal{T}, \quad (5c)$$

$$\sum_{m \in \mathcal{V}_z} B_{im} \hat{\theta}_{mz}^t = \hat{p}_i^t - \hat{d}_i, \forall t \in \mathcal{T}, \quad (5d)$$

where decision variables are indicated with a (\cdot) notation, and the rest are the parameters available to an adversary. The unknown load magnitude \hat{d}_i at node i of interest is modelled as a decision variable. An adversary seeks the value of \hat{d}_i that minimizes the Euclidean distance between the voltage variables $\hat{\theta}_z^{t+1}$ modeled in the adversarial problem and the voltage solution $\hat{\theta}_z^{t+1}$ released by the sub-problem at all iterations $t \in \mathcal{T}$. By penalizing the distance with a sufficiently large coefficient Υ , an adversary identifies the load magnitude that produces the same voltage solution as that released by the sub-problem, thus identifying the unknown load magnitude.

VI. NUMERICAL EXPERIMENTS

This section examines the proposed Algorithms 2 and 1 using a standard IEEE 118-node test case with a 3-zone

lay-out taken from [13, case 118-3]. The algorithms are compared in terms of their robustness to privacy attacks, convergence properties, and fidelity with respect to the non-private ADMM algorithm. By default, we set ADMM penalty factor $\rho = 100$, iteration limit $K = 300$, algorithm tolerance $\gamma = 0.5$, and coefficient $\Upsilon = 10^6$. The privacy requirements are selected such that the privacy loss is fixed $\varepsilon = 1$ whereas the adjacency coefficient varies in the range $\alpha = \{1, 2.5, 5, 7, 10\}\%$. For the given algorithmic parameters, the standard non-private ADMM converges to the optimal OPF solution in 59 iterations.

1) Robustness to the Privacy Attacks: The robustness of the algorithms to the load inference is assessed by using the adversarial model in (5). The adversarial model identifies *all* network loads if the standard ADMM is used. The random perturbations of sub-problem solutions, however, prevent the adversary from inferring the actual loads. The results focus on the load at bus 20, which has a median load in the first zone. As per Theorem 3, by specifying the adjacency coefficient α , the algorithms guarantee that, at a given iteration k , an adversary cannot distinguish the magnitude of unknown load d_{20} from any other magnitude in the range $d_{20} \pm \alpha$.

The load inference results for the DP-ADMM algorithm are shown in Fig. 1. The plots show the inferred load at every iteration of the algorithm assuming that only a single iteration is available to an adversary. The inferred load is given as a probability density with each observation corresponding to a single iteration. By increasing α , the inferred load deviates more substantially from the true value of 9 MW, hence, the probability of recovering the true load magnitude reduces. The load obfuscation with SP-ADMM is depicted in Fig. 2. Since the noise is fixed across iterations, the results display 1000 ADMM runs. Similarly to the DP-ADMM algorithm, increasing values of α result in wider distributions of inferred loads. It is important to note that the attacker observes only one sample from these distributions. Observe that the variance of load distributions is notably larger than that of DP-ADMM for a given adjacency value. Moreover, the support of the distributions in Fig. 2 extends drastically with increasing values of α , making the load inference essentially equivalent to a random guess.

Fig. 2 further shows that the use of upper bound on the global sensitivity Δ_z in SP-ADMM, which is set to the largest installed load in the system, results in much stronger privacy protection than the use of local sensitivity, which is set to be at least as much as the maximum local sensitivity observed across DP-ADMM iterations, i.e., $\bar{\delta}_z = \max_k \{\delta_z^k\}_{k=1}^K$. Although both methods enable privacy protection, the formal privacy guarantees provided by SP-ADMM are only achieved with the use of global sensitivity.

Finally, observe that every new iteration of DP-ADMM reveals more information to an adversary, as shown on the left plot in Fig. 3. If the attack budget, i.e., the number of compromised iterations, increases up to T , an adversary recovers the load more precisely. To overcome this limitation, Theorem 4 can be applied to preserve ε -differential privacy

TABLE I
OPTIMALITY LOSS INDUCED BY DP-ADMM AND SP-ADMM (%)

$\alpha, \%$	1	2.5	5	7	10
DP-ADMM	0.48	0.92	1.23	1.51	3.83
SP-ADMM	0.28	4.33	11.0	11.35	20.41

across T iterations. This requires to scale the noise parameters by T . The corresponding results in the right plot in Fig. 3 show that the magnitude of the noise increases substantially, thus reducing the quality of load inference even with more information available to an adversary.

2) Convergence analysis: The convergence statistics of the two algorithms obtained with 100 simulation runs are summarized in Fig. 4. The figure shows the evolution of the aggregated primal residual across iterations highlighting important differences between dynamic and static perturbations of sub-problem solutions. With dynamic perturbations, the DP-ADMM algorithm perturbs the sub-problem solutions at every iteration, and the magnitude of the noise increases with α . While the non-private ADMM converges in 59 iterations on this test case, the DP-ADMM requires up to 300 iterations in average, depending on the choice of α . In contrast, the SP-ADMM exhibits a similar computational complexity as the non-private ADMM algorithm. Moreover, in average, the convergence of SP-ADMM is not affected by the choice of adjacency coefficient.

3) Fidelity analysis: It remains to quantify the loss in efficiency of differentially-private OPF solutions. The average optimality loss induced by DP-ADMM and SP-ADMM algorithms for 100 runs is provided in Table 4. The results for attack budget $T = 1$ show that with increasing privacy requirements, both algorithms converge in sub-optimal solutions as compared to the non-private ADMM solution. However, due to dynamically updated zero-mean perturbations, the DP-ADMM has notably better fidelity than the SP-ADMM, which fixes the noise across iterations and constantly steers the OPF dispatch from the optimal solution. This unfolds the following trade-offs among the algorithms: despite better convergence properties of SP-ADMM, it yields a larger optimality gap compared to the DP-ADMM, which demonstrates weaker convergence statistics.

VII. CONCLUSIONS

Although the distributed algorithms have been long trusted to preserve the privacy of network parameters in OPF computations, this paper shows that the standard distributed algorithms do not ensure the information integrity as the sensitive parameters, e.g., electrical loads, are leaked through the exchange of coordination signals. To overcome this limitation, this paper introduces two privacy-preserving OPF ADMM algorithms that satisfy the definition of ε -differential privacy. The algorithms provide privacy by means of either static or dynamic perturbations of the sub-problem solutions at each iteration. The paper shows theoretically and through numerical results that the two algorithms are able to negate the adversarial inference of sensitive information from coordination signals. Despite their complementary privacy properties, the numerical performance of the two algorithms is

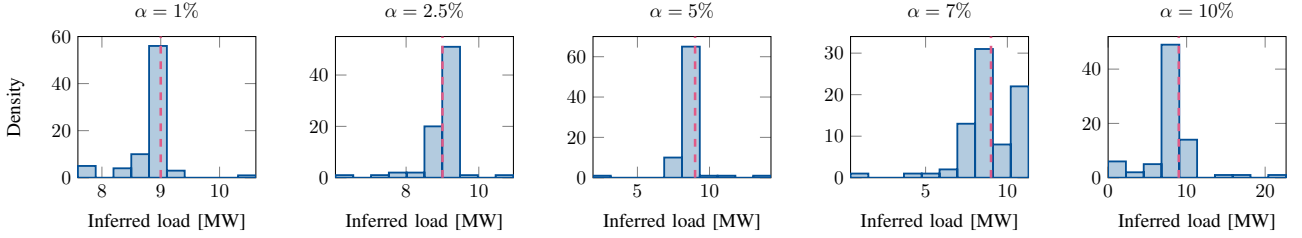


Fig. 1. DP-ADMM: Results of privacy attack on the load sited at node 20. The plots show the densities of inferred load by an adversary across iterations for different adjacency coefficients for a single simulation run.

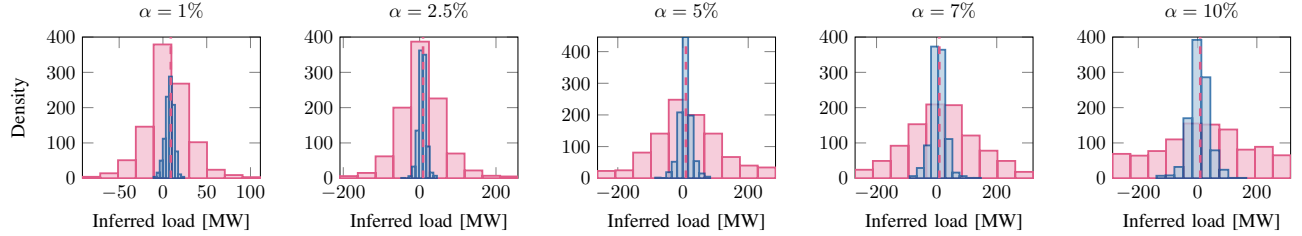


Fig. 2. SP-ADMM: Results of privacy attack on the load sited at node 20. The plots depict the distribution of inferred load by an adversary across 1000 simulation runs for different adjacency coefficient. The red and blue distributions are given for the global and local sensitivities Δ_z and $\bar{\Delta}_z$, respectively.

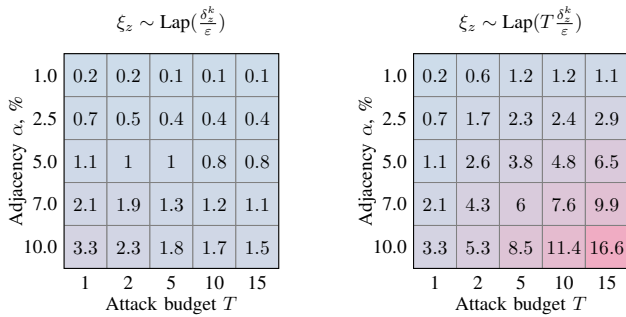


Fig. 3. DP-ADMM: Mean absolute inference error, i.e., mismatch between the actual and inferred loads in MWh, across last T iterations with (right) and without (left) application of Theorem 4 for 100 simulation runs.

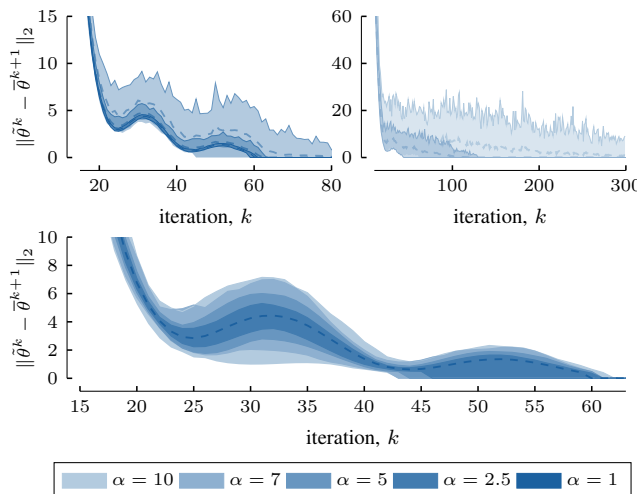


Fig. 4. Convergence of DP-ADMM (top) and SP-ADMM (bottom) algorithms on the 3-zone IEEE 118-node system for different adjacency coefficient α in %. The dashed lines indicate the average residual across 100 runs, whereas the colored areas indicate the spread between the minimum and maximum values of the residual at iteration k . Best view in colors.

mutually exclusive: if static perturbations demonstrate a more robust convergence, their fidelity with respect to the non-private solution is lower than that of dynamic perturbations with weaker convergence statistics.

REFERENCES

- [1] D. K. Molzahn *et al.*, “A survey of distributed optimization and control algorithms for electric power systems,” *IEEE Transactions on Smart Grid*, vol. 8, no. 6, pp. 2941–2962, 2017.
- [2] R. Shokri *et al.*, “Membership inference attacks against machine learning models,” in *2017 IEEE Symposium on Security and Privacy (SP)*, 2017, pp. 3–18.
- [3] C. Dwork and A. Roth, “The algorithmic foundations of differential privacy,” *Foundations and Trends® in Theoretical Computer Science*, vol. 9, no. 3–4, pp. 211–407, 2014.
- [4] C. Dwork *et al.*, “Calibrating noise to sensitivity in private data analysis,” in *Theory of cryptography conference*. Springer, 2006, pp. 265–284.
- [5] K. Chatzikokolakis *et al.*, “Broadening the scope of differential privacy using metrics,” in *International Symposium on Privacy Enhancing Technologies Symposium*. Springer, 2013, pp. 82–102.
- [6] T. Zhang and Q. Zhu, “Dynamic differential privacy for ADMM-based distributed classification learning,” *IEEE Transactions on Information Forensics and Security*, vol. 12, no. 1, pp. 172–187, 2016.
- [7] S. Han, U. Topcu, and G. J. Pappas, “Differentially private distributed constrained optimization,” *IEEE Transactions on Automatic Control*, vol. 62, no. 1, pp. 50–64, 2016.
- [8] T. W. Mak, F. Fioretto, and P. Van Hentenryck, “Privacy-preserving obfuscation for distributed power systems,” *arXiv preprint arXiv:1910.04250*, 2019.
- [9] F. Fioretto and P. Van Hentenryck, “Constrained-based differential privacy: Releasing optimal power flow benchmarks privately,” in *CRAIOPR*. Springer, 2018, pp. 215–231.
- [10] F. Fioretto, T. W. Mak, and P. Van Hentenryck, “Differential privacy for power grid obfuscation,” *arXiv preprint arXiv:1901.06949*, 2019.
- [11] T. Erseghe, “A distributed approach to the OPF problem,” *EURASIP Journal on Advances in Signal Processing*, vol. 2015, no. 1, pp. 1–13, 2015.
- [12] S. Boyd *et al.*, “Distributed optimization and statistical learning via the alternating direction method of multipliers,” *Foundations and Trends® in Machine learning*, vol. 3, no. 1, pp. 1–122, 2011.
- [13] J. Guo, G. Hug, and O. K. Tonguz, “Intelligent partitioning in distributed optimization of electric power systems,” *IEEE Transactions on Smart Grid*, vol. 7, no. 3, pp. 1249–1258, 2015.

[Paper E] Differentially private convex optimization with feasibility guarantees

Authors:

V. Dvorkin, F. Fioretto, P. Van Hentenryck, J. Kazempour and P. Pinson.

Differentially Private Convex Optimization with Feasibility Guarantees

Vladimir Dvorkin

Technical University of Denmark
Lyngby, Denmark
vladvo@elektro.dtu.dk

Ferdinando Fioretto

Syracuse University
Syracuse, NY, USA
ffiorett@syr.edu

Pascal Van Hentenryck

Georgia Institute of Technology
Atlanta, GA, USA
pvh@isye.gatech.edu

Jalal Kazempour

Technical University of Denmark
Lyngby, Denmark
seykaz@elektro.dtu.dk

Pierre Pinson

Technical University of Denmark
Lyngby, Denmark
ppin@elektro.dtu.dk

Abstract

This paper develops a novel differentially private framework to solve convex optimization problems with sensitive optimization data and complex physical or operational constraints. Unlike standard noise-additive algorithms, that act primarily on the problem data, objective or solution, and disregard the problem constraints, this framework requires the optimization variables to be a function of the noise and exploits a chance-constrained problem reformulation with formal feasibility guarantees. The noise is calibrated to provide differential privacy for identity and linear queries on the optimization solution. For many applications, including resource allocation problems, the proposed framework provides a trade-off between the expected optimality loss and the variance of optimization results.

1 Introduction

Differential privacy (Dwork et al., 2006) is a rigorous definition of privacy that quantifies and bounds the risk of disclosing sensitive attributes of datasets used in computations. Differentially private algorithms ensure privacy by introducing a calibrated noise to the inputs, outputs, or objectives of computations. It has been successfully applied to a variety of contexts, including histogram queries (Li et al., 2010), census surveys (Abowd, 2018; Fioretto and Van Hentenryck, 2019), linear regression (Chaudhuri et al., 2011) and deep learning (Abadi et al., 2016) to name but a few examples. However, their applications to *constrained* optimization problems remains limited, because it is generally hard to certify the feasibility of differentially private optimization solution.

This paper considers a parametric constrained optimization problems of the form

$$\underset{z}{\text{minimize}} \quad c(z) \quad \text{subject to} \quad \mathcal{Z} \triangleq \{z \mid Az \leq b, Gz = d\}, \quad (1)$$

with variables $z \in \mathbb{R}_+^n$, convex cost function $c : \mathbb{R}^n \mapsto \mathbb{R}$, and convex, compact and non-empty feasible space \mathcal{Z} with parameters $A \in \mathbb{R}^{m \times n}$, $b \in \mathbb{R}^m$, $G \in \mathbb{R}^{\ell \times n}$, and $d \in \mathbb{R}^\ell$, with $m > 0$ and $\ell > 0$. The paper assumes elements c, A, b and G as public, non-sensitive information about the system design, whereas vector $d = \{d_i\}_{i=1}^\ell$ contains private, sensitive data of every user i , e.g. the customer loads in an electrical power system. In such applications, the feasible space \mathcal{Z} encodes hard operational constraints or physical laws that must be satisfied.

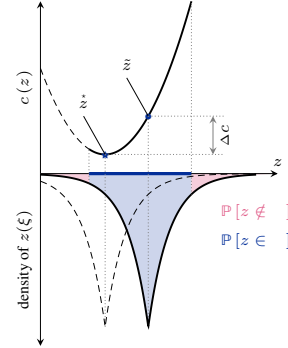
Releasing queries over the solutions of problem (1) may leak information about the sensitive data d . For example, in energy network operations, releasing the nodal energy supplies using identity queries,

or aggregated supply quantities using sum queries, exposes the allocation of energy demand d across the network (Zhou et al., 2019). Therefore, the goal of this work is to compute such solution z that makes queries over z differentially private, while also being feasible for problem constraints.

While there exist various differential privacy algorithms to solve convex optimization problems, their application to constrained problems is limited because they do not generally guarantee that the privacy-preserving result necessarily satisfies the feasibility conditions. Algorithms based on input perturbation of the sensitive data d modify the feasible space \mathcal{Z} (Dwork et al., 2006; Fukuchi et al., 2017), thus returning an approximate solution to (1) that may not satisfy the original constraints. The output perturbation mechanisms (Chaudhuri and Monteleoni, 2009; Rubinstein et al., 2012), that add noise to the optimization results, generally cannot be certified feasible for \mathcal{Z} ; see, for example, the impossibility results of Hsu et al. (2014). The feasibility and near-optimality of the privacy-preserving results can be restored by leveraging the post-processing immunity of differential privacy. This, however, requires solving bilevel optimization problems (Mak et al., 2020).

This paper addresses these limitations and develops a new framework that provides both privacy and feasibility guarantees for constrained optimization problems. Instead of applying the noise to either the parameters or the results of the optimization, the framework solves a stochastic chance-constrained optimization problem whose solution is used to sample a solution to (1), which guarantees privacy and ensures feasibility with high probability. The approach requires a linear dependency between the optimization variables and the noise (Georghiou et al., 2019) and reveals a novel connection between differential privacy and stochastic chance-constrained optimization.

The functioning of the framework is illustrated in the adjacent figure, showing the projections of solutions z onto cost function c and feasible space \mathcal{Z} . Consider the optimal solution \hat{z} returned by problem (1). The output perturbation of \hat{z} results in solutions whose density $\tilde{z}(\xi)$ (dashed line on the bottom of the figure) is prone to lie outside the feasible space \mathcal{Z} . By restricting the optimization variables to be a linear function of the noise, e.g., $z(\xi) = \tilde{z} + f(\xi)$ where \tilde{z} is the expected value of the solution with respect to the random variable distribution and $f(\xi)$ is the linear functional recourse, the stochastic problem optimizes \tilde{z} and $f(\xi)$ providing a new probability density of solution z (solid line). This new density renders any realization of the noise ξ feasible within a *prescribed* probability $\mathbb{P}[\tilde{z} + f(\xi) \in \mathcal{Z}]$, specified by the curator of problem (1). If the functional recourse $f(\xi)$ is made independent from the sensitive data d , the framework enjoys both privacy and feasibility guarantees. However, it introduces a trade-off between privacy and the optimality loss with expected value $\Delta c = \mathbb{E}[c(z(\xi)) - c(\hat{z})]$.



The chance-constrained optimization always ensures the satisfaction of the system $Gz = d$, which may represent flow conservation constraints and other physical laws that cannot be violated. This setting, however, restricts the queries to be made only on strict subsets of solution z , because the perturbation needs to be redistributed among the variables to guarantee the feasibility of the system. By separating the solution into released and non-released variables, the latter can be optimized to provide trade-offs between the optimality loss and its variance, as well as the trade-offs between the optimality loss and the overall solution variance. The contributions of this work can be summarized as follows: **(1)** It develops a novel differentially private framework for the release of identity and sum queries over the solutions of constrained convex programs, using stochastic chance-constrained optimization (Section 3). **(2)** The released solutions are guaranteed feasible with a high probability. The feasibility guarantees are studied for individual and joint constraint satisfaction, providing higher or lower optimality losses, respectively (Section 4). **(3)** The framework establishes a trade-off between the expected and the worst-case errors by controlling the variance of the optimization results and the optimality loss (Section 5). **(4)** On the benchmark energy optimization datasets, the framework is shown to outperform the standard output perturbation algorithm (Section 6).

Notation Upper and lower case symbols are used to denote, respectively, matrices and vectors. The indexed notation A_i is used to denote the i^{th} row vector of matrix A . The operator $\text{diag}(a)$ returns the diagonal matrix with entries of vector a , and $\text{diagv}(A)$ returns the vector of diagonal elements of matrix A . The ceil $\lceil r \rceil$ maps real number r into the least succeeding integer. Notation \circ denotes a Schur product. $\mathbf{0}$ and $\mathbf{1}$ respectively denote vectors of zeros and ones of proper dimensions.

2 Preliminaries

Across the paper, it is assumed that the optimal solution to problem (1) exists and is unique and that the data d_i , contributed by each individual i , in d are not correlated. Thus, the problem can be seen as an algorithm $\mathcal{M} : \mathbb{R}^\ell \mapsto \mathbb{R}^n$ with a unique mapping of datasets d to optimization results. To enable private queries over the optimization results, this work considers a differentially private counterpart $\tilde{\mathcal{M}}$ of \mathcal{M} . While the traditional differential privacy definition aims at protecting the *participation* of an individual data (Dwork et al., 2006), this work focuses on obfuscating the *magnitude* d_i associated with participant i of the input vector d . To capture this privacy notion, the paper focuses on the *indistinguishability* framework proposed by Chatzikokolakis et al. (2013), which protects the sensitive data of each individual up to some measurable quantity $\alpha > 0$ and defines two neighboring datasets d, d' (written \sim_α) as

$$d \sim_\alpha d' \iff \exists i \text{ s.t. } |d_i - d'_i| \leq \alpha \wedge d_j = d'_j, \forall j \neq i,$$

where d and d' are input vectors to problem (1) and α is a positive real value. Following previous work (Muñoz et al., 2019), this relation requires the assumption that the neighboring datasets are feasible for problem (1), which is not restrictive, as only feasible solutions are of interest to release.

Differential privacy requires that the maximum divergence of the algorithm output distributions on neighboring inputs to be bounded by privacy parameters ε and δ , such that

$$\mathbb{P} [\tilde{\mathcal{M}}(d) = O] \leq \mathbb{P} [\tilde{\mathcal{M}}(d') = O] \exp(\varepsilon) + \delta$$

for a random algorithm $\tilde{\mathcal{M}}$ and any output O , where \mathbb{P} denotes the probability over runs of $\tilde{\mathcal{M}}$. If $\delta = 0$, $\tilde{\mathcal{M}}$ is said to be ε -differentially private.

The *global sensitivity* methods are known to provide differential privacy by augmenting the output of computations with the noise calibrated to the ℓ_1 - or ℓ_2 -sensitivity. The ℓ_p -sensitivity

$$\Delta_\alpha \triangleq \max_{d \sim_\alpha d'} \|\mathcal{M}(d) - \mathcal{M}(d')\|_p, \quad p = 1, 2,$$

is used to bound the change in the algorithm output induced by any two α -indistinguishable inputs. In many applications of interest, $G \in \{0, 1\}^{\ell \times n}$ is a binary matrix and the domain of datasets d is normalized in $[0, 1]$. Thus, Δ_α is directly upper-bounded by α .

Let $\text{Lap}(\lambda)^n$ denote the i.i.d. Laplace distribution over n dimensions with 0 mean and scale λ . The following ubiquitous result provides an ε -differentially private algorithm (Dwork et al., 2006).

Theorem 1 (Laplace mechanism). *Let \mathcal{M} be an algorithm with ℓ_1 sensitivity Δ_α that maps datasets d to \mathbb{R}^n . The Laplace mechanism $\mathcal{M}(d) + \xi$, with $\xi \sim \text{Lap}(\Delta_\alpha/\varepsilon)^n$, attains ε -differential privacy.*

3 Internalizing global sensitivity methods into constrained optimization

The direct application of Theorem 1 to the optimal optimization solution may produce a result that violates the problem constraints. This section introduces a suitable transformation of problem (1) into a stochastic chance-constrained problem that internalizes the global sensitivity methods to establish both privacy and constraint feasibility guarantees. This section first discusses the Laplace mechanism and then extends the results to the Gaussian mechanism.

Consider a random perturbation $\xi \in \mathbb{R}^p$ calibrated to Laplace distribution $\mathbb{P}_\xi = \text{Lap}(\Delta_\alpha/\varepsilon)^p$ for some arbitrary dimension p , and assume that the solution z depends on the realization of ξ as

$$z(\xi) = \tilde{z} + f(\xi) = \tilde{z} + Z\xi, \tag{2}$$

where $\tilde{z} \in \mathbb{R}^n$ is the expected value of the solution with respect to distribution \mathbb{P}_ξ and $Z\xi$ is the linear functional recourse with recourse decision $Z \in \mathbb{R}^{n \times p}$, which is used to adjust the expected solution to any realization of ξ . Therefore, any query made over $z(\xi)$ will constitute the expected and random components. To provide privacy guarantees, the random component is required to be independent from data d . This can be achieved by enforcing additional, query-specific, constraints \mathcal{Q} on the recourse Z . While the framework can accommodate the general class of linear queries over solution $z(\xi)$, for ease of presentation, this work focuses on identity and sum queries.

Definition 1 (Identity query). This query releases a specified subset of solution $z(\xi)$. Consider a random perturbation $\xi \in \mathbb{R}^n$ and a diagonal matrix $I \in \mathbb{R}^{n \times n}$, such that

$$\xi_i = \begin{cases} \text{Lap}(\Delta_\alpha/\varepsilon), & I_{ii} = 1, \\ 0, & \text{otherwise.} \end{cases} \quad I_{ii} = \begin{cases} 1, & \text{if } i^{\text{th}} \text{ element of vector } z(\xi) \text{ is subject to release,} \\ 0, & \text{otherwise.} \end{cases}$$

The identity query release is thus $Iz(\xi) = I\tilde{z} + IZ\xi$ for $Z \in \mathbb{R}^{n \times n}$. The random component $IZ\xi$ is made independent from the dataset d if the recourse decision Z is constrained as follows

$$Z \in \mathcal{Q}(I) \triangleq \{Z \mid Z \circ I = I, Z \circ (I - \text{diag}(I)\mathbb{1}_n^\top) = \mathbb{0}_{n \times n}\},$$

$$\text{which yields } Iz(\xi) = \begin{cases} \tilde{z}_i + \xi_i, & \text{if } I_{ii} = 1, \\ 0, & \text{otherwise.} \end{cases}$$

Definition 2 (Sum query). This query releases p sum statistics over non-intersecting subsets of $z(\xi)$. Consider a random perturbation $\xi \in \mathbb{R}^p$ and a matrix $S \in \mathbb{R}^{p \times n}$, such that

$$S_{ij} = \begin{cases} 1, & \text{if element } z_j(\xi) \text{ participates in sum statistic } i, \\ 0, & \text{otherwise.} \end{cases}$$

The sum query releases $Sz(\xi) = S\tilde{z} + SZ\xi$ for $Z \in \mathbb{R}^{n \times p}$. The random component $SZ\xi$ is made independent from the dataset d if the recourse decision Z is constrained as follows

$$Z \in \mathcal{Q}(S) \triangleq \{Z \mid SZ = \text{diag}(\mathbb{1}_p)\},$$

which yields $Sz(\xi) = S\tilde{z} + \xi$.

To produce random solutions to (1), function (2) is optimized using the following stochastic program

$$\underset{\tilde{z}, Z \in \mathcal{Q}}{\text{minimize}} \quad \mathbb{E}^{\mathbb{P}_\xi} [c(\tilde{z} + Z\xi)] \quad (3a)$$

$$\text{subject to} \quad \mathbb{P}_\xi [A(\tilde{z} + Z\xi) \leq b] \geq 1 - \eta, \quad (3b)$$

$$G(\tilde{z} + Z\xi) = d \quad \mathbb{P}_\xi\text{-a.s.,} \quad (3c)$$

which optimizes \tilde{z} and Z by anticipating all realizations of the random variable ξ . This problem minimizes the expected value of the convex cost function (3a) with respect to the random variable ξ . The problem constraints are given by a set of probabilistic constraints. The joint chance constraint (3b) requires the satisfaction of the inequality constraints with a *prescribed* probability $1 - \eta$, specified by the curator of problem (3). The almost sure constraint (3c) requires the equality constraints to hold with probability 1. Note that, if problem (3) is infeasible, it follows that the privacy parameters α and ε are too strong for the feasibility requirement η .

As the recourse of problem (3) amounts to finitely-dimensional linear functions, objective function (3a) and chance constraint (3b) admit computationally tractable reformulations (Ben-Tal et al., 2009) (additional details will be given in Section 4). The almost sure constraint (3c) includes a random variable and, therefore, satisfying it is computationally intractable. However, it can be equivalently reformulated using the following set of equations:

$$G\tilde{z} = d, \quad GZ = \mathbb{0}. \quad (4)$$

If variables \tilde{z} and Z are subject to (4), their optimal solution satisfies the equality constraint (3c) for any realization of ξ . The structural properties of G restrict the set of potential queries and a query is said to be implementable if there exists $Z \in \mathcal{Q}$ such that $GZ = \mathbb{0}$ holds.

Example (Flow conservation constraint). Assume $G \in \mathbb{R}^{\ell \times n}$ represents the incidence matrix of a fully connected graph \mathcal{G} (its rank is $n - 1$) and that $Gz = d$ represents a flow conservation constraint. Consider an identity query $Iz(\xi) = I\tilde{z} + IZ\xi$ and $Z \in \mathcal{Q}(I)$ as in Definition 1. The identity query is implementable if $\text{Tr}[I] < n$, i.e., not all elements of Z are constrained by $\mathcal{Q}(I)$ and $GZ = \mathbb{0}$ holds.

The constraint $GZ = \mathbb{0}$ plays a critical role: it balances the perturbation between the released and non-disclosed variables. As a result, the query should leave enough degree of freedom to satisfy the equality constraint. This limitation is solely induced by the need to preserve the satisfaction of the equality constraint and it is not seen as a limiting factor for many applications (see Section 6).

Algorithm 1: Private identity query (PIQ)

- 1 **Input:** $d, \Delta_\alpha, \varepsilon, \eta, I$
 - 2 $(\hat{z}, \hat{Z}) \leftarrow \text{Solve (3) for } Z \in \mathcal{Q}(I)$
 - 3 $\hat{\xi} \leftarrow \text{Sample from } \text{Lap}(\Delta_\alpha/\varepsilon)^n$
 - 4 Compute solution to (1) as $\hat{z} = \hat{z} + \hat{Z}\hat{\xi}$
 - 5 **Release:** $I\hat{z}$
-

Algorithm 2: Private sum query (PSQ)

- 1 **Input:** $d, \Delta_\alpha, \varepsilon, \eta, S$
 - 2 $(\hat{z}, \hat{Z}) \leftarrow \text{Solve (3) for } Z \in \mathcal{Q}(S)$
 - 3 $\hat{\xi} \leftarrow \text{Sample from } \text{Lap}(\Delta_\alpha/\varepsilon)^p$
 - 4 Compute solution to (1) as $\hat{z} = \hat{z} + \hat{Z}\hat{\xi}$
 - 5 **Release:** $S\hat{z}$
-

Private identity query (PIQ) algorithm The procedure is summarized in Algorithm 1, which takes as inputs the dataset d , the ℓ_1 -sensitivity of the identity query, the privacy ε and feasibility η requirements, the known covariance Σ , and the query specification I . Upon receiving the optimal chance-constrained solution (line 2), the algorithm draws a sample from the Laplace distribution (line 3) and computes a $(1 - \eta)$ -feasible solution for problem (1) (line 4). The algorithm returns an ε -differentially private identity query which satisfies problem (1) constraints with probability $(1 - \eta)$.

Theorem 2 (ε -differentially PIQ). *Algorithm 1 is ε -differentially private, i.e.,*

$$\mathbb{P}[I(\hat{z}(d) + \hat{Z}(d)\xi) = O] \leq \mathbb{P}[I(\hat{z}(d') + \hat{Z}(d')\xi) = O] \exp(\varepsilon)$$

for any two α -neighboring datasets d and d' and output solutions O .

Private sum query (PSQ) algorithm The procedure is summarized in Algorithm 2, which differs from Algorithm 1 by the query specification S and the noise dimension.

Theorem 3 (ε -differentially PSQ). *Algorithm 2 is ε -differentially private, i.e.,*

$$\mathbb{P}[S(\hat{z}(d) + \hat{Z}(d))\xi = O] \leq \mathbb{P}[S(\hat{z}(d') + \hat{Z}(d'))\xi = O] \exp(\varepsilon) \quad (5)$$

for any two α -neighboring datasets d and d' and output solutions O .

In addition to releasing a privacy-preserving answer with a probabilistic feasibility certificate, the proposed framework also allows to verify the feasibility of the sampled solution \hat{z} without incurring an additional privacy loss. Since the equality constraint holds due to (4), it is sufficient to verify the feasibility of constraint $A\hat{z} \leq b$ without accessing the original data d . The operation is private by post-processing immunity of differential privacy (Dwork et al., 2014).

Furthermore, since formulation (3) is independent from the distribution of the noise, the framework can accommodate other global sensitivity methods. In particular, the following result holds.

Theorem 4 (Gaussian algorithms). *Let $\delta, \varepsilon \in (0, 1)$ and let Δ_α^2 be the ℓ_2 -sensitivity. Algorithms 1 and 2 that calibrate $\xi \in \mathcal{N}(0, \sigma^2)$ to the Gaussian distribution with $\sigma \geq \Delta_\alpha^2 \sqrt{2 \ln(1.25/\delta)/\varepsilon}$ satisfy (ε, δ) -differential privacy.*

The relation between the feasibility requirement η and the privacy parameters ε and δ is implicit in the formulation of the chance-constrained problem: the variance of the noise affects the ability to satisfy the problem constraints within the feasibility requirement and vice-versa. To render this relation explicit, Appendix D discusses a version of Algorithms 1 and 2 that iterates lines 3 to 5 an optimal number T of times to guarantee the release of a feasible solution with probability $1 - \mu$, for some $0 < \mu < 1$.

Theorem 5 (Composition to improve feasibility). *Given feasibility requirement η , privacy parameter ε/T , and value $0 < \mu < 1$, the iterative variants of Algorithms 1 and 2 return an ε -differentially private solution that is feasible with probability at least $1 - \mu$ within $T = \lceil \frac{\log(\mu)}{\log(\eta)} \rceil$ steps.*

4 Reformulations and feasibility guarantees

The optimization problem (3) is intractable because it constitutes the optimization of a random variable. However, due to the convexity assumption on (1), linear functional recourse and known distribution of ξ , problem (3) admits tractable reformulations. There are several avenues to reformulate the joint chance constraint (3) with different degrees of conservatism in terms of expected optimality loss (Nemirovski and Shapiro, 2007). This work provides a conservative joint constraint satisfaction guarantee, using a *sample* approximation, and a less conservative individual constraint satisfaction guarantee, using an *analytic* reformulation. The objective function is reformulated as follows.

Objective function reformulation Consider a quadratic cost function with first- and second-order coefficients $c_1 \in \mathbb{R}^n$ and $c_2 \in \mathbb{R}^n$, and a *diagonal* covariance matrix $\Sigma = \mathbb{E}[\xi\xi^\top]$ with diagonal elements being equal to $\lambda = \Delta_\alpha/\varepsilon$. Then, the objective function (3a) reformulates as

$$\mathbb{E}^{\mathbb{P}_\xi} [c_1^\top (z + Z\xi) + (z + Z\xi)^\top \text{diag}(c_2)(z + Z\xi)] = c_1^\top z + z^\top \text{diag}(c_2)z + \text{Tr}[Z^\top \text{diag}(c_2)Z\Sigma],$$

which follows from the zero-mean distribution \mathbb{P}_ξ and the fact that $\mathbb{E}[\xi\xi^\top] = \Sigma$. Notice that for the affine cost functions, the analytic reformulation of (3a) reduces to $c_1^\top z$.

Sample approximation This approximation substitutes the chance constraint (3b) with a finite number of deterministic constraints, each enforced on a specific realization of random perturbation (Campi and Garatti, 2008; Alamo et al., 2010; Margellos et al., 2014). This work invokes the sample approximation method from (Margellos et al., 2014), which enforces (3b) on the vertices of the rectangular sample set extracted from distribution \mathbb{P}_ξ , i.e., for $\xi \in \mathbb{R}^p$

$$\mathbb{P}_\xi [(A(z + Z\xi) \leq b)] \geq 1 - \eta \equiv Az \leq b - AZ\hat{\xi}^v, \quad \forall v = 1, \dots, 2^p, \quad (6)$$

where $\hat{\xi}^v \in \mathbb{R}^{2^p}$ is the v^{th} vertex of the extracted sample set. Margellos et al. (2014) show that the joint constraint satisfaction is attained if the number of samples N from \mathbb{P}_ξ is properly chosen.

Theorem 6 (Margellos et al. (2014)). *The equivalence (6) holds with confidence $(1 - \beta)$ if the rectangular set is built upon S samples extracted from \mathbb{P}_ξ , with N at least as much as*

$$N \geq \left\lceil \frac{1}{\eta} \frac{e}{e-1} \left(2p - 1 + \ln \frac{1}{\beta} \right) \right\rceil.$$

Finally, notice that this approximation requires an additional input β to Algorithms 1 and 2 to accommodate the confidence level of the data curator.

Analytic reformulation The joint chance constraint (3b) can be rewritten as a union of individual chance constraints. For some vector $\bar{\eta} \in \mathbb{R}_+^m$ of individual constraint violation probabilities, the individual chance constraints can be reformulated exactly using second-order cone constraints (Ben-Tal and Nemirovski, 2001):

$$A_i z \leq b_i - f(1 - \bar{\eta}_i) \|A_i Z \Sigma^{1/2}\|_2, \quad \forall i = 1, \dots, m, \quad (7)$$

where $f(1 - \bar{\eta}_i)$ is a distribution-dependent safety parameter and $\Sigma^{1/2}$ is the lower triangular matrix resulting from the Cholesky factorization of Σ . For any symmetric and unimodal distribution of ξ , $f(1 - \bar{\eta}_i)$ amounts to $(2/9\bar{\eta}_i)^{1/2}$ if $0 \leq \bar{\eta}_i \leq 1/6$ (see the result from Van Parys et al. (2016)). For the Gaussian distribution of ξ , $f(1 - \bar{\eta}_i)$ amounts to the inverse CDF of the standard Gaussian distribution at $(1 - \bar{\eta}_i)$ -quantile (Ben-Tal and Nemirovski, 2001). Observe that, for the fixed parameter $\bar{\eta}_i$, the last term in the right-hand side of (7) is a safety margin, which reduces the feasible space of the original problem (1) to guarantee individual constraint feasibility for $(1 - \bar{\eta}_i)$ realizations of ξ .

If $\mathbb{1}^\top \bar{\eta} \leq \eta$ holds, the individual chance constraints guarantee joint constraint satisfaction probability η . Yet, finding the optimal value $\bar{\eta}$ is an NP-hard problem (Xie et al., 2019). Section 6, shows that, for small problem instances, the choice $\bar{\eta} = \eta$ results in the desired joint constraint satisfaction while providing a significantly less conservative solution than the sample approximation.

5 Variance-aware differentially private algorithms

For many systems governed by the solution of problem (1), e.g. energy networks, it is important to control the impact of the differentially private solutions on the optimality loss (e.g., extra supply cost) and the variance of the state variables (e.g., supply and flow allocations). This section extends Algorithms 1 and 2 to provide a minimal variance solution without affecting the privacy guarantees.

Minimal variance of optimality loss The chance-constrained problems of Algorithms 1 and 2 optimize against the expected value of the cost function. Its solution provides the estimate of the expected optimality loss relative to the solution of problem (1). The worst-case outcome of the

optimality loss, however, may significantly exceed the expected value. A trade-off between the expected and worst-case outcomes can be attained by controlling the variance of the optimality loss.

As the value of the cost function of problem (1) is deterministic, it is sufficient to control the variance of (3a) to attain the desired result. For a linear cost function, the variance admits a convex expression $\text{Var}[c_1^\top(z + Z\xi)] = \text{Tr}[Z^\top \text{diag}(c_1)\text{diag}(c_1)Z\Sigma]$ in recourse variable Z . Therefore, it can be minimized by optimizing, instead, the following objective function

$$\underset{z, Z \in \mathcal{Q}}{\text{minimize}} \quad (1 - \varphi)\mathbb{E}^{\mathbb{P}_\xi}[c_1^\top(z + Z\xi)] + \varphi \left\| \Sigma^{1/2} Z^\top c_1 \right\|_2, \quad (8)$$

which optimizes the trade-off between the expected value and the standard deviation of the cost function for some factor $\varphi \in [0, 1]$. Thus, varying the factor φ establishes a Pareto frontier between the optimality loss and its variance. Since the recourse decision Z is subject to query-specific constraints \mathcal{Q} , the results of Theorems 2 and 3 hold. Finally, the variance of the non-affine cost functions does not permit convex formulations and is not considered in this paper.

Minimal variance of optimization variables The variance of the optimization solution $z(\xi) = z + Z\xi$ admits a convex expression $\text{Var}[z(\xi)] = \text{Tr}[Z^\top \Sigma Z]$ in Z . Therefore, it can be controlled by optimizing the recourse decision Z using the following objective function

$$\underset{z, Z \in \mathcal{Q}}{\text{minimize}} \quad (1 - \varphi)\mathbb{E}^{\mathbb{P}_\xi}[c(z + Z\xi)] + \varphi \left\| Z \Sigma^{1/2} \mathbf{1} \right\|_2, \quad (9)$$

which finds the optimal trade-off between the expected cost and the standard deviation of the optimization variables for some factor $\varphi \in [0, 1]$. Since the optimal recourse is still guided by the query-specific constraints, the privacy guarantees provided by Theorems 2 and 3 are preserved.

6 Experiments

Problem description The proposed framework is applied to the energy resource allocation problem using a set of benchmark networks from (Coffrin et al., 2018). The problem goal is to compute the cost-optimal supply allocations across the network to satisfy nodal demands while respecting the supply and network limits. The problem is described by an undirected graphs $\mathcal{G}(N, E)$ with a set of nodes N and a set of edges E , connecting those nodes. The graph typology is represented by the weighted Laplacian matrix B formed from non-negative edge weights $\beta \in \mathbb{R}_+^{|E|}$. The nodal supply $p \in \mathbb{R}_+^{|N|}$ is allocated in the network to meet nodal demand $d \in \mathbb{R}_+^{|N|}$. The flow along the edges is modeled considering a vector of nodal potentials $\theta \in \mathbb{R}^{|N|}$, their difference is proportional to the network flows, i.e., the flow in edge ℓ amounts to $f_\ell(\theta) = \beta_\ell(\theta_{s(\ell)} - \theta_{r(\ell)})$, $\forall \ell \in E$, with operators $s(\ell)$ and $r(\ell)$ returning the sending and receiving nodes of edge ℓ , respectively. Finally, the nodal supply incurs costs computed by function $c : \mathbb{R}^{|N|} \mapsto \mathbb{R}$. This allocation problem gives rise to the following optimization

$$\underset{p, \theta}{\text{minimize}} \quad c(p) \quad (10a)$$

$$\text{subject to} \quad B\theta = p - d \quad (10b)$$

$$\underline{p} \leq p \leq \bar{p} \quad (10c)$$

$$\underline{f} \leq f(\theta) \leq \bar{f}. \quad (10d)$$

The objective function minimizes the total supply cost, while the equality constraint balances nodal demand, supply, and net flow injection. The inequality constraints respect the minimum and maximum nodal supply and the network flow limits $\underline{p}, \bar{p} \in \mathbb{R}_+^{|N|}$, $\underline{f} \in \mathbb{R}_-^{|E|}$, $\bar{f} \in \mathbb{R}_+^{|E|}$. A rearrangement of the terms in (10b)-(10d) makes the problem representable in the form expressed by problem (1), thus its chance-constrained counterpart is achieved as detailed in Sections 3 and 4.

The experiments concern the identity and sum queries made over the subset of nodal supplies p and make use of the ℓ_1 -sensitivity Δ_α of vector p on the two α -indistinguishable datasets d and d' . Consider the optimal supply allocations \hat{p} and \hat{p}' obtained, respectively, on datasets d and d' .

Proposition 1. $\Delta_\alpha = \|\hat{p} - \hat{p}'\|_1 \leq \alpha$.

Experimental setup The experiments are organized as follows. For every network instance, the variable limits are fixed, while cost coefficients and nodal demands are i.i.d. drawn from the following uniform distributions $c_1 \sim U(1, 3)$, $c_2 \sim U(1/10, 3/10)$, and $d \sim U(1/2, 1)$. The results are thus reported for 100 independent simulation runs. The identity and sum queries are made over an arbitrary set of 30% of nodal supplies, which is sampled at every simulation run. The privacy loss parameter ϵ is set to 1 and the indistinguishability parameter α is set to 0.1 for identity queries and 0.5 for sum queries. As ℓ_1 -sensitivity Δ_α is bounded by α , random perturbations thus obey the Laplace distribution $\text{Lap}(\alpha)$. The feasibility requirements for the joint and individual constraint satisfaction are set uniformly at $\eta = \bar{\eta} = 2.5\%$, and the out-of-sample empirical constraint violation probability is obtained for 1000 samples at every simulation run.

Privacy-preserving algorithms The algorithm abbreviations PIQ and PSQ are appended by `-a` or `-s` to indicate whether the chance constraints are reformulated, respectively, analytically or by samples (Section 4). They are compared with the output perturbation OP algorithm, which adds noise to the query answer. The OP solution is said to be feasible if problem (1) returns a feasible solution for the fixed solution of the OP algorithm.

Implementation The simulations were carried out using the standard PC with Intel Core i5 3.4 GHz processor and 8 GB memory. Solving optimization problems with the analytic reformulation requires less than a few seconds on average, whereas the sample approximation of the chance constraints requires by at most 78 seconds on average. The optimization models were implemented in the Julia Language and the source code can be accessed at https://github.com/wdvorkin/DP_CO_FG.

Algorithm comparison The algorithms are compared in terms of their ability to release private queries while satisfying the feasibility requirement. Table 1 summarizes the results for identity query answers obtained on several networks differing by the number of variables (n) and constraints ($|\mathcal{Z}|$). The results indicate that the OP algorithm returns private answers that violate the problem constraints at a far greater rate than the one imposed by the requirement η . Additionally, its performance degrades with the increase of the problem size. The application of PIQ-a, on the other hand, provides formal guarantees for the individual constraint satisfaction. These guarantees suffice to attain the desired feasibility requirement for smaller network instances. However, with an increasing network size, the probability of violating multiple constraints increases, and the average PIQ-a feasibility performance reduces. To guarantee the joint constraint satisfaction within the prescribed probability $1 - \eta$, the PIQ-s uses a sample approximation. While the guarantees are attained, notice that (last four columns of the table) this algorithm generates solutions with larger optimality loss than those generated by PIQ-a, reflecting the discussion in Section 5.

Next, Table 2 reports the results for the sum queries made over the largest test case `118_ieee`. These sum queries return a single aggregated statistic for the subset of selected nodes (first row of the table), or return the sums over 3, 6, or 9 partitions of the selected nodes. A single statistic requires one perturbation, which is accommodated by all algorithms in a feasible manner. With an increasing number of statistics, however, the differences between OP and PSQ algorithms are clearly observed.

Variance-aware differentially private optimization The last experiments show the ability of the chance-constrained framework to control the variance of the optimization results by means of Equations (8) and (9). Due to the inherent dependency between the optimality loss and the cost values, the results are given for different degrees of sparsity (\bar{c}) of supply cost among network nodes. Figure 1 illustrates the results for the PSQ-a algorithm releasing 9 sum statistics for the `118_ieee` case and for the various assignments of the trade-off parameter $\varphi \in [0, 1]$. The left plot shows that independently of cost sparsity, the algorithm can produce a differentially private output at zero variance of the optimality loss. The right plot demonstrates the drastic reduction of the overall solution variance $\text{Var}[z(\xi)] = \text{Tr}[\mathbf{Z}^\top \Sigma \mathbf{Z}]$, almost to the $\text{Tr}[\Sigma]$ total variance of the 9 random perturbations. Both results, however, require larger conservatism of the solution in terms of optimality loss.

7 Related work

There is a large body of work on differentially private algorithms for convex optimization in the context of empirical risk minimization (ERM) problems. Output perturbation algorithms (Chaudhuri and Monteleoni, 2009; Rubinstein et al., 2012) focus on adding the noise to the optimization results.

Table 1: Identity query summary for 100 network data samples

Case ID	$n \times \mathcal{Z} $	Empirical constraint violation $\mathbb{P}[\hat{z} \notin \mathcal{Z}] [\%]$						Optimality loss $\Delta c [\%]$			
		OP		PIQ-a		PIQ-s		PIQ-a		PIQ-s	
		mean	std	mean	std	mean	std	mean	std	mean	std
3_lmbd	6×17	29.7	23.07	0.64	0.34	0.27	0.31	3.42	3.55	5.72	7.64
5_pjm	10×29	18.32	22.94	0.39	0.41	0.12	0.3	1.22	2.07	2.04	3.03
14_ieee	28×84	52.24	26.85	1.48	0.78	0.27	0.25	1.55	1.33	3.45	2.88
39_epri	78×211	95.56	4.69	4.86	1.32	0.49	0.35	2.17	0.81	4.7	1.68
57_ieee	114×333	98.59	1.91	7.17	1.50	1.28	1.06	2.4	0.78	5.51	5.06
118_ieee	236×728	99.99	0.02	14.35	2.06	1.51	0.47	2.46	0.56	4.89	1.20

Table 2: Sum query summary for 100 network data samples

queries #	Empirical constraint violation $\mathbb{P}[\hat{z} \notin \mathcal{Z}] [\%]$						Optimality loss $\Delta c [\%]$			
	OP		PSQ-a		PSQ-s		PSQ-a		PSQ-s	
	mean	std	mean	std	mean	std	mean	std	mean	std
1	0.00	0.00	0.00	0.00	0.00	0.00	0.00	0.00	0.00	0.00
3	0.62	0.03	0.00	0.00	0.00	0.00	0.07	0.04	0.12	0.11
6	16.48	20.2	1.39	0.84	0.2	0.24	0.58	0.32	1.81	0.82
9	59.83	23.6	4.94	1.11	1.00	0.92	2.36	1.01	13.35	7.31

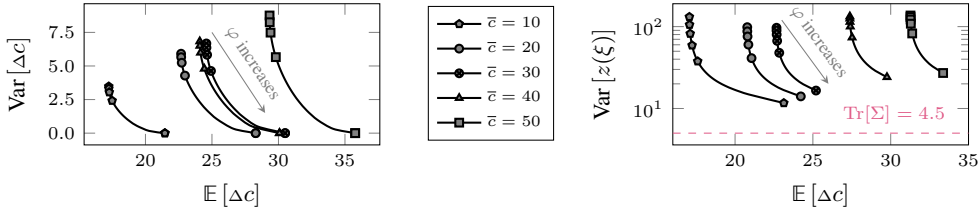


Figure 1: Trade-offs: expected value of optimality loss vs. variance (left) and vs. variance of optimization solution (right). The results are given for $c_1 \sim U[1, \bar{c}]$ and averaged over 100 runs.

Objective perturbation algorithms (Chaudhuri et al., 2011) perturb the optimization objective and perform well for smooth loss functions. Exponential sampling algorithms (McSherry and Talwar, 2007; Bassily et al., 2014) rely on an evaluation function to select a candidate output, while achieving $(\varepsilon, 0)$ -differential privacy that may be difficult to implement due to the exponential nature of evaluation function. Finally, noisy stochastic gradient descent (SGD) algorithms (Abadi et al., 2016; Song et al., 2013; Bassily et al., 2014; Wang et al., 2015) provide a privacy-preserving version of SGD that can be combined with accountant methods to provide tight bounds. All these algorithms, however, are meant for a particular class of *unconstrained* or *regularized* convex optimization problems and do not focus on reporting solutions that must satisfy problem constraints.

The contributions on differentially private *constrained* convex optimization for generic decision-making problems are much more sparse. Gupta et al. (2010) studied differential privacy in combinatorial optimization problems and derived information-theoretic bounds on the task utility. Hsu et al. (2014) proposed to solve linear programs privately using a differentially private variant of the multiplicative weights mechanism. Han et al. (2014) focused on a particular class of convex optimization problems whose objective function is piecewise affine, with the possibility of including linear inequality constraints. Fioretto et al. (2020) proposed a private data-release mechanism relying on projections to restore the feasibility of the violated constraints due to input perturbation. Finally, Muñoz et al. (2019) developed a differentially private algorithm for a class of linear programs that solely include the inequality constraints whose right-hand side contains sensitive data. The work relies on the input perturbation of the inequality right-hand sides to achieve (ε, δ) -differential privacy.

There are also differential privacy proposals for the distributed convex optimization. A privacy-preserving version of the alternating direction method of multipliers (Boyd et al., 2011) has been studied in the context of the unconstrained ERM problem (Zhang and Zhu, 2016; Ding et al., 2019) and constrained energy resource allocation problem (Dvorkin et al., 2019). Han et al. (2016) proposed a

private distributed projected gradient descent algorithm for constrained convex optimization problems. This collection of work, however, minimizes the privacy leakage by acting on the information exchanged by agents during the coordination process and does not provide privacy guarantees for the release of optimization solution.

8 Conclusion

The paper proposed a novel framework to release privacy-preserving solutions of constrained convex optimization problems that contain complex feasibility constraints. The framework relies on a combination of differential privacy and stochastic optimization theory and provides the foundations for two algorithms answering privacy-preserving identity and sum queries over the optimization solutions. The feasibility guarantees were studied for both individual and joint constraint satisfaction and the paper examined the trade-off between the expected and the worst-case errors by controlling the variance of the solutions and the optimality loss. Finally, the proposed framework was shown to outperform standard output perturbation algorithms on several energy benchmark networks.

References

- M. Abadi, A. Chu, I. Goodfellow, H. B. McMahan, I. Mironov, K. Talwar, and L. Zhang. Deep learning with differential privacy. In *Proceedings of the 2016 ACM SIGSAC Conference on Computer and Communications Security*, pages 308–318. ACM, 2016.
- J. M. Abowd. The us census bureau adopts differential privacy. In *Proceedings of the 24th ACM SIGKDD International Conference on Knowledge Discovery & Data Mining*, pages 2867–2867. ACM, 2018.
- T. Alamo, R. Tempo, and A. Luque. On the sample complexity of randomized approaches to the analysis and design under uncertainty. In *Proceedings of the 2010 American Control Conference*, pages 4671–4676, 2010.
- R. Bassily, A. Smith, and A. Thakurta. Private empirical risk minimization: Efficient algorithms and tight error bounds. In *2014 IEEE 55th Annual Symposium on Foundations of Computer Science*, pages 464–473, 2014.
- A. Ben-Tal and A. Nemirovski. *Lectures on modern convex optimization: analysis, algorithms, and engineering applications*, volume 2. Siam, 2001.
- A. Ben-Tal, L. El Ghaoui, and A. Nemirovski. *Robust optimization*, volume 28. Princeton University Press, 2009.
- S. Boyd, N. Parikh, E. Chu, B. Peleato, and J. Eckstein. Distributed optimization and statistical learning via the alternating direction method of multipliers. *Foundations and Trends® in Machine learning*, 3(1):1–122, 2011.
- M. C. Campi and S. Garatti. The exact feasibility of randomized solutions of uncertain convex programs. *SIAM Journal on Optimization*, 19(3):1211–1230, 2008.
- K. Chatzikokolakis, M. E. Andrés, N. E. Bordenabe, and C. Palamidessi. Broadening the scope of differential privacy using metrics. In *International Symposium on Privacy Enhancing Technologies Symposium*, pages 82–102. Springer, 2013.
- K. Chaudhuri and C. Monteleoni. Privacy-preserving logistic regression. In *Advances in Neural Information Processing Systems*, pages 289–296, 2009.
- K. Chaudhuri, C. Monteleoni, and A. D. Sarwate. Differentially private empirical risk minimization. *Journal of Machine Learning Research*, 12(Mar):1069–1109, 2011.
- C. Coffrin, R. Bent, K. Sundar, Y. Ng, and M. Lubin. Powermodels. jl: An open-source framework for exploring power flow formulations. In *2018 Power Systems Computation Conference (PSCC)*, pages 1–8, 2018.
- J. Ding, Y. Gong, C. Zhang, M. Pan, and Z. Han. Optimal differentially private ADMM for distributed machine learning. *arXiv preprint arXiv:1901.02094*, 2019.
- V. Dvorkin, P. Van Hentenryck, J. Kazempour, and P. Pinson. Differentially private distributed optimal power flow. *arXiv preprint arXiv:1910.10136*, 2019.
- C. Dwork, F. McSherry, K. Nissim, and A. Smith. Calibrating noise to sensitivity in private data analysis. In *TCC*, volume 3876, pages 265–284. Springer, 2006.

- C. Dwork, A. Roth, et al. The algorithmic foundations of differential privacy. *Foundations and Trends® in Theoretical Computer Science*, 9(3–4):211–407, 2014.
- F. Fioretto and P. Van Hentenryck. Differential privacy of hierarchical census data: An optimization approach. In *Principles and Practice of Constraint Programming - 25th International Conference, CP*, pages 639–655, 2019.
- F. Fioretto, T. W.K. Mak, and P. Van Hentenryck. Bilevel optimization for differentially private optimization, 2020.
- K. Fukuchi, Q. K. Tran, and J. Sakuma. Differentially private empirical risk minimization with input perturbation. In *International Conference on Discovery Science*, pages 82–90. Springer, 2017.
- A. Georghiou, D. Kuhn, and W. Wiesemann. The decision rule approach to optimization under uncertainty: methodology and applications. *Computational Management Science*, 16(4):545–576, 2019.
- A. Gupta, K. Ligett, F. McSherry, A. Roth, and K. Talwar. Differentially private combinatorial optimization. In *Proceedings of the twenty-first annual ACM-SIAM symposium on Discrete Algorithms*, pages 1106–1125. SIAM, 2010.
- S. Han, U. Topcu, and G. J. Pappas. Differentially private convex optimization with piecewise affine objectives. In *53rd IEEE conference on decision and control*, pages 2160–2166, 2014.
- S. Han, U. Topcu, and G. J. Pappas. Differentially private distributed constrained optimization. *IEEE Transactions on Automatic Control*, 62(1):50–64, 2016.
- J. Hsu, A. Roth, T. Roughgarden, and J. Ullman. Privately solving linear programs. In *International Colloquium on Automata, Languages, and Programming*, pages 612–624. Springer, 2014.
- C. Li, M. Hay, V. Rastogi, G. Miklau, and A. McGregor. Optimizing linear counting queries under differential privacy. In *Proceedings of the twenty-ninth ACM SIGMOD-SIGACT-SIGART Symposium on Principles of Database Systems*, pages 123–134. ACM, 2010.
- T. W. K. Mak, F. Fioretto, L. Shi, and P. Van Hentenryck. Privacy-preserving power system obfuscation: A bilevel optimization approach. *IEEE Transactions on Power Systems*, 35(2):1627–1637, March 2020.
- K. Margellos, P. Goulart, and J. Lygeros. On the road between robust optimization and the scenario approach for chance constrained optimization problems. *IEEE Transactions on Automatic Control*, 59(8):2258–2263, 2014.
- F. McSherry and K. Talwar. Mechanism design via differential privacy. In *48th Annual IEEE Symposium on Foundations of Computer Science (FOCS'07)*, pages 94–103, 2007.
- A. Muñoz, U. Syed, S. Vassilvitskii, and E. Vitercik. Private linear programming without constraint violations. 2019.
- A. Nemirovski and A. Shapiro. Convex approximations of chance constrained programs. *SIAM Journal on Optimization*, 17(4):969–996, 2007.
- B. I. Rubinstein, P. L. Bartlett, L. Huang, and N. Taft. Learning in a large function space: Privacy-preserving mechanisms for svm learning. *Journal of Privacy and Confidentiality*, 4(1):65–100, 2012.
- S. Song, K. Chaudhuri, and A. D. Sarwate. Stochastic gradient descent with differentially private updates. In *2013 IEEE Global Conference on Signal and Information Processing*, pages 245–248, 2013.
- B. P. Van Parys, P. J. Goulart, and D. Kuhn. Generalized gauss inequalities via semidefinite programming. *Mathematical Programming*, 156(1-2):271–302, 2016.
- Y.-X. Wang, S. Fienberg, and A. Smola. Privacy for free: Posterior sampling and stochastic gradient monte carlo. In *International Conference on Machine Learning*, pages 2493–2502, 2015.
- W. Xie, S. Ahmed, and R. Jiang. Optimized bonferroni approximations of distributionally robust joint chance constraints. *Mathematical Programming*, pages 1–34, 2019.
- T. Zhang and Q. Zhu. Dynamic differential privacy for ADMM-based distributed classification learning. *IEEE Transactions on Information Forensics and Security*, 12(1):172–187, 2016.
- F. Zhou, J. Anderson, and S. H. Low. Differential privacy of aggregated DC optimal power flow data. In *2019 American Control Conference (ACC)*, pages 1307–1314, 2019.

A Proof of Theorem 2

Proof. Without loss of generality, consider that the identity query $Iz(\xi) = I\tilde{z} + IZ\xi$ requires releasing first k items of $z(\xi)$, such that the diagonal matrix I can be described as

$$I = \begin{bmatrix} \text{diag}(\mathbb{1})_{k \times k} & \\ & \text{diag}(\mathbb{0})_{n-k \times n-k} \end{bmatrix},$$

the perturbation vector ξ as

$$\xi = [\xi_1, \dots, \xi_k, \mathbb{0}_{n-k}^\top]^\top,$$

and an arbitrary identity outcome O as

$$O = [O_1, \dots, O_k, \mathbb{0}_{n-k \times n-k}^\top]^\top.$$

Denote the optimal solution of the chance-constrained problem (3) by $\hat{\tilde{z}}$ and \hat{Z} . It needs to be shown that the ratio of probabilities that the algorithm returns the same outcome O on two α -indistinguishable input datasets d and d' is bounded by a constant $\exp(\varepsilon)$:

$$\mathbb{P}\left[I\left(\hat{\tilde{z}}(d) + \hat{Z}(d)\xi\right) = O\right] / \mathbb{P}\left[I\left(\hat{\tilde{z}}(d') + \hat{Z}(d')\xi\right) = O\right] \leq \exp(\varepsilon).$$

It follows that:

$$\begin{aligned} & \frac{\mathbb{P}\left[I\hat{\tilde{z}}(d) + I\hat{Z}(d)\xi = O\right] / \mathbb{P}\left[I\hat{\tilde{z}}(d') + I\hat{Z}(d')\xi = O\right]}{\mathbb{P}\left[\begin{bmatrix}\hat{\tilde{z}}_1(d) \\ \vdots \\ \hat{\tilde{z}}_k(d) \\ \mathbb{0}_{n-k}\end{bmatrix} + \begin{bmatrix}\xi_1 \\ \vdots \\ \xi_k \\ \mathbb{0}_{n-k}\end{bmatrix} = \begin{bmatrix}O_1 \\ \vdots \\ O_k \\ \mathbb{0}_{n-k}\end{bmatrix}\right] / \mathbb{P}\left[\begin{bmatrix}\xi_1 \\ \vdots \\ \xi_k \\ O_k\end{bmatrix} = \begin{bmatrix}O_1 \\ \vdots \\ O_k \\ \hat{\tilde{z}}_1(d)\end{bmatrix} - \begin{bmatrix}\hat{\tilde{z}}_1(d) \\ \vdots \\ \hat{\tilde{z}}_k(d)\end{bmatrix}\right]} \\ & \stackrel{(i)}{=} \frac{\mathbb{P}\left[\begin{bmatrix}\hat{\tilde{z}}_1(d') \\ \vdots \\ \hat{\tilde{z}}_k(d') \\ \mathbb{0}_{n-k}\end{bmatrix} + \begin{bmatrix}\xi_1 \\ \vdots \\ \xi_k \\ \mathbb{0}_{n-k}\end{bmatrix} = \begin{bmatrix}O_1 \\ \vdots \\ O_k \\ \mathbb{0}_{n-k}\end{bmatrix}\right] / \mathbb{P}\left[\begin{bmatrix}\xi_1 \\ \vdots \\ \xi_k \\ O_k\end{bmatrix} = \begin{bmatrix}O_1 \\ \vdots \\ O_k \\ \hat{\tilde{z}}_1(d')\end{bmatrix} - \begin{bmatrix}\hat{\tilde{z}}_1(d') \\ \vdots \\ \hat{\tilde{z}}_k(d')\end{bmatrix}\right]}{\mathbb{P}\left[\begin{bmatrix}\hat{\tilde{z}}_1(d') \\ \vdots \\ \hat{\tilde{z}}_k(d') \\ \mathbb{0}_{n-k}\end{bmatrix} + \begin{bmatrix}\xi_1 \\ \vdots \\ \xi_k \\ \mathbb{0}_{n-k}\end{bmatrix} = \begin{bmatrix}O_1 \\ \vdots \\ O_k \\ \mathbb{0}_{n-k}\end{bmatrix}\right] / \mathbb{P}\left[\begin{bmatrix}\xi_1 \\ \vdots \\ \xi_k \\ O_k\end{bmatrix} = \begin{bmatrix}O_1 \\ \vdots \\ O_k \\ \hat{\tilde{z}}_1(d')\end{bmatrix} - \begin{bmatrix}\hat{\tilde{z}}_1(d') \\ \vdots \\ \hat{\tilde{z}}_k(d')\end{bmatrix}\right]} \\ & \stackrel{(iii)}{=} \frac{\prod_{i=1}^k \exp\left(-\frac{\varepsilon \|O_i - \hat{\tilde{z}}_i(d)\|_1}{\Delta_\alpha}\right)}{\prod_{i=1}^k \exp\left(-\frac{\varepsilon \|O_i - \hat{\tilde{z}}_i(d')\|_1}{\Delta_\alpha}\right)} = \prod_{i=1}^k \exp\left(\frac{\varepsilon \|O_i - \hat{\tilde{z}}_i(d')\|_1 - \varepsilon \|O_i - \hat{\tilde{z}}_i(d)\|_1}{\Delta_\alpha}\right) \\ & \stackrel{(iv)}{\leq} \prod_{i=1}^k \exp\left(\frac{\varepsilon \|\hat{\tilde{z}}_i(d) - \hat{\tilde{z}}_i(d')\|_1}{\Delta_\alpha}\right) = \exp\left(\frac{\varepsilon \|\hat{\tilde{z}}(d) - \hat{\tilde{z}}(d')\|_1}{\Delta_\alpha}\right) \stackrel{(v)}{\leq} \exp(\varepsilon), \end{aligned}$$

where (i) is obtained from the primal feasibility condition $Z \in \mathcal{Q}(I)$, which enforces independence between the query random component and the sensitive data (see Definition 1), (ii) comes from rearranging the terms and removing zero entries, (iii) is due to the definition of the probability density function of the Laplace distribution, (iv) follows the reverse inequality of norms, and (v) is from the definition of ℓ_1 -sensitivity on α -indistinguishable input datasets. \square

B Proof of Theorem 3

Proof. Without loss of generality, consider that the sum query $Sz(\xi) = S(\tilde{z} + Z\xi)$ requires releasing p amount of sum statistics over non-intersecting subsets of $z(\xi)$. We thus need to show that the ratio of probabilities that the algorithm returns the same outcome $O \in \mathbb{R}^p$, i.e.,

$$\mathbb{P}\left[S(\hat{\tilde{z}}(d) + \hat{Z}(d))\xi = O\right] / \mathbb{P}\left[S(\hat{\tilde{z}}(d') + \hat{Z}(d'))\xi = O\right] \leq \exp(\varepsilon),$$

Algorithm 3: Private identity query (PIQ)

```

1 Input:  $d, \Delta_\alpha, \varepsilon, \eta, \mu, I$ 
2  $(\hat{z}, \hat{Z}) \leftarrow$  Solve (3) for  $Z \in \mathcal{Q}(I)$  and
    $\xi \sim \text{Lap}(T\Delta_\alpha/\varepsilon)$ 
3 for  $i = 1, \dots, T = \lceil \frac{\log(\mu)}{\log(\eta)} \rceil$  do
4    $\hat{\xi} \leftarrow$  Sample from  $\text{Lap}(T\Delta_\alpha/\varepsilon)^n$ 
5   Compute solution to (1) as  $\hat{z} = \hat{z} + \hat{Z}\hat{\xi}$ 
6   if  $A\hat{z} \leq b \vee i = T$  then
7     | Release:  $I\hat{z}$ 
8   end
9 end

```

Algorithm 4: Private sum query (PSQ)

```

1 Input:  $d, \Delta_\alpha, \varepsilon, \eta, \mu, S$ 
2  $(\hat{z}, \hat{Z}) \leftarrow$  Solve (3) for  $Z \in \mathcal{Q}(S)$  and
    $\xi \sim \text{Lap}(T\Delta_\alpha\varepsilon)$ 
3 for  $i = 1, \dots, T = \lceil \frac{\log(\mu)}{\log(\eta)} \rceil$  do
4    $\hat{\xi} \leftarrow$  Sample from  $\text{Lap}(T\Delta_\alpha/\varepsilon)^p$ 
5   Compute solution to (1) as  $\hat{z} = \hat{z} + \hat{Z}\hat{\xi}$ 
6   if  $A\hat{z} \leq b \vee i = T$  then
7     | Release:  $S\hat{z}$ 
8   end
9 end

```

is bounded by a constant $\exp(\varepsilon)$, where $S \in \mathbb{R}^{p \times n}$ and $\xi \in \mathbb{R}^p$ as in Definition 2. By denoting the optimal solution of the chance-constrained problem (3) by \hat{z} and \hat{Z} , this ratio writes as

$$\begin{aligned}
& \frac{\mathbb{P} [S\hat{z}(d) + S\hat{Z}(d)\xi = O]}{\mathbb{P} [S\hat{z}(d') + S\hat{Z}(d')\xi = O]} \stackrel{(i)}{=} \frac{\mathbb{P} [S\hat{z}(d) + \xi = O]}{\mathbb{P} [S\hat{z}(d') + \xi = O]} = \frac{\mathbb{P} [\xi = O - S\hat{z}(d)]}{\mathbb{P} [\xi = O - S\hat{z}(d')]} \\
& \stackrel{(ii)}{=} \frac{\prod_{i=1}^p \exp\left(-\frac{\varepsilon \|O_i - [S\hat{z}(d)]_i\|_1}{\Delta_\alpha}\right)}{\prod_{i=1}^p \exp\left(-\frac{\varepsilon \|O_i - [S\hat{z}(d')]_i\|_1}{\Delta_\alpha}\right)} = \prod_{i=1}^p \exp\left(\frac{\varepsilon \|O_i - [S\hat{z}(d')]_i\|_1 - \varepsilon \|O_i - [S\hat{z}(d)]_i\|_1}{\Delta_\alpha}\right) \\
& \stackrel{(iii)}{\leqslant} \prod_{i=1}^p \exp\left(\frac{\varepsilon \| [S\hat{z}(d)]_i - [S\hat{z}(d')]_i \|_1}{\Delta_\alpha}\right) = \exp\left(\frac{\varepsilon \|S\hat{z}(d) - S\hat{z}(d')\|_1}{\Delta_\alpha}\right) \stackrel{(iv)}{\leqslant} \exp(\varepsilon),
\end{aligned}$$

where (i) follows from the primal feasibility condition $Z \in \mathcal{Q}(S)$, which requires the random component of the sum query to be independent from the data (see Definition 2), (ii) is due to the definition of the probability density function of the Laplace distribution, (iii) follows from the reserve inequality of norms, and (iv) is from the ℓ_1 -sensitivity of the sum query, which is identical to the ℓ_1 -sensitivity of the identity query. \square

C Proof of Theorem 4

Similarly to the proofs of Theorems 2 and 3, the random components of the identity and linear queries can be shown to be independent from a datasets d and d' using the query specific feasibility conditions \mathcal{Q} . The reminder of the proof can be obtained by following the same steps of the proof in (Dwork et al., 2006, Appendix A), using notation $f(d) = I\hat{z}(d)$ for the identity query and $f(d) = S\hat{z}(d)$ for the sum query, where $f(\cdot)$ is the function of interest in (Dwork et al., 2006, Appendix A).

D Proof of Theorem 5

The iterative versions of the Algorithms 1 and 2 are provided, respectively, in Algorithms 3 and 4.

Proof. Consider the optimal solution (\hat{z}, \hat{Z}) returned by the chance constraint problem (line 2) and recall that the sampling process (lines 4–5) generates a $(1 - \eta)$ -feasible solution \hat{z} .

The new algorithms, illustrated in Algorithms 3 and 4, alternate this step with a constraint satisfaction test (line 6) for a maximum number of number T of times with the goal of generating a solution that satisfies the problem constraints with probability at least $1 - \mu$. Recall that the constraint satisfaction test, performed in line 6, can be achieved at no extra privacy loss (see Section 3 for details).

The repetition of such process can be seen as a sequence of independent Bernulli trials, each with probability $1 - \eta$ of success (i.e., \hat{z} satisfies the problem constraints) and probability η of failure (i.e.,

\hat{z} violates the problem constraints). Let FAIL be the discrete random variable describing the number of unsuccessful trials prior to the first success. Thus, FAIL is described by a Geometric random variable with probability $(1 - \eta)$. Formally, the goal is described by the following problem:

$$T \triangleq \arg \min_T \mathbb{P}(\text{FAIL} \geq T) \leq \mu,$$

requiring that the first success is seen after T trials with probability no larger than μ . Using a Geometric distribution of order T , it follows that:

$$\begin{aligned} \mathbb{P}(\text{FAIL} \geq T) &= 1 - \mathbb{P}(\text{FAIL} < T) \\ &= 1 - (1 - \eta) \sum_{i=1}^{T-1} \eta^i \\ &= 1 - (1 - \eta) \frac{1 - \eta^T}{1 - \eta} = \eta^T \end{aligned}$$

Thus, the solution to the minimizer above is for $T = \left\lceil \frac{\log(\mu)}{\log(\eta)} \right\rceil$. \square

E Proof of Proposition 1

Proof. The equality constraint (10b) requires the balance between the total supply and total demand. By construction, $\sum_{i \in N} [B \dot{\theta}]_i = 0$, thus from (10b) it follows

$$\begin{aligned} \sum_{i \in N} \dot{p}_i - \sum_{i \in N} d_i &= 0 \\ \sum_{i \in N} \dot{p}'_i - \sum_{i \in N} d'_i &= 0, \end{aligned}$$

therefore,

$$\sum_{i \in N} \dot{p}_i - \sum_{i \in N} \dot{p}'_i = \sum_{i \in N} d_i - \sum_{i \in N} d'_i \leq \alpha,$$

because the datasets d and d' differ by at most α in one entry, i.e., $\|d - d'\|_1 \leq \alpha$. Therefore, $\Delta_\alpha = \|\dot{p} - \dot{p}'\|_1 \leq \alpha$. \square

[Paper F] Differentially private optimal power flow for distribution grids

Authors:

V. Dvorkin, F. Fioretto, P. Van Hentenryck, P. Pinson and J. Kazempour.

Submitted to:

IEEE Transactions on Power Systems

Differentially Private Optimal Power Flow for Distribution Grids

Vladimir Dvorkin Jr., *Student member, IEEE*, Ferdinando Fioretto, Pascal Van Hentenryck, *Member, IEEE*, Pierre Pinson, *Fellow, IEEE*, and Jalal Kazempour, *Senior Member, IEEE*

Abstract—Although distribution grid customers are obliged to share their consumption data with distribution system operators (DSOs), a possible leakage of this data is often disregarded in operational routines of DSOs. This paper introduces a privacy-preserving optimal power flow (OPF) mechanism for distribution grids that secures customer privacy from unauthorised access to OPF solutions, e.g., current and voltage measurements. The mechanism is based on the framework of *differential privacy* that allows to control the participation risks of individuals in a dataset by applying a carefully calibrated noise to the output of a computation. Unlike existing private mechanisms, this mechanism does not apply the noise to the optimization parameters or its result. Instead, it optimizes OPF variables as affine functions of the random noise, which weakens the correlation between the grid loads and OPF variables. To ensure feasibility of the randomized OPF solution, the mechanism makes use of chance constraints enforced on the grid limits. The mechanism is further extended to control the optimality loss induced by the random noise, as well as the variance of OPF variables. The paper shows that the differentially private OPF solution does not leak customer loads up to specified parameters.

Index Terms—Data obfuscation, optimization methods, privacy

I. INTRODUCTION

THE increasing observability of distribution grids enables advanced operational practices for distribution system operators (DSOs). In particular, high-resolution voltage and current measurements available to DSOs allow for continuously steering the system operation towards an optimal power flow (OPF) solution [1]–[3]. However, when collected, these measurements expose distribution grid customers to privacy breaches. Several studies have shown that the measurements of OPF variables can be used by an adversary to identify the type of appliances and load patterns of grid customers [4], [5]. The public response to these privacy risks has been demonstrated by the Dutch Parliament’s decision to thwart the deployment of smart meters until the privacy concerns are resolved [6].

Although grid customers tend to entrust DSOs with their data in exchange for a reliable supply, their privacy rights are often disregarded in operational routines of DSOs. To resolve this issue, this paper augments the OPF computations with the preservation of customer privacy in the following sense.

V. Dvorkin Jr., P. Pinson, and J. Kazempour are with the Technical University of Denmark, Kgs. Lyngby, Denmark. F. Fioretto is with the Syracuse University, Syracuse, NY, USA. P. Van Hentenryck is with the Georgia Institute of Technology, Atlanta, GA, USA.

Definition 1 (Customer privacy). *The right of grid customers to be secured from an unauthorized disclosure of sensitive information that can be inferred from the OPF solution.*

To ensure this right, privacy needs to be rigorously quantified and guaranteed. Differential privacy (DP) [7] is a strong privacy notion that quantifies and bounds privacy risks in computations involving sensitive datasets. By augmenting the computations with a carefully calibrated *random noise*, a DP mechanism guarantees that the noisy results do not disclose the attributes of individual items in a dataset. Chaudhuri *et al.* [8] and Hsu *et al.* [9] introduced several mechanisms to solve optimization models while preventing the recovery of the input data from optimization results. These mechanisms apply noise to either the parameters or the results of an optimization. The applied noise, however, fundamentally alters the optimization problem of interest. Therefore, the direct application of these mechanisms to OPF problems has been limited. First, they may fail to provide a *feasible* solution for constrained optimization problems. To restore feasibility, they require an additional level of complexity such as the post-processing steps proposed in [10], [11]. Second, although these mechanisms provide bounds on the worst-case performance, they do not consider the *optimality loss* as a control variable. As a result, they cannot provide appropriate trade-offs between the expected and the worst-case mechanism performances. Finally, the previously proposed mechanisms overlook the impact of the noise on the *variance* of the optimization results. Hence, their direct application to OPF problems may lead to undesired overloads of system components [12].

Contributions: To overcome these limitations, this paper proposes a novel differentially private OPF mechanism that does not add the noise to the optimization parameters or to the results. Instead, it obtains DP by optimizing OPF variables as *affine functions* of the noise, bypassing the above-mentioned theoretical drawbacks. More precisely, the paper makes the following contributions:

1. The proposed mechanism produces a random OPF solution that follows a Normal distribution and guarantees (ϵ, δ) —differential privacy [7]. Parameters ϵ and δ , respectively, bound the multiplicative and additive differences between the probability distributions of OPF solutions obtained on adjacent datasets (i.e., differing in at most one load value). The mechanism is particularly suitable for protecting grid loads from unauthorized access to OPF solutions, as fine-tuned (ϵ, δ) values make randomized OPF solutions similar, irrespective of the used load dataset.

2. The mechanism enforces chance constraints on random OPF variables to guarantee solution feasibility for a given constraint satisfaction probability. This way, it does not require a post-processing step to restore OPF feasibility, as in [10] and [11]. Since the OPF variables are affine in the Gaussian noise, the chance constraints are reformulated into computationally efficient second-order cone constraints.
3. The mechanism enables the control of random OPF outcomes without weakening the DP guarantees. Using results from stochastic programming [13], the optimality loss induced by the noise is controlled using Conditional Value-at-Risk (CVaR) risk measure, enabling a trade-off between the expected and the worst-case performance. Furthermore, with a variance-aware control from [14], the mechanism attains DP with a smaller variance of OPF variables.

Broader Impact: Distribution OPF proposals have been around for at least a decade, though their adoption in real operations is complicated by the need of utilizing load datasets, which raises significant privacy concerns by many regulators worldwide. The adoption of the proposed mechanism, in turn, extends standard OPF models to enable a privacy-cognizant utilization¹ of this data, thus facilitating the digitization of the energy sector. The mechanism treats the DSOs as trustworthy parties and places them on the same ground with the digital service providers, e.g. Amazon, enabling the regulation and securing legal responsibility of the digitalized distribution grids under modern data protection and privacy standards, including the General Data Protection Rights (GDPR) in the European Union, the California Consumer Privacy Act (CCPA) and the New York Privacy Act (NYPA) in the United States. Moreover, the mechanism provides the means to hedge the financial risks of the DSOs by avoiding the cost incurred by privacy violations, such as legal costs, as it relies on a strong quantification of privacy and co-optimizes the joint cost of energy supply and privacy.

Related Work: Thanks to its strong privacy guarantees, DP has been recently applied to private OPF computations. In particular, the mechanism of Zhou *et al.* [15] releases aggregated OPF statistics, e.g., aggregated load, while ensuring the privacy for individual loads, even if all but one loads are compromised. The proposals by Fioretto *et al.* [10] and Mak *et al.* [11] provide a differentially private mechanism to release high-fidelity OPF datasets (e.g., load and network parameters) from real power systems while minimizing the risks of disclosing the actual system parameters. The mechanisms, however, are meant for the private release of aggregate statistics and input datasets and do not provide the OPF solution itself.

Private OPF computations have also been studied in a decentralized and distributed setting. Dvorkin *et al.* [16] designed a distributed OPF algorithm with a differentially private exchange of coordination signals, hence preventing the leakage of the sensitive information contained in the algorithm subproblems. Han *et al.* [17] proposed a privacy-aware distributed coordination scheme for electrical vehicle charging. The privacy frameworks in [16] and [17], however,

¹Note that privacy concerns a safe utilization of the data, not its storage, which falls within the field of cyber-security.

are not suitable for centralized computations and solely focus on the privacy leakage through the exchange of coordination signals. Moreover, to negate the privacy loss induced at every iteration, they require scaling the parameters of the random perturbation, thus involving larger optimality losses and poorer convergence. The centralized mechanisms proposed in this work, however, allow obtaining the private OPF solution in a single computation run. In distribution systems, Zhang *et al.* [18], among other proposals reviewed in [6], designed a privacy-aware optimization of behind-the-meter energy storage systems to prevent the leakage of consumption data from the smart meter readings. However, they disregard OPF feasibility of distribution systems, which has to be preserved in all circumstances.

Paper Organization: Following the preliminaries in Section II, Section III formalizes the privacy goals and provides an overview of the proposed solution. Section IV provides the formulation of the proposed privacy-preserving OPF mechanism and its properties, whereas Section V presents its extensions. Section VI provides numerical experiments and Section VII concludes. The proofs are relegated to the appendix.

II. PRELIMINARIES

A. Optimal Power Flow Problem

The paper considers a low-voltage radial distribution grid with controllable distributed energy resources (DERs). A DSO is responsible for controlling the DERs and supplying power from the high-voltage grid while meeting the technical limits of the grid. The grid is modeled as a graph $\Gamma(\mathcal{N}, \mathcal{L})$, where $\mathcal{N} = \{0, 1, \dots, n\}$ is the set of nodes and $\mathcal{L} = \mathcal{N} \setminus \{0\}$ is the set of lines connecting those nodes. The root node, indexed by 0, is a substation with a large capacity and fixed voltage magnitude $v_0 = 1$. The radial topology, depicted in Fig. 1, associates each node $i \in \mathcal{N}$ with the sets \mathcal{U}_i and \mathcal{D}_i of, respectively, upstream and downstream nodes, as well as with the set \mathcal{R}_i of nodes on the path to the root node.

Each node i is characterized by its fixed active d_i^p and reactive d_i^q power load and by its voltage magnitude $v_i \in [\underline{v}_i, \bar{v}_i]$. For modeling convenience, the voltage variables are substituted by $u_i = v_i^2$, $\forall i \in \mathcal{N}$. A controllable DER sited at node i outputs an amount of active $g_i^p \in [g_i^p, \bar{g}_i^p]$ and reactive $g_i^q \in [g_i^q, \bar{g}_i^q]$ power. Its costs are linear with a cost coefficient c_i . To model the relation between the active and reactive DER power output, the constant power factor $\tan \phi_i$ is assumed for each node i . The active and reactive power flows, f_ℓ^p and f_ℓ^q , $\forall \ell \in \mathcal{L}$, respectively, are constrained by the apparent power limit \bar{f}_ℓ , and each line is characterized by its resistance r_ℓ and reactance x_ℓ . The deterministic OPF model is formulated as:

$$\text{D-OPF: } \min_{g^\dagger, f^\dagger, u} \sum_{i \in \mathcal{N}} c_i g_i^p \quad (1a)$$

$$\text{s.t. } g_0^\dagger = \sum_{i \in \mathcal{D}_0} (d_i^\dagger - g_i^\dagger), \quad u_0 = 1, \quad (1b)$$

$$f_\ell^\dagger = d_\ell^\dagger - g_\ell^\dagger + \sum_{i \in \mathcal{D}_\ell} (d_i^\dagger - g_i^\dagger), \quad \forall \ell \in \mathcal{L}, \quad (1c)$$

$$u_i = u_0 - 2 \sum_{\ell \in \mathcal{R}_i} (f_\ell^p r_\ell + f_\ell^q x_\ell), \quad \forall i \in \mathcal{L}, \quad (1d)$$

$$(f_\ell^p)^2 + (f_\ell^q)^2 \leq \bar{f}_\ell^2, \quad \forall \ell \in \mathcal{L}, \quad (1e)$$

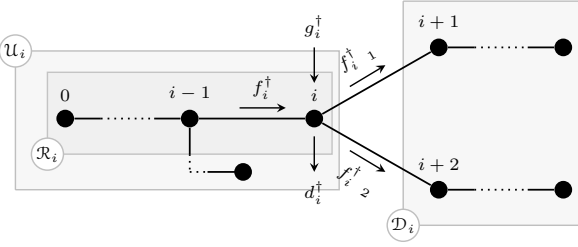


Fig. 1. Topology of the distribution grid relative to node i , $\dagger = \{p, q\}$.

$$\underline{g}_i^\dagger \leq g_i^\dagger \leq \bar{g}_i^\dagger, \forall i \in \mathcal{N}, \quad (1f)$$

$$\underline{v}_i^2 \leq u_i \leq \bar{v}_i^2, \forall i \in \mathcal{N} \setminus \{0\}, \quad (1g)$$

where superscript $\dagger = \{p, q\}$ indexes active and reactive power. The objective is to minimize the total operational cost subject to the OPF equations (1b)–(1d), that balance the grid based on the *LinDistFlow* AC power flow equations [19, equations (9)] for distribution grids, and grid limits (1e)–(1g). Equation (1b) requires the total mismatch between power generation and loads in the distribution grid to be compensated for by the power from the substation at the root node. Equation (1c) requires the balance between the power flow along every edge ℓ , power mismatch at the in-flow node ℓ as well as that at the downstream nodes. The last term in (1c) can be also rewritten as the sum of power flows in the adjacent downstream lines, but kept as it is in the interest of the subsequent derivations. Last, equation (1d) models the voltage drop along the path from the root node to the node of interest.

Although OPF equations (1b)–(1d) establish the affine relation between the OPF variables, which is necessary for the subsequent chance-constrained formulation, they neglect distribution grid losses. The losses, however, can be included in an affine manner using various linearization techniques, such as in [20], [21] and [22] to mention but a few examples.

B. Differential Privacy

The paper uses the framework of *differential privacy* [7] to quantify and control the privacy risks of the customer loads. It considers datasets $D \in \mathbb{R}^n$ as n -dimensional vectors describing the *active* load values, denoted by d_i for each node i . To protect the participation of the load in the i^{th} entry of the dataset, the following *adjacency relation* is introduced:

$$D \sim_{\beta} D' \Leftrightarrow \exists i \text{ s.t. } |d_i - d'_i| \leq \beta_i \text{ and } d_j = d'_j, \forall j \neq i,$$

where D and D' are two adjacent datasets, $\beta \in \mathbb{R}^n$ is a vector of positive real values, and values d_i and d'_i are the load values corresponding to customer i in D and D' , respectively. The adjacency relates two load vectors that differ in at most one item, at position i , by a value not greater than β_i .

If a mechanism satisfies the definition of differential privacy, it returns similar results on adjacent datasets in a probabilistic sense. This intuition is formalized in the following definition.

Definition 2 (Differential Privacy). *Given a value $\beta \in \mathbb{R}_+^n$, a randomized mechanism $\tilde{\mathcal{M}}: \mathcal{D} \rightarrow \mathcal{R}$ with domain \mathcal{D} and range*

\mathcal{R} is (ε, δ) -differential private if, for any output $s \subseteq \mathcal{R}$ and any two adjacent inputs $D \sim_{\beta} D' \in \mathbb{R}^n$

$$\mathbb{P}[\tilde{\mathcal{M}}(D) \in s] \leq e^{\varepsilon} \mathbb{P}[\tilde{\mathcal{M}}(D') \in s] + \delta,$$

where \mathbb{P} denotes the probability over runs of $\tilde{\mathcal{M}}$.

In the context of OPF problem (1), domain \mathcal{D} includes all feasible load datasets, mechanism \mathcal{M} denotes the OPF problem itself, and $\tilde{\mathcal{M}}$ is its randomized counterpart, and range \mathcal{R} denotes the feasible region of the OPF problem.

The level of privacy is controlled by DP parameters (ε, δ) . The former corresponds to the maximal multiplicative difference in distributions obtained by the mechanism on adjacent datasets, whereas the latter defines the maximal additive difference. Consequently, smaller values of ε and δ provide stronger privacy protection. Definition 2 extends the metric-based differential privacy introduced by Chatzikokolakis *et al.* [23] to control of *individual* privacy risks.

If a mechanism satisfies Definition 2, it features two important properties. First, by acting on adjacent datasets D and D' , it provides privacy for each item i *irrespective* of the properties of all remaining items in a dataset. Second, it is immune to the so-called side attacks, i.e., it ensures that even if an attacker acquires the data of all other users but i , when accessing the output $\tilde{\mathcal{M}}(D)$ of the differential private mechanism, it will not be able to infer the load value of user i up to differential privacy bounds ε and δ [24].

The differentially private design of any mechanism is obtained by means of randomization using, among others, Laplace or Gaussian noise for numerical queries and exponential noise for the so-called non-numerical events [24]. The DP requirements for an optimization problem are achieved by introducing a calibrated noise to the input data [9] or to the output or objective function of the mechanism itself [8]. Regardless of the strategy adopted to attain DP, the amount of noise to inject depends on the mechanism *sensitivity*. In particular, the L_2 -sensitivity of a deterministic mechanism \mathcal{M} on β -adjacent datasets, denoted by Δ^β , is defined as:

$$\Delta^\beta = \max_{D \sim_{\beta} D'} \|\mathcal{M}(D) - \mathcal{M}(D')\|_2.$$

This work employs the Gaussian mechanism, because the Gaussian noise allows for the exact analytic reformulation of chance constraints into tractable second-order cone constraints.

Theorem 1 (Gaussian mechanism [24]). Let \mathcal{M} be a mechanism of interest that maps datasets D to \mathbb{R}^n , and let Δ^β be its L_2 -sensitivity. For $\varepsilon \in (0, 1)$ and $\gamma^2 > 2 \ln(\frac{1.25}{\delta})$, the Gaussian mechanism that outputs $\tilde{\mathcal{M}}(D) = \mathcal{M}(D) + \xi$, with ξ noise drawn from the Normal distribution with 0 mean and standard deviation $\sigma \geq \gamma \frac{\Delta^\beta}{\varepsilon}$ is (ε, δ) -differentially private.

When the DP mechanism produces solutions to an optimization problem, it is also important to quantify the *optimality loss*, i.e., the distance between the optimal solutions of the original mechanism $\mathcal{M}(D)$ and its differentially private counterpart $\tilde{\mathcal{M}}(D)$ evaluated on the original dataset D .

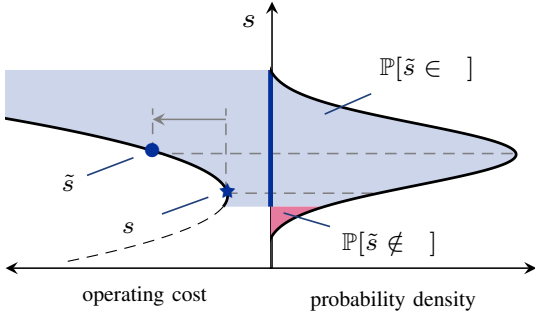


Fig. 2. Projections of OPF solutions onto operating cost and feasibility space.

III. PROBLEM STATEMENT

In the context of the underlying dispatch problem, the DSO collects a dataset $D = \{d_i^p\}_{i \in \mathcal{N}}$ of customer *sensitive* loads and dispatches the DER according to the solution of the OPF model (1). The OPF model acts as a mechanism $\mathcal{M} : D \mapsto s$ that maps the dataset D into an optimal OPF solution s^* . The solution is a tuple comprising generator set points $\{g_i^p, g_i^q\}_{i \in \mathcal{N}}$, power flows $\{f_\ell^p, f_\ell^q\}_{\ell \in \mathcal{L}}$, and voltages $\{u_i\}_{i \in \mathcal{N}}$, as depicted on the left plane in Fig. 2. However, the release of s^* poses a privacy threat: an adversary with access to the items in s^* could *decode* the customers activities [4], [5]. For instance, the voltage sags at a node of interest discloses the activity of residential customers (e.g., charging an electrical vehicle). Voltages and flows (currents) also encode information about the technology, production patterns, and other commercial data of industrial customers [10].

To minimize privacy risks, this work proposes a mechanism $\tilde{\mathcal{M}}$ for the DSO, which returns a feasible solution \tilde{s} at the expense of an optimality loss, as shown in Fig. 2. A non-trivial benefit of choosing \tilde{s} over s^* is that the former includes a particular perturbation of the optimal solution and thus carries less information about the real load data D . For instance, the sub-optimal solution can feature a more intensive deployment of expensive DERs instead of purchasing less expensive power from the high-voltage grid. To ensure that $\tilde{\mathcal{M}}$ returns a differentially private solution, \tilde{s} has to follow a carefully calibrated noise distribution, as depicted on the right plane in Fig. 2. In other words, the mechanism must satisfy Definition 2, i.e., on adjacent load datasets, it must output distributions that differ by at most ε and δ in multiplicative and additive terms, respectively. However, with smaller ε and δ , the variance of the OPF solutions and hence the probability of producing an infeasible solution increases. The mechanism thus needs to address this feasibility issue. Finally, the last desired property is the ability to control the induced optimality loss Θ in order to ensure cost-effective grid operations.

To provide differentially private OPF solutions, the work focuses on the randomization of active power flows as their sensitivities to grid loads can be directly upper-bounded by the load magnitudes in radial grids. Since the OPF equations (1b)–(1d) couple OPF variables, the randomization of power flows will also induce the randomization of reactive power flows and voltages. Therefore, the randomized OPF mechanism $\tilde{\mathcal{M}}$ is now seen as a mapping from a dataset D to the active power

flow solution f^p . Let $F^p \in \mathbb{R}^{|\mathcal{L}|}$ be a particular realization of the randomized active power flows. The privacy goal of this work is to ensure that $\tilde{\mathcal{M}}$ satisfies

$$D \sim_{\beta} D' : \mathbb{P}[\tilde{\mathcal{M}}(D) \in F^p] \leq e^{\varepsilon} \mathbb{P}[\tilde{\mathcal{M}}(D') \in F^p] + \delta, \text{ i.e.,}$$

the definition of (ε, δ) -DP on β -adjacent load datasets.

IV. DIFFERENTIALLY PRIVATE OPF MECHANISM

This section provides a mathematical description of mechanism $\tilde{\mathcal{M}}$ and details its application. Section IV-A describes the perturbation of generator outputs to attain the randomization of power flows, Section IV-B details the chance-constrained program that accommodates the perturbation in a feasible manner, and Section IV-C explains the mechanism application as well as its feasibility and privacy guarantees.

A. Random Perturbation of OPF Solutions

Consider a random perturbation $\xi \in \mathbb{R}^{|\mathcal{L}|}$ which obeys a Gaussian distribution $\mathcal{N}(0, \Sigma)$ with covariance matrix

$$\Sigma = \text{diag}([\sigma_1^2, \dots, \sigma_{|\mathcal{L}|}^2]) = \text{diag}(\sigma^2) \in \mathbb{R}^{|\mathcal{L}| \times |\mathcal{L}|}.$$

Throughout the paper, Σ , σ^2 , and σ are used interchangeably to discuss the perturbation parameters. The power flows are conditioned on perturbation ξ when the following affine policies are imposed on DERs and substation supplies:

$$\tilde{g}_i^p(\xi) = g_i^p + \sum_{\ell \in \mathcal{D}_i} \alpha_{i\ell} \xi_\ell - \sum_{\ell \in \mathcal{U}_i} \alpha_{i\ell} \xi_\ell, \quad \forall i \in \mathcal{N}, \quad (2a)$$

where $\tilde{g}_i^p(\xi)$ and g_i^p are, respectively, the random and nominal (mean) active power outputs, and $\alpha_{i\ell}$ is the portion of random perturbation ξ_ℓ provided by the supplier at node i , modeled as a free variable. The policies in (2a) are viable when the following balancing conditions are enforced:

$$\sum_{i \in \mathcal{U}_\ell} \alpha_{i\ell} = 1, \quad \sum_{i \in \mathcal{D}_\ell} \alpha_{i\ell} = 1, \quad \forall \ell \in \mathcal{L}, \quad (2b)$$

such that for each line ℓ , the upstream suppliers adjust their aggregated output by ξ_ℓ and the downstream DERs counterbalance this perturbation by ξ_ℓ , thus satisfying power balance.

The policies in (2) differ from those in stochastic dispatch models in [2], [3], [14], [25], [26], where the overall generator recourse compensates for the mismatch between grid loads and renewable forecast error realizations. However, since the affine nature of generator response remains similar, the proposed policy directly extends to balance renewable forecast errors.

To provide a succinct representation of the randomized OPF variables, consider a topology matrix $T \in \mathbb{R}^{|\mathcal{N}| \times |\mathcal{L}|}$ whose elements are such that:

$$T_{i\ell} = \begin{cases} 1, & \text{if line } \ell \text{ is downstream w.r.t. node } i, \\ -1, & \text{if line } \ell \text{ is upstream w.r.t. node } i \\ 0, & \text{otherwise.} \end{cases}$$

Consider also an auxiliary row vector $\rho_i^p = T_i \circ \alpha_i$ that returns a Schur product of i^{th} row of T and i^{th} row of α , and set $\rho_i^q = \rho_i^p \tan \phi_i$. If the grid DERs allow, the later can be relaxed to model variable DER power factors. Using this notation, the

perturbed OPF solution is modeled as the following set of random variables:

$$\tilde{g}_i^\dagger(\xi) = g_i^\dagger + \rho_i^\dagger \xi, \forall i \in \mathcal{N}, \quad (3a)$$

$$\tilde{f}_\ell^\dagger(\xi) = f_\ell^\dagger - \left[\rho_\ell^\dagger + \sum_{j \in \mathcal{D}_\ell} \rho_j^\dagger \right] \xi, \forall \ell \in \mathcal{L}, \quad (3b)$$

$$\begin{aligned} \tilde{u}_i(\xi) = u_i + 2 \sum_{j \in \mathcal{R}_i} [r_j (\rho_j^p + \sum_{k \in \mathcal{D}_j} \rho_k^p) + \\ x_j (\rho_j^q + \sum_{k \in \mathcal{D}_j} \rho_k^q)] \xi, \forall i \in \mathcal{L}, \end{aligned} \quad (3c)$$

where the randomized power flows \tilde{f}_i^\dagger are obtained by substituting generator policy (2a) into (1c), and randomized voltage magnitudes \tilde{u}_i are expressed by substituting \tilde{f}_i^\dagger into (1d), refer to Appendix A for details. Each variable is thus represented by its nominal component and its random component whose realization depends on ξ . Furthermore, the random components of power flows in (3b) and voltages (3c) also depend on the generator dispatch decisions ρ^\dagger . Therefore, by properly calibrating the parameters of ξ and finding the optimal dispatch decisions, the randomized OPF solution in (3) provides the required privacy guarantees (see Section IV-C, Theorem 2). However, there is yet no guarantee that the randomized OPF solution in (3) is feasible.

B. The Chance-Constrained Optimization Program

To obtain a feasible dispatch, the proposed mechanism uses a chance-constrained program which optimizes the affine functions in (3) to make OPF solution feasible for any realization of random variable ξ with a high probability. The chance-constrained program is obtained by substituting variables (3) into the base OPF model (1) and enforcing chance constraints on the grid limits. Its tractable formulation is provided in (5), which is obtained considering the following reformulations.

1) Objective Function Reformulation: The chance-constrained program minimizes the *expected* cost, which is reformulated as follows:

$$\mathbb{E}_\xi \left[\sum_{i \in \mathcal{N}} c_i \tilde{g}_i^p \right] = \mathbb{E}_\xi \left[\sum_{i \in \mathcal{N}} c_i (g_i^\dagger + \rho_i^\dagger \xi) \right] = \sum_{i \in \mathcal{N}} c_i g_i^p, \forall i \in \mathcal{N},$$

due to the zero-mean distribution of ξ .

2) Inner Polygon Approximation of the Quadratic Power Flow Constraints: The substitution of the random power flow variables in (3b) into the apparent power flow limit constraints (1e) results in the following expression

$$(\tilde{f}_\ell^p)^2 + (\tilde{f}_\ell^q)^2 \leq \bar{f}_\ell^2, \forall \ell \in \mathcal{L},$$

which exhibits a quadratic dependency on random variable ξ , for which no tractable chance-constrained reformulation is known. To resolve this issue, the above quadratic constraint is replaced by the inner polygon [22], [27], which writes as

$$\gamma_c^p \tilde{f}_i^p + \gamma_c^q \tilde{f}_i^q + \gamma_c^s \bar{f}_i \leq 0, \forall i \in \mathcal{L}, \forall c \in \mathcal{C}, \quad (4)$$

where $\gamma_c^p, \gamma_c^q, \gamma_c^s$ are the coefficients for each side c of the polygon. The cardinality $|\mathcal{C}|$ is arbitrary, but a higher cardinality brings a better accuracy. Equation (4) is not a relaxation but an inner convex approximation: if the power flow solution is feasible for (4), it is also feasible for the original quadratic constraint (1e).

Algorithm 1: DP CC-OPF mechanism $\tilde{\mathcal{M}}$

- 1 **Input:** $D, \varepsilon, \delta, \beta, \eta^g, \eta^u, \eta^f$
 - 2 Define covariance $\Sigma = f(\varepsilon, \delta, \beta)$ as per Theorem 2
 - 3 Solve $\dot{\mathcal{V}} \leftarrow \text{argmin}$ problem (5) using D and Σ
 - 4 Sample random perturbation $\hat{\xi} \sim \mathcal{N}(0, \Sigma)$
 - 5 Obtain final OPF solution from (3) using $\dot{\mathcal{V}}$ and $\hat{\xi}$
 - 6 **Release:** $\tilde{f}^\dagger(\hat{\xi}), \tilde{u}(\hat{\xi}), \tilde{g}^\dagger(\hat{\xi})$
-

3) Conic Reformulation of Linear Chance Constraints: For the normally distributed variable ξ with known moments, the chance constraint of the form $\mathbb{P}_\xi[\xi^\top x \leq b] \geq 1 - \eta$ is translated into a second-order cone constraint as [28, Chapter 4.2.2]:

$$z_\eta \|\text{std}(\xi^\top x)\|_2 \leq b - \mathbb{E}_\xi[\xi^\top x],$$

where $z_\eta = \Phi^{-1}(1 - \eta)$ is the inverse cumulative distribution function of the standard Gaussian distribution at the $(1 - \eta)$ quantile, and η is the constraint violation probability. Therefore, the individual chance constraints on the generation, voltage, and power flow variables are formulated in a conic form in (5c)–(5g), respectively. The resulting tractable formulation of the chance-constrained OPF program is as follows:

$$\text{CC-OPF: } \min_{\mathcal{V} = \{g^\dagger, f^\dagger, u, \rho^\dagger\}} \sum_{i \in \mathcal{N}} c_i g_i^p \quad (5a)$$

$$\text{s.t. Equations (1b) – (1d), (2b),} \quad (5b)$$

$$z_{\eta^g} \|\rho_i^\dagger \sigma\|_2 \leq \bar{g}_i^\dagger - g_i^\dagger, \forall i \in \mathcal{N}, \quad (5c)$$

$$z_{\eta^g} \|\rho_i^\dagger \sigma\|_2 \leq g_i^\dagger - \underline{g}_i^\dagger, \forall i \in \mathcal{N}, \quad (5d)$$

$$\begin{aligned} z_{\eta^u} \left\| \left[\sum_{j \in \mathcal{R}_i} [r_j (\rho_j^p + \sum_{k \in \mathcal{D}_j} \rho_k^p) + x_j (\rho_j^q + \sum_{k \in \mathcal{D}_j} \rho_k^q)] \right] \sigma \right\|_2 \\ \leq \frac{1}{2} (\bar{u}_i - u_i), \forall i \in \mathcal{L}, \end{aligned} \quad (5e)$$

$$\begin{aligned} z_{\eta^u} \left\| \left[\sum_{j \in \mathcal{R}_i} [r_j (\rho_j^p + \sum_{k \in \mathcal{D}_j} \rho_k^p) + x_j (\rho_j^q + \sum_{k \in \mathcal{D}_j} \rho_k^q)] \right] \sigma \right\|_2 \\ \leq \frac{1}{2} (u_i - \underline{u}_i), \forall i \in \mathcal{L}, \end{aligned} \quad (5f)$$

$$\begin{aligned} z_{\eta^f} \left\| \left(\gamma_c^p [\rho_\ell^\dagger + \sum_{i \in \mathcal{D}_\ell} \rho_i^p] + \gamma_c^q [\rho_\ell^\dagger + \sum_{i \in \mathcal{D}_\ell} \rho_i^q] \right) \sigma \right\|_2 \\ - \gamma_c^p f_\ell^p - \gamma_c^q f_\ell^q - \gamma_c^s \bar{f}_\ell, \forall \ell \in \mathcal{L}, \forall c \in \mathcal{C}. \end{aligned} \quad (5g)$$

C. The Privacy-Preserving Mechanism and Guarantees

The functioning of the privacy-preserving mechanism $\tilde{\mathcal{M}}$ is explained in Algorithm 1. The Algorithm first computes the covariance matrix Σ that encodes the DP parameters (ε, δ) , and adjacency parameter β . The mechanism then solves the optimization problem in (5) to obtain an optimal chance-constrained solution $\dot{\mathcal{V}}$. Last, the mechanism samples the random perturbation and obtains the final OPF solution using equations (3). By design of problem (5), the sampled OPF solution is guaranteed to satisfy grid limits and customer loads up to specified violation probabilities η^g, η^u and η^f , of the generator, voltage, and power flow constraints.

The privacy guarantees, in turn, depend on the specification of DP parameters (ε, δ) and the vector of adjacency coefficients β . For simplicity, the DP parameters are assumed to be uniform for all customers and specified by the DSO,

whereas customer privacy preferences are expressed in the submitted adjacency coefficients. In this setting, the load of every customer i is guaranteed to be indistinguishable from any other load in the range $[d_i^p - \beta_i, d_i^p + \beta_i]$ in the release of OPF solution related to node i up to DP parameters (ε, δ) . This guarantee is formalized by the following result.

Theorem 2 (Privacy Guarantees). *Let $(\varepsilon, \delta) \in (0, 1)$ and $\sigma_i \geq \beta_i \sqrt{2 \ln(1.25/\delta)/\varepsilon}$, $\forall i \in \mathcal{L}$. Then, if problem (5) returns an optimal solution, mechanism $\tilde{\mathcal{M}}$ is (ε, δ) -differentially private for β -adjacent load datasets. That is, the probabilities of returning a power flow solution in set F^p on any two β -adjacent datasets D and D' are such that*

$$\mathbb{P}[\tilde{\mathcal{M}}(D) \in F^p] \leq e^\varepsilon \mathbb{P}[\tilde{\mathcal{M}}(D') \in F^p] + \delta,$$

where \mathbb{P} denotes the probability over runs of $\tilde{\mathcal{M}}$.

Proof. The full proof is available in Appendix B and relies on two intermediate results summarized in Lemmas 1 and 2. The first lemma shows that the standard deviation of power flow related to customer i is at least as much as σ_i . Therefore, by specifying σ_i , the DSO attains the desired degree of randomization. The second lemma shows that $\beta_i \geq \Delta_i^\beta$, i.e., if σ_i is parameterized by β_i , then σ_i is also parameterized by sensitivity Δ_i^β , required by the Gaussian mechanism in Theorem 1. \square

V. MECHANISM EXTENSIONS

A. OPF Variance Control

Due to the radial topology of distribution grids, the flow perturbations along the same radial branch induce larger flow variances than those intended by the covariance matrix Σ . This section extends the mechanism $\tilde{\mathcal{M}}$ to reduce the overall flow variance while still preserving privacy guarantees. Two strategies are proposed to achieve this goal.

1) *Total Variance Minimization:* The flow standard deviation, obtained from (3b), depends on the DER participation variables ρ^\dagger . Therefore, the variance of power flows can be controlled by optimizing the DER dispatch. This variance control strategy is enabled by replacing problem (5) at the core of mechanism $\tilde{\mathcal{M}}$ by the following optimization:

$$\text{ToV-CC-OPF: } \min_{\mathcal{V} \cup \{t\}} \sum_{i \in \mathcal{N}} c_i g_i^p + \sum_{\ell \in \mathcal{L}} \psi_\ell t_\ell \quad (6a)$$

$$\text{s.t. } \left\| [\rho_\ell^p + \sum_{i \in \mathcal{D}_\ell} \rho_i^p] \sigma \right\|_2 \leq t_\ell, \forall \ell \in \mathcal{L}, \quad (6b)$$

$$\text{Equations (5b) -- (5g),} \quad (6c)$$

where the decision variable t_ℓ represents the standard deviation of the active power flow in line ℓ , which is penalized in the objective function by a non-negative parameter ψ_ℓ . By choosing $\psi_\ell, \forall \ell \in \mathcal{L}$, the DSO minimizes the total variance at the expense of operational cost. Note that, by Lemma 1, optimization (6) does not violate the privacy guarantees.

2) *Pursuing Target Variance:* This strategy solely perturbs the flow in the selected line of the radial branch (e.g., adjacent to the customer with the strongest privacy requirement) and constrains the DERs to maintain the flow variance in each line as required by the original matrix Σ . It specifies a new

matrix $\hat{\Sigma} = \text{diag}([\hat{\sigma}_1^2, \dots, \hat{\sigma}_{|\mathcal{L}|}^2])$, $\mathbb{1}^\top \hat{\sigma}^2 \leq \mathbb{1}^\top \sigma^2$, that contains a smaller number of perturbations. This control is enabled by replacing problem (5) by the following optimization:

$$\text{TaV-CC-OPF: } \min_{\mathcal{V} \cup \{t, \tau\}} \sum_{i \in \mathcal{N}} c_i g_i^p + \sum_{\ell \in \mathcal{L}} \psi_\ell \tau_\ell \quad (7a)$$

$$\text{s.t. } \left\| [\rho_\ell^p + \sum_{i \in \mathcal{D}_\ell} \rho_i^p] \hat{\sigma} \right\|_2 \leq t_\ell, \forall \ell \in \mathcal{L}, \quad (7b)$$

$$\left\| t_\ell - \sigma_\ell \right\|_2 \leq \tau_\ell, \forall \ell \in \mathcal{L}, \quad (7c)$$

$$\text{Equations (5b) -- (5g) with } \hat{\sigma}, \quad (7d)$$

where, t_ℓ returns the resulting flow standard deviation, while constraint (7c) yields the distance τ_ℓ between the resulting standard deviation and original one $\sigma_\ell = \Sigma_{\ell, \ell}^{1/2}$ required to provide customer at node ℓ with differential privacy. By penalizing this distance in the objective function, the DSO attains privacy at a smaller amount of random perturbations. Note, as optimization (7) acts on covariance matrix $\hat{\Sigma}$ instead of Σ , the DSO needs to verify a posteriori that $t_\ell \geq \sigma_\ell, \forall \ell \in \mathcal{L}$.

B. Optimality Loss Control

The application of mechanism $\tilde{\mathcal{M}}$ necessarily leads to an optimality loss compared to the solution of non-private mechanism \mathcal{M} . This section slightly abuses the notation and denotes the cost of the non-private OPF solution and that of the proposed DP mechanism when evaluated on a dataset D by $\mathcal{M}(D)$ and $\tilde{\mathcal{M}}(D)$, respectively. The optimality loss Θ is measured in expectation as the L_2 distance, i.e.,

$$\mathbb{E}[\Theta] = \|\mathcal{M}(D) - \mathbb{E}[\tilde{\mathcal{M}}(D)]\|_2,$$

as $\mathcal{M}(D)$ always provides a deterministic solution. However, the worst-case realization of $\tilde{\mathcal{M}}(D)$ may significantly exceed the expected value and lead to a larger optimality loss. To this end, this section introduces the optimality loss control strategy using the Conditional Value-at-Risk (CVaR) measure [13].

Consider $\varrho\%$ of the worst-case realizations of the optimality loss. The expected value of these worst-case realizations can be modeled as a decision variable using the CVaR measure as

$$\text{CVaR}_\varrho = \mu_c + \sigma_c \phi(\Phi^{-1}(1 - \varrho)) / \varrho, \quad (8)$$

where μ_c and σ_c represent the expected value and standard deviation of operational costs, while ϕ and $\Phi^{-1}(1 - \varrho)$ denote the probability density function and the inverse cumulative distribution function at the $(1 - \varrho)$ quantile of the standard Normal distribution. From Section (IV-B), it follows that

$$\mu_c = \mathbb{E}[c^\top \tilde{g}^p] = \mathbb{E}[c^\top (g^p + \rho \xi)] = c^\top g^p,$$

for zero-mean ξ , and the standard deviation finds as

$$\sigma_c = \text{std}[c^\top (g^p + \rho \xi)] = \text{std}[c^\top (\rho \xi)] = \|c^\top (\rho \sigma)\|_2,$$

providing a convex reformulation of the CVaR in (8). Therefore, for some trade-off parameter $\theta \in [0, 1]$, the DSO can trade off the mean and CVaR_ϱ of the optimality loss by substituting problem (5) at the core of mechanism $\tilde{\mathcal{M}}$ by the following optimization CVaR-CC-OPF:

$$\min_{\mathcal{V} \cup \sigma_c} (1 - \theta) c^\top g^p + \theta [c^\top g^p + \sigma_c \phi(\Phi^{-1}(1 - \varrho)) / \varrho] \quad (9a)$$

$$\text{s.t. } \|c^\top(\rho\sigma)\|_2 \leq \sigma_c, \quad (9b)$$

$$\text{Equations (5b) -- (5g),} \quad (9c)$$

where the standard deviation σ_c is modeled as a decision variable. Notice, the optimality loss control by means of (9) does not violate the privacy guarantees as per Lemma 1.

VI. NUMERICAL EXPERIMENTS

The experiments consider a modified 15-node radial grid from [29], which includes network parameters taken from [30], nodal loads as given in Table I, and nodal DERs with cost coefficients drawn from Normal distribution $c_i \sim \mathcal{N}(10, 2)$ \$/MWh, generation limits $\underline{g}_i^p = 0$ MW, $\bar{g}_i^p = 8$ MW, and power factor $\tan\phi_i = 0.5$, $\forall i \in \mathcal{N}$. The constraint violation probabilities are set as $\eta^g = 1\%$, $\eta^u = 2\%$ and $\eta^f = 10\%$. The DP parameters are set to $\varepsilon \rightarrow 1$, $\delta = 1/n = 0.071$ with n being a number of grid customers, while the adjacency parameters $\beta_i, \forall i \in \mathcal{L}$, vary across the experiments. All models are implemented in Julia using the JuMP package [31], and all data and codes are relegated to the e-companion [32].

A. Illustrative Example

The purpose of the illustrative example is to simulate and obfuscate periodic components of the load profile in power flow and voltage measurements. Assume that the customer at node 7 has an atypical load pattern representing its production technology. Her pattern is obtained by multiplying the maximum load by $k(t)$, a multiplier with the following three periodic components:

$$k(t) = \max \left\{ \sin \frac{5}{10^2} t, \frac{7}{10} \right\} + \frac{5}{10^2} \sin \frac{5}{10^2} t + \frac{25}{10^3} \sin \frac{75}{10^2} t$$

where t is the time step. The parameters of multiplier $k(t)$ are selected such that the load components have different magnitudes and frequencies. The non-private OPF solution provided by the D-OPF model leaks the information about this pattern through the power flow f_7^p and voltage v_7 readings, as displayed on the left plots in Fig. 3. To obfuscate the load pattern in the OPF solution, the customer submits the privacy preference β_7 , which is accommodated by the DSO using mechanism $\tilde{\mathcal{M}}$. Figure 3 shows that by setting $\beta_7 \rightarrow 0.07$ MW, the presence of the smallest periodic component is obfuscated through randomization, while the presence of the two remaining components is still distinguished. With an increasing β_7 , the mechanism further obfuscates the medium and largest periodic components.

B. Privacy Guarantees

To illustrate the privacy guarantees of Theorem 2, consider the same grid customer at node 7 with the load of 2.35 MW. For β_7 , consider two adjacent load datasets D' and D'' , containing $d_7^p = d_7^p - \beta_7$ and $d_7''^p = d_7^p + \beta_7$, respectively. The non-private OPF mechanism returns the following power flows

$$\mathcal{M}(D') = 2.05 \text{ MW}, \mathcal{M}(D) = 2.35 \text{ MW}, \mathcal{M}(D'') = 2.65 \text{ MW},$$

for $\beta_7 = 0.3$ MW, clearly distinguishing the differences in datasets through power flow readings. The differentially

private mechanism $\tilde{\mathcal{M}}$ in Algorithm 1, in turn, obfuscates the load value used in the computation. Figure 4 shows that the mechanism makes the OPF solutions on the three datasets similar in the probabilistic sense, thus providing privacy guarantees for the original load dataset D . The maximal difference between the distributions of power flow solutions is bounded by the parameters ε and δ . Observe that the larger specification $\delta = 0.75$ results in weaker guarantees, as the distributions slightly stand out from one another. On the other hand, $\delta = 0.07$ yields a larger noise magnitude overlapping the support of the three distributions. The OPF solution to be implemented is obtained from a single sample drawn from the blue distribution. By observing a single sample, an adversary cannot distinguish the distribution, and thus the dataset, it was sampled from. Finally, Fig. 4 shows randomized OPF solutions obtained on a given load dataset. The parameters of the noise, however, are independent from load dataset (see Theorem 2), and the privacy guarantee for the customer at node 7 is independent from the loads and their variations at other grid nodes.

C. OPF Variance Control

Consider the application of the mechanism when all grid customers have their adjacency coefficients set to 10% of their loads. The non-private D-OPF and private OPF solutions, obtained with the variance-agnostic CC-OPF and variance-aware ToV- and TaV-CC-OPF models, are summarized in Table I: Each row i presents the power flow and voltage solutions related to customer i , and the bottom rows report the expected operational cost, optimality loss $\mathbb{E}[\Theta]$ in %, sum of power flow standard deviations, percentage $\hat{\eta}$ of infeasible instances on 5000 noise samples, and CPU times.

The table shows that, unlike non-private, deterministic D-OPF model, the DP mechanisms return OPF variables as probability densities with given means and standard deviations. For all three DP mechanisms, the flow standard deviations are at least as much as those required by Theorem 2, thus providing differential privacy. However, due to the noise applied to each network flow, the flow standard deviations provided by the CC-OPF model exceed the intended quantities, e.g., by 458% for the first customer close to the substation. To minimize the OPF variance, the ToV-CC-OPF and TaV-CC-OPF models are used with the uniform variance penalty factor $\psi_\ell = 10^5, \forall \ell \in \mathcal{L}$. The ToV-CC-OPF model also perturbs each flow in the network but it alters the optimal DER dispatch to reduce the sum of flow standard deviations by 50%. The TaV-CC-OPF model, in turn, introduces a limited number of perturbations to lines $\{1, 5 - 7, 9, 11 - 13\}$ and constrains the DERs to maintain the intended standard deviation σ across the entire network, reducing the flow standard deviation by 63%. As ToV-CC-OPF and TaV-CC-OPF prioritize the flow variance over expected cost, the models provide larger optimality loss than the CC-OPF model.

The OPF solution to be implemented by the DSO is a sample drawn from the probability densities reported in Table I. The empirical probability of the joint constraint violation $\hat{\eta}$ demonstrates an appropriate out-of-sample performance.

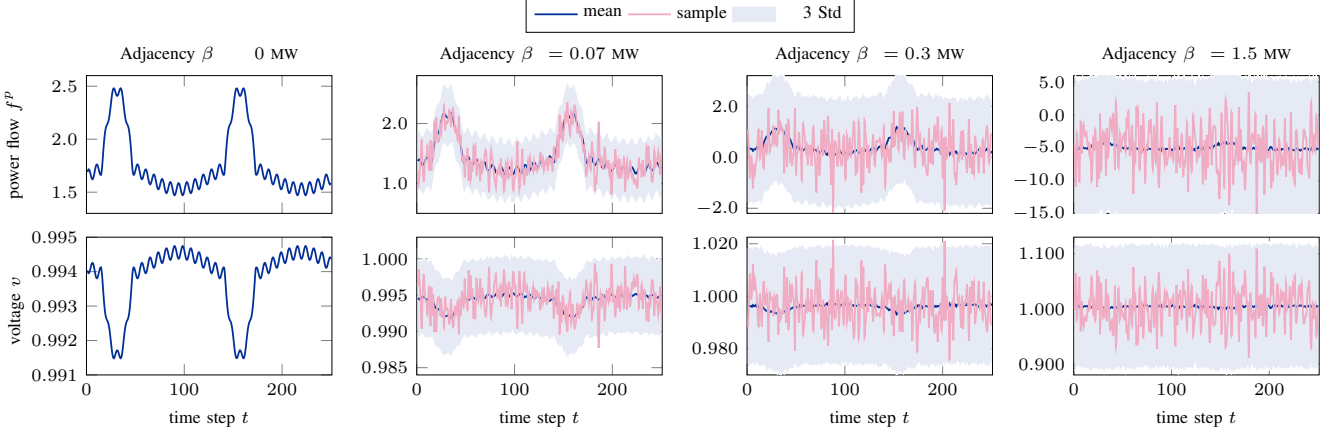


Fig. 3. Power flow and voltage magnitude at node 7 as functions of adjacency coefficient β_7 . The flow and voltage solutions are given by their mean value (blue) and the range of ± 3 standard deviations (light blue). The OPF solution implemented by the DSO is given by sample trajectories (red).

TABLE I
SOLUTION SUMMARY FOR THE NON-PRIVATE AND DIFFERENTIALLY PRIVATE OPF MECHANISMS.

i	d_i^p	σ_i	D-OPF, Eq. (1)		CC-OPF, Eq. (5)				ToV-CC-OPF, Eq. (6)				TaV-CC-OPF, Eq. (7)			
			f_i^p	v_i	mean	std	mean	std	f_i^p	v_i	mean	std	f_i^p	v_i	mean	std
0	0	—	—	1.00	—	—	1.00	—	—	—	1.00	—	—	—	1.00	—
1	2.01	0.48	8.5	1.00	11.3	2.68	1.00	0.0016	12.6	0.69	1.00	0.0004	13.0	0.48	1.00	0.0003
2	2.01	0.48	6.5	1.00	9.3	2.68	0.99	0.0057	11.4	0.71	0.99	0.0015	11.0	0.48	0.99	0.0010
3	2.01	0.48	4.4	1.00	7.3	2.68	0.99	0.0123	10.2	0.78	0.97	0.0033	9.0	0.48	0.98	0.0022
4	1.73	0.41	-8.0	1.00	-1.4	1.72	0.99	0.0128	3.6	0.69	0.97	0.0034	1.7	0.41	0.98	0.0023
5	2.91	0.70	5.1	1.00	3.1	0.87	0.99	0.0128	2.5	0.82	0.97	0.0035	1.9	0.70	0.98	0.0024
6	2.19	0.52	2.2	1.00	0.1	0.87	0.99	0.0128	0.7	0.63	0.97	0.0038	1.0	0.52	0.98	0.0024
7	2.35	0.56	2.3	0.99	0.9	0.63	0.98	0.0134	0.9	0.61	0.97	0.0039	1.0	0.56	0.98	0.0024
8	2.35	0.56	10.5	0.99	6.7	1.18	0.98	0.0130	5.8	0.78	0.97	0.0036	6.4	0.56	0.98	0.0023
9	2.29	0.55	5.8	0.99	3.5	0.88	0.98	0.0132	3.1	0.70	0.97	0.0037	3.6	0.55	0.98	0.0023
10	2.17	0.52	3.5	0.99	1.2	0.88	0.98	0.0135	1.6	0.65	0.97	0.0038	1.3	0.52	0.97	0.0023
11	1.32	0.32	1.3	0.99	0.4	0.39	0.98	0.0135	0.4	0.40	0.97	0.0038	0.6	0.32	0.97	0.0023
12	2.01	0.48	6.5	1.00	3.6	1.23	1.00	0.0008	3.3	0.73	1.00	0.0004	3.6	0.48	1.00	0.0003
13	2.24	0.54	4.5	0.99	1.6	1.23	1.00	0.0034	2.1	0.72	1.00	0.0019	3.2	0.54	0.99	0.0012
14	2.24	0.54	2.2	0.99	-0.6	1.23	1.00	0.0050	0.8	0.64	0.99	0.0027	1.0	0.54	0.99	0.0018
cost ($\mathbb{E}[\Theta]$)			\$396.0 (0\%)		\$428.0 (8.1\%)				\$463.5 (17.1\%)				\$459.3 (16.0\%)			
$\sum_i \text{std}[f_i^p]$			0 MW		19.1 MW				9.5 MW				7.1 MW			
infeas. η			0%		3.3%				6.9%				5.5%			
CPU time			0.016s		0.037s				0.043s				0.052s			

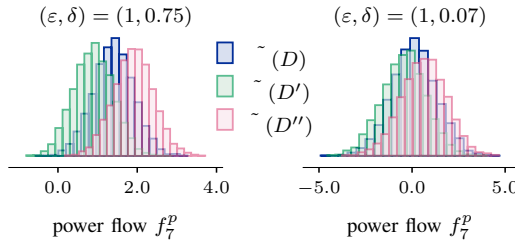


Fig. 4. The overlay of power flow probability densities obtained on the three β_7 -adjacent load datasets for $\delta = 0.75$ and $\delta = 0.07$ (5000 samples).

However, if the DP mechanism returns an infeasible sample, the DSO may re-sample the OPF solution, yet it comes at the expense of the relaxation of privacy guarantees: every resampling round increases the privacy loss linearly, by ε , as per composition of DP [24, Theorem 3.14]. Finally, the privacy-

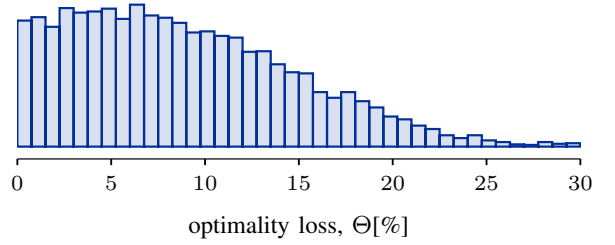


Fig. 5. CVaR-CC-OPF: Empirical out-of-sample density of the optimality loss for a trade-off parameter $\theta = 0$ (5000 samples)

preserving mechanisms keep the CPU time within the same time-frame as the standard, non-private D-OPF mechanism.

D. Optimality Loss Control

The application of mechanism $\tilde{\mathcal{M}}$ yields an optimality loss with respect to the solution of the standard, non-private OPF

TABLE II
TRADE-OFFS OF THE EXPECTED AND CVaR_{10%} PERFORMANCE

θ	exp. value		CVaR _{10%}		$\sum_i \text{std}[f_i^p]$, MW
	cost, \$	$\Theta, \%$	cost, \$	$\Theta, \%$	
0.0	428.0	8.1	478.1	20.7	19.1
0.1	428.0	8.1	476.3	20.3	19.4
0.2	428.3	8.2	475.0	19.9	19.6
0.3	428.9	8.3	473.3	19.5	19.8
0.4	431.9	9.1	467.8	18.1	17.3
0.5	434.5	9.7	464.4	17.3	15.7
0.6	438.2	10.7	461.7	16.6	14.6
0.7	452.9	14.4	452.9	14.4	13.0

mechanism. For the same setting as in the previous experiment, the out-of-sample empirical distribution of the cost is depicted in Fig. VI-D. Observe that the probability mass is centered at 8.1% of optimality loss and that the distribution is biased towards smaller optimality losses. Although the probability of the worst-case outcomes is shown very small on out-of-sample, the expected value over 10% of the worst-case outcomes is at relatively large 20.7%. The DSO, however, is capable to trade off between the expected and the worst-case optimality loss by substituting the CC-OPF model in mechanism $\tilde{\mathcal{M}}$ by the CVaR-CC-OPF model in (9). For a trade-off parameter $\theta \in [0, 1]$, the expected optimality loss in $\varrho = 10\%$ of the worst-case scenarios is contrasted with the expected loss in Table II. For $\theta = 0$, the CVaR_{10%} significantly exceeds the expected value. However, by increasing θ , the DSO alters the DER dispatch to reduce the worst-case optimality loss at the expense of increasing the expected value. For $\theta \geq 0.7$, the expected value corresponds to CVaR_{10%}, thus providing differential privacy at a fixed cost. Eventually, the choice of θ is driven by the DSO's risk preference. Finally, the optimality loss can be further reduced by relaxing the feasibility guarantee with larger probabilities η , though it may result in an increasing out-of-sample violation probability $\hat{\eta}$.

E. Comparison with the Output Perturbation Mechanism

It remains to compare the proposed privacy-preserving OPF mechanism with the standard, non-adapted to the specifics of OPF problems, output perturbation (OP) mechanism [24]. The functioning of this mechanism is depicted in Algorithm 2: it solves the deterministic OPF problem, perturbs the optimal power flow solution with the random noise, and then finds the feasible DER and substation dispatch that satisfies AC-OPF equations for the perturbed values of power flows. If exists, the mechanism returns an (ε, δ) -differentially private OPF solution on β -adjacent datasets, or reports infeasibility otherwise. Observe, unlike the proposed mechanism in Algorithm 1, the output perturbation mechanism does not offer feasibility guarantees, because the perturbation step is done independently from the OPF computations.

To compare the two mechanisms, consider the provision of differential privacy for sets of nodes $1 : n$, i.e., from 1 to n , for which $\beta_i \rightarrow 10\%$. By increasing n , the amount of noise that the DSO needs to accommodate in the grid increases. Table III summarizes the feasibility statistics for

Algorithm 2: Output Perturbation (OP) Mechanism

```

1 Input:  $D, \varepsilon, \delta, \beta$ 
2 Solve  $\{f_\ell^p\}_{\ell \in \mathcal{L}} \leftarrow \text{argmin}$  problem (1) using  $D$ 
3 Sample  $\hat{\xi}_\ell \sim \mathcal{N}(0, \beta_\ell \sqrt{2 \ln(1.25/\delta)/\varepsilon}), \forall \ell \in \mathcal{L}$ 
4 Perturb power flows  $\hat{f}_\ell^p = f_\ell^p + \hat{\xi}_\ell, \forall \ell \in \mathcal{L}$ 
5 Re-solve problem (1) for the fixed  $f_\ell^p = \hat{f}_\ell^p, \forall \ell \in \mathcal{L}$ 
6 if problem (1) feasible then
7 | Implement perturbed solution
8 else
9 | Report infeasibility
10 end

```

TABLE III
PERCENTAGE OF INFEASIBLE OPF INSTANCES (5000 SAMPLES) [%]

Mechanism	Node set $1 : n$ (with non-zero adjacency β_i)						
	1	1:2	1:3	1:4	1:5	...	1:14
OP	52.1	87.0	97.9	99.7	100	...	100
CC-OPF	0.1	0.9	0.9	1.0	1.1	...	3.3

the two algorithms. Observe, even for a single customer, the output perturbation mechanism produces infeasible solutions in 52.1% of instances, and its performance further reduces in n . By optimizing affine functions in (3), the proposed mechanism, instead, produces feasible OPF instances with a high probability, e.g. 96.7% for the entire set of customers.

VII. CONCLUSIONS AND FUTURE WORK

This paper introduced a differentially private OPF mechanism for distribution grids, which provides formal privacy guarantees for grid customer loads. The mechanism parametrizes OPF variables as affine functions of a carefully calibrated noise to weaken the correlations between grid loads and OPF variables, thus preventing the recovery of customer loads from the voltage and power flow measurements. Furthermore, the mechanism was extended to enable the DSO to control the OPF variance induced by the noise in the computations, providing better practices for systems with more emphasis on component overloads than on operational costs. Finally, the optimality loss induced by the mechanism translates into privacy costs. To minimize the risk of large privacy costs, the mechanism was extended to enable the trade-off between the expected and worst-case performances.

There are several avenues for future work. To understand the impacts of the privacy preservation on distribution electricity pricing, one can explore the connection between DP parameters and distribution locational marginal prices following price decomposition approach from [22] and [29]. Alternatively, the coalition game theory can be used to find an adequate privacy cost allocation among customers, similar to game-theoretic reserve cost allocation in [33]. Finally, the private OPF mechanism has been developed in a technically suitable ecosystem: it builds upon LinDistFlow OPF equations neglecting the effects of power losses, adopts a constant DER power factor, and does not include the control of stochastic DERs. Although these three factors are well-studied in the context of the chance-constrained OPF problems under uncertainty, it remains valid,

if not crucial, for future work to explore their effects on the limits of the differential privacy provision in distribution grids.

APPENDIX

A. System Response to the Random Perturbation

The affine dependency of power flows on the random perturbation is obtain by substituting generator response policy (2a) into OPF equations (1c), that is:

$$\begin{aligned} \tilde{f}_\ell^\dagger(\xi) &= d_\ell^\dagger - g_\ell^\dagger(\xi) + \sum_{i \in \mathcal{D}_\ell} (d_i^\dagger - g_i^\dagger(\xi)) \\ &= d_\ell^\dagger - g_\ell^\dagger - \rho_\ell^\dagger \xi + \sum_{i \in \mathcal{D}_\ell} (d_i^\dagger - g_i^\dagger - \rho_i^\dagger \xi) \\ &= d_\ell^\dagger - g_\ell^\dagger + \sum_{i \in \mathcal{D}_\ell} (d_i^\dagger - g_i^\dagger) - [\rho_\ell^\dagger \xi + \sum_{i \in \mathcal{D}_\ell} \rho_i^\dagger \xi] \\ &\stackrel{\text{due to (1c)}}{=} f_\ell^\dagger - \left[\rho_\ell^\dagger + \sum_{j \in \mathcal{D}_\ell} \rho_j^\dagger \right] \xi, \quad \forall \ell \in \mathcal{L}, \end{aligned} \quad (10a)$$

where f_ℓ^\dagger is the nominal (average) component and the last term is the random flow component. The affine dependency of voltages on the random perturbation is obtain by substituting (10a) into voltage drop equation (1d), that is:

$$\begin{aligned} \tilde{u}_i(\xi) &= u_0 - 2 \sum_{\ell \in \mathcal{R}_i} (\tilde{f}_\ell^p(\xi) r_\ell + \tilde{f}_\ell^q(\xi) x_\ell) \\ &= u_0 - 2 \sum_{\ell \in \mathcal{R}_i} (f_\ell^p r_\ell + f_\ell^q x_\ell) \\ &\quad + 2 \sum_{\ell \in \mathcal{R}_i} [r_\ell (\rho_\ell^p + \sum_{k \in \mathcal{D}_\ell} \rho_k^p) + x_\ell (\rho_\ell^q + \sum_{k \in \mathcal{D}_\ell} \rho_k^q)] \xi \\ &\stackrel{\text{due to (1d)}}{=} u_i + 2 \sum_{\ell \in \mathcal{R}_i} [r_\ell (\rho_\ell^p + \sum_{k \in \mathcal{D}_\ell} \rho_k^p) + x_\ell (\rho_\ell^q + \sum_{k \in \mathcal{D}_\ell} \rho_k^q)] \xi, \end{aligned} \quad (10b)$$

where u_i is the nominal (average) component and the last term is the random voltage component. Together with the response policy in (2a), equations (10) constitute the model of system response to the random perturbation, given in equations (3).

B. Proof of Theorem 2

The proof of Theorem 2 relies on Lemmas 1 and 2. The first lemma shows that the standard deviation of power flow related to customer i is at least as much as σ_i . Therefore, by specifying σ_i , the DSO attains the desired degree of randomization.

Lemma 1. *If OPF mechanism (5) returns optimal solution, then σ_ℓ is the lower bound on $\text{std}[\tilde{f}_\ell^p]$.*

Proof. Consider a single flow perturbation with $\xi_\ell \sim \mathcal{N}(0, \sigma_\ell^2)$ and $\xi_j = 0, \forall j \in \mathcal{L} \setminus \ell$. The standards deviation of active power flow (3b) in optimum finds as

$$\begin{aligned} \text{std} \left[\tilde{f}_\ell^p - \left[\rho_\ell^p + \sum_{j \in \mathcal{D}_\ell} \rho_j^p \right] \xi \right] &= \text{std} \left[\left[\rho_\ell^p + \sum_{j \in \mathcal{D}_\ell} \rho_j^p \right] \xi \right] \\ &= \text{std} \left[\sum_{j \in \mathcal{D}_\ell} \alpha_{j\ell}^* \xi_\ell \right] \stackrel{(2b)}{=} \text{std}[\xi_\ell] = \sigma_\ell, \end{aligned} \quad (11)$$

where the second to the last equality follows from balancing conditions (2b). As for any pair $(\ell, j) \in \mathcal{L}$ the covariance

matrix returns $\Sigma_{\ell,j} = 0$, σ_ℓ is a lower bound on $\text{std}[\tilde{f}_\ell^p]$ in the optimum for any additional perturbation in the network. \square

Remark 1. *The result of Lemma 1 holds independently from the choice of objective function and is solely driven by the feasibility conditions.*

The second lemma shows that $\beta_i \geq \Delta_i^\beta$, i.e., if σ_i is parameterized by β_i , then σ_i is also parameterized by sensitivity Δ_i^β .

Lemma 2. *Let D and D' be two adjacent datasets differing in at most one load d_i^p by at most $\beta_i > 0$. Then,*

$$\Delta_i^\beta = \max_{\ell \in \mathcal{L}} \|\mathcal{M}(D)|_{f_\ell^p} - \mathcal{M}(D')|_{f_\ell^p}\|_2 \leq \beta_i,$$

where the notation $\mathcal{M}(\cdot)|_{f_\ell^p}$ denotes the value of the optimal active power flow on line ℓ returned by the computation $\mathcal{M}(\cdot)$.

Proof. Let \tilde{f}_ℓ^p be the optimal solution for the active power flow in line ℓ obtained on input dataset $D = (d_1^p, \dots, d_n^p)$. From OPF equation (1c), it can be written as

$$\tilde{f}_\ell^p = d_\ell^p - g_\ell^p + \sum_{i \in \mathcal{D}_\ell} (d_i^p - g_i^p),$$

which expresses the flow as a function of the downstream loads and the optimal DER dispatch. A change in the active load d_ℓ^p translates into a change of power flow as

$$\begin{aligned} \frac{\partial \tilde{f}_\ell^p}{\partial d_\ell^p} &= \underbrace{\frac{\partial d_\ell^p}{\partial d_\ell^p}}_1 - \underbrace{\frac{\partial g_\ell^p}{\partial d_\ell^p}}_0 + \sum_{i \in \mathcal{D}_\ell} \left(\underbrace{\frac{\partial d_i^p}{\partial d_\ell^p}}_0 - \underbrace{\frac{\partial g_i^p}{\partial d_\ell^p}}_1 \right) \\ &= 1 - \frac{\partial g_\ell^p}{\partial d_\ell^p} - \sum_{i \in \mathcal{D}_\ell} \frac{\partial g_i^p}{\partial d_\ell^p}, \end{aligned} \quad (12)$$

where the last two terms are always non-negative due to convexity of model (1). The value of (12) attains maximum when

$$g_k^p = \bar{g}_k^p \mapsto \frac{\partial g_k^p}{\partial d_\ell^p} = 0, \quad \forall k \in \{\ell\} \cup \mathcal{D}_\ell. \quad (13)$$

Therefore, by combining (12) with (13) we obtain the maximal change of power flows as

$$\frac{\partial \tilde{f}_\ell^p}{\partial d_\ell^p} = 1.$$

Since the dataset adjacency relation considers loads d_ℓ^p that differ by at most β_ℓ , it suffices to multiply the above by β_ℓ to attain the result. It finds similarly that for a β_i change of any load $i \in \mathcal{N}$, all network flows change by at most β_i . \square

Proof of Theorem 2. Consider a customer at non-root node i . Mechanism $\tilde{\mathcal{M}}$ induces a perturbation on the active power flow f_i^p by a random variable $\xi_i \sim \mathcal{N}(0, \sigma_i^2)$. The randomized active power flow \tilde{f}_i^p is then given as follows:

$$\tilde{f}_i^p = \tilde{f}_i^p - \left[\rho_i^p + \sum_{j \in \mathcal{D}_i} \rho_j^p \right] \xi_i,$$

where \star denotes optimal solution for optimization variables. For privacy parameters (ε, δ) , the mechanism specifies

$$\sigma_i \geq \beta_i \sqrt{2\ln(1.25/\delta)/\varepsilon}, \forall i \in \mathcal{L}.$$

As per Lemma 1, we know that σ_i is the lower bound on the standard deviation of power flow f_i^p . From Lemma 2 we also know that the sensitivity Δ_i^β of power flow in line i to load d_i^p is upper-bounded by β_i , so we have

$$\text{std}[\tilde{f}_i^p] \geq \sigma_i \geq \Delta_i^\beta \sqrt{2\ln(1.25/\delta)/\varepsilon}.$$

Since the randomized power flow follow is now given by a Normal distribution with the standard deviation $\text{std}[\tilde{f}_i^p]$ as above, by Theorem 1, mechanism $\tilde{\mathcal{M}}$ satisfies (ε, δ) -differential privacy for each grid customer up to adjacency parameter β . \square

REFERENCES

- [1] E. Dall'Anese and A. Simonetto, "Optimal power flow pursuit," *IEEE Trans. Smart Grid*, vol. 9, no. 2, pp. 942–952, 2016.
- [2] S. Bolognani, E. Arcari, and F. Dörfler, "A fast method for real-time chance-constrained decision with application to power systems," *IEEE Contr. Syst. Lett.*, vol. 1, no. 1, pp. 152–157, 2017.
- [3] R. Mieh and Y. Dvorkin, "Data-driven distributionally robust optimal power flow for distribution systems," *IEEE Contr. Syst. Lett.*, vol. 2, no. 3, pp. 363–368, 2018.
- [4] C. Duarte *et al.*, "Non-intrusive load monitoring based on switching voltage transients and wavelet transforms," in *2012 Future of Instrumentation International Workshop Proceedings*. IEEE, 2012, pp. 1–4.
- [5] A. I. Cole and A. Albicki, "Data extraction for effective non-intrusive identification of residential power loads," in *IMTC/98 Conference Proceedings*, vol. 2. IEEE, 1998, pp. 812–815.
- [6] Z. Erkin *et al.*, "Privacy-preserving data aggregation in smart metering systems: An overview," *IEEE Signal Processing Magazine*, vol. 30, no. 2, pp. 75–86, 2013.
- [7] C. Dwork *et al.*, "Calibrating noise to sensitivity in private data analysis," in *Theory of Cryptography Conference*. Springer, 2006, pp. 265–284.
- [8] K. Chaudhuri, C. Monteleoni, and A. D. Sarwate, "Differentially private empirical risk minimization," *Journal of Machine Learning Research*, vol. 12, no. Mar, pp. 1069–1109, 2011.
- [9] J. Hsu *et al.*, "Privately solving linear programs," in *International Colloquium on Automata, Languages, and Programming*. Springer, 2014, pp. 612–624.
- [10] F. Fioretto, T. W. Mak, and P. Van Hentenryck, "Differential privacy for power grid obfuscation," *IEEE Trans. Smart Grid*, vol. 11, no. 2, pp. 1356–1366, 2019.
- [11] T. W. Mak *et al.*, "Privacy-preserving power system obfuscation: A bilevel optimization approach," *IEEE Trans. Power Syst.*, vol. 35, no. 2, pp. 1627–1637, 2019.
- [12] S. S. Baghsorkhi and I. A. Hiskens, "Impact of wind power variability on sub-transmission networks," in *2012 IEEE Power and Energy Society General Meeting*. IEEE, 2012, pp. 1–7.
- [13] A. Shapiro, D. Dentcheva, and A. Ruszczynski, *Lectures on stochastic programming: modeling and theory*. SIAM, 2009.
- [14] D. Bienstock and A. Shukla, "Variance-aware optimal power flow: Addressing the tradeoff between cost, security, and variability," *IEEE Control Netw. Syst.*, vol. 6, no. 3, pp. 1185–1196, 2019.
- [15] F. Zhou, J. Anderson, and S. H. Low, "Differential privacy of aggregated DC optimal power flow data," *arXiv preprint arXiv:1903.11237*, 2019.
- [16] V. Dvorkin *et al.*, "Differentially private distributed optimal power flow," *arXiv preprint arXiv:1910.10136*, 2019.
- [17] S. Han, U. Topcu, and G. J. Pappas, "Differentially private distributed constrained optimization," *IEEE Trans. Autom. Control*, vol. 62, no. 1, pp. 50–64, 2016.
- [18] Z. Zhang *et al.*, "Cost-friendly differential privacy for smart meters: Exploiting the dual roles of the noise," *IEEE Trans. Smart Grid*, vol. 8, no. 2, pp. 619–626, March 2017.
- [19] M. Baran and F. F. Wu, "Optimal sizing of capacitors placed on a radial distribution system," *IEEE Trans. Power Deliv.*, vol. 4, no. 1, pp. 735–743, 1989.
- [20] L. A. Roald, "Optimization methods to manage uncertainty and risk in power systems operation," Ph.D. dissertation, ETH Zurich, 2016.
- [21] A. Bernstein, C. Wang, E. Dall'Anese, J.-Y. Le Boudec, and C. Zhao, "Load flow in multiphase distribution networks: Existence, uniqueness, non-singularity and linear models," *IEEE Trans. Power Syst.*, vol. 33, no. 6, pp. 5832–5843, 2018.
- [22] R. Mieth and Y. Dvorkin, "Distribution electricity pricing under uncertainty," *arXiv preprint arXiv:1905.07526*, 2019.
- [23] K. Chatzikokalakis *et al.*, "Broadening the scope of differential privacy using metrics," in *International Symposium on Privacy Enhancing Technologies Symposium*. Springer, 2013, pp. 82–102.
- [24] C. Dwork and A. Roth, "The algorithmic foundations of differential privacy," *Foundations and Trends® in Theoretical Computer Science*, vol. 9, no. 3–4, pp. 211–407, 2014.
- [25] L. Roald, S. Misra, T. Krause, and G. Andersson, "Corrective control to handle forecast uncertainty: A chance constrained optimal power flow," *IEEE Trans. Power Syst.*, vol. 32, no. 2, pp. 1626–1637, 2016.
- [26] V. Dvorkin, J. Kazempour, and P. Pinson, "Chance-constrained equilibrium in electricity markets with asymmetric forecasts," *arXiv preprint arXiv:2005.11749*, 2020.
- [27] T. Akbari and M. T. Bina, "Linear approximated formulation of AC optimal power flow using binary discretisation," *IET Generation, Transmission & Distribution*, vol. 10, no. 5, pp. 1117–1123, 2016.
- [28] S. Boyd and L. Vandenberghe, *Convex optimization*. Cambridge university press, 2004.
- [29] A. Papavasiliou, "Analysis of distribution locational marginal prices," *IEEE Trans. Smart Grid*, vol. 9, no. 5, pp. 4872–4882, 2017.
- [30] R. Mieth and Y. Dvorkin. Code supplement - DLMPs under uncertainty. [Online]. Available: https://github.com/korpuske191/DLMP_uncertainty_CodeSupplement
- [31] M. Lubin and I. Dunning, "Computing in operations research using julia," *INFORMS J Comput.*, vol. 27, no. 2, pp. 238–248, 2015.
- [32] V. Dvorkin *et al.* Online Appendix to DP-CC-OPF. [Online]. Available: https://github.com/wdvorkin/DP_CC_OPF
- [33] O. Karaca, S. Delikaraoglu, G. Hug, and M. Kamgarpour, "Enabling inter-area reserve exchange through stable benefit allocation mechanisms," *arXiv preprint arXiv:1912.09933*, 2019.

Department of Electrical Engineering

Center for Electric Power and Energy (CEE)

Technical University of Denmark

Elektrovej, Building 325

DK-2800 Kgs. Lyngby

Denmark

www.elektro.dtu.dk/cee

Tel: (+45) 45 25 35 00

Fax: (+45) 45 88 61 11

E-mail: cee@elektro.dtu.dk